AD-A035 743 NAVAL POSTGRADUATE SCHOOL MONTEREY CALIF F/G 17/2.1
A SIMULATOR FOR SHIPBOARD RADIO FREQUENCY INTERFERENCE IN SATEL--ETC(U)
OCT 76 E S BRICK, J E OHLSON
UNCLASSIFIED NPS-620L76109 NL

1 OF 3
AD-A
035 743

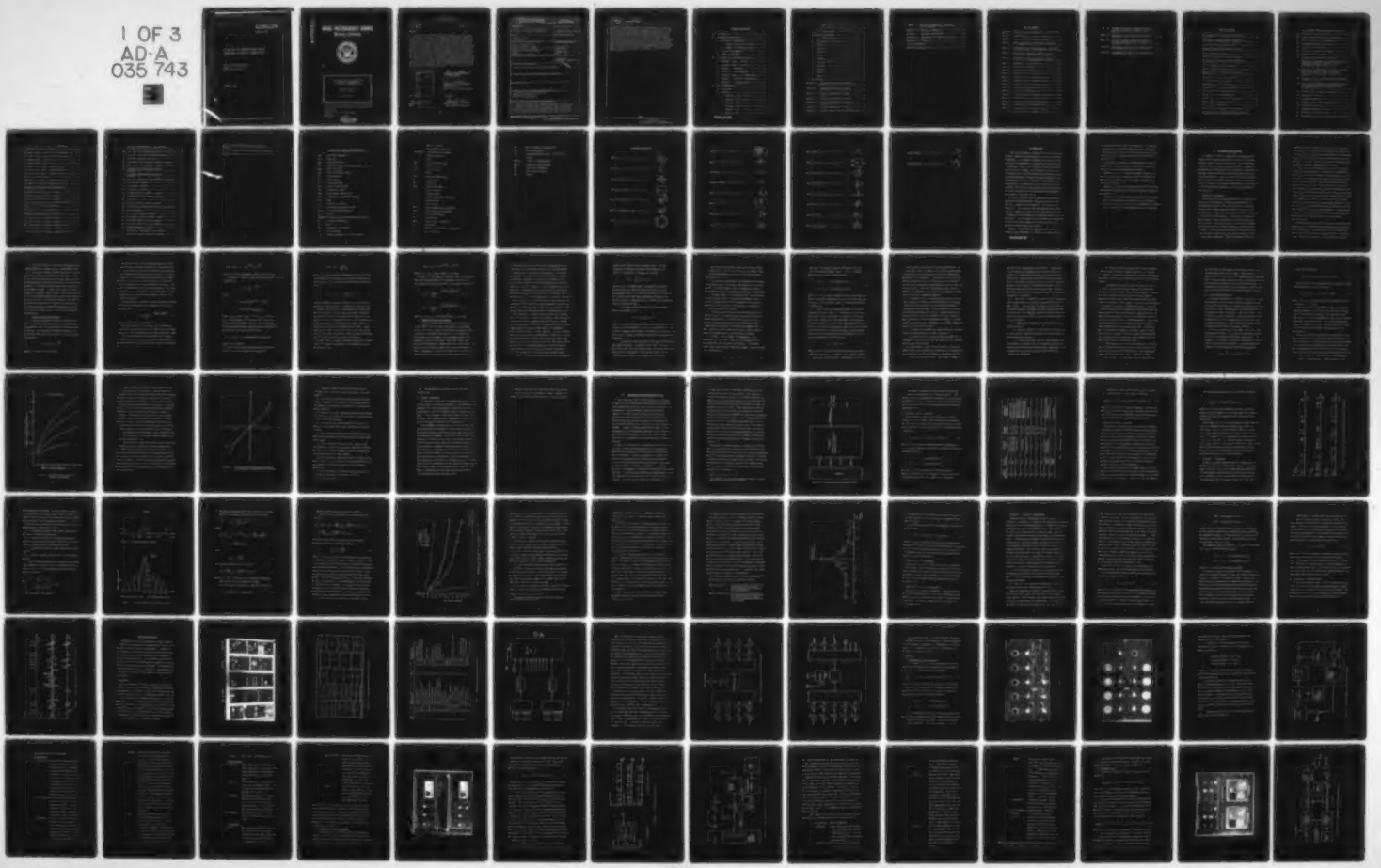

A SIMULATOR FOR SHIPBOARD RADIO FREQUENCY INTERFERENCE IN SATELLITE COMMUNICATIONS

NAVAL POSTGRADUATE SCHOOL
MONTEREY, CALIFORNIA

OCTOBER 1976

NPS-62OL76109

NAVAL POSTGRADUATE SCHOOL

Monterey, California

A SIMULATOR FOR SHIPBOARD RADIO FREQUENCY INTERFERENCE IN SATELLITE COMMUNICATIONS

Eduardo S. Brick
John E. Ohlson

October 1976

Approved for public release: Distribution Unlimited

A task under the Shipboard RFI in UHF SATCOM Project

Prepared for:

Naval Electronic Systems Command
PME 106
Washington, D. C. 20360

NAVAL POSTGRADUATE SCHOOL
Monterey, California

Rear Admiral Isham Linder
Superintendent
30 October 1976

Jack R. Borsting
Provost

ABSTRACT

A simulator for shipboard radio frequency interference, intended to be used in the characterization of UHF satellite communications terminals such as the AN/WSC-3 and AN/SSR-1, has been developed. Analytical results for the performance of various types of communications systems in white gaussian noise is available in the open literature. Performance in other types of channels, such as between a satellite and ship, is not known yet due to unavailability of analytical models for the additive type of interference found in the ship's environment. A physical-statistical model for shipboard interference, based on Middleton's model for urban noise, is given. The model developed incorporates the relevant physical aspects of the various possible interferers and postulates a statistical framework in which these signals are inserted. A simulator based on the developed model was built to serve as a tool for study of the effects of the various interferers upon shipboard satellite communications systems. The simulator is capable of generating 10 types of complex emitters and of providing linear and nonlinear processing of them. It is also capable of generating a PSK modulated test signal for performance measurements of UHF terminals. Results of performance measurements are presented. These results demonstrate the ability of the simulator to reproduce the shipboard electromagnetic environment.

This report was prepared by:

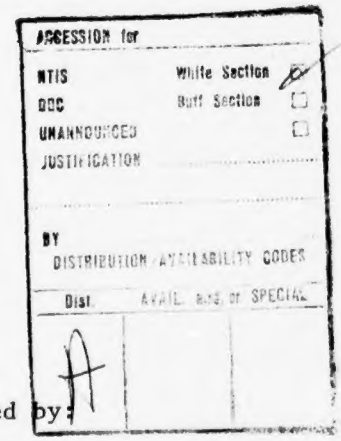

EDUARDO S. BRICK
LT, Brazilian Navy

JOHN E. OHLSON
Associate Professor
Department of Electrical Engineering

Approved by:

DONALD E. KIRK
Chairman
Dept. of Electrical Engineering

Released by:

ROBERT R. FOSSUM
Dean of Research Administration

UNCLASSIFIED

SECURITY CLASSIFICATION OF THIS PAGE (When Data Entered)

REPORT DOCUMENTATION PAGE		READ INSTRUCTIONS BEFORE COMPLETING FORM
1. REPORT NUMBER NPS-62OL76109	2. GOVT ACCESSION NO.	3. RECIPIENT'S CATALOG NUMBER
4. TITLE (and Subtitle) A Simulator for Shipboard Radio Frequency Interference in Satellite Communications		5. TYPE OF REPORT & PERIOD COVERED Technical Report 6. PERFORMING ORG. REPORT NUMBER
7. AUTHOR(s) Eduardo S. Brick John E. Ohlson		8. CONTRACT OR GRANT NUMBER(s)
9. PERFORMING ORGANIZATION NAME AND ADDRESS Naval Postgraduate School Monterey, California 93940		10. PROGRAM ELEMENT, PROJECT, TASK AREA & WORK UNIT NUMBERS N0003976WRT9053
11. CONTROLLING OFFICE NAME AND ADDRESS Naval Electronic Systems Command PME 106 Washington, D. C. 20360		12. REPORT DATE October 1976 13. NUMBER OF PAGES 264
14. MONITORING AGENCY NAME & ADDRESS(if different from Controlling Office)		15. SECURITY CLASS. (of this report) Unclassified 15a. DECLASSIFICATION/DOWNGRADING SCHEDULE

16. DISTRIBUTION STATEMENT (of this Report)

Approved for public release; distribution unlimited.

17. DISTRIBUTION STATEMENT (of the abstract entered in Block 20, if different from Report)

18. SUPPLEMENTARY NOTES

19. KEY WORDS (Continue on reverse side if necessary and identify by block number)

Shipboard Radio Frequency Interference
Satellite Communications
UHF Satellite Communications

20. ABSTRACT (Continue on reverse side if necessary and identify by block number)

A simulator for shipboard radio frequency interference, intended to be used in the characterization of UHF satellite communications terminals such as the AN/WSC-3 and AN/SSR-1, has been developed. Analytical results for the performance of various types of communications systems in white gaussian noise is available in the open literature. Performance in other types of channels, such as between a satellite and ship, is not known yet due to

DD FORM 1 JAN 73 1473 EDITION OF 1 NOV 65 IS OBSOLETE
S/N 0102-014-6601

UNCLASSIFIED

SECURITY CLASSIFICATION OF THIS PAGE (When Data Entered)

(20. ABSTRACT Continued)

unavailability of analytical models for the additive type of interference found in the ship's environment. A physical-statistical model for shipboard interference, based on Middleton's model for urban noise, is given. The model developed incorporates the relevent physical aspects of the various possible interferers and postulates a statistical framework in which these signals are inserted. A simulator based on the developed model was built to serve as a tool for study of the effects of the various interferers upon shipboard satellite communications systems. The simulator is capable of generating 10 types of complex emitters and of providing linear and nonlinear processing of them. It is also capable of generating a PSK modulated test signal for performance measurements of UHF terminalls. Results of performance measurements are presented. These results demonstrate the ability of the simulator to reproduce the shipboard electromagnetic environment.

TABLE OF CONTENTS

LIST OF TABLES

LIST OF FIGURES

GLOSSARY OF TERMS AND ABBREVIATIONS

AM	Amplitude modulation
AMP	Amplifier
AND	Logical AND gate
APD	Amplitude probability distribution. $P(y > y_o)$
BPS	Bits per second
BSM	Basic statistical model
BW	3 dB bandwidth
CP	Clock pulse
CW	Continuous wave
DBM	Double balanced mixer
DC	Directional coupler
DPDT	Double-pole double-throw
DPSK	Differential phase-shift keying
DS	Lamp
E[·]	Statistical average
ESM	Equivalent statistical model
EX.OR	Logical EXCLUSIVE-OR gate
FL	Filter
FLTSATCOM	Fleet Satellite Communications System
FM	Frequency modulation
FS	Fuse
FSK	Frequency shift keying
HF	High frequency
h(t)	Impulse response of a linear network

I	Logical inverter
IF	Intermediate frequency
INTERMODS	Intermodulation products
J	Female connector
K	Relay
LED	Light emitting diode
LO	Local oscillator
LOS	Line of sight
M	Meter
MIM	Metal-insulator-metal
MR	Master reset
MS	Master set
NAND	Logical NAND gate
OR	Logical OR gate
P	Male connector
p(·)	Probability density function
PD	Power divider
PN	Pseudo noise
PRBS	Pseudo random binary sequence
PRF	Pulse repetition frequency
PSK	Phase shift keying
PTT	Push-to-talk
PTTS	Push-to-talk statistics
PW	Pulse width
R	Resistor, attenuator or termination
RF	Radio frequency

RFI	Radio frequency interference
RMS	Root mean squared
$R(\tau)$	Autocovariance function. $E[y(t) \cdot y(t-\tau)]$
S	Switch
SATCOM	Satellite communications
SPDT	Single-pole double-throw
UHF	Ultra high frequency
VHF	Very high frequency
XTAL	Crystal

GLOSSARY OF SYMBOLS

Amplifier ----------

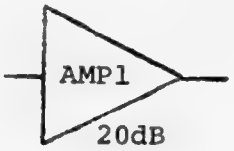

And gate ----------

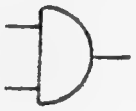

Double balanced mixer ----------

Directional Coupler ----------

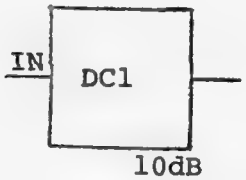

Light emitting diode ----------

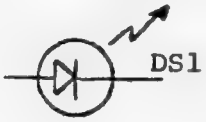

Lamp. (incandescent, neon) ----------

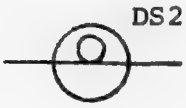

Flip-flop ----------

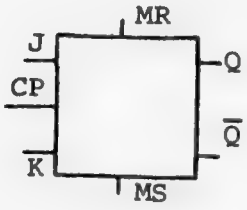

Filter ----------

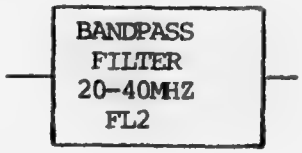

Fuse ----------

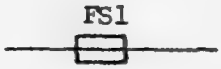

Inverter ----------

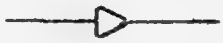

Female connector ----------

Relay ----------

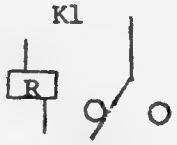

Meter ----------

Nand gate ----------

Or gate ----------

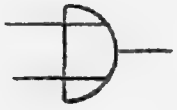

Male connector ---------- 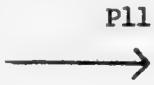

Power divider ---------- 

Rotary attenuator ---------- 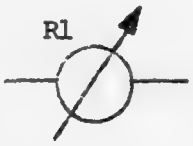

Fixed attenuator (pad) ---------- 

Resistive termination ---------- 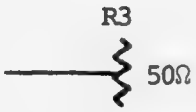

Potentiometer ---------- 

Switch (RF-SPDT) ---------- 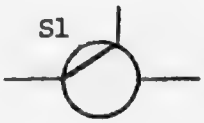

Switch (RF-TRANSFER) ---------- 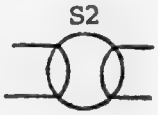

Switch (TOGGLE) ----------

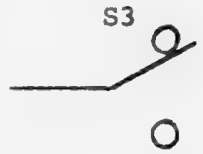

Switch (ROTARY) ----------

I. INTRODUCTION

With the forthcoming introduction of a satellite UHF tactical communications system for the U.S. Naval Fleet (FLTSATCOM), it has become apparent that a better under standing of shipboard RFI and its effect on this system is necessary. This is so, because of the high receiver sensitivities involved. The objective of this work is to characterize the UHF shipboard RFI problem and devise the means necessary to determine the performance of the SATCOM system in this environment. Very early in the investigation it became obvious that this could only be achieved, with the time and economic constraints available, by direct simulation of the shipboard electromagnetic environment in the laboratory.

The first step was then to study previous efforts of modeling on electromagnetic interference with a view to the final objective of simulation. This was done in Chapter II. The shipboard UHF interference model established in Chapter III was a natural derivation of results in Chapter II and knowledge of measurements data on various Navy ships. It is a model that is suitable for simulation and, we hope, could become a first step taken in the direction of more analytical results.

Chapter IV describes the simulator built in the Communications Laboratory of the Naval Postgraduate School

using the model established in Chapter III. It presents a description at the block diagram level of the system implemented and also gives a detailed description of controls and ports available on the front panel of the various units.

In Chapter V the results of measurements of various parameters on the simulator and pictures and graphs of the various emitters implemented are shown.

Appendices 1 to 8 give detailed descriptions of the various units built and present schematic diagrams for them. These appendices are of interest primarily for system maintenance.

Appendix 9 gives detailed description of the STATISTICS GENERATOR board and explains how the different statistics were obtained.

Appendix 10 presents operating instructions; Appendix 11 gives an interconnection table for all connectors on the back panels of the various units and Appendix 12 contains a list of parts used in the implementation of the system.

II. INTERFERENCE BACKGROUND

In order to be able to simulate the complex electromagnetic environment aboard ships, a model of this interference process will be of great help. As a first step in model building, identification of the main sources and mechanisms of interference will be necessary, together with whatever characterization of them has already been made. With that purpose in mind, a review of the various models of RFI found in the open literature, as well as identification of the main sources of electromagnetic interference in the shipboard environment, was done and presented in this chapter.

A. IMPULSIVE INTERFERENCE

Communications systems employing digital signaling are particularly vulnerable to impulsive interference. A shipboard environment, with its multitude of electrical machinery and complex electronic systems, many of them deliberately of impulsive nature such as radars, is plagued by this kind of interference. In addition to these man-made sources, ships are subjected to noise from precipitation static. This noise arises as a result of charged particles striking a receiving antenna or ship isolated structure. A ship traveling through a precipitation area picks up such a charge which when lost produces a corona or small spark discharge. These disturbances also have an

impulsive nature. Another important cause of impulsive interference, now the subject of closer investigation, is the noise that is observed in synchronism with radar pulses and has been attributed to some tunneling effect due to currents or voltages induced in the ship's superstructure nonlinearities when illuminated by the radar.

If the only cause of problems to the UHF shipboard communications systems were the impulsive interference, it would be possible to establish a mathematical model for this kind of interference and actually calculate the performance of these systems in this environment or even design optimum receivers. When we want to consider the whole problem, this approach, although not impossible, will certainly delay some necessary results, such as performance evaluation, that can be inferred more readily from simulation.

In order to establish a model for the interference process we relied heavily on the measured data [Ref. 1] but we also tried to benefit from the various models that have been proposed for impulsive interference. This approach, we hope, has allowed us to get our immediate results and, at the same time, pave the way for more analytical considerations.

Although nothing was found in the open literature about modeling of man-made interference generated in the particular environment of a ship, several kinds of atmospheric and man-made noise have been proposed and can be generally classified for our purposes in the following categories:

i. Empirical models – fitting of experimental amplitude probability distribution by a recognizable function.

ii. Analytical models – models designed to represent the entire random interference process itself, which, in turn, could be subdivided into filtered impulse models, Markov processes models and higher-order statistics models (product of a slowly varying regime process and a narrowband random process). In this last class, the model developed by Middleton [Ref. 2] has combined precise description of interference sources with mathematical tractability and may very well, in the future, offer a good tool to analyze the effects of both impulsive interference and interference caused by topside nonlinearities because it is the only model to date able to treat narrowband interference.

1. Summary of Empirical Models

Empirical models are usually restricted to the fitting of experimental data on the amplitude probability distribution (APD) of the envelope of the process after filtering. For a Gaussian bandlimited process, it is well known that the noise envelope (y) has the Rayleigh distribution

$$P(y > y_0) = a^{-ay_0^2} \tag{2.1}$$

where a is chosen to fit the data.

This model is not able to represent impulsive interference because a Gaussian process with the same average power as an impulsive one will not exhibit the large tails on the probability distribution of the latter. In order to account for the large impulsive tails found in atmospheric and man-made noise, many authors have proposed a variety of models with variable degrees of success. Summaries of these models have already been made in the works of Hall [Ref. 3], Ibukun [Ref. 4], Giordano [Ref. 5] and Spaulding [Ref. 6] and the most prominent ones will be considered here again.

In 1954 Hesperper, Kessler, Sullivan and Wells proposed the log normal distribution for atmospheric noise (see Spaulding, Ref. 6).

$$p(y) = \frac{1}{\sigma\sqrt{2\pi}} e^{-\left(\frac{\log y - \log \mu}{\sigma}\right)^2} \qquad (2.2)$$

where $\mu = E[y]$ and $\sigma = E[(y-\mu)^2]$.

This model gave good fit to the tails of measured distributions but did not agree very well with the Gaussian character of the interference at the lower amplitude levels.

In 1956 various models were proposed with variable success. Likhter unsuccessfully used a combination of two Rayleigh distributions for atmospheric noise (see Spaulding, Ref. 6).

$$P(y > y_0) = (1 - c)e^{-ay_0^2} + ce^{-by_0^2} \qquad (2.3)$$

where a, b, c are parameters chosen to fit the data.

Reference 7 mentions that Watt proposed the following distribution:

$$P(y > y_0) = e^{-x^2} \qquad (2.4)$$

where

$$x = a_1 y_0 + a_2 y_0^{(b+1)/2} + a_3 y_0^b$$

$$b = 0.6[20 \log(y_{rms}/y_{avg})]$$

where $y_{avg} = E[y]$, $y_{rms} = E[(y - y_{avg})^2]$ and b, a_1, a_2, a_3 are parameters to fit the data. Iuhara et. al. are also credited by [Ref. 7] with, after improvements on the measurement methods, having proposed a combination of Rayleigh and log normal distributions,

$$P(y > y_0) = (1 - c)(\text{Rayleigh}) + c(\text{log normal}) \qquad (2.5)$$

where c is a constant.

Also in 1956 Horner and Harwood were mentioned by [Ref. 8] as having proposed the expression

$$P(y > y_0) = \frac{\gamma^2}{y_0^q + \gamma^2} \tag{2.6}$$

where γ and q are parameters depending on the data, and the Department of Scientific and Industrial Research of Great Britain (DSIR) proposed the following distribution [Ref. 4]

$$P(y > y_0) = \left[1 + \left(\frac{\alpha y_0}{\bar{y}}\right)^r\right]^{-1} \tag{2.7}$$

where $\bar{y}$ is average envelope voltage, α is a function of geographical location and r a parameter to fit the data.

In 1960, Crichlow et. al. proposed to represent the APD of atmospheric noise by three functions: Rayleigh distribution at the lower amplitudes to account for the Gaussian nature of atmospheric noise at low levels and two other expressions for the medium and higher levels to represent the impulsive character of the noise. These distributions gave a good fit to data over a wide range and are being used by the CCIR as the "standard" representation of atmospheric radio noise (see Ref. 6).

Galejs (1966) proposed a weighted summation of exponentials with reasonable agreement with atmospheric noise data (see Ref. 6).

$$P(y > y_0) = (1-\delta)e^{-\alpha_1 y_0} + \delta e^{-\alpha_2 y_0} \qquad (2.8)$$

where α, δ_1, and δ_2 were chosen to fit data.

Finally, in 1970 Nakai and Nagatani [Ref. 9] represented the amplitude distribution of atmospheric noise with a log normal distribution for each of two ranges of amplitude

$$p(y) = \frac{1}{\sigma_1\sqrt{2\pi}} e^{-\left(\frac{\log y - \log \mu_1}{\sigma_1}\right)^2} \qquad B < y < \infty$$

$$P(y) = \frac{1}{\sigma_2\sqrt{2\pi}} e^{-\left(\frac{\log y - \log \mu_2}{\sigma_2}\right)^2} \qquad 0 < y < B \qquad (2.9)$$

where σ_1, σ_2, μ_1, μ_2 and B were chosen to fit data.

2. Summary of Analytical Models

In the previous section we gave a succinct summary of the models that have been used mostly for atmospheric noise. They were all empirical models that sought primarily to obtain an expression that would fit the envelope of the filtered noise process in the broadest range of the parameters involved (bandwidth, amplitude, epoch, etc.). The main disadvantage of these models for our purpose is the total lack of physical insight that can be inferred from them. Consequently little or no help at all will be available when we try to simulate the interference process.

On the other hand, many authors have presented analytical models for the interference process with variable degrees of complexity and of physical justification. It should be mentioned that this last characteristic of the model is of paramount importance for simulation purposes. The first class of models is the one representing the noise process by a sum of randomly occurring impulses with random amplitude. Representatives of this class are the models developed by Furutsu and Ishida [Ref. 7], Beckman [Ref. 6], Giordano [Ref. 5]. These models have, of course, incorporated the physics of the noise sources and are very suitable for simulation of the particular noise processes that were considered. On the other hand, they are very limited in scope because they were directed primarily at atmospheric noise or, more generally, broadband type of impulsive interference. In Reference 7, Furutsu and Ishida, following results of Schonland (1953) and Watt and Maxwell (1957), showed that the atmospheric discharges comprise a slowly developing leader stroke of about one msec duration followed by a return stroke of about 100 μsec duration. By also observing that the leader stroke (predischarge) is made up of a series of discrete leaders occurring according to a Poisson law with a rate of about one every 25 to 100 μsec, they modeled the noise due to the predischarge as a Poisson noise of 1 msec duration and consisting of the basic impulses of about 1 μsec duration. Since the whole process repeats itself with a Poisson distribution at some rate the atmospheric

noise may be called Poisson-Poisson noise. The model developed by Furutsu and Ishida thus represents the noise by a summation of signals as follows:

$$n(t) = \sum_{i=1}^{N} a_i \, h(t - t_i)$$

where the a_i are independent, identically distributed random variables with distributions postulated to fit experimental data; h(t) gives the response of the receiver IF filter to the individual atmospheric impulses and t_i are the times of occurrence of the N individual lightening strokes (N being random).

The response of the receiver for an elementary pulse was assumed to be

$$r = r(t,a) \cos(\omega t + \Psi) \qquad (2.11)$$

where t is the time length from the time of pulse occurrence to the time of observation, r(t,a), the envelope, is a time function changing very slowly in the period $2\pi/\omega$ (narrow band case) and a denotes the parameter specifying the amplitude statistics.

Atmospheric noise modeled in this way has shown good agreement with data. As noted by Hall [Ref. 3] this is due to the fact that the Furutsu model is strongly physically motivated and atmospheric noise behaves closely to the Poisson-Poisson model with clusters of noise pulses, where

the pulses within each cluster occur in a Poisson fashion with mean rate r' (10^4 to 4×10^4 pulses per second) while the clusters themselves occur also in a Poisson fashion with mean rate $r < r'$).

Furutsu and Ishida have also considered the important physical aspect of spatial distribution of the noise sources. In 1962 Beckmann [Ref. 6] employed a similar model suggesting that propagation conditions be considered.

Ottesen [Ref. 6] and Giordano [Ref. 5] also used a filtered impulse model to represent atmospheric noise. Giordano, following the work of Beckmann, took into consideration various spatial distributions of sources as well as propagation conditions.

Markov process modeling has also been applied to impulsive noise. In these models there are at least two recognizable states — B (Burst) and N (No burst) with transition probabilities q_B and q_N respectively which correspond to burst start and burst stop probabilities. Each transition that brings the system to state B has an associated probability q_I of producing an impulse.

Gilbert (1960), Berger and Mandelbrot (1963) and Shaver et. al. (1972) [Ref. 6], are examples of researchers who have employed this approach. The latter group used a particularly interesting model. They represent the interference as

$$z(t) = n_0(t) + \gamma_0(t) \qquad (2.12)$$

where $n_0(t)$ represents Gaussian background noise and $\gamma_0(t)$ represents man-made noise. $\gamma_0(t)$ is a process described by a two-state Markov chain,

$$q_0 = 0 \qquad \text{with probability } p(a)$$
$$q_0 = n_1(t) \quad \text{with probability } p(b) \tag{2.13}$$

where $n_1(t)$ is a complex Gaussian process with a RMS value that can be large compared with $n_0(t)$, and p(b) very small. The appeal of this model is that it leads quite naturally to simulation.

A third class of analytical models is the one inaugurated by Hall [Ref. 3]. Although it is an analytical model in its application, it also has a totally empirical formulation in the sense that Hall perceived that the variation in time of the dynamic range of atmospheric noise could be explained by the notion of a "regime" process controlling a Gaussian process, and then postulated that the narrowband received atmospheric noise y(t) could be considered to have the form

$$y(t) = a(t)\ n(t) \tag{2.14}$$

where n(t) is a zero-mean narrowband gaussian process with covariance function $R_n(\tau)$ and a(t), the "regime" process, is a stationary random process, independent of n(t) whose

statistics were to be chosen to match measured data. As will be shown later in Chapter III, the Hall model applies quite nicely to one component of the total interference generated by our simulator. Omura [Ref. 6] has also presented a model that fits in the class of the Hall model but that gave agreement with measurements only at the higher envelope levels. The great advantage of this class of models is the mathematical tractability although the price paid is the lack of physical support.

Middleton [Ref. 2] perceived the fragility of the lack of physical grounds of the Hall model and developed a model that he called the Statistical-Physical Model, to overcome these problems. He then applied it to characterize man-made urban radio noise. Because Middleton's approach will be used as a reference for our simulation model building, it will be described in detail. In what follows, we will be more interested in the model formulation than in the analytical results.

Middleton's formulation follows along the following lines, as described by that author (see Ref. 2):

i. Construction of a primarily physical model of the propagation fields arising from the spatially and temporally distributed noise sources.

ii. Development of the so-called "basic statistical model" (BSM) which provides the framework for incorporating quantitatively the principal physical mechanisms and features as will be described later. This model consists of

the sum of two independent noise fields. A high-density Poisson field with asymptotically gaussian statistical properties, representing the general interference background and a low-density Poisson field which represents the few high-level and distinct sources of RFI. From the physical description of this composite ambient field the detailed structure of the mean intensity and covariance functions can be derived, which constitute the "statistical parameters" of the BSM.

iii. The use of a modified version of Hall's atmospheric noise model which he called the "equivalent statistical model" (ESM). This was used initially to avoid the complex determination of probability distributions directly from the BSM. The important features incorporated in this formulation and that makes it very suitable for simulation are the following:

a) Geometrical distribution of the various interfering sources,

b) Physical character of the noise fields generated by these sources and their conversion into waveforms upon reception by the receiver.

c) A statistical model which is phenomenologically broad enough to account for the principal observed interference effects and which has sufficient physical structure to enable one to identify the pertinent individual interference mechanisms.

d) Various special features such as directionality effects; mixed classes of interference, i.e., a variety of different interference mechanisms; effects of operational patterns of the various interference sources, and multipath effects.

Summarizing Middleton's model we can say that it is in reality a hybrid model that "borrows" the desirable features of various models previously developed. It starts by giving a precise description of the noise sources, propagation conditions, receiving antenna directivity and receiver filtering. This roughly follows the ideas developed in the models of Furutsu, Giordano and others. The statistical mechanisms are introduced by postulating that the sources have a Poisson distribution in space and also that each source represents a transient and impulsive event in time with starting time as a random parameter. Again, this follows the basic idea of the filtered impulse response models although in a more generalized form. In the last part of the model development, Middleton uses the Hall model with the exception that the statistical parameters are calculated from his physical model instead of being empirically chosen as was done by Hall.

Concluding this review of RFI modeling, we can say that the empirical models will be of little help for the simulation of the interference process. The analytical models, on the other hand, offer a variety of tools to attack the problem. The Middleton model is very flexible

and will allow incorporation of practically any kind of interference source to the model. Other models, like Hall's or Shaver et. al.'s, will also be useful, expecially when trying to model impulsive types of interference where the individual impulses are not well characterized. In Chapter III these models will be referred to again during the actual model building of the interference process.

B. TOPSIDE NONLINEARITIES

Shipboard communication systems, in addition to having to operate in an environment that is inherently noisier due to the concentration of electrical and electronic gear in a small volume, having another unsuspected source of impairment to their operation in that environment. Nonlinearities found in the ship's superstructure have been determined to cause the generation of high order intermodulation products causing interference systems operating at bands far away from the original sources.

It is well known that a nonlinear device will cause intermodulation which is the sum and difference products of two or more signals of different frequencies. For example, if we feed two signals at frequencies f_1 and f_2 to a nonlinear system without memory, the intermodulation products can be calculated by applying the operator

$$g[x] = a_0 + a_1 x + a_2 x^2 + a_3 x^3 + \ldots \qquad (2.15)$$

to the signal expression

$$x(t) = E_1 \sin 2\pi f_1 t + E_2 \sin 2\pi f_2 t \qquad (2.16)$$

The results of such computations will yield the various intermodulation products of the form

$$y_{|m|+|p|}(t) = k \sin 2\pi(mf_1 \pm pf_2) \qquad (2.17)$$

where $|m| + |p|$ is the "order" of the product and k is a constant. $N = |m|+|p|$.

Figure 1 taken from Reference 10 shows the number of generated products as a function of the number of input signals of different frequency. The family of curves drawn has as its third parameter the order of the products generated. From this figure, it can be seen that the number of products rises very rapidly both with the order of the product and the number of signals fed to the nonlinearity.

The Naval Electronics Laboratory Center (NELC) in San Diego, California, has conducted extensive studies on topside nonlinearities and developed an algorithm to determine the lowest order intermodulation product due to two discrete frequencies that will occur at a given frequency. They also have made progress on the techniques to localize and nullify sources of intermodulation (nonlinearities) on the ship's superstructure. Representative of this

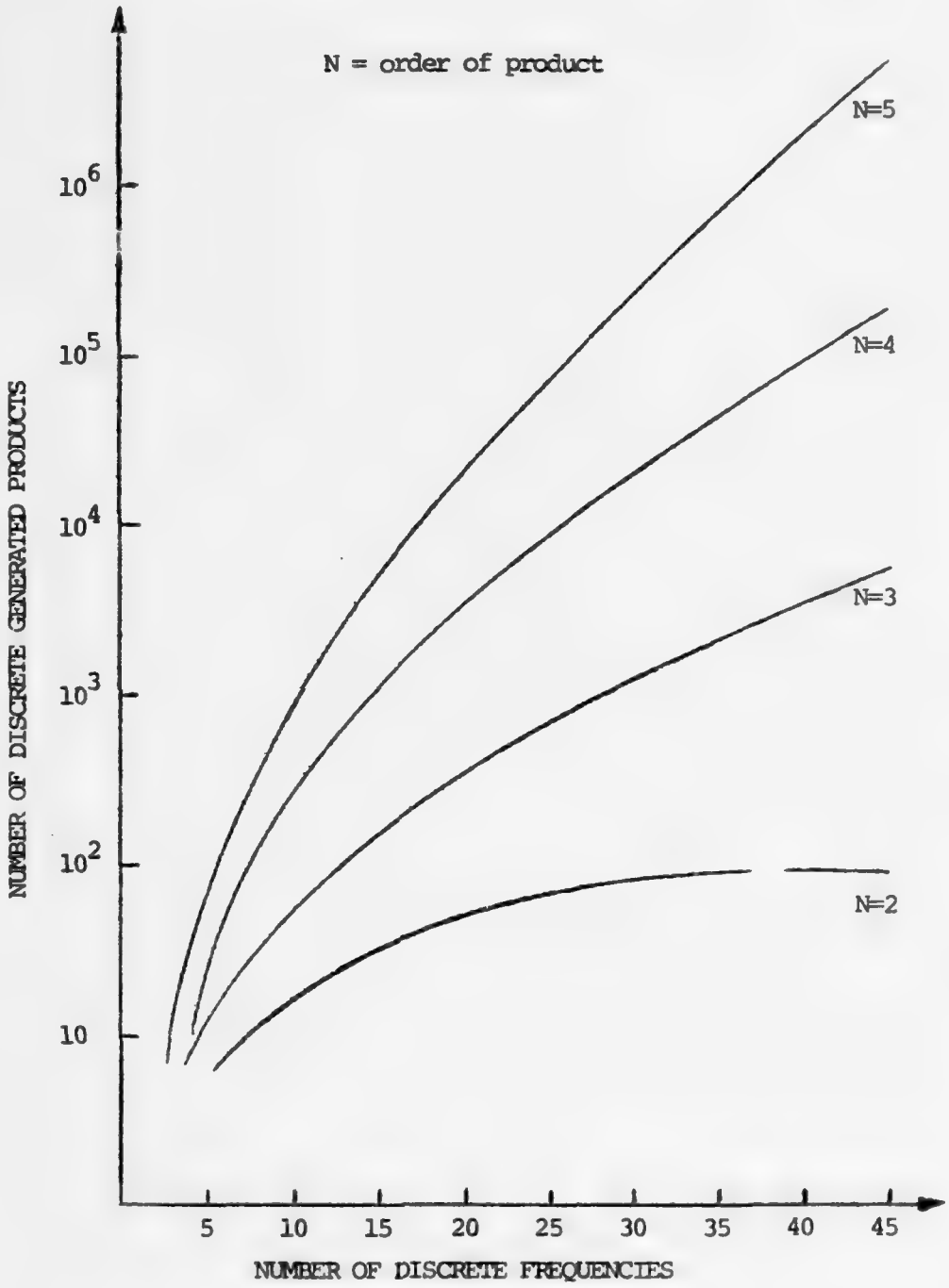

Figure 1: Intermodulation generation from discrete frequencies.

effort are the technical documents and technical reports listed as References 11 through 15. Another source of information about the characterization of topside nonlinearities can be found in the work of Higa [Ref. 16] which analyzed and gave an explanation to the tunneling effect through MIM (metal-insulator-metal, Al-Al_2O_3-Al) junctions existing on 26 m and 64 m diameter paraboloidal antennas operated by the Jet Propulsion Laboratory, Pasadena, California. As pointed out by Higa, there are various indications that the nonlinearities will be of the type depicted in Figure 2 with the additional fact that the i-v characteristics shown are neither uniform nor stable. The facts leading to this conclusion are the following:

i) The nonlinearities exhibit a power threshold effect,

ii) The spectrum of the spurious signals generated are relatively narrowband, and

iii) Generation of random noise bursts occurs with single or multiple frequency excitation of the nonlinearities.

The randomly varying conductivities of the junctions produce random amplitude modulation of incident signals that explain the noise bursts observed in the case of single or multiple carriers. Although the study of shipboard topside nonlinearities is still in a very crude state, the following general assertions can be made about the shipboard intermodulation problem:

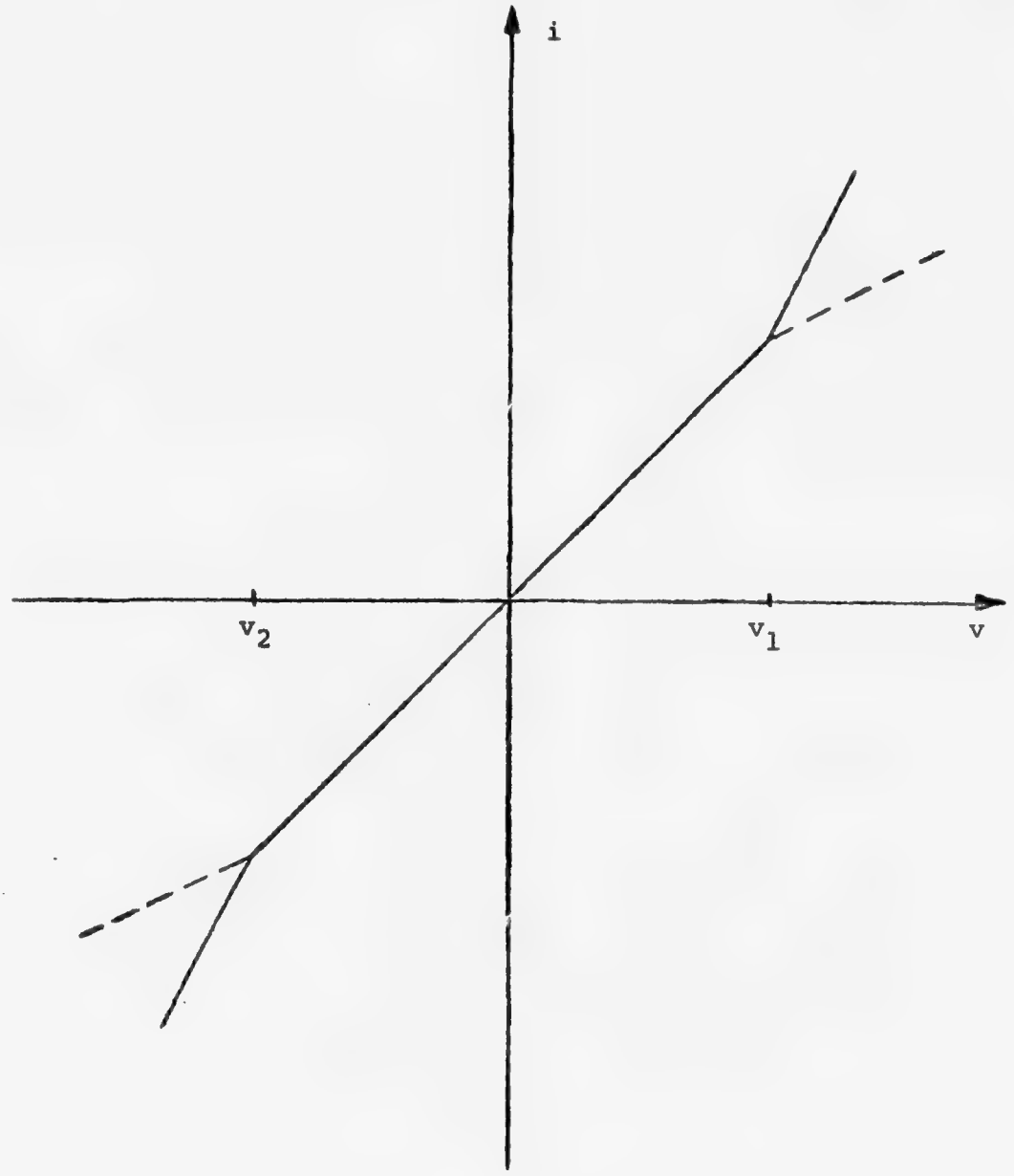

Figure 2: Two Kinds of Nonlinearities Generated by MIM (Metal-Insulator-Metal) Junctions.

i. Spurious signals are generated when strong radiated energy impinges on nonlinearities on the ship's topside.

ii. The number of possible intermodulation products increases greatly as the number of transmitted signals is increased, increasing the probability of interference correspondingly.

iii. The level of the intermodulation product generated is a function of the order of that product, being stronger for the lower order products.

iv. The greater the system sensitivity, the more damage to it because higher order products will become relevant.

v. Most environment-generated intermodulations have many random, extremely intermittent sources located somewhere topside.

vi. It is possible that, due to the nature of the nonlinearities, noise is generated on them by the simpler excitation of a carrier frequency, which indicates that the nonlinearities are very unstable.

The above comments, based on observed evidence [References 1 and 11 to 15], indicates that three effects of the nonlinearities will be dominant on the interference generation:

i. UHF Intermodulation products generated by two or more UHF/LOS, UHF/PSK or UHF/RADAR interferers,

ii. HF harmonics and

iii. Intermodulation products from HF (or VHF) systems and UHF ones.

C. DIRECT INTERFERERS

In addition to the kind of problems mentioned in items A and B above, of much more concern to the FLTSATCOM system operation will be the degradation caused by the direct interference from other systems sharing the same frequency band. In this category, UHF search radars and UHF line-of-sight (LOS) communications transmitters will be the ones to be considered as pointed out in Reference 1.

The UHF/RADAR interferer, due to its high peak power, wide bandwidth and closeness in the frequency spectrum, reaches the receiver with such a large power that blanking is practically necessary. The effect of this radar interference will thus be a major one. The UHF/LOS communications systems will also affect the FLTSATCOM receiver operation due to desensitization caused by its high level and closeness in frequency as pointed out by Reference 17. Another related problem is the one caused by the switching type operation of LOS systems in which the operator turns the transmitter ON and OFF in a random fashion. The other type of direct interferers are the UHF/PSK systems employed for satellite and also LOS operation and that will cause direct interference in the same fashion as the UHF/LOS voice modulated system mentioned above.

Because these types of interferers are such important pieces of the overall interference process, special attention will be given to their modeling in the next chapter.

III. SHIPBOARD UHF INTERFERENCE MODELING

One of the main tasks of this study was to establish a model for the interference process that exists aboard a ship platform and that will have a relevant effect on the performance of the FLTSATCOM communications system. In Chapter II we have reviewed some previous efforts in modeling of noise processes and we concluded that the physical-statistical model developed by Middleton [Ref. 2] was the most promising one in offering a tool to attack our problem. Indeed, a similar approach was taken in order to characterize the interference observed in the 240-400 MHz portion of the UHF band, in such a way that the model derived is very adequate for simulation of the interference process.

There is no doubt that the surest way to test a system against a hostile environment would be to exhaustively measure the performance of the system while operating in that environment. Since this approach is usually ruled out by cost considerations, the best option remaining is to try to reproduce the hostile environment in the laboratory, as closely to reality as possible. To dothis, first of all it is necessary to correctly characterize the problem and then, if possible make simplifying assumptions to reduce its complexity while maintaining all relevant factors present. With the risk of being too simplistic, we can

say that the problem of shipboard interference at UHF is characterized mainly by two factors – the existence of a variety of sources of signals[1] (emitters) operating concomitantly with the SATCOM system and the random and nonlinear processing performed on these signals by the complex ship's superstructure. This nonlinear processing aggravates the already difficult problems of frequency allocation and has been observed to cause severe impairment even to less sensitive systems at HF. Based on the above characterizations, our modeling approach was to try to reproduce all the relevant physical parts of the interference problem (emitters and processing) and insert these physical entities in a statistical framework in a similar fashion to the model developed by Middleton, except that we were directed toward simulation instead of analytical results.

Extensive measurements made by the RFI group at NPGS [Ref. 1] have shown that practically any electronic system that irradiates aboard a ship may be a cause of interference. Based on this experimental knowledge we decided to simulate 10 kinds of emitters and submit them to linear and nonlinear processing before combining them with the SATCOM signal input. Figure 3 shows the block diagram of the physical realization of this model.

---

[1]By "signals" we mean both signals containing intelligent information and noise-like interference.

Figure 3: Shipboard UHF Interference Model.

The emitters considered to be the most relevant and that have been implemented are listed in Table 1. Each emitter that was implemented has retained its main physical characteristic and, in addition to that, the most important ones (the ones at UHF) have incorporated some statistical parameters as well.

A. EMITTERS 1 AND 2 – UHF/PSK

The existence of data links at UHF with satellite relaying or line of sight (LOS) operation made necessary the inclusion of a signal of this type as one of the interference sources. The expression for a PSK modulated signal is given by:

$$y_{PSK}(t) = A \sin\left(2\pi ft + \psi + \frac{\pi}{2} a(t)\right) \qquad (3.1)$$

where Ψ is a uniformly distributed random variable and $a(t)$ a binary random process which can assume two states and represents the data.

$$a(t) = 1 \quad \text{with probability } 1/2$$

$$a(t) = -1 \quad \text{with probability } 1/2$$

That, of course, corresponds to the ideal case of a maximum entropy source of information (random data) but is considered to approach very closely real situations.

EMITTER DESIGNATION	TYPE OF MODULATION	MODULATING SIGNAL	FREQUENCY BAND(MHz)	STATISTICAL PARAMETERS
E1	PSK	Pseudo-Random Data	200 - 400	Modulating Signal
E2	PSK	Pseudo-Random Data	200 - 400	Modulating Signal
E3	AM	Voice Process	225 - 400	Modulating Signal and Push-To-Talk Statistics
E4	AM	Voice Process	225 - 400	Modulating Signal and Push-To-Talk Statistics
E5	Pulse	Variable PRF and PW	200 - 224 420 - 470	Pulsed Noise
E6	CW	——	40 - 75 108 - 200	——
E7	CW	——	10 - 16 16 - 26	——
E8	CW	——	0 - 10	——
E9	Impulsive Noise	Pseudo-Random Poisson Process	0 - 500	Random Time of Occurrence and Pulse Format
E10	Gaussian Noise	——	0 - 500	Signal Format

TABLE 1. Characteristics of Emitters

In addition to that, this signal can be filtered to limit its bandwidth in which case we would get

$$y_{PSK}(t) = \int_{-\infty}^{\infty} h(t-\delta)A \sin(2\pi f\delta + \Psi + \frac{\pi}{2}a(\delta))\, d\delta \qquad (3.2)$$

where h(t) is the filter impulse response. We thus see that emitters 1 and 2 retain the exact physical characteristics of a real world interferer, including the statistical parameters given by the modulating signal.

B. EMITTERS 3 AND 4 — UHF/LOS

Following the pattern set by the UHF/PSK interferers, interference caused by UHF/LOS communications systems will present a clear signature of these signals and thus will have to be simulated by generating a signal which must have the same physical characteristics as the ones used aboard ships. The interference caused by this kind of emitter will be narrowband and this also leads us naturally to a model similar to the one used by Middleton, i.e., we must construct a replica of a "typical" signal generated by one of these systems and incorporate it into a set of statistical assumptions which will describe the main statistical features of these signals.

For UHF/LOS interferers the signals used will be AM signals and the statistical assumptions that the modulating signal will be voice and that the transmitter will be keyed according to a Push-To-Talk statistics (PTTS) as described below.

The interference process y(t), will then be described by:

$$y_{LOS}(t) = a(t)[1 + m(t)] \sin \omega_c t \qquad (3.3)$$

where m(t) is the voice modulating process, ω_c is the angular center frequency of the signal and a(t) is again a "regime" process that characterizes the PTT operation of the emitter.

The process a(t) is a two-state Markov process derived from two independent Poisson processes $P_1(t)$ and $P_0(t)$ with rates γ_1 and γ_0 in the following fashion. Process "1" (a start signal) sets a(t) to state 1 (a(t) = 1) iff a(t) = 0. Process "0" (a stop signal) sets a(t) to state 0 (a(t) = 0) iff a(t) = 1. Typical sample functions of $P_1(t)$, $P_0(t)$ and a(t) can be seen in Figure 4. This corresponds to the situation in which the operation of these emitters occurs in a random fashion and the duration of emissions also occurs in a random fashion.

C. EMITTER 5 — UHF/RADAR

Probably the most damaging kind of interferer to the SATCOM system will be the UHF search radars. Their importance is due not only to their high power and proximity in the frequency spectrum but also to the fact that low order INTERMODS falling in the SATCOM assigned band will be generated by the simultaneous operation of HF, VHF and

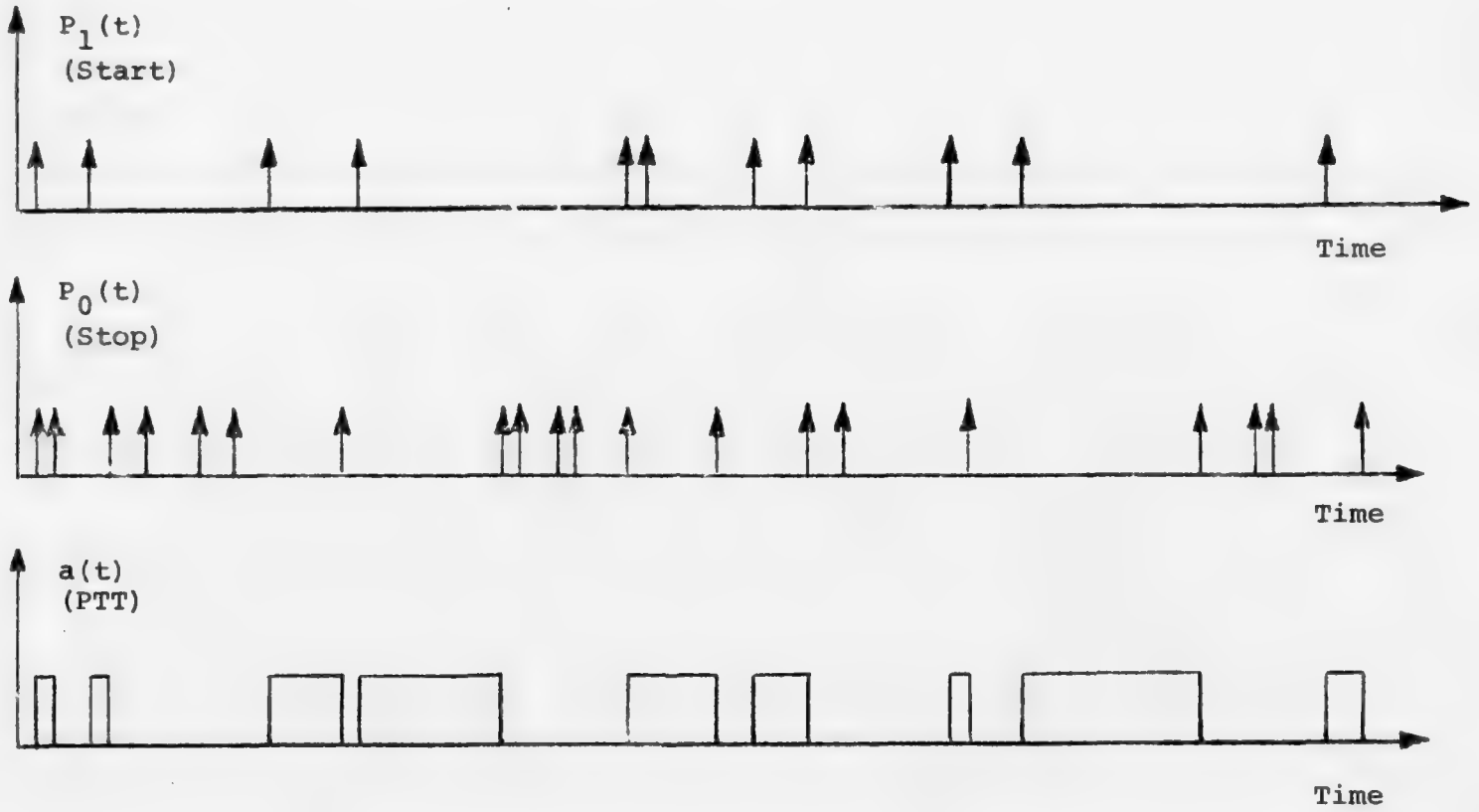

Figure 4: Typical PTT Signal Generation from two Poisson Processes.

UHF communications systems. For this reason, a correct representation of the interference effects of this particular kind of signal is very important for the ultimate goal of simulating the interference process.

The UHF radar interferer was designed with the following mechanisms of interference in mind:

a) Interference caused by the radar pulse spectrum falling in the receiver bandwidth;

b) Interference caused by INTERMODS generated by mixing of radar pulses and other interferers on the ship's topside nonlinearities or receiver front end;

c) Interference caused by radar transmitter wideband noise;

d) Effects of radar antenna scan on the interference process.

A usual first approximation to a pulsed radar envelope is to consider a periodic train of rectangular pulses as shown in Figure 5. The expression for the modulating signal is given by:

$$s(t) = \begin{cases} A & -T_p/2 \leq t \leq T_p/2 \\ 0 & -T/2 \leq t \leq T_p/2 \quad \text{and} \\ & T_p/2 \leq t \leq T/2 \end{cases} \qquad (3.4)$$

s(t) periodic with period T

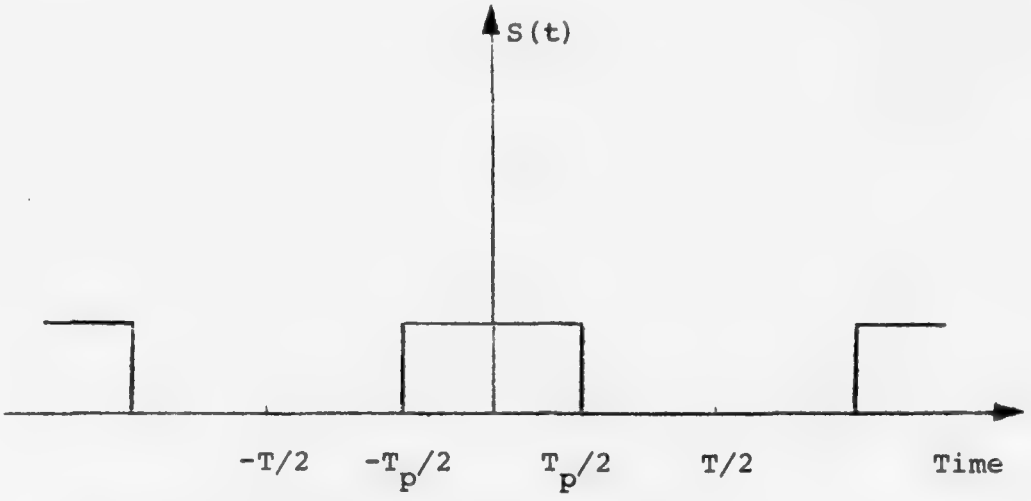

Figure 5: Radar Modulating Signal.

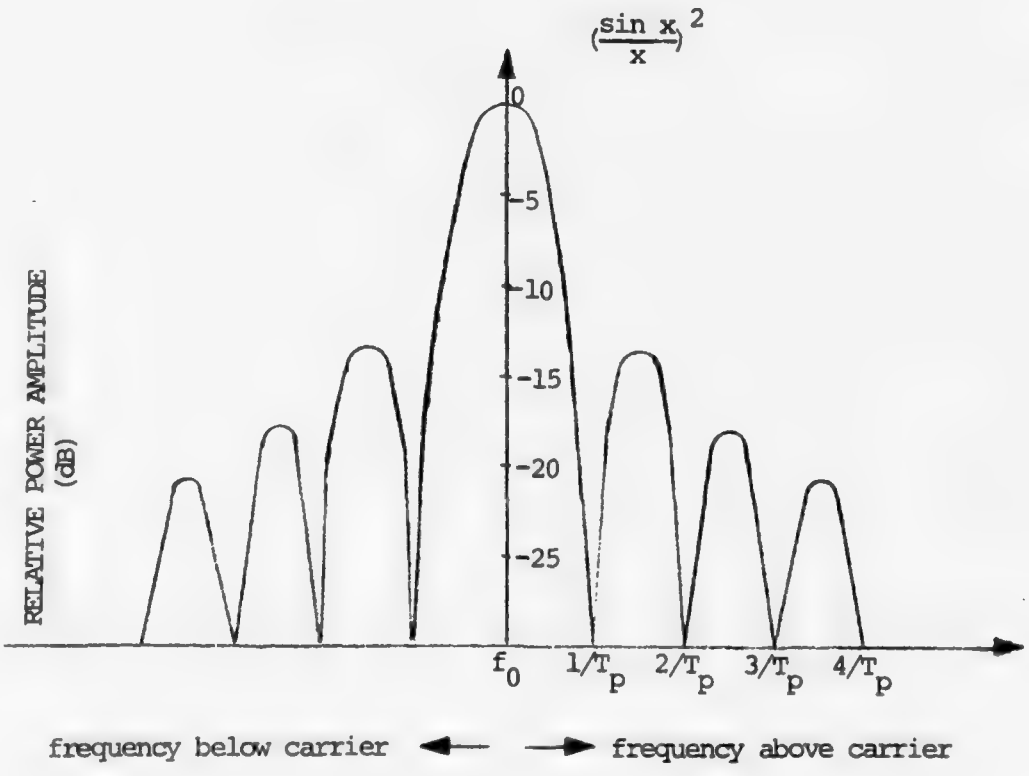

Figure 6: Spectrum Envelope of Pulsed RF Carrier.

The frequency representation of this signal can be obtained by utilizing the complex form of the Fourier series:

$$s(t) = \sum_{n=-\infty}^{n=+\infty} s_n e^{j\omega_n t} \tag{3.5}$$

where,

$$s_n = \frac{1}{T} \int_{-T/2}^{T/2} e^{-j\omega_n t}\, s(t)\, dt = \frac{AT_p}{T} S_a\left(\frac{\omega_n T_p}{2}\right) \tag{3.6}$$

$$\omega_n \equiv \frac{2\pi n}{T} = 2\pi f_r n \tag{3.7}$$

and

$$S_a(x) \equiv \frac{\sin x}{x} \tag{3.8}$$

The Fourier transform of s(t) will be:

$$S(f) = \frac{AT_p}{T} \sum_{n=-\infty}^{+\infty} S_a\left(\frac{\omega_n T_p}{2}\right)\, \delta(f - nf_r) \tag{3.9}$$

where $f_r \equiv \frac{1}{T}$ is the radar pulse repetition frequency.

The signal s(t) will modulate a carrier $c(t) = B \sin(2\pi f_0 t)$ whose Fourier transform is given by:

$$C(f) = \frac{B}{2}\delta(f - f_0) + \frac{B}{2}\delta(f + f_0) \tag{3.10}$$

The Fourier transform of the pulsed R.F. Signal $f(t) = s(t)c(t)$ can be obtained by the convolution of $S(f)$ with $C(f)$.

$$F(f) = S(f) \quad c(f) = \frac{ABT_p}{2T} \sum_{n=-\infty}^{\infty} S_a\left(\frac{\omega_n T_p}{2}\right) \delta(f - nf_r - f_0) + \\ + \frac{ABT_p}{2T} \sum_{n=-\infty}^{\infty} S_a\left(\frac{\omega_n T_p}{2}\right) \delta(f - nf_r + f_0) \tag{3.11}$$

The relative magnitude of the nth line of the power spectrum referred to the carrier power is

$$\frac{P_n}{P_0} = S_a^2 \left(\frac{\omega_n T_p}{2}\right) \tag{3.12}$$

From Eq. (3.12) we see that the envelope of the power spectrum follows a $\sin^2(x)/x^2$ function, shown in Figure 6. For a real system, however, there are many differences from the above idealized situation. In the first place, the modulating signal either presents finite rise and fall times or has a different format. These effects produce different power-spectra. To illustrate this, Figure 7, taken from Reference 18, shows the envelope of the power spectra of four different types of pulse waveforms. This gives a good idea of the envelope of a pulsed RF carrier having as modulating signal one of these waveforms. The point to make is that different radars, operating at the same frequency will deliver a different amount of power to a receiver close in

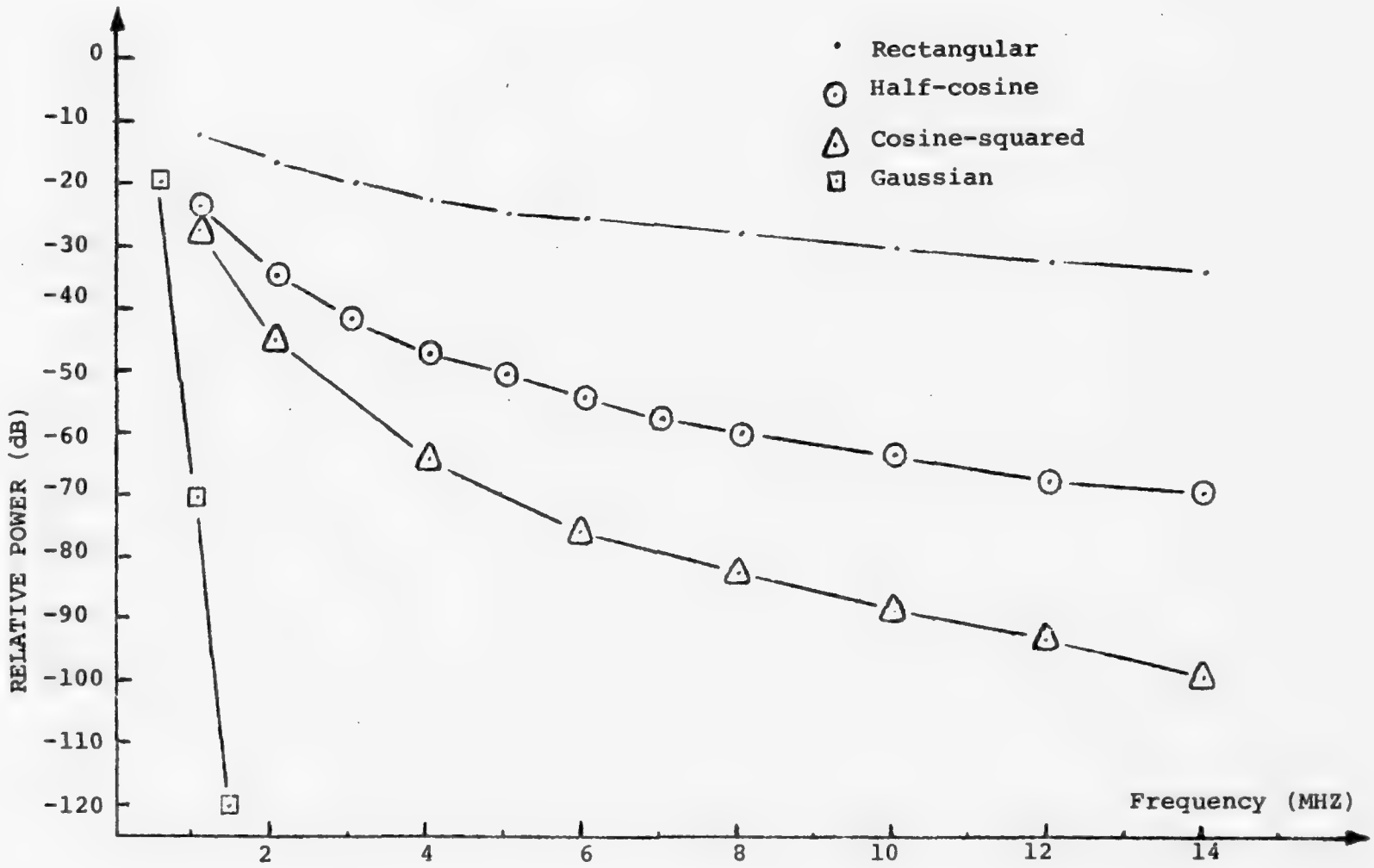

Figure 7: Envelopes of power spectra for different pulse shapes. (Pulse energy constant. 1 μsec pulses.)

frequency due to this difference in pulse waveforms alone. So, in order to faithfully simulate real life radars, the simulator must be able to deliver variable amounts of power at a specified band for a given peak carrier power. Another source of difficulty in trying to adequately characterize radar signals in general is given by the fact that in addition to variable pulse shape, FM of the carrier (CHIRP) is used in certain systems.

In order to be able to account for the main effects of direct radar interference, certain assumptions were made based on the following practical considerations:

a) Since the PRF of UHF radars is of the order of 200 to 400 PPS and the SATCOM receiver bandwidth is many times larger than 400 Hz, a large number of spectrum lines from the radar signal will fall in this bandwidth;[2]

b) Since the pulse widths span the range from 5 to 150 μs, the zeros of the power spectra envelope will probably be more than 20 KHz apart or will not exist at all because the FMing of the carrier will tend to eliminate the zeros (the signals with pulse widths in the upper part of the range above usually are CHIRP signals);

c) In many circumstances the radar level at the receiver will be so high that blanking is mandatory so that the

---

[2]An important exception occurs when the system is operating with a 75 BPS rate.

radar pulse waveform will be of secondary importance relative to the event, "a pulse is being transmitted by the radar."

The effect of the above considerations is that we can consider, in a first approximation, the pulsed interference as seen by the receiver to have a constant and continuous power spectrum density. An appropriate model will then be that of a pulsed Gaussian noise source that, while maintaining the impulsive characteristic of the radar signal, will allow for easy control of the amount of power delivered to the interfered receiver as a result of variation in pulse shape and modulation.

This model alone would account for the effects if direct interference from the radar but, as mentioned before, this is not the only interference mechanism that we would like to consider. In many circumstances radars operating at higher frequencies (such as L band) will also be of concern due to the effect of the ship's nonlinearities. Although the model above could represent this effect in a first approximation, we choose to include a true sinusoidal RF carrier with the signal so that the mixing effect can be best studied since this phenomena is still the subject of investigation.

Radar transmitter noise as well as any other system-generated broadband noise will be accounted for by a Gaussian noise source.

The last important factor considered in the simulation of the radar emitter is that of antenna radiation pattern and scan. Figure 8 shows a typical high gain antenna pattern. Since the antenna rotates at very low speed (less than 1 RPS) we can see that when the main beam illuminates a receiver antenna (or a nonlinearity) the interference signal will reach a maximum and thus we can expect to find from the receiver standpoint that the radar pulses occur in clusters. This is clearly a very important characteristic of radar caused interference and was taken into account in the simulator by providing an antenna scan modulation of the pulsed radar signals. Since the implementation of the antenna scan modulator uses a computer to generate the antenna pattern, and since this can be done with a resolution of 1°, no simplifying assumptions need to be made about the antenna patterns because we can reproduce any antenna pattern with 1° resolution by simple change of memory contents in the computer.

The preceding comments about the radar interferer can be summarized by the following radar hypothesis.

Radar Hypothesis I: The radar signal, as seen by the SATCOM receiver, will have approximately continuous power density spectrum.

Radar Hypothesis II: The effect of instability in nonlinearities will be simulated by the generation of bursts of noise in synchronism with the radar pulses.

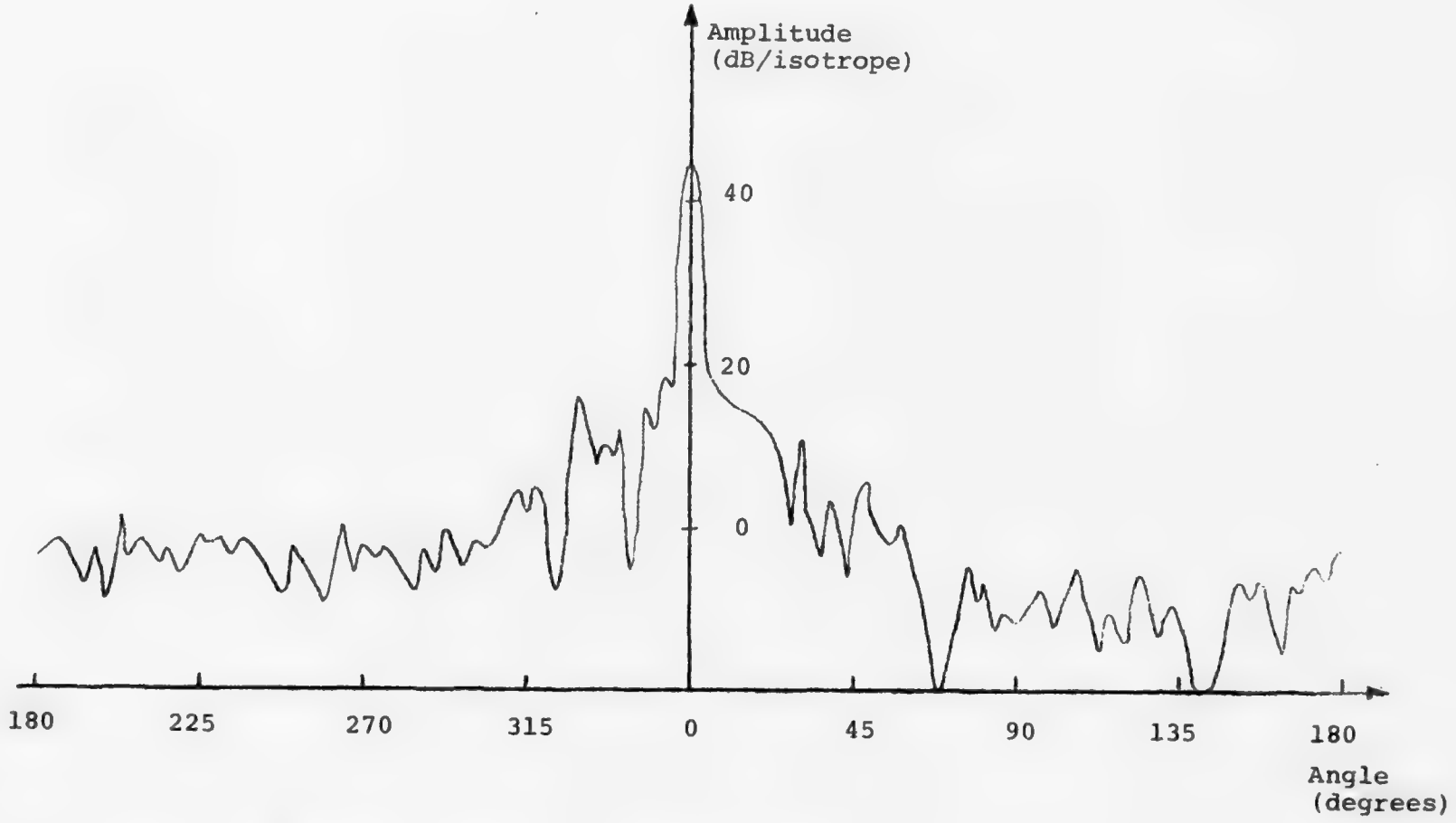

Figure 8: Typical high-gain antenna pattern.

Since the effects of broadband noise and of nonlinearities will be considered in its totality, no hypothesis need be made for them.

A suitable expression for the UHF/RADAR interferer will be as follows:

$$y(t) = a(t)s(t)[n(t) + B \sin(2\pi f_c t)] \qquad (3.13)$$

where a(t) is a "regime" modulating signal representing the effect of antenna scan and antenna pattern on the signal, s(t) is a pulse modulating signal as in (3.4) and n(t) is a broadband Gaussian noise process with one-sided power spectrum density $\frac{N_0}{2}$ watts/Hz.

D. EMITTER 6 – VHF INTERFERER

In the real world this kind of source of interference is of the same type as the UHF/LOS interferer. Since the likely interference effects of this emitter will be due to intermodulation products generated by the nonlinearities, we have in a first approximation considered it to be a CW signal only.

E. EMITTERS 7 AND 8 – HF INTERFERERS

Again, as in the case of EMITTER 6, despite the fact that a true representation of real life interferers would possess some kind of modulation (often a 16 channel multiplexed FSK), we choose to generate only CW signals as a first approximation.

F. EMITTER 9 – IMPULSIVE INTERFERENCE

Impulsive noise found aboard ships is due to a variety of causes: Switching of electrical and electronic equipments, operation of digital equipment such as computers and digital communications, use of fluorescent lamps and in general, the use of all electrical and electronic gear that makes a ship's environment possess a high density electromagnetic field. Previous physical models for impulsive noise have considered and found the random occurrence of a given type of a transient waveform to give a good fit to data in numerous occasions. Such was the case for atmospheric and ignition noise where the type of waveform occurring was of a definite type in either case. Again, as in the case of the radar interferer modeling, we tried to characterize this type of interference by considering the main aspects of it which are basically the following:

a) The interference process will likely be extremely broadband and possibly even affecting the whole SATCOM band. It will certainly be broadband with respect to the receiver bandwidth.

b) Since it is an impulsive phenomenon, it will occur discretely rather than continuously in time.

What this amounts to is that a certain level of energy will be delivered to the receiver filter in a "random" (in time) fashion. What "random" here really means will depend, of course, on the source of interference. If a radar is the cause, it will not be random at all but will have a

clear periodicity, and that hypothesis must also be considered in our model. As we anticipated in the introduction, various models previously proposed take these aspects into consideration. Middleton's model, although the more precise, will be of no help in this case because of the above mentioned lack of better knowledge of the types of impulsive waveforms that make up the interference process. On the other hand some of the analytical models which treat the problem by considering only its more general characteristics, such as by Hall [Ref. 3] or Shaver et. al. [Ref. 6] will be much more suitable for simulation at this stage of knowledge. Both models consider the impulsive part of the interference process to be a Gaussian process modulated by another "regime" process that accounts for the variation of the dynamic range of the process in time.

In the case of Hall's model, which was applied to atmospheric noise, this is accomplished by considering y(t) (the interference process after being filtered by the receiver) to be of the form:

$$y(t) = a(t)\, n(t) \tag{3.14}$$

where n(t) is a zero-mean narrowband Gaussian process with covariance functions $R_n(\tau)$ and a(t), the "regime" process, is a stationary random process, independent of n(t) whose statistics were to be chosen to match measured data. If a(t) is a 2-state process which occurs randomly in time with

$$P(0) = \text{probability of } a(t) = 0$$

$$P(1) = \text{Probability of } a(t) = 1$$

we see that this model would apply exactly to a Gaussian noise process multiplied by a randomly occurring sequence of rectangular pulses. If they occur with a rate $\gamma(\text{sec}^{-1})$ and have a pulse width PW(sec), the probability of being in the state 1 will be $\gamma \times PW$.

The approach taken by Shaver et. al. [Ref. 6] considers y(t) to be a two-state Markov chain:

$$\begin{aligned} y(t) &= 0 \qquad \text{with probability } P(0) \\ y(t) &= n(t) \quad \text{with probability } P(1) \end{aligned} \tag{3.15}$$

where n(t) is a zero-mean Gaussian process.

Although this model was applied to the impulsive noise found in telephone channels, we see that they are remarkably similar in format to each other, and that is due to the fact that they represented the interference process by considering only their more general physical and statistical characteristics instead of precisely defining all the physical aspects of the sources of noise. That fact gave us the confidence to use a similar model for the impulsive noise that will be likely to be found aboard ships. The first important characteristic of an impulsive phenomenon

is its randomness in time and thus we have modeled it as a sequence of pulses occurring randomly in time. The next important characteristic would be the format of the pulses. Since, as we mentioned before, we do not have enough information to accurately characterize it, we have used as an approximation, a truncated sample function from a broad band Gaussian noise source. Such a model can be represented by the same expression used by Hall:

$$y(t) = a(t)\ n(t) \tag{3.14}$$

where a(t) will be a sequence of randomly occurring pulses with pulse width PW and n(t) is as described before. Figure 9 shows typical sample functions of a(t), n(t) and y(t). The pulse's starting time t_i occurs according to a Poisson process with rate γ, which can be varied and together with pulse width (PW) and noise power spectrum density (N_0), constitute the parameters for our model.

G. EMITTER 10 – GAUSSIAN NOISE

It has been observed [Refs. 1 and 15] that the overall noise level aboard ships varies with the general activity of the ship. In order to account for this increase in the background noise level, we have modeled it as a broadband Gaussian noise process, covering the SATCOM band.

Figure 9: Typical Sample Functions for a(t), n(t) and y(t).

IV. SYSTEM DESCRIPTION

In Chapter III we have established a model intended to characterize the problem of shipboard RFI at UHF. This model has basically two major components: sources of electromagnetic interference (emitters) and processing of these signals which includes propagation, coupling and effects of nonlinearities. In this chapter we will describe the system that was physically implemented using the above model to simulate the RFI problem. A photograph of the system setup is shown in Figure 10. Identification of the various units shown in the figure is given by Figure 11 and Table 2.

A. PROCESSING

The block diagram in Figure 12 shows the system configuration. There are 10 emitters, implemented following the description in Chapter III, two nonlinearities (N1 and N2) and a combining unit (C1) which adds linearly the results of nonlinearity processing on Emitters 1 to 8, with Emitters 1 to 5, 9, 10 the signal and also any externally generated interferer. The combination of all those signals is available on an "OUTPUT" jack on the front panel of C1. A "TEST OUT" jack on the front panel of C1 also provides an attenuated (20 dB down) version of the output signal for monitoring purposes with a spectrum analyzer.

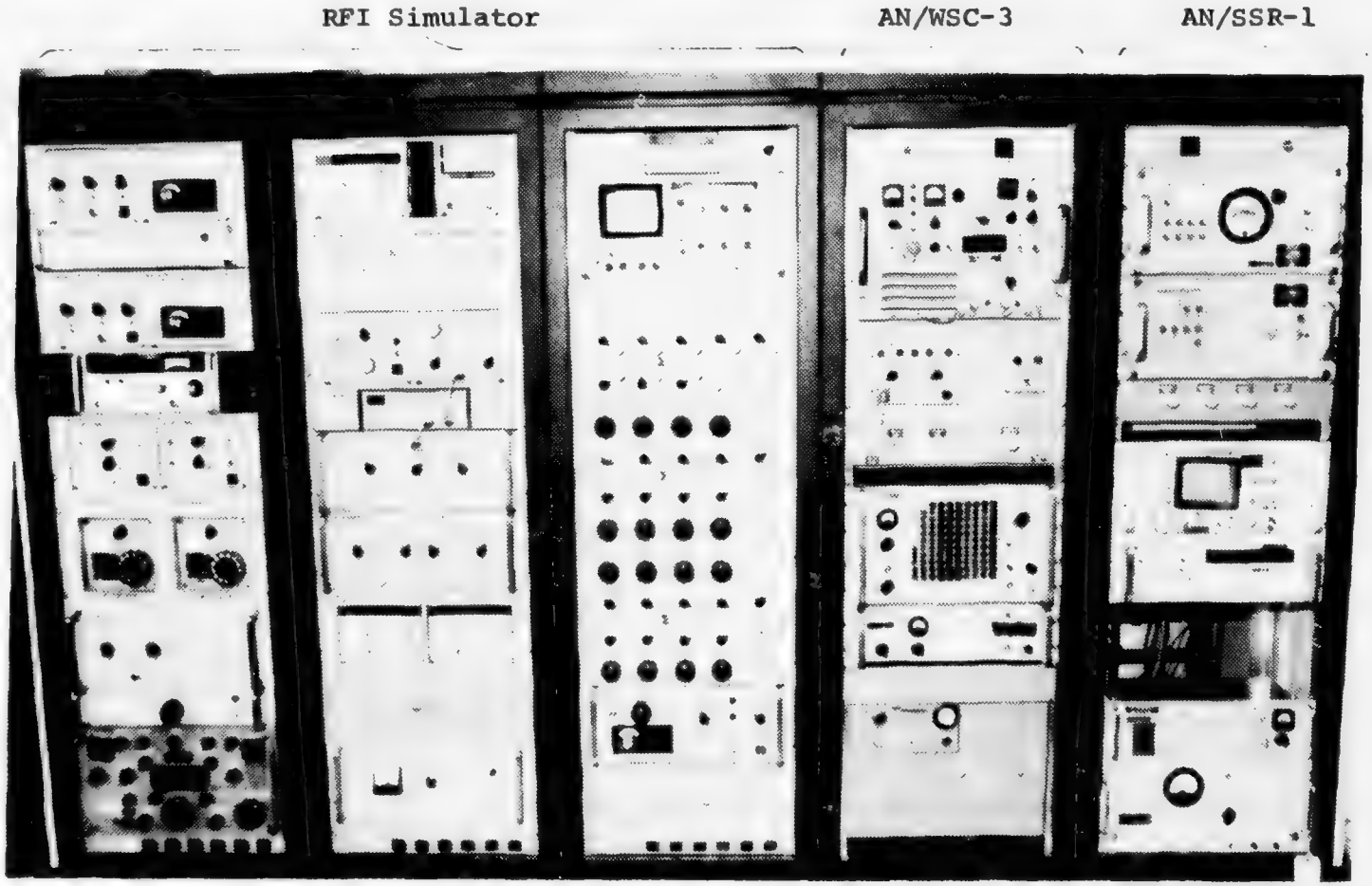

Figure 10: Overall view of simulator and satellite terminals.

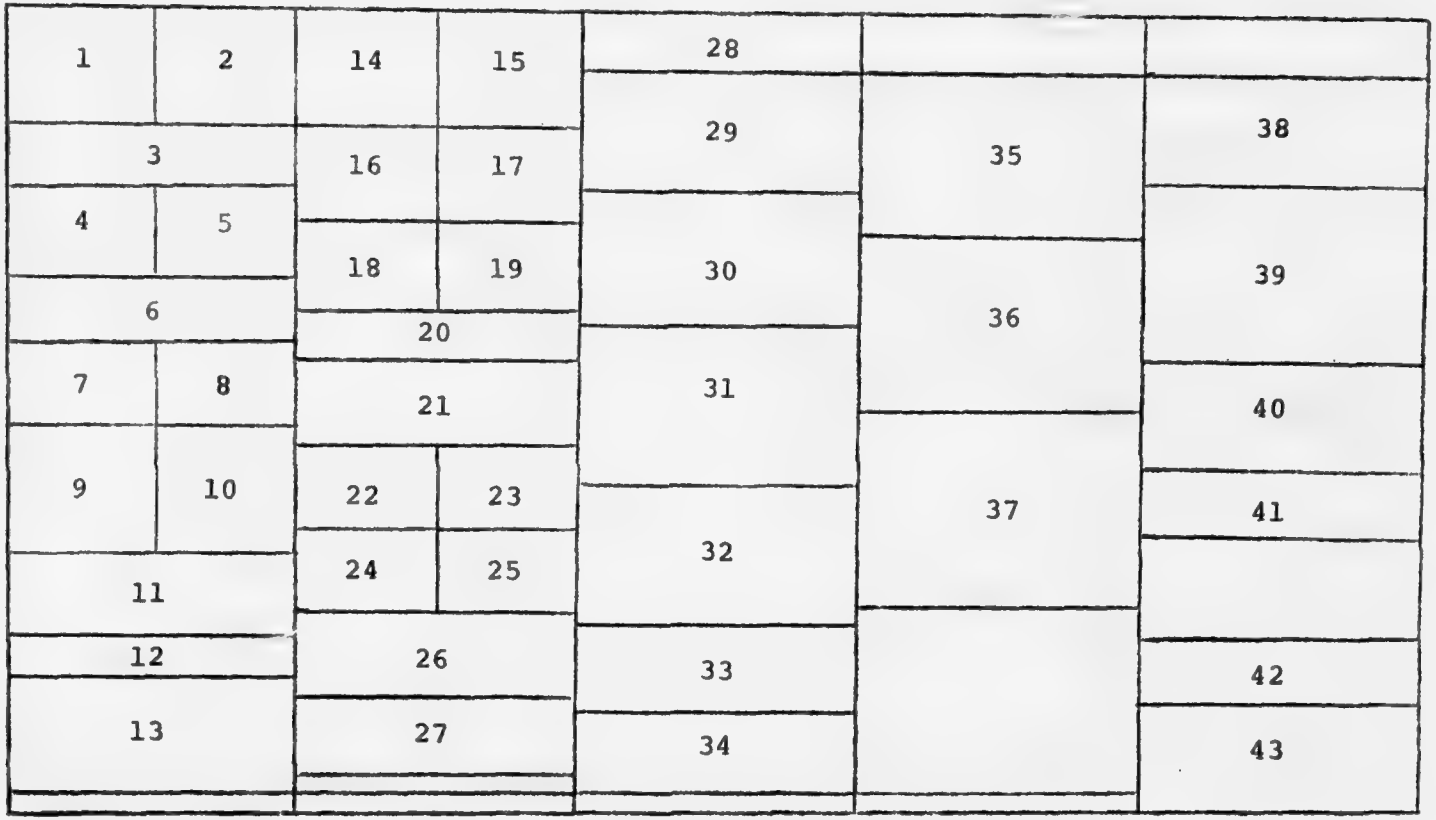

Figure 11: Identification of Units in Figure 10.

UNIT	DESCRIPTION	UNIT	DESCRIPTION
1	E1A - UHF/PSK modulator	23	E7 - HF Interferer
2	E1B - UHF/PSK filter	24	HP-3200B Signal Generator
3	E1C/E2C - UHF/PSK Amplifiers	25	HP-3200B Signal Generator
4	E2A - UHF/PSK Modulator	26	Drawer
5	E2B - UHF/PSK Filter	27	PS1 - Power Supply
6	Wavetek-3000 Signal Generator	28	Counter
7	E3A - UHF/LOS Modulator	29	Spectrum Analyzer
8	E4A - UHF/LOS Modulator	30	C1 - Combining Unit
9	E3B - UHF/LOS Frequency Selector	32	N1 - Nonlinearity #1
10	34B - UHF/LOS Frequency Selector	32	N2 - Nonlinearity #2
11	E8 - HF Interferer	35	S1 - Signal
12	E10 - Gaussian Noise	34	Drawer
13	R-390A Receiver	35	AN/WSC-3
14	HP-3200B - Signal Generator	36	AN/WSC-3
15	HP-435A - Power Meter	37	HP-5105A Frequency Synthesizer
16	HP-8011A - Pulse Generator	38	AN/SSR-1
17	HP-8011A - Pulse Generator	39	AN/SSR-1
18	E9 - Impulsive Noise	40	HP-3580A - Spectrum Analyzer
19	E5A - Radar Pulse Modulator	41	HP-1645A Data Error Analyzer
20	E5B - Radar Amplifier	42	AM-2123 (V)U - Distribution Amplifier
21	E5C - Radar Scan Modulator	43	0-471/U Frequency Standard
22	E6 0 VHF Interferer		

TABLE 2: Identification of Units in Figure 10

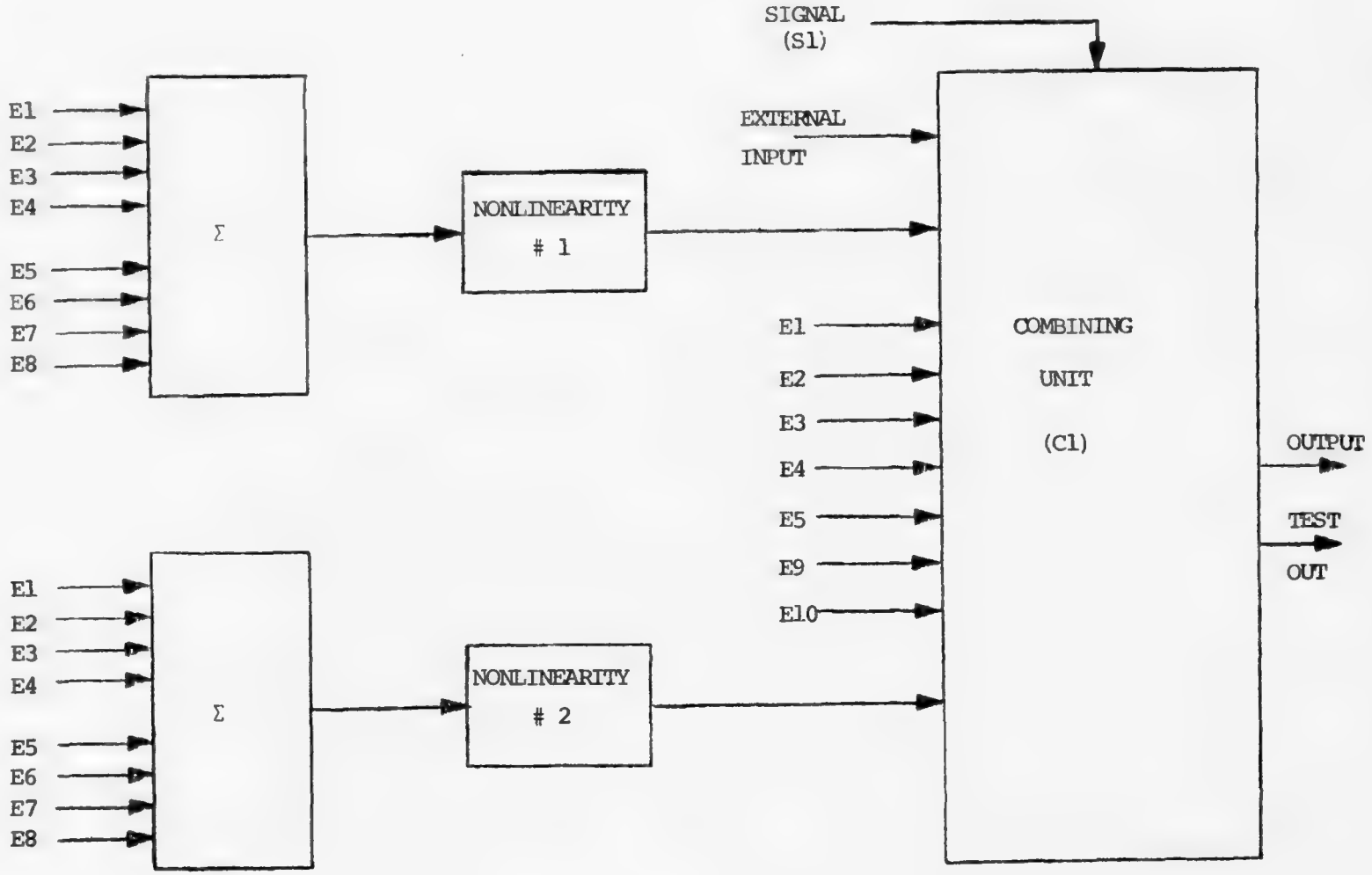

Figure 12: RFI Simulator Block Diagram.

Each of the emitters being fed to nonlinearities N1 or N2 can be individually controlled in amplitude as well as be totally cut off from the nonlinearity by an RF switch as shown in Figure 13. The result of nonlinear processing on the emitters can also be attenuated and/or cut off before being fed to the COMBINING UNIT. When in the OFF position, the emitters are dissipated in internal loads as shown in Figure 13. On the COMBINING UNIT (Figure 14) Emitters 1 through 5 have front panel control of amplitude and ON/OFF. When in the ON position, the emitters are combined with the signal and are available at the "OUTPUT" and "TEST OUT" terminals. In the "OFF" position, the emitters are available at jacks on the front panel and are not combined with the signal. The levels of the emitters at these outputs is nominally 6 dB above the ones obtained at the "OUTPUT" jack for Emitters 1 through 4 and 5 dB for Emitter 5.

Emitters 9, 10 and the signal (S1) have individual ON/OFF controls and are also available at front panel jacks when in the OFF position. The level of these signals at these points is nominally 13, 31 and 19 dB above the level obtained at the "OUTPUT" port, respectively.

An external input can be fed to the appropriate jack on the front panel and will be attenuated by 19 dB before reaching the "OUTPUT" port. The signals from NONLINEARITIES 1 and 2 will be attenuated by 17 dB in C1, before reaching the "OUTPUT" port. Controls for these signals are not available in the COMBINING UNIT but are available in N1

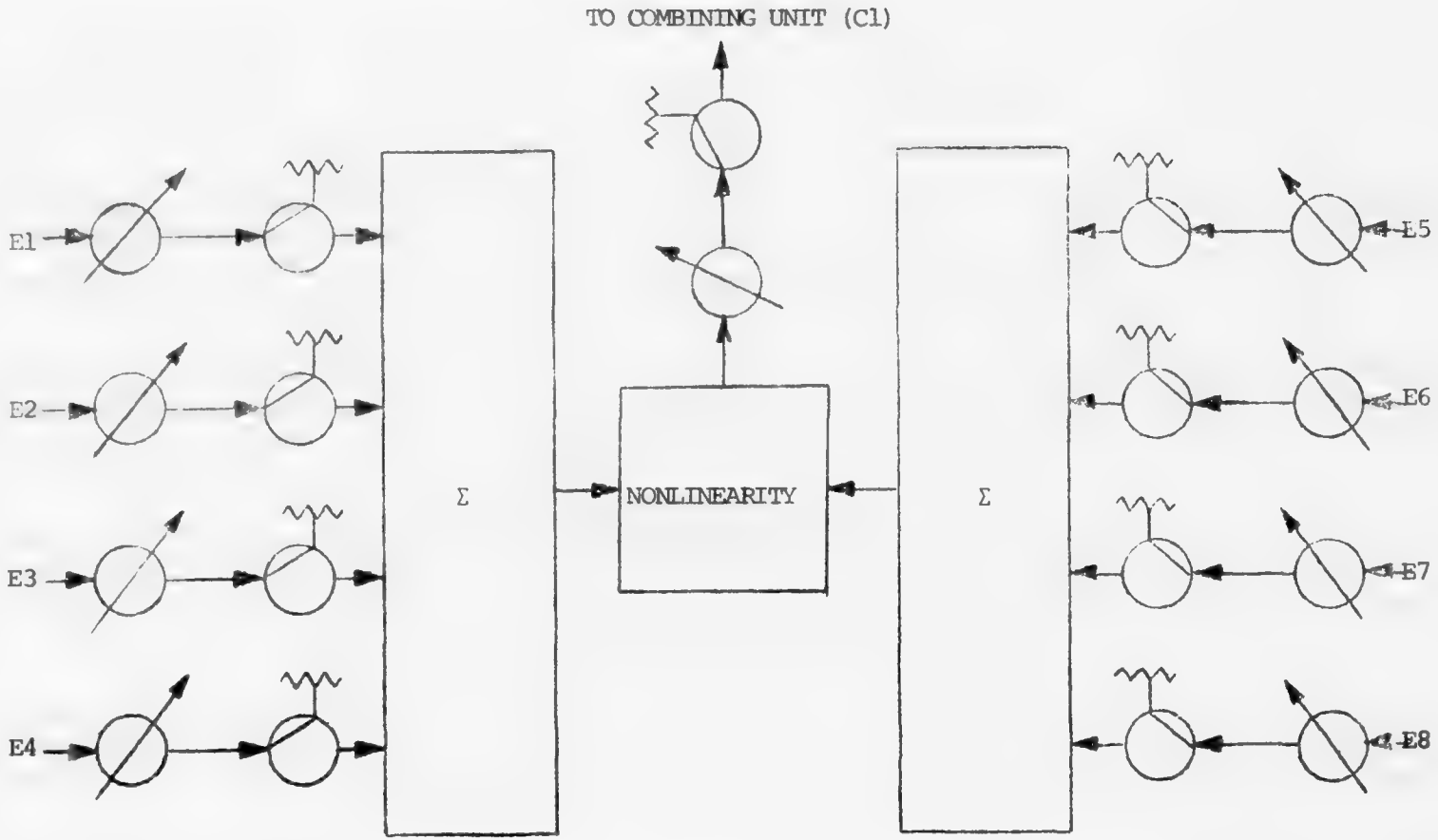

Figure 13: Nonlinearity #1 or #2 Block Diagram.

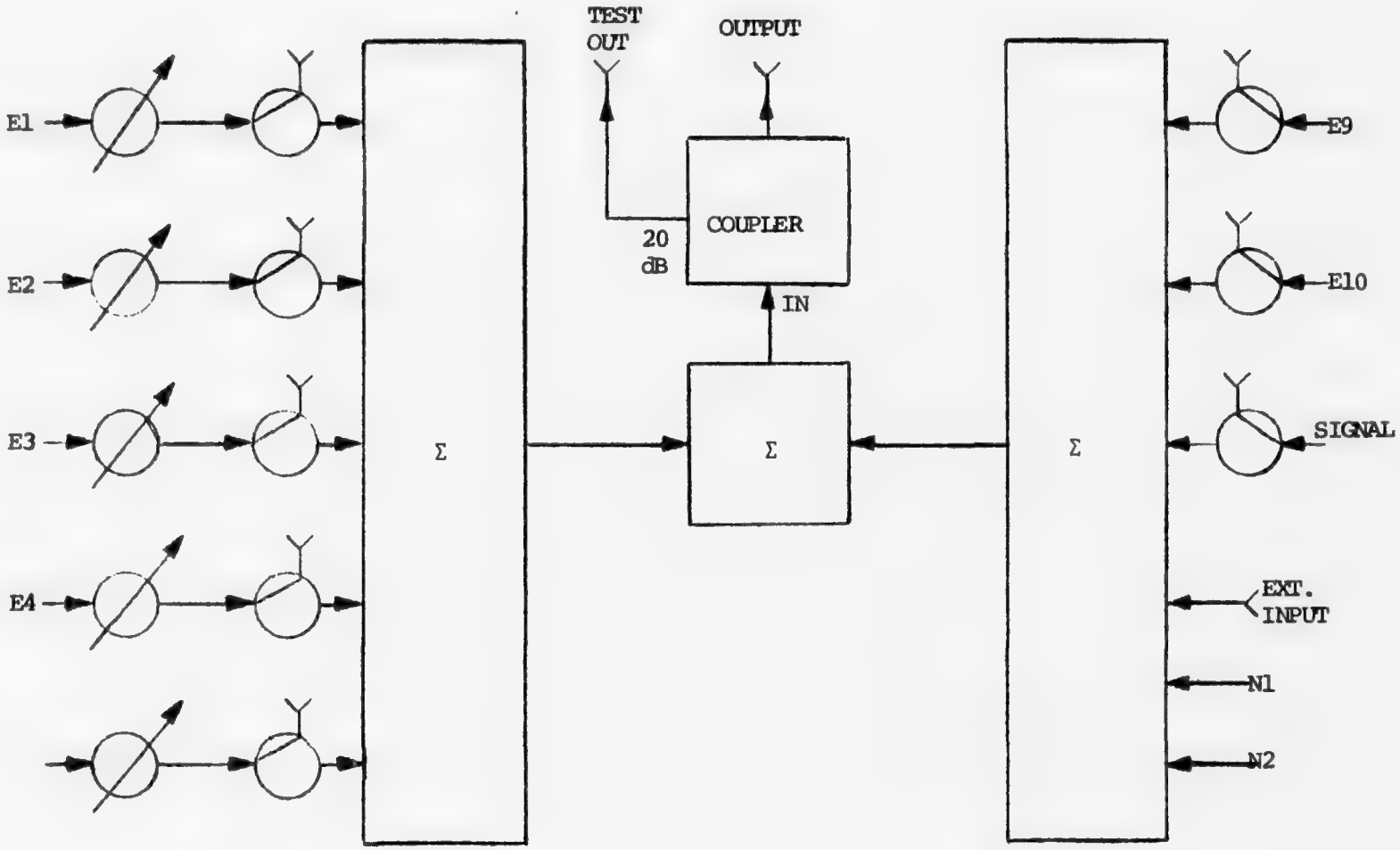

Figure 14: Combining Unit (C1) Block Diagram.

and N2 as explained before. Detailed schematic diagrams of C1-COMBINING UNIT, N1-NONLINEARITY #1 and N2-NONLINEARITY #2 are available in Appendix 1. Photographs of the front panel of C1 – Combining Unit and N1 – Nonlinearity #1 are shown in Figures 15 and 16.

B. EMITTERS

1. Emitters 1 and 2 (E1 and E2)

In Chapter III, E1 and E2 were modeled as a PSK random data modulated and filtered carrier as expressed by Eqs. (3.2), repeated here for convenience.

$$y_{PSK}(t) = \int_{-\infty}^{\infty} h(t-\delta)A \sin(2\pi f\delta + \Psi + \frac{\pi}{2} a(\delta))\, d\delta \qquad (3.2)$$

where h(t) is the filter impulse response, A a constant, Ψ a uniformly distributed random variable expressing the phase uncertainty on the RF source and a(t) a binary random process which can assume two states.

$$a(t) = 1 \quad \text{with probability } 1/2$$

$$a(t) = -1 \quad \text{with probability } 1/2$$

The implementation of this random data stream was done by using a pseudo-random binary sequence (PRBS) generator (a maximum length PN sequence). This was achieved by using shift registers of selectable lengths 5, 10 and 20

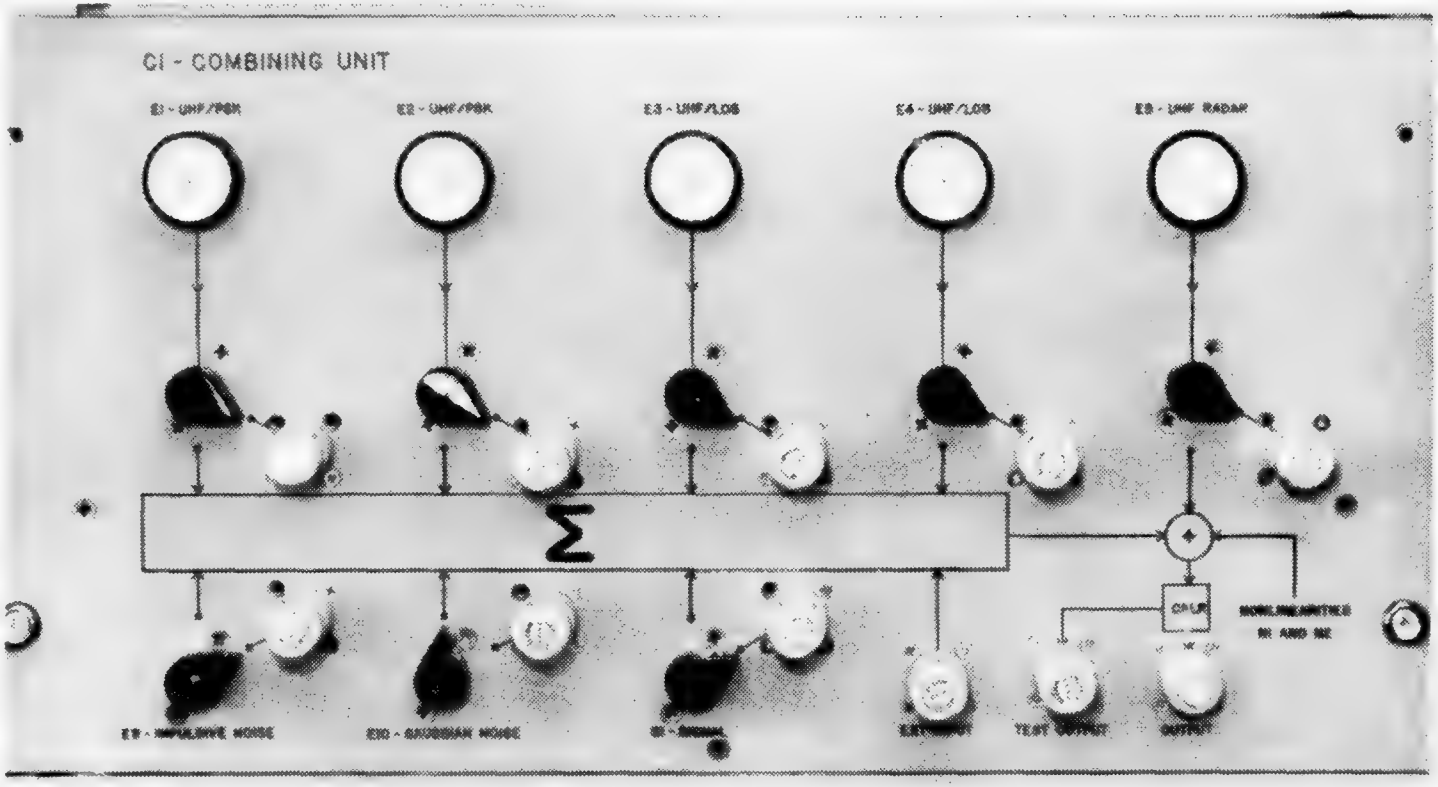

Figure 15: Front Panel of C1-COMBINING UNIT

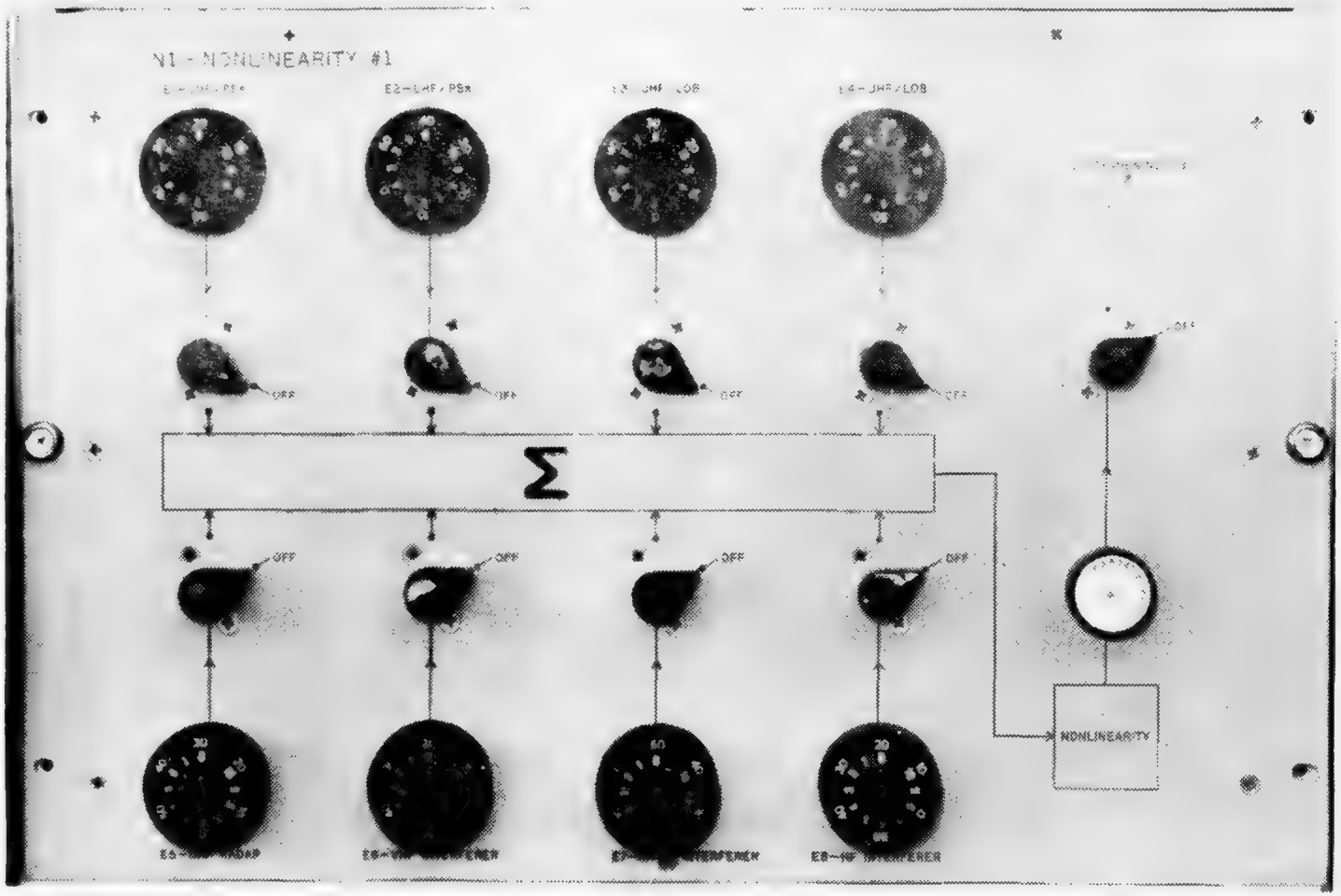

Figure 16: Front Panel of N1-NONLINEARITY #1

with feedback from the first and fourth element in the chain according to Reference 19.

In Figure 17, a block diagram of the UHF/PSK interferers is drawn. Each emitter is realized with the help of three units:

UHF/PSK MODULATOR - E1A (E2A)

UHF/PSK AMPLIFIER - E1C/E2C

UHF/PSK FILTER - E1B (E2B)

In addition, a stable 30 MHz reference signal (frequency and level controlled) and a local oscillator (LO) are used to obtain the signal.

As shown in Figure 17 a pseudo-random binary sequence bi-phase modulates (0° or 180°) the 30 MHz carrier which then is filtered by a 30 kHz bandwidth crystal filter giving the desired signal as expressed by (3.2). After that the signal is up-converted to the 200-400 MHz band in the mixer, is amplified in unit E1C/E2C and filtered in the filter unit E1B (E2B) to eliminate one of the sidebands and recover a higher level version of the original signal.

The operator has access to the following controls and ports on the front panels.

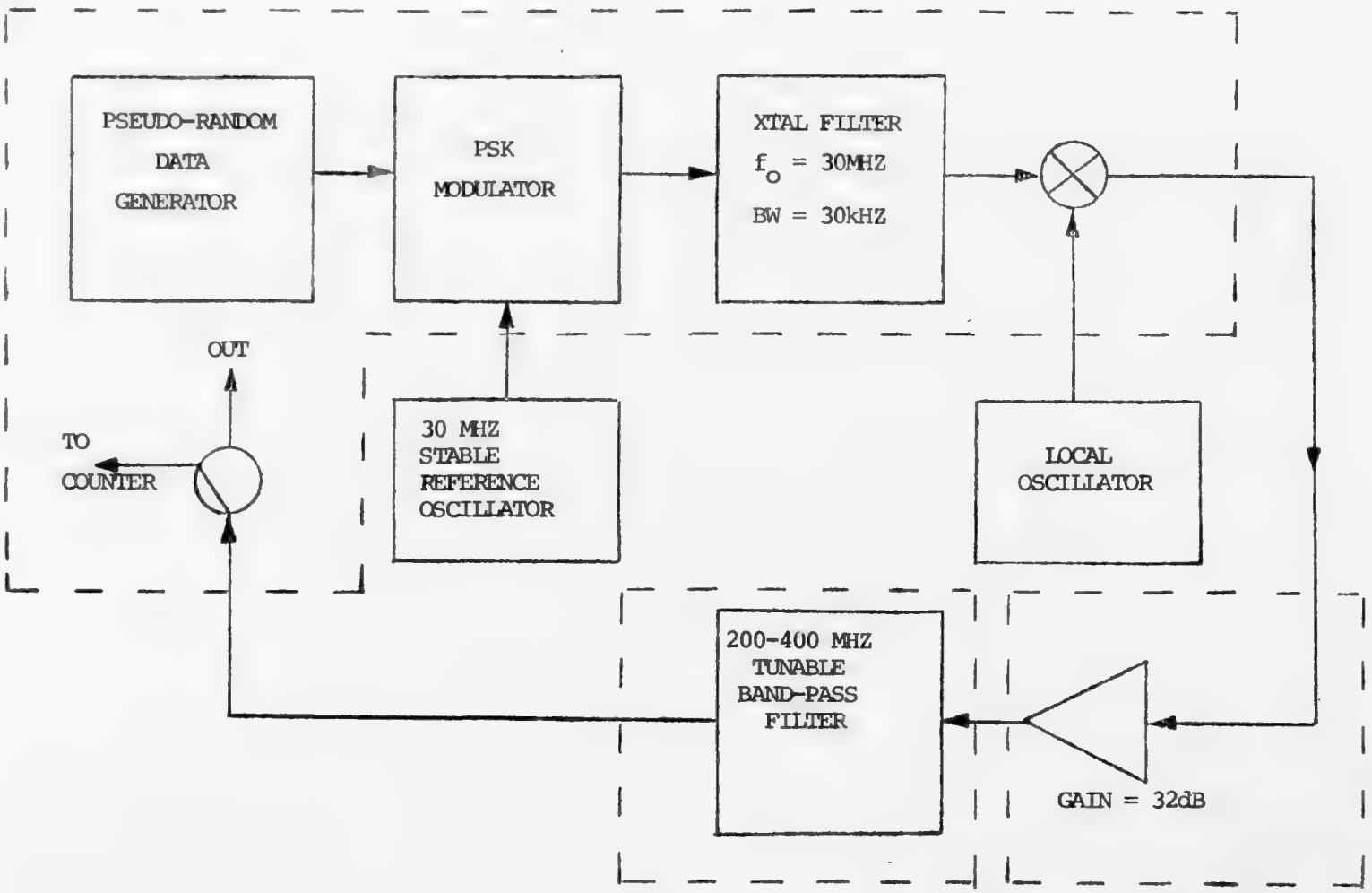

Figure 17: E1(E2)-UHF/PSK Interferer Block Diagram

a) Unit E1A(E2A) UHF/PSK MODULATOR

DATA SECTION:

--"SYNC OUT": This output connector provides a synchronism signal each time a sequence period is completed, when the "REGISTER LENGTH" switch is in position 5. On the other positions (10 and 20) this is just a pseudo-random output obtained by detecting a subsequence of length 5 on the PN sequences generated. This signal is derived from a TTL line driver and will accept a 50 Ωload.

--"REGISTER LENGTH": This switch selects the size of the register being used to generate the PRBS. Options available are 5, 10 and 20. In all positions feedback is made from flip-flops 1 and 4 in the register.

--"ENCODING": This is a two-position switch with options "PSK" and "DPSK." In the "PSK" position the carrier is PSK modulated with the data (either internal or external). In the "DPSK" position the data is differentially encoded before modulating the carrier.

--"SOURCE": This switch can select the source of data that will modulate the carrier. In the "INT" position the internally generated PRBS is used and is also available at the "OUT" port, derived from a TTL line driver (accepts 50Ω loads). In the "EXT" position, any data fed to the TTL compatible "IN" port will be used as the source of modulating signal. In that case, the same data will be available at the "OUT" terminal. The external data must have transitions on the leading edge of the clock which, in addition, must also be available in order that the encoding circuit can work properly.

--"OUT": Data output derived from a TTL line driver (accepts 50Ω load). When "SOURCE" switch is in "INT," the output is the internally generated sequence. When "SOURCE" switch is in "EXT" and a data source is connected to "IN" port, the output is the same as the external data. "ENCODING" switch does not affect this port.

--"IN": Data input. TTL COMPATIBLE CIRCUITRY.

CLOCK SECTION:

--"OUT": Clock output port. Provides internally generated or externally applied clock, depending on the position of "SELECTION" switch. Accepts 50Ω load.

--"IN": Clock input port. TTL compatible input for an external clock. (Must be used when using external data. Minimum rate is 75 Hz.)

--"RATE": Rate selection switch. Allows the selection of five clock rates (1.2, 2.4, 4.8, 9.6, 19.2 kHz) from the internal clock. It has no function when an external clock is being used.

--"SELECTION": Two position switch: "EXT" and "INT". Selects external or internal clock.

RF SECTION:

--"IN": This N-type connector is the input port for the local oscillator. Signal level of 7 dBm, 30 MHz above or below the desired frequency, are required at this port.

--"MODULATION": This switch commands the modulation of the carrier. In the "OFF" position the carrier is unmodulated, in which case the RF switch can be used to select the signal to the COUNTER so that the carrier frequency can be measured. In the "ON" position the carrier is modulated.

--"RF": This RF switch can select the signal to the COUNTER (in which case be sure MODULATION is OFF) or to the COMBINING UNIT and NONLINEARITIES N1 and N2.

E1B(E2B) has a tuning knob on the front panel and E1C/E2C has an ON/OFF switch that switches a 24V DC supply and a cooling fan on the unit. A detailed description of the operation of emitters 1 and 2 together with schematic diagrams of units E1A(E2A), E1B(E2B), E1C/E2C is given in Appendix 2. Photograph of front panel of Emitters 1 and 2 is shown in Figure 18.

2. EMITTERS 3 and 4 (E3 and E4)

The model for a UHF/LOS emitter as established in Chapter III was one of a voice modulated AM signal which would be on or off according to push-to-talk (PTT) statistics, postulated taking into consideration the fact that the

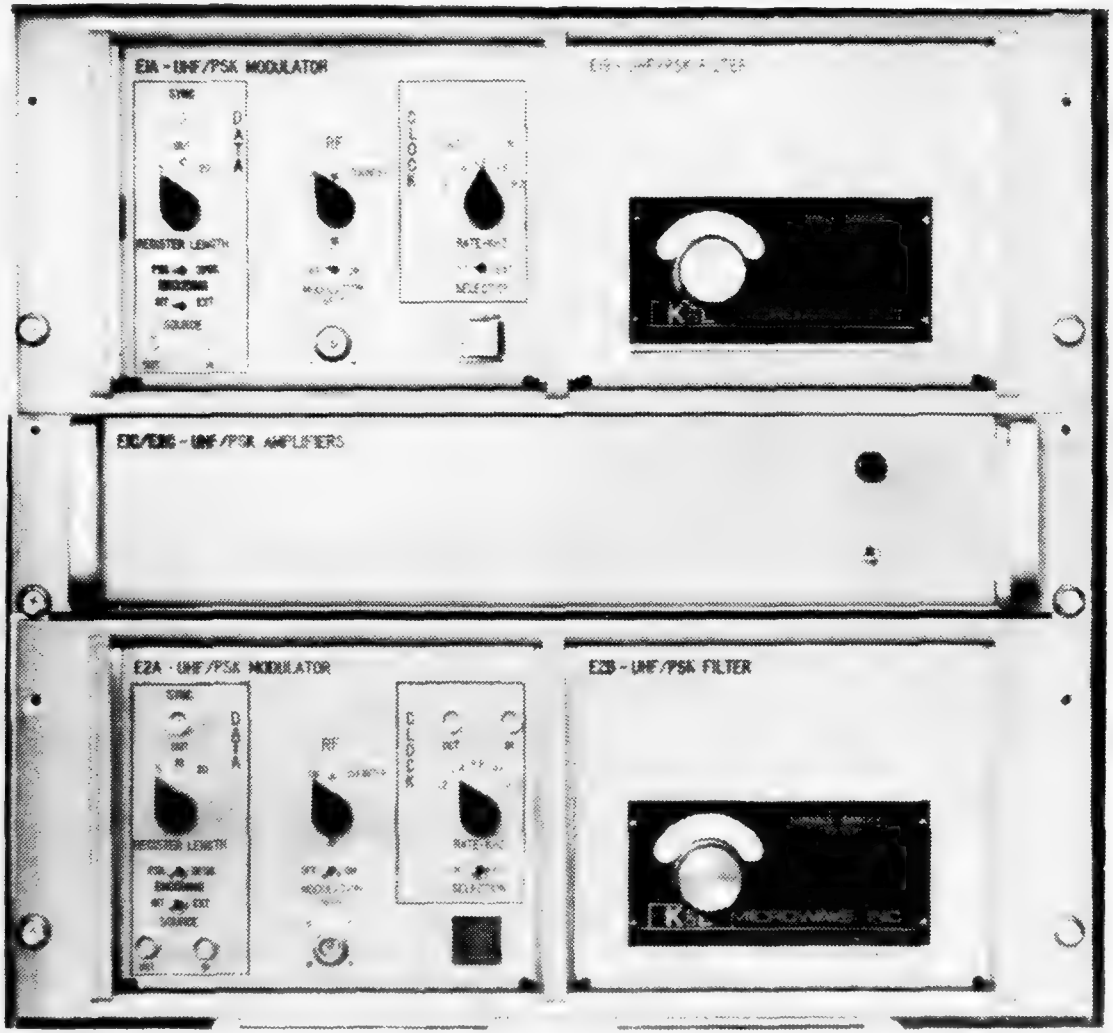

Figure 18. Front Panel of Emitters 1 and 2.

emitter would be turned on in a random fashion and off also randomly and independently of the on time. This model leads to the expression (3.3) which was established in Chapter III and repeated below.

$$y_{LOS}(t) = a(t)[1 + m(t)] \sin \omega_c t \qquad (3.3)$$

where m(t) is a "voice process, ω_c is the carrier angular frequency and a(t) is a process describing the push-to-talk statistics as described in Chapter III.

The "voice" process m(t) was obtained by using an audio signal derived from a broadcast receiver (in our case, a R-390A receiver) tuned to one of the local news stations. The PTT process a(t) was obtained in the following way. Two independent pseudo-Poisson processes, $S_1(t)$ and $S_2(t)$, derived from PN sequences as explained in Appendix 9 were used to reset and set a flip-flop as shown in Figure 19. When the flip-flop is "ON," the J input is at "0", the K input is at "1", the stop signal $S_1(t)$ is connected to CP (clock pulse input) and the start signal $S_2(t)$ is disabled. Thus all the start pulses are blocked and the first stop pulse will reset the slip-flop reversing the process. The signal a(t) is then used to switch ON and OFF a transmitter. In Figure 20 an overall block diagram of emitters 3 and 4 is given.

The signal m(t) as explained is derived from the broadcast receiver R-390A and can be switched on and off by

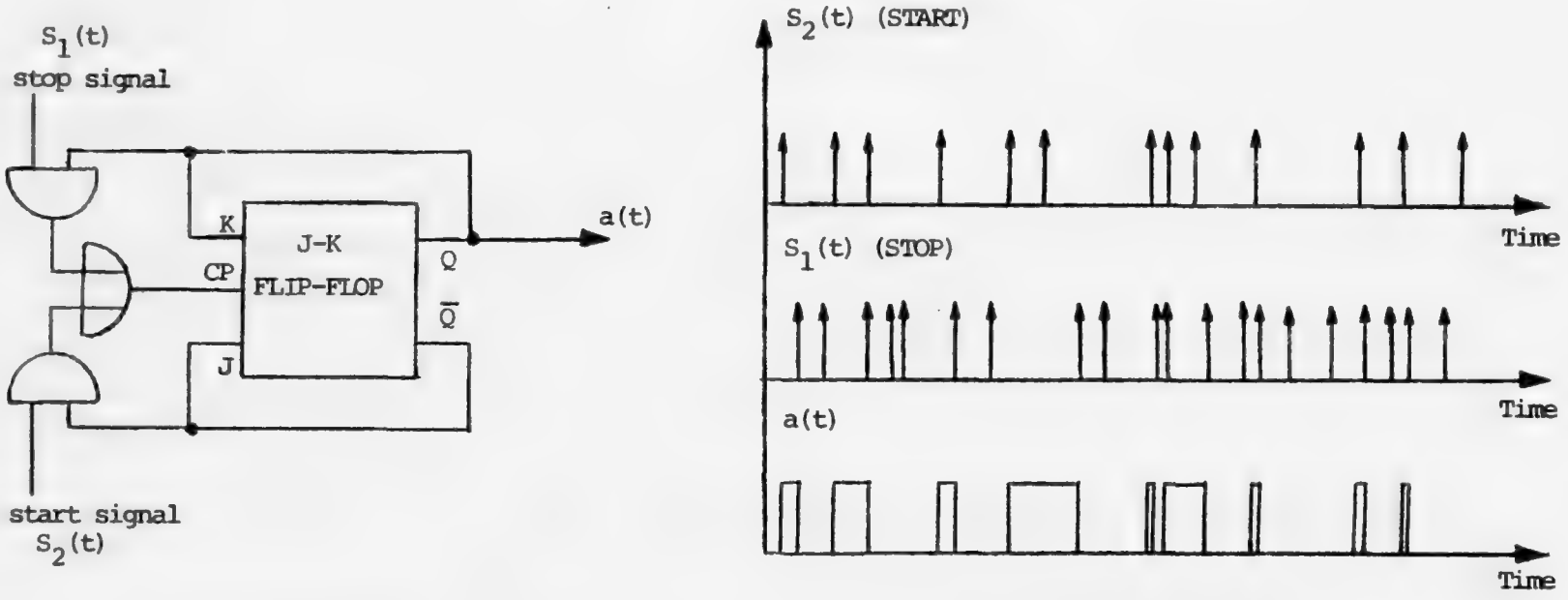

a) PTT generator

b) Signal waveforms

Figure 19: PTT Statistics Generation.

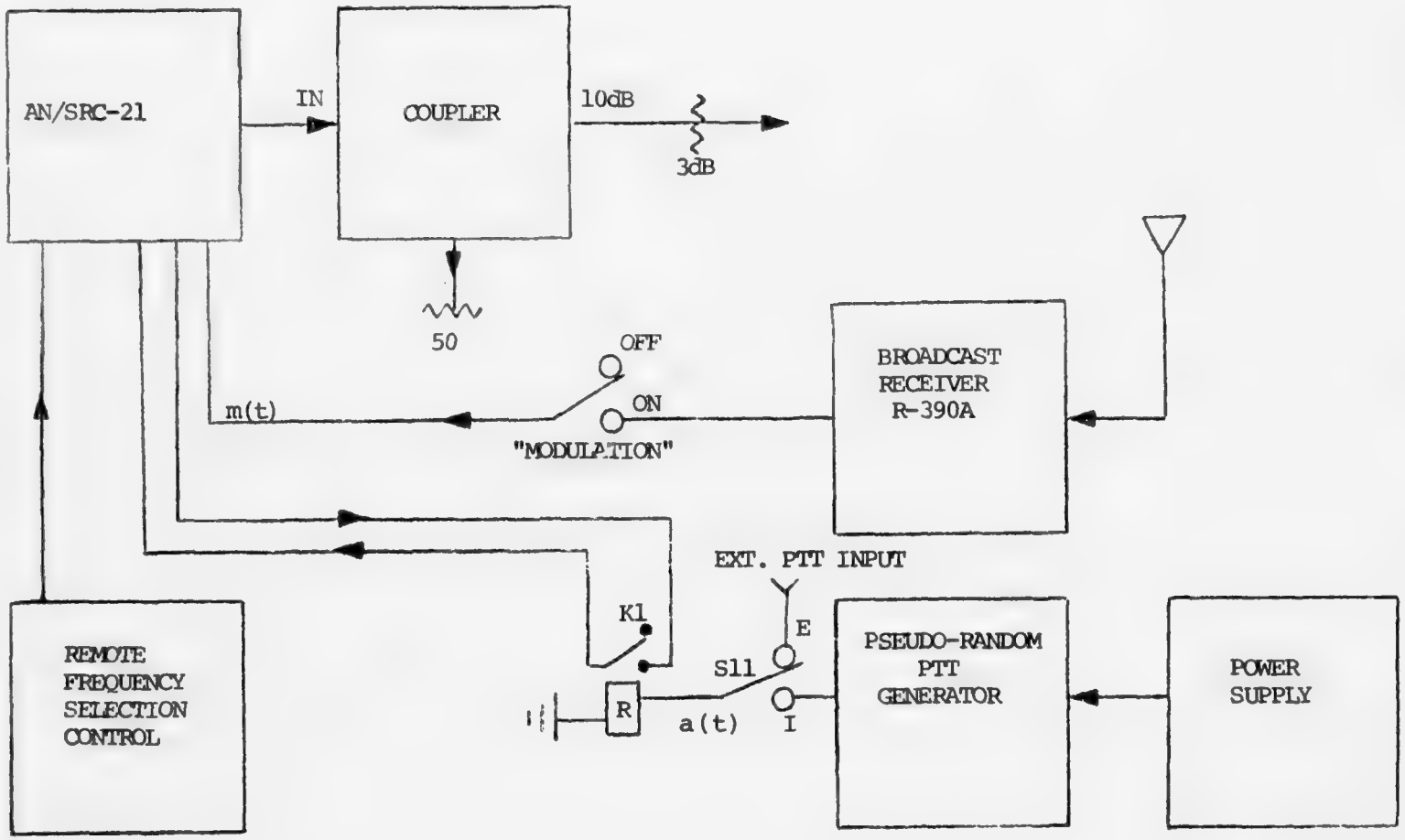

Figure 20: E3(E4) UHF/LOS Interferer Block Diagram.

the switch "MODULATION" on the front panel of units E3A or E4A. Units E3B and E4B are two remote controls that allow selection of one of 19 frequencies programmed in the transceiver AN/SRC-21 used as the signal source. Relay K1 on units E3A (E4A) controls the operation of the AN/SRC-21 transmitter when set for remote operation. This relay can be controlled either by the PTT signal a(t) generated in E3A (E4A) or by any external signal (TTL compatible) fed to connector J11 on the back of E3A (E4A). Internal (I) or external (E) control is selected by "PTT" switch (S11) also on the back of E3A (E4A). The m(t)-AM-modulated and a(t)-switched carrier of the AN/SRC-21 with a level up to 20 watts average is fed to a 10 dB coupler and the coupled output after attenuated by a 3 dB pad is available as emitters 3 and 4 to the COMBINING UNIT C1 and NONLINEARITIES N1 and N2.

The operator has access to the following controls and ports on the front panels of the various units.

a) Unit E3A(E4A) UHF/LOS MODULATOR

"PTT RATE" This 5-position switch selects the rate of the start pseudo-random signal $S_2(t)$. The rate unit is minute^{-1} and the options available are 0.5, 1, 2, 4, 8.

"PTT AVG ON TIME" This is also a 5-position switch which selects the rate

of the stop pseudo-random signal $S_1(t)$. The panel selection indicates the inverse of the rate and its unit is in seconds.

"CLOCK #1" Two-position switch commanding the selection of the clock that drives the start signal $S_2(t)$. On the "INT" position the clock is internal and "PTT RATE" switch is calibrated. Clock output is available in connector J14 on the back. In the "EXT" position any clock fed to J15 on the back (TTL compatible input) will command the on rate as explained in Appendix 3. J14 will in both cases provide a TTL line driver derived output of the working clock. (J14 accepts a 50Ω load.)

"CLOCK #2" Has the same functions as "CLOCK #1" switch except that it works with the clock that drives the stop signal $S_1(t)$ and the clock input and output connectors are J13 and J12 on the back of E3A(E4A).

"MODE" 3-positions toggle switch. In the "OFF" position the transmitter is turned off and so is Emitter 3(4). In the "CONT" position the transmitter is continuously turned on. In the "PTT" position the transmitter is under the control of relay K1 on E3A(E4A) and thus can be switched on and off either by the PTT signal a(t) or by any external signal as explained before.

"MODULATION" Two-position toggle switch which controls the modulating signal m(t) to the transmitter.

b) Unit E3B(E4B) UHF/LOS FREQUENCY SELECTOR

"ON/OFF" Turns unit on and off.

"DIAL" Any of the 19 pre-programmed frequencies on the AN/SRC-21 can be selected by dialing. Channels 1 to 9 can be directly dialed. Channels 10 to 19 are dialed by substituting the first digit (1) by the A on the dial.

Detailed description and schematic diagrams of emitters 3 and 4 are given in Appendix 3. Detailed description of

controls and operation of AN/SRC-21 and R-390A can be found in the respective technical manuals. Photograph of front panels of Emitters 3 and 4 is shown in Figure 21.

3. EMITTER 5 (E5)

As seen in Chapter III the radar interferer was modeled as:

$$y_{RADAR}(t) = a(t)\ s(t)\ [n(t) + B \sin 2\pi f_0 t] \qquad (3.13)$$

where a(t) is a scan modulating signal, s(t) a periodic train of rectangular pulses, n(t) a broadband Gaussian noise process and f_0 the carrier frequency.

The actual implementation of this interferer was done as seen in Figure 22, in a slightly different manner than the analytic model. A filter was used after the RF amplifier in order to eliminate the contribution of the amplifier noise to the noise level at the receiver. A correct expression for this emitter would then be:

$$y_{RADAR}(t) = a(t)s(t)n(t) + B \int_{-\infty}^{\infty} h(t-\delta)a(\delta)s(\delta)\sin(2\pi f_0\delta)d\delta \qquad (4.1)$$

where h(t) is the impulse response of the bandpass filter.

The block diagram of Emitter 5 is shown in Figure 22. A RF source (with an 18 dBm power capability) and a broadband Gaussian noise source are processed in parallel in a similar fashion. First a digitally controlled pin-diode attenuator, commanded by the antenna scan pattern

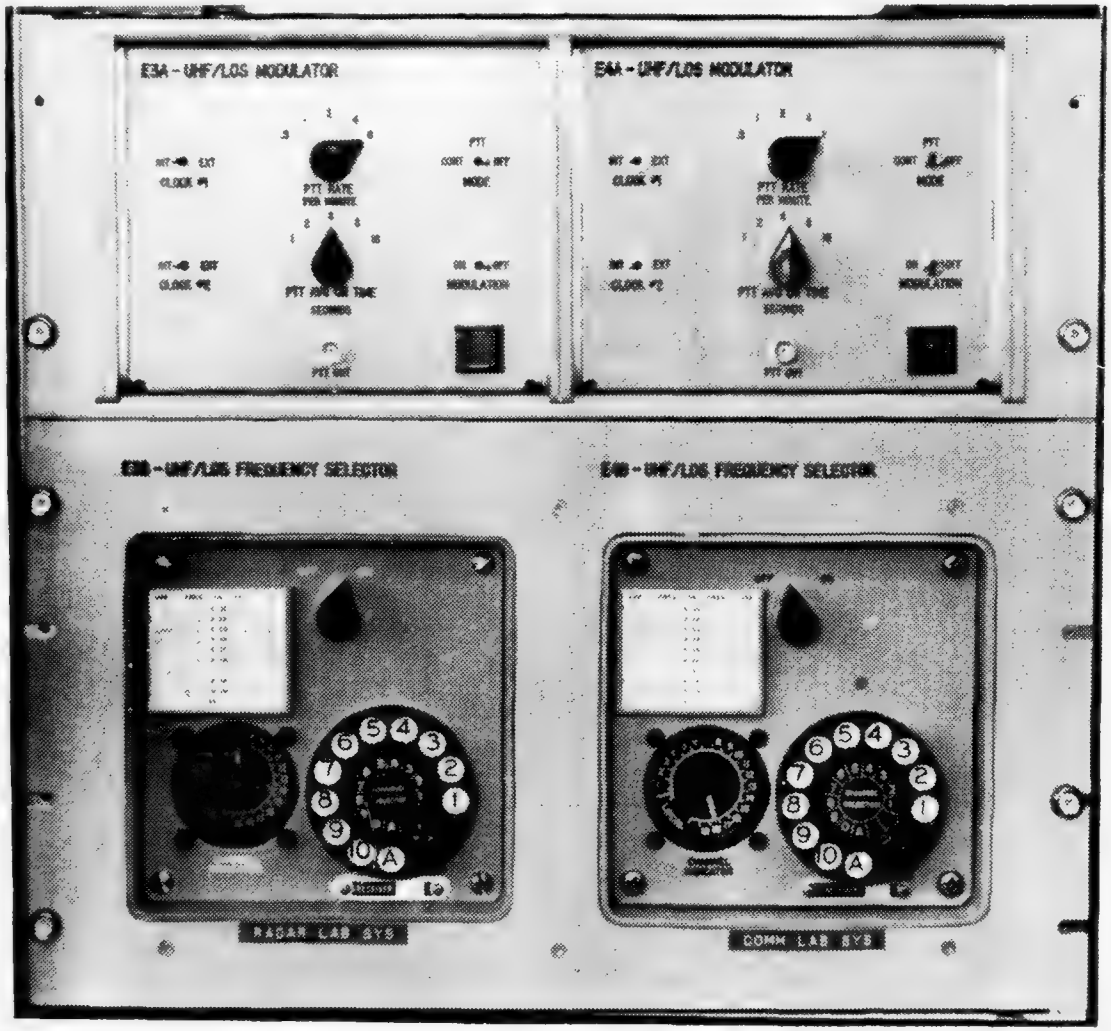

Figure 21: Front Panel of E3A(E4A) UHF/LOS Modulator and E3B(E4B) UHF/LOS Frequency Selector.

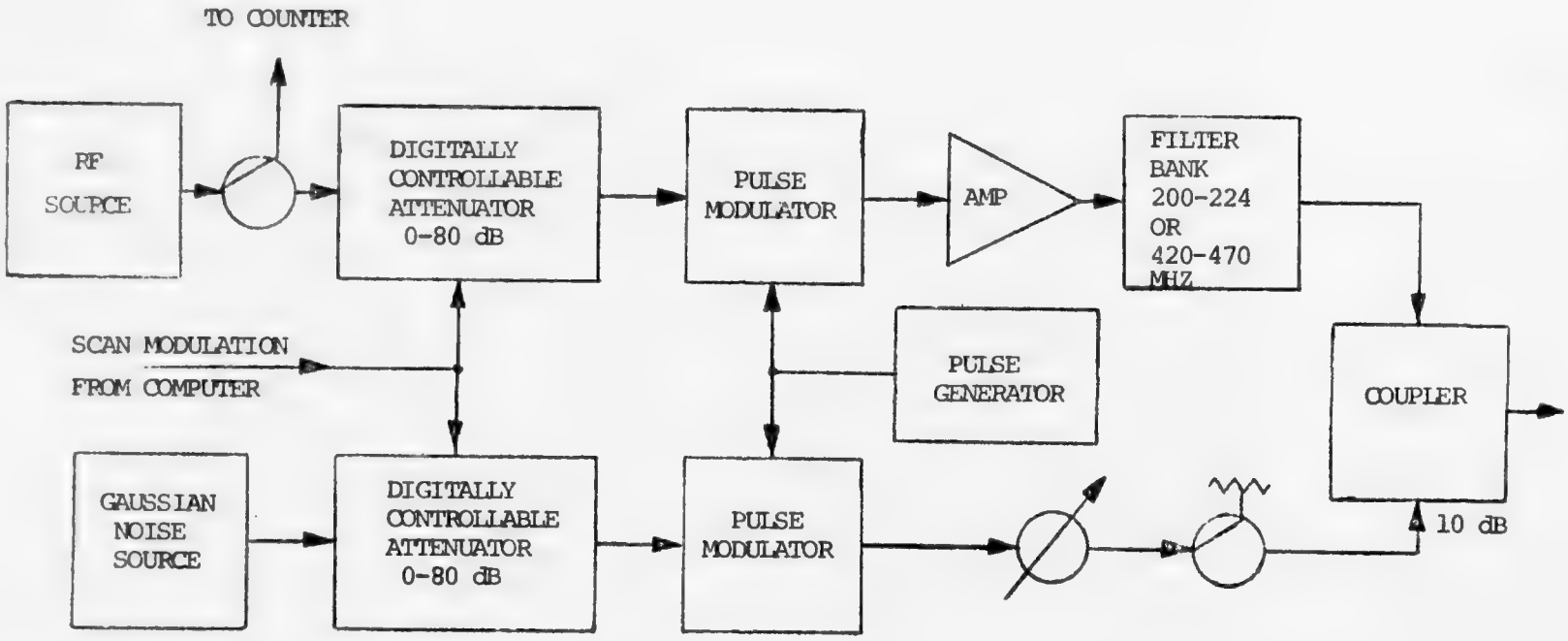

Figure 22: E5-UHF/RADAR Interferer Block Diagram

AD-A035 743 NAVAL POSTGRADUATE SCHOOL MONTEREY CALIF F/G 17/2.1
A SIMULATOR FOR SHIPBOARD RADIO FREQUENCY INTERFERENCE IN SATEL--ETC(U)
OCT 76 E S BRICK, J E OHLSON
UNCLASSIFIED NPS-620L76109 NL

2 OF 3
AD-A
035 743

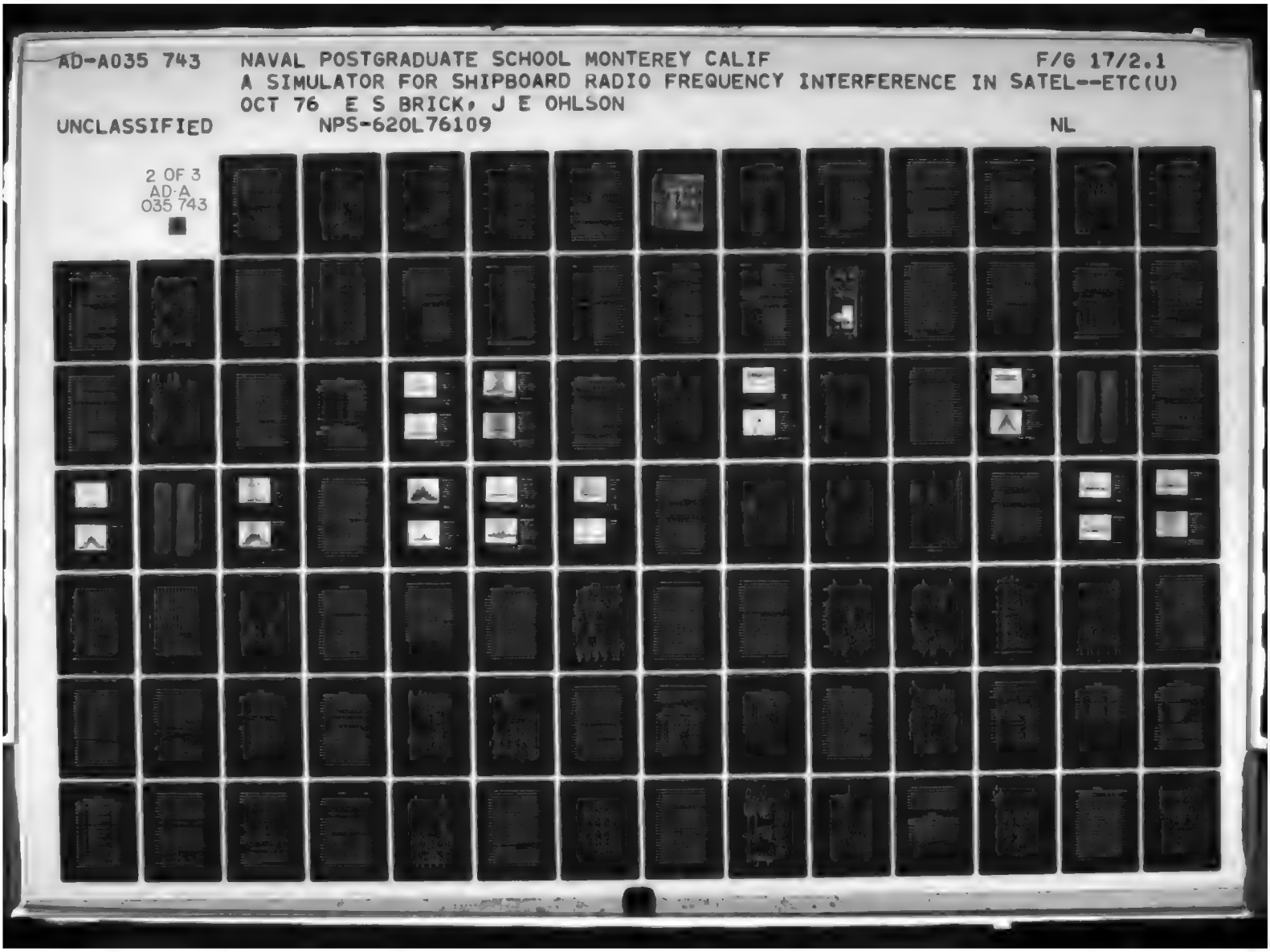

at the scan rate (a(t)), modulates both the carrier and the noise. Both signals are also pulse modulated at two different pulse modulators but by the same modulating signal s(t). The modulated RF carrier is then amplified by a 30 dB gain, 36 dBm 1 dB compression point linear amplifier and filtered by one of two band-pass filters selectable by switches on the panel of one of the units. The modulated noise can be attenuated or turned on and off, also by front panel control, before being comgined with the modulated RF by a 10 dB directional coupler.

The E5 emitter is divided in 6 different units in order to perform its function. A brief description of the functions performed by each unit is given below and an interconnection diagram of the various units is given in Figure 23.

Unit	Description
E5A-RADAR PULSE MODULATOR	Performs pulse modulation of noise and carrier. Also performs attenuation on noise and provides ON/OFF control for noise.
E5B-RADAR AMPLIFIER	Amplifier for the modulated RF carrier.
E5C-RADAR SCAN MODULATOR	Generates the scan repetition frequency, performs the scan modulation of both RF and noise, performs the filtering of the

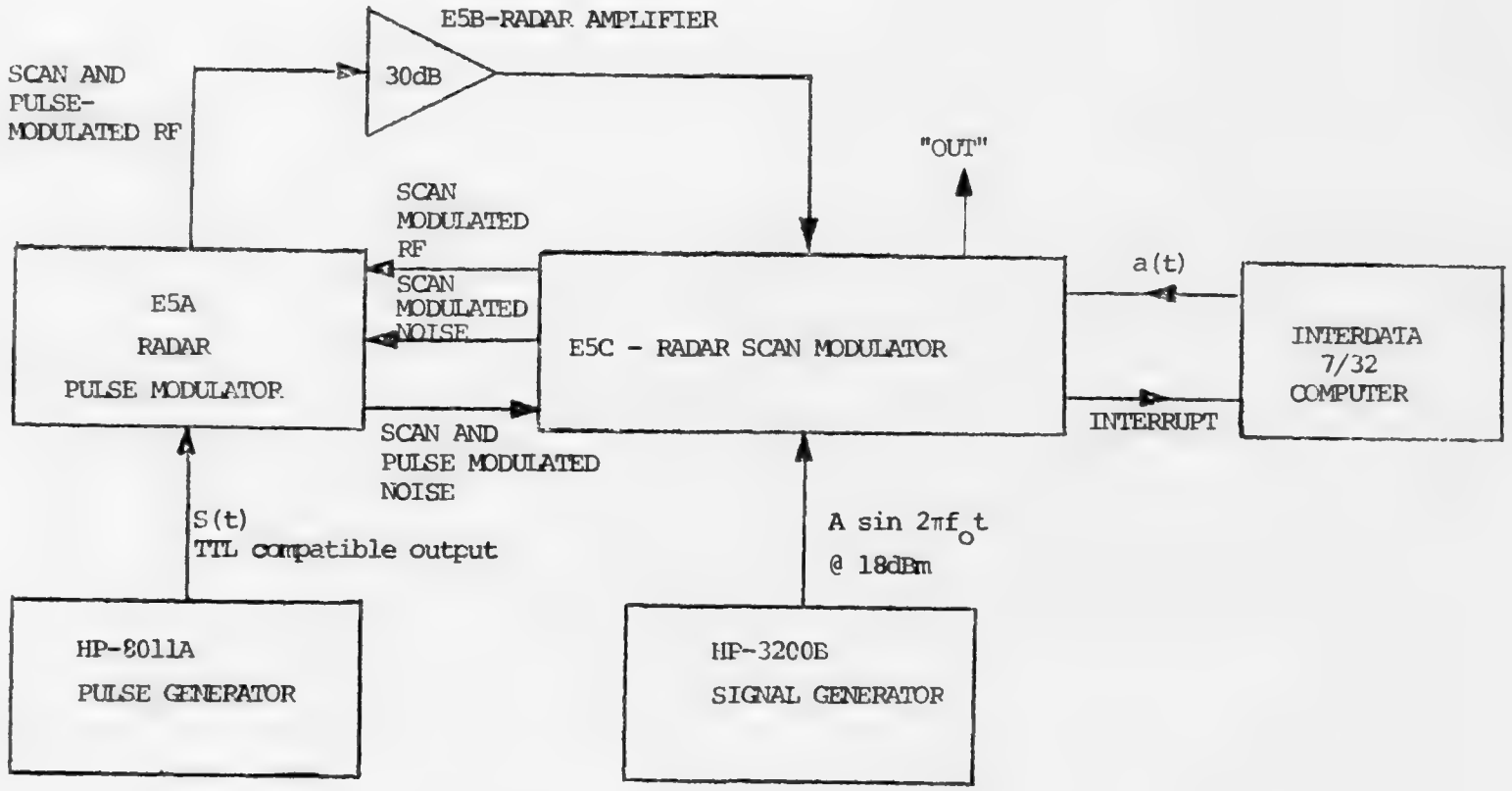

Figure 23: Interconnection of Units in E5.

	modulated RF carrier, provides ON/OFF control for the RF, adds the modulated RF and noise to give the E5 output.
PULSE GENERATOR	A HP-8011A pulse generator with continuous control of PRF and PW.
RF SOURCE	HP-3200B VHF-oscillator. Capable of delivering more than 18 dBm of power in the band of interest.
COMPUTER	INTERDATA 7/32. Provides programming and storage capability to generate the scan modulating signal. Works on a real time basis triggered by interrupts generated in Unit E5C at 360 times the antenna scan rate.

The operator has access to the following control and ports on the front panels of the different units:

a) Unit E5A - RADAR PULSE MODULATOR

NOISE SECTION:

"ATTENUATION"	When in the 0 dB position the noise, when pulsed on, will correspond to a level ~60 dB above thermal at the simulator

	output ("OUTPUT" port at C1) when the E5 attenuator on C1 is also at 0 dB.
"ON/OFF"	This switch will turn on and off the noise component of the radar emitter.

PULSE SECTION:

"PULSE IN"	TTL compatible input for the pulse modulating signal s(t) (50Ω input impedance).
COUNTER SWITCH	SPDT RF switch. Directs the modulating signal s(t) either to pulse modulators driver or to the counter in order to measure PRF.
"PULSED RF OUT"	Type N connector providing the scan and pulse modulated RF carrier to be connected to the input of the E5B RADAR AMPLIFIER.

b) Unit E5B - RADAR AMPLIFIER

This unit has only an ON/OFF power switch and RF INPUT and OUTPUT connectors.

c) Unit E5C - RADAR SCAN MODULATOR

"BAND"	DPDT RF Switch selecting the desired filter for the modulated RF carrier. The two options

	correspond to 3 dB bandwidth band-pass filters of 200-224 MHz and 420-470 MHz.
"SCAN RATE"	Selects the internally generated scan rate frequency in RPM. The options are 5, 6, 7, 12, 15 RPM.
"RF"	SPDT RF switch commanding the input from the signal generator. The RF carrier is either turned on ("ON" position) or fed to the counter ("COUNTER" position) for frequency measurement.
"PULSED RF INPUT"	Connected to the OUT of the E5B RADAR AMPLIFIER.

d) Description of controls and operation of the three remaining units (HP-8011A, HP-3200B and INTERDATA 7/32) can be found in the technical manuals of those units.

Detailed description with inclusion of schematic diagrams for Emitter 5 is restricted to Appendix 4. Photograph of front panels of Emitters 5 and 9 is shown in Figure 24.

4. EMITTERS 6 and 7 (E6 and E7)

For Emitters 6 and 7 the only requirement was the generation of a high level (close to 30 dBm) CW signal at the used VHF or HF communications bands. The block diagram in Figure 25 shows how this was achieved. The carried from the signal generator is amplified by a 16 dB gain amplifier,

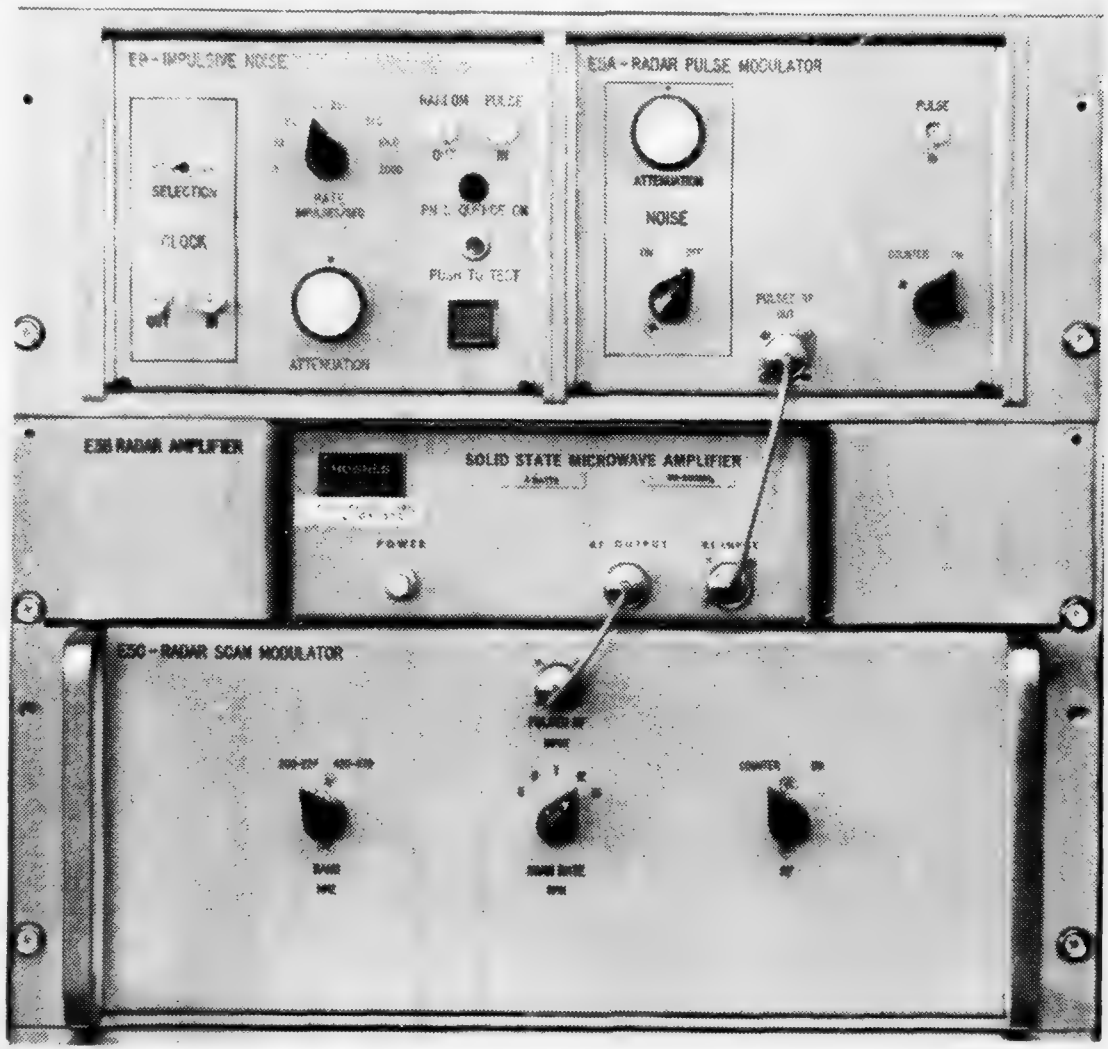

Figure 24: Front Panel of Units E5A, E5B, E5C and E9.

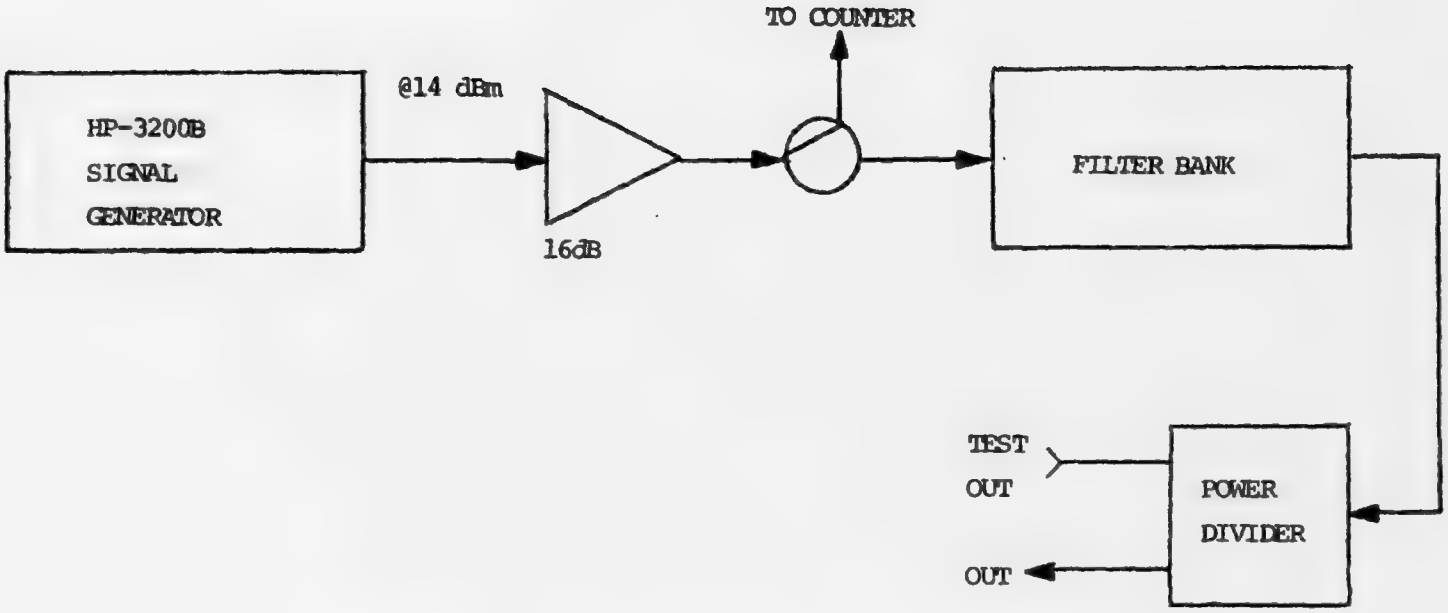

Figure 25: E6(E7) Interferer Block Diagram.

with a 1 dB compression point of 30 dBm. The amplified signal is then filtered by one of two filters depending on the selected frequency. This signal is split in two equal parts, one being the emitter signal the other being available at a "TEST OUTPUT" port on the front panel for monitoring or any other desired purpose. Emitters 6 and 7 are located in the same unit and both have the following control ports on the front panel.

"BAND"	DPDT RF switch commanding the selection of the proper bandpass filter. For Emitter 6 the options are 40-75 MHz or 108-200 MHz. For Emitter 7 the options are 10-16 or 16-26 MHz.
"RF"	SPDT RF switch that can direct the signal to the nonlinearities for processing ("ON" position) or to the counter for frequency measurement ("COUNTER" position).
"TEST OUT"	Provides a replica of the signal for monitoring or any other purpose. (CAUTION: level up to 29 dBm.)

Schematic diagrams and detailed description of Emitters 6 and 7 are given in Appendix 5.

5. EMITTER 8 (E8)

The requirements for Emitter 8 were the same as for Emitters 6 and 7. The only difference between them is in

the physical implementation. Emitter 8 was derived directly from a HF transmitter (T-827B/URT) located in the Communications Laboratory. This unit (T-827B/URT) is actually a synthesizer with a preamplifier capable of delivering up to 28 dBm of power and thus we have used this signal directly without the need for an amplifier. The block diagram for E8 is identical to the one for E6 and E7 if we substitute the signal generator and the amplifier for the T-827B/URT transmitter. The operator has the same controls on the front panel with the exception that the filters available are 0-6 MHz and 6-10 MHz.

Located in the same unit E8, but completely isolated from Emitter 8 is the circuit to generate the 30 MHz stable reference frequency for Emitters 1 and 2 and the signal. This was done in order to use the empty space in the unit. Detailed description of Emitter 8 as well as the 30 MHz reference circuit is reserved for Appendix 5.

6. Emitter 9 (E9)

An impulsive source of interference was included in our model not only because previous sources of man-made noise have shown to possess an impulsive characteristic but also because we believe that the interference caused by many radars (in a task force, for example) firing at random, will give rise to a similar kind of signal. The model adopted was a general one with the hope that this will cover the widest span of possible sources of impulsive interference. A randomly occurring stream of random-like pulse waveforms was considered

to be very appropriate for that purpose and the mathematical model was established by expression (3.14)

$$y(t) = a(t)\ n(t) \qquad (3.14)$$

where a(t) is a sequence of randomly occurring pulses of variable pulse width and pulse rate and n(t) is a broadband Gaussian noise process.

The block diagram of Emitter 9 is given in Figure 26. A pseudo-random Poisson process is generated in the same way used to generate the PTT statistics for Emitters 3 and 4, and is used to trigger a pulse generator whose pulse width (PW) can be continuously varied. The output of the pulse generator is then fed to a driver circuitry to pulse modulate a source of Gaussian noise. The result is a random stream of samples of a Gaussian noise source that constitutes Emitter 9. The controls abailable to the operator on the front panel of E9 are as follows.

"SELECTION" Selects the source of the clock that will determine the impulse rate. In "INT", the internal clock is used and the "RATE" switch is correctly calibrated. In "EXT", any TTL compatible external clock fed to the "IN" port will determine the impulse rate.

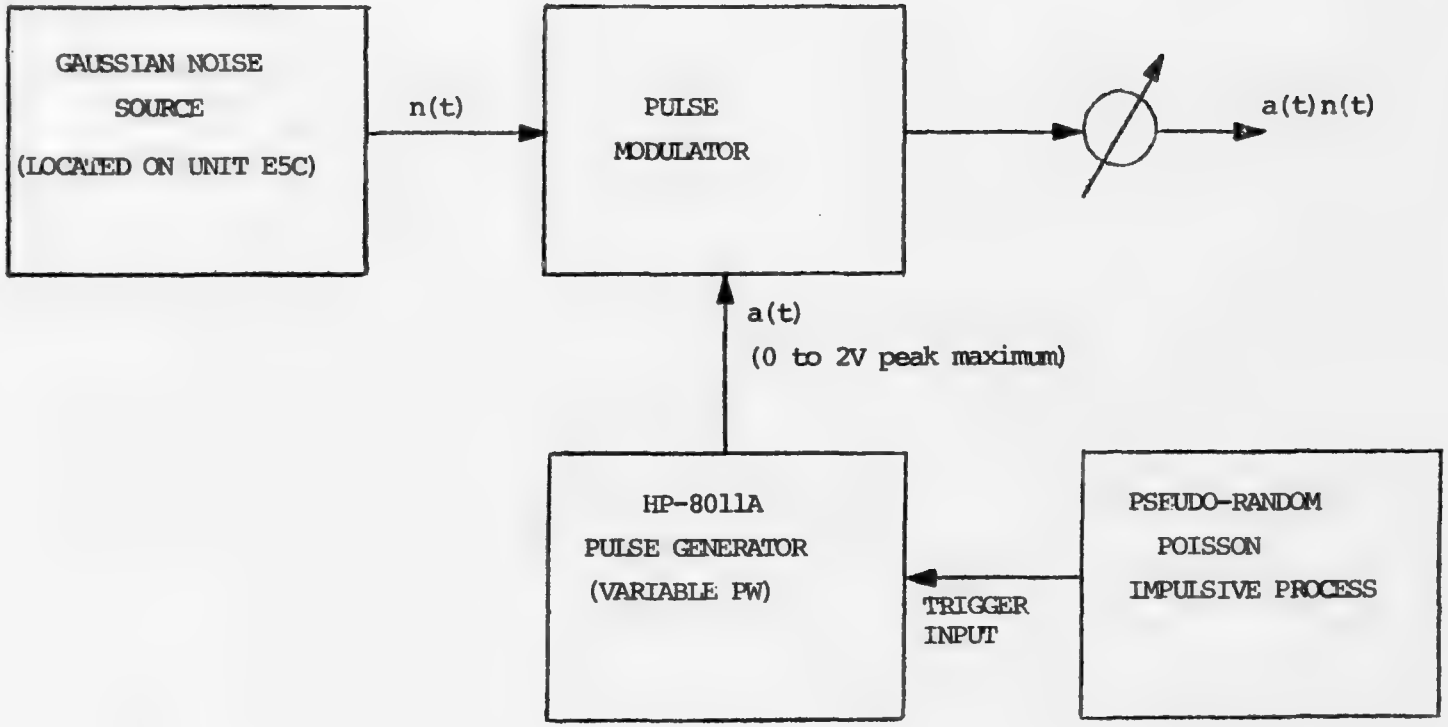

Figure 26: E9 Impulsive Noise Block Diagram.

"OUT"	This output port provides a replica of the clock being used (either internal or external) by the unit and is derived from a TTL line driver and thus accepts a 50Ω load.
"IN"	TTL compatible input for an external clock.
"RATE"	Eight-positions rotary switch selecting the desired impulse rate in seconds^{-1}. The nominal available rates are: 15, 30, 60, 125, 250, 500, 1000 and 2000 sec^{-1}.
"RANDOM OUT"	OUTPUT derived from a TTL line driver (50Ω load accepted) representing the pseudo-Poisson process that will trigger the pulse generator.
"PULSE IN"	Pulse-modulator driver input from the pulse generator. CAUTION: This is not a TTL input. It is a 50Ω input requiring a 0 to 1.5-2.5 volts peak signal. A signal exceeding 3V will damage the mixers used to pulse modulate the noise.
"PN SEQUENCE ON"	LED used to indicate that the PN sequence used to derive the pseudo-Poisson process is working properly.

"PUSH-TO-TEST"	Monitoring switch used only to test the "PN SEQUENCE ON" LED.
"ATTENUATION"	Rotary attenuator providing control of the overall emitter level. When in the 0 dB position the level of the pulsed noise at the "OUTPUT" port of C1 (output of the simulator) will be of 40 dB above thermal noise.

Detailed description of Emitter 9 is given in Appendix 6. Photograph of front panel of Emitter 9 is shown in Figure 24.

7. EMITTER 10 (E10)

The background Gaussian noise interference was simulated by using a Gaussian noise source capable of delivering a signal with a power of 40 dB above thermal at the simulator output terminal. A 0-60 dB, 1 dB step attenuator provides control of the level of this emitter. Evidently any attenuation greater than 40 dB will completely nullify this signal at the "OUTPUT" port.

Schematics and detailed description for E10 are found in Appendix 8.

8. Signal

In order to be able to test the performance of a SATCOM receiver in the interference environment a signal source had to be built. Figure 27 contains the block diagrams of the signal source. The construction of the

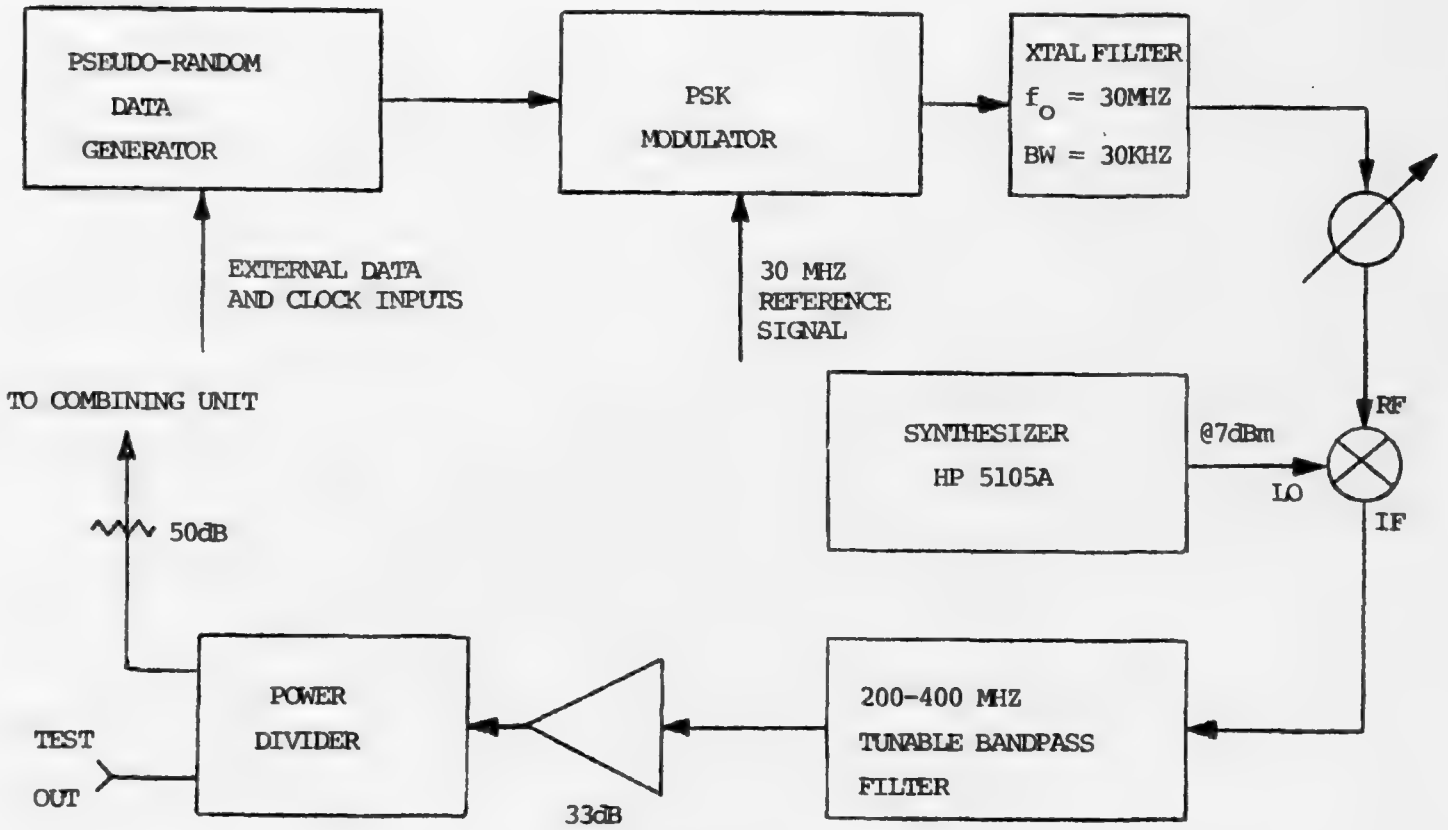

Figure 27: S1 - Signal Block Diagram.

signal is similar to the one used for E1 and E2 Emitters with some noticeable differences. The PRBS internally generated or as an externally provided data, PSK modulates a 30 MHz stable reference carrier. This signal can be filtered by a 30 kHz bandpass filter which can be turned on and off by a coaxial transfer switch commanded electrically by a toggle switch on the front panel of the unit. The signal can then be attenuated in 1 dB steps from 0 to 60 dB's before being up-converted in a mixer whose local oscillator is derived from a HP5105A synthesizer. The signal is then filtered by a 3% bandwidth, tunable bandpass filter before being amplified by a 33 dB gain amplifier which is used to elevate the signal to a level where it can be accurately monitored by a power meter at the "TEST OUT" port. The signal power level measured at the "TEST OUT" is reduced by a total of 102.9 dB (50 and 3 dB attenuators in S1 and 50 dB attenuator in C1) plus the attenuation due to processing in Unit C1 as given by the calibration chart in Figure 28. The accuracy of the total attenuation can be calculated by adding the uncertainty of individual components and measurements as follows:

50 dB attenuator - 50.04 dB ± .5 dB

50 dB attenuator - 50.07 dB ± .5 dB

3 dB attenuator - 2.77 dB. Less than ± .1 dB

Power measurement with HP435A - less than ± .1 dB

Accuracy of Calibration Chart - less than ± .1 dB

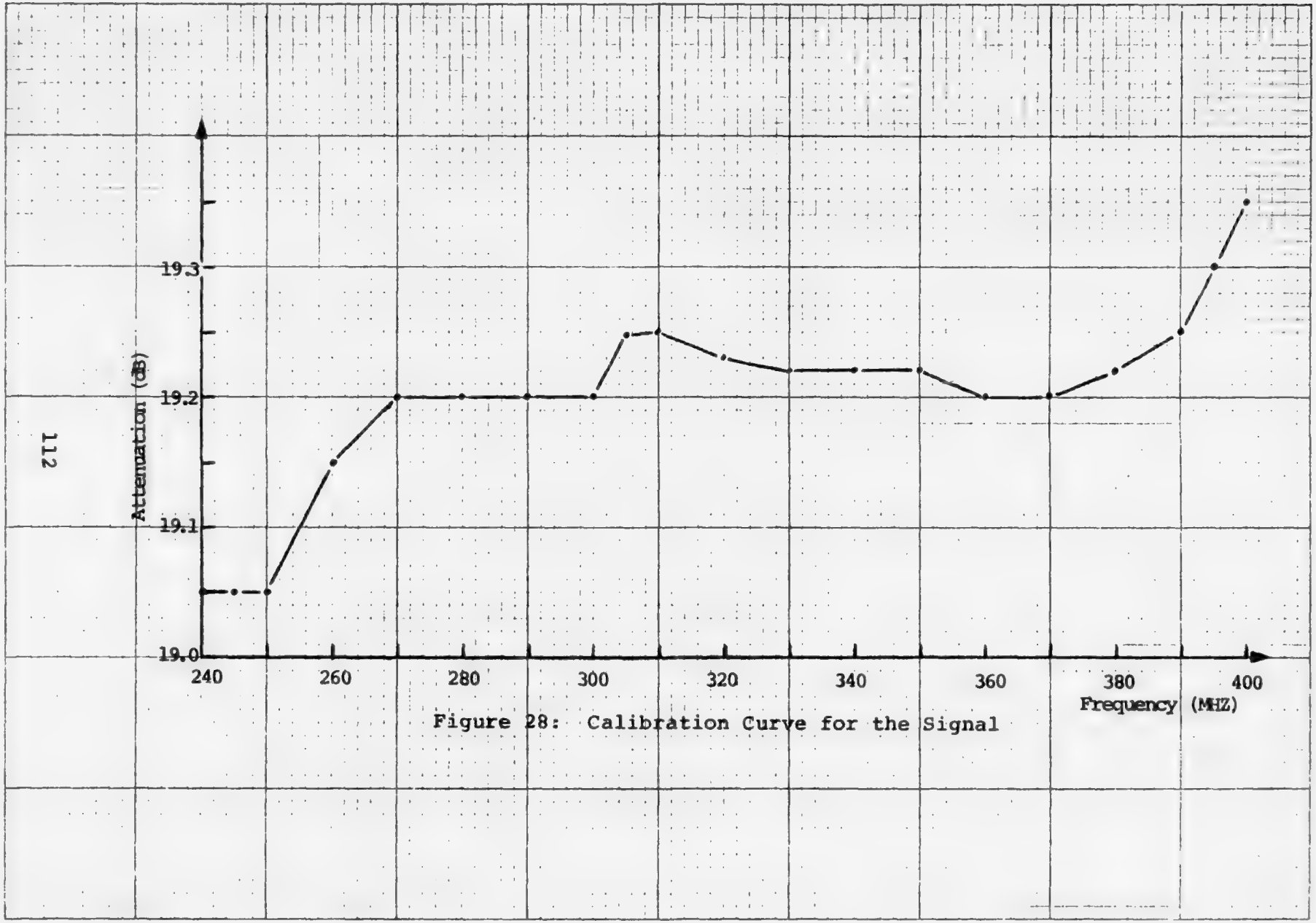

Figure 28: Calibration Curve for the Signal

Since the maximum power level measured at the "TEST OUT" terminal is about 17 dBm and the nominal attenuation on unit C1 is 19 dB, a 37 dB variation of signal level (power meter measuring from 17 dBm to -20 dBm) will provide a signal at the receiver port varying from -105 to -142 dBm. This is adequate to measure performance of receivers operating with rates up to 9.6 kHz in white Gaussian noise. For higher data rates, a 3 dB pad on the back of the unit can be removed changing the span of signal level to -102 dBm down to -135 dBm.

The operator has access to the following controls and ports on the front panel of the unit.

DATA SECTION:

"SYNC OUT" — This output connector provides a synchronism signal each time a sequence period is completed, when the "REGISTER LENGTH" switch is in position 5. On the other positions (10 and 20) this output is just a pseudo-random output obtained by detecting a subsequence of length 5 on the PN sequences that are being generated as data. This signal is derived from a TTL line driver and will accept a 50Ω load.

"REGISTER LENGTH"	This switch selects the size of the register being used to generate the PN sequence. Options available are 5, 10 and 20. Ir all positions, feedback is made from flip-flops 1 and 4 in the register.
"ENCODING"	This is a toggle switch with options "PSK" and "DPSK". In the "PSK" position the carrier is PSK modulated with the data (either internal or external). In the "DPSK" position the data is differentially encoded before modulating the carrier.
"SOURCE"	Toggle switch used to select the source of data that will modulate the carrier. In the "INT" position, the internally generated PRBS is used and is also available at the "OUT" port. In the "EXT" position, any TTL compatible data sequence fed to the "IN" port will be used as the source of modulation. In that case the "OUT" port will also provide a replica of the external signal.*

*Any external data must have transitions at the leading edge of the clock which, in addition, must also be available in order that the encoding circuit can work properly.

"OUT" — Data output derived from a TTL line driver (accepts a 50Ω load). When "SOURCE" switch is in "INT", the output is the internally generated sequence. When "SOURCE" switch is in "EXT" and a data source is connected to the "IN" port, this terminal will provide a replica of the external data. "ENCODING" switch has no effect on the signal at this port.

"IN" — Data input. TTL compatible circuitry.

CLOCK SECTION:

"OUT" — Clock output port. Provides output of internally generated or externally applied clock, depending on the position of the "SELECTION" switch. This output is derived from TTL line driver and accepts a 50Ω load.

"IN" — Clock input port. TTL compatible input for an external clock. Lowest clock rate acceptable is 75 Hz. MUST BE USED when selecting external data source.

"RATE" — Clock rate selection switch. Allows the selection of five different clock rates (1.2, 2.4, 4.8, 9.6 and 19.2

KHz) from the internal clock. It has no function when an external clock is being used.

"SELECTION" — Toggle switch with two positions: "EXT" and "INT". Selects external or internal clock source.

Other Controls:

"LO IN" — N-type connector. Input for the local oscillator at a level of 7 dBm (from HP 5105A).

"MODULATION" — This switch commands the modulation of the carrier. In the "OFF" position the signal is unmodulated. In the "ON" position the carrier is PSK modulated by the data ("ENCODING" switch in "PSK") or by a differential version of it ("ENCODING" switch in "DPSK").

"30 kHz FILTER" — Toggle switch that commands electrically the transfer switch used to insert a 30 KHz bandwidth filter on the filter line. Two indicator LEDS are lighted from DC lines that are switched together with the RF part of the transfer switch, giving reliable indication of the status of the filter (whether ON or OFF).

"ATTENUATION"	Rotary attenuator, 0 to 60 dB in 1 dB steps used to control the signal level.
"TEST OUT"	OUTPUT Port containing a high level (up to 17 dBm) version of the signal, used to accurately measure the power level of the signal at the receiver terminals.

Detailed description of the signal unit as well as schematic diagrams have been reserved for Appendix 7. Photograph of the front panel of S1 signal is shown in Figure 29.

9. Other Units

In addition to all the above mentioned units the system has also a power supply unit (PS1) which provides the following DC voltages:

+15V	to the pin-diode attenuator driver in E5C-RADAR SCAN MODULATOR
-15V	to the pin-diode attenuator driver in E5C-RADAR SCAN MODULATOR
+ 5V	to the pin diode attenuator driver in E5C-RADAR SCAN MODULATOR and the pulse-modulator driver in E5A-RADAR PULSE MODULATOR.
+24V	To amplifiers in E1C/E2C UHF/PSK AMPLIFIERS, E6/E7 - VHF/HF INTERFERERS, N1 and N2 NONLINEARITIES and to the Gaussian noise source located in E5C-RADAR SCAN modulator.

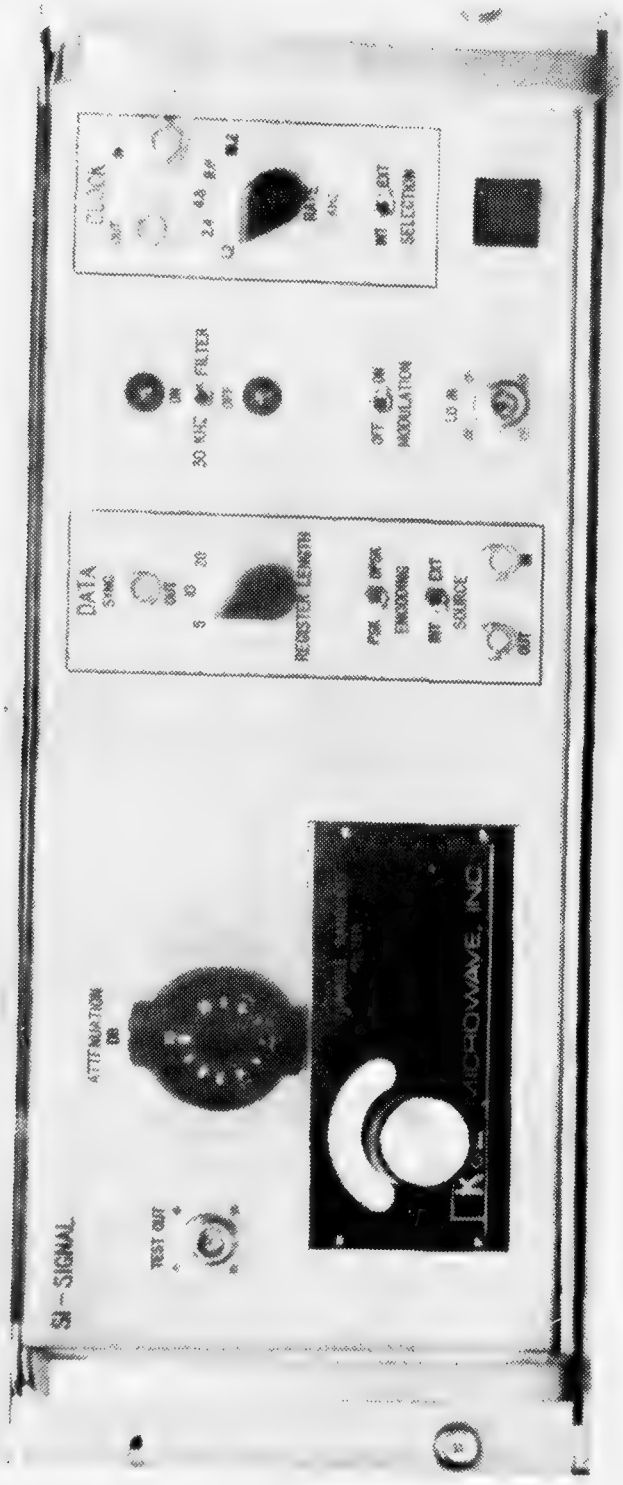

Figure 29: Front Panel of S1-SIGNAL

In addition to these supplies located in PS1 and the individual power supplies in the various units such as E1A, E2A, E3A, E4A and S1, there is still another +15V power supply located in E10-GAUSSIAN NOISE that supplies power to the amplifiers of the 30 MHz reference signal in E8.

The last part of the system remaining to be described is the COUNTER. It is a HP 5383A counter with a selection circuit with 8 input ports and one output. All the input ports are terminated in a 1 Watt, 50Ω load and the selected channel is attenuated by at least 20 dB before being available at the "OUT" port. Because the signals being fed at the input port can be as high as 1 Watt and the counter sensitivity is as low as -20 dBm, cross talk between channels may disturb the measurement when two or more signals are present at the input ports. For that reason, when making frequency measurements, the operator must make sure that only one emitter is connected to the "COUNTER" position. When not making measurements, the COUNTER switch on the various emitters can be turned to the "COUNTER" position because in this situation the signals will be dissipated on the 50Ω loads at the counter input ports. The COUNTER switches in this situation will be operating as ON/OFF switches. Schematics for unit PS1 and selection circuit for the counter can be found in Appendix 8.

10. General Remarks

All units of the simulator are installed in three, 63-inch high, standard 19-inch wide racks with the exception

of the UHF/LOS transmitters, the HF transmitter, the computer and the 5 MHz standard which are located elsewhere in the Communications and Radar Laboratories. The racks are positioned side by side with two other racks containing the AN/WSC-3 satellite communications set and the AN/SSR-1 receiver which will be tested against interference. Figures 10, 15, 16, 18, 24 and 25 show photographs of the whole setup and of some of the individual units.

Concerning the construction of the units, all RF cabling was done with semi-rigid .141" coaxial cables, all amplifiers were extensively protected with RFI filters and all components processing RF were built in shielded cases. In addition, all power supply connectors were filtered with low-pass π filters in our attempt to reduce RF leaking from the individual units.

Interconnection of different units was done with RG-223/U or RG-214/U (double shielded cables) to reduce picking up of spurious radiation by the individual cables. The interconnection table for the various units is presented in Appendix 11.

V. SIMULATOR PERFORMANCE

The system described in Chapter IV has been built and its performance is given in this chapter.

A. C1 - COMBINING UNIT

This unit can be best described by giving the measured attenuation of various emitters from the input ports on the back of the units to the "OUTPUT" port when all attenuators are set to zero. This was done and the results are listed in Table 3.

Table 3

Attenuation of the Various Signals in C1

FREQUENCY (MHz)	200	250	300	350	400	EMITTER
ATTENUATION (dB)	19.4	19.5	19.3	19.5	19.5	E1
	20.6	21.0	21.0	19.9	19.5	E2
	19.2	19.8	19.0	19.4	19.2	E3
	19.0	19.8	19.2	19.3	19.3	E4
	4.9	4.2	4.0	3.8	3.4	E5
	12.2	12.3	12.5	12.2	12.4	E9
	33.3	33.4	34.1	34.6	34.3	E10
	18.9	18.9	19.0	19.2	19.0	S1 (*)
	18.9	18.9	19.0	19.2	19.0	EXT. INPUT

(*) Precise measurements for S1 are given in Figure 28: Add 50 dB to the values shown.

Another set of data that gives an indication of the overall performance of the simulator is the power available from each emitter at the "OUTPUT" port when in normal operation. The results of measurements are given in Table 4 for Emitters 1 through 5.

Table 4

Power Available from Emitters 1 Through 5 at OUTPUT port in C1

EMITTER	AVG. POWER (dBm)	CONDITIONS OF MEASUREMENT
E1	0.5 @ 240 MHZ; 2.3 @ 320 MHZ; 0.3 @ 400 MHZ	MODUL."ON"; REG. LENGTH "5"; PSK; RATE "19.2 kHz".
E2	-0.5 @ 240 MHZ; 0.5 @ 320 MHZ; 0.5 @ 400 MHZ	MODUL."ON"; REG. LENGTH "5"; "DPSK"; RATE "4.8 kHz".
E3	6.5 @ 237.5 MHZ; 7.6 @ 319.1 MHZ; 9.1 @ 353.8 MHZ	MODE "CONT"; MODUL. "OFF".
E4	9.2 @ 237.5 MHZ; 7.4 @ 319.1 MHZ; 11.2 @ 353.8 MHZ	MODE "CONT"; MODUL. "OFF".
E5	18.8 @ 210 MHZ; 22.4 @ 445 MHZ	PRF=1 kHz; PW=100 μsec.

B. NONLINEARITIES N1 AND N2

As explained in Appendix 1 the nonlinearities are realized by loading a 50Ω micro-strip transmission line with two back-to-back Schottky diodes. The sum of all emitters is amplified by an amplifier before being fed to the nonlinearities with the double purpose of raising the level of the weakest

signals to the threshold of nonlinearities and provide a sufficient reverse isolation to cut down the level of the INTERMODS that would travel back on the various signal lines after being generated at the nonlinearities. The nonlinearity threshold was measured by defining a 1 dB EXPANSION POINT as follows.

1 dB EXPANSION POINT - fundamental power at which a given harmonic of the signal will experience a 1 dB increase relative to its normal level measured on a linear processing setup.

In other words we measure the power of a given harmonic versus the power of the fundamental with or without the nonlinearity inserted in the circuit. The fundamental power at the point where we observe a 1 dB increase on the harmonic level is the 1 dB EXPANSION POINT. This quantity may be, of course, a function of the relative amplitude of the harmonic to the fundamental, frequency and other variables but we found these possible variations to be irrelevant to the purpose of defining a nonlinearity threshold for intermodulation generation.

The threshold measurement set-up and the results are given in Figure 30. Based on these results we established that a minimum power level of 10 dBm from each emitter would be necessary to drive the nonlinearities well into the nonlinear region. We thus calibrated the system so that the weakest signal would be capable of delivering at least 10

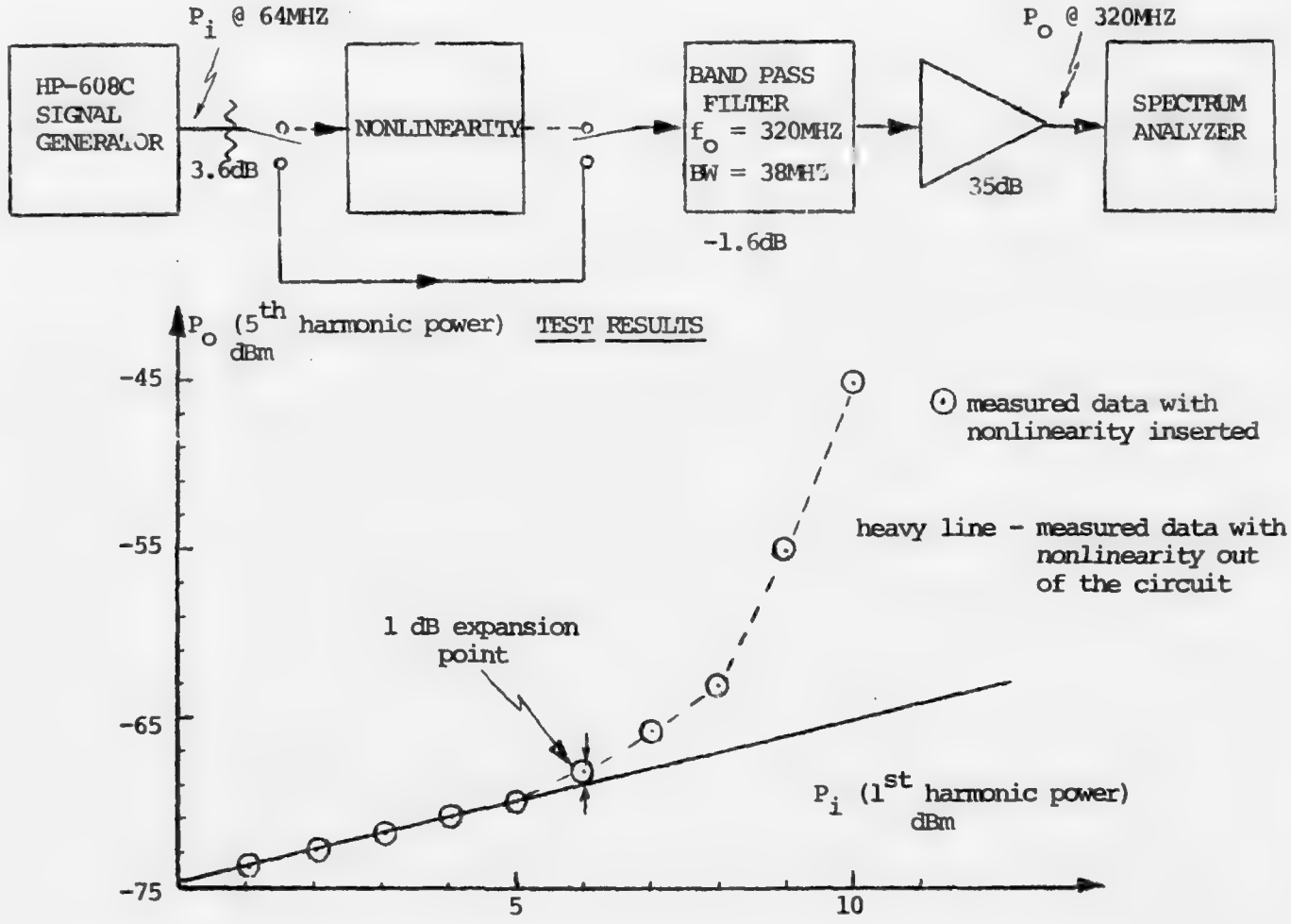

Figure 30: Nonlinearity Threshold Measurement.

dBm of power to the nonlinearities. Since there is a wide difference in the power of the different emitters it may happen that some emitters will saturate the amplifier preceding the nonlinearity. In that case the intermodulation products would be generated both at the amplifier and at the nonlinearity. In order to establish the minimum amount of attenuation that each emitter should have in order to individually keep the amplifier in the linear region, measurements were made of the power available from each emitter at the amplifier input. The results of these measurements are given in Table 5. Since the gain of the amplifiers is 33 dB and the 1 dB compression point is 22 dBm we see that each emitter should be restricted to a maximum -11 dBm level at the amplifier input. The amount of power available as given by Table 5 indicates the minimum attenuation that each emitter must have in order to keep the amplifier in the linear region.

Another set of measurements that is relevant to describe the performance of N1 and N2 is the one giving the total amount of attenuation from the emitters input terminals to the amplifier input terminal in each nonlinearity. These results are given in Tables 6 and 7.

The ultimate performance test on Units N1 and N2 was done by showing that the units are able to generate INTERMODS from a combination of input signals as shown in Figures 31 to 34.

Table 5

Available Power at Nonlinearities Amplifiers Inputs from Each of the Emitters

EMITTER	Power at N1 (dBm)	Power at N2 (dBm)	OBS
E1	-12.0	-12.3	320 MHZ,REG.LENGTH="5", RATE=19.2 kHZ.
E2	-12.5	-12.9	320 MHZ,REG.LENGTH="5", RATE=4.8 kHZ.
E3	- 5.7	- 4.4	353.8 MHZ,MODUL.="OFF".
E4	- 3.5	- 3.0	353.8 MHZ,MODUL."OFF".
E5	- 1.5	- 1.4	Peak power, 445 MHZ, PRF=1 kHZ, PW=100 sec.
E6	- 3.8	- 3.7	60 MHZ.
E7	- 4.4	- 4.4	20 MHZ.
E8	- 4.8	- 4.5	5 MHZ.

Table 6

Attenuation from Input Ports to Input of Amplifiers in Nonlinearities N1 and N2

FREQUENCY (MHz)	200		250		300		350		400	
UNIT	N1	N2	N1	N2	N1	N2	N1	N2	N1	N2
E1	32.2	32.2	32.7	32.5	33.0	33.0	33.1	33.4	33.5	33.6
E2	33.8	33.9	33.7	33.7	34.3	34.3	34.0	34.3	33.6	33.7
E3	32.1	31.8	32.3	32.3	33.1	32.9	34.1	33.3	33.5	33.6
E4	32.2	31.9	32.4	32.4	33.1	32.8	33.9	33.4	33.3	33.8
E5	37.7	36.1	37.5	37.0	37.4	37.4	37.9	38.4	39.0	38.7

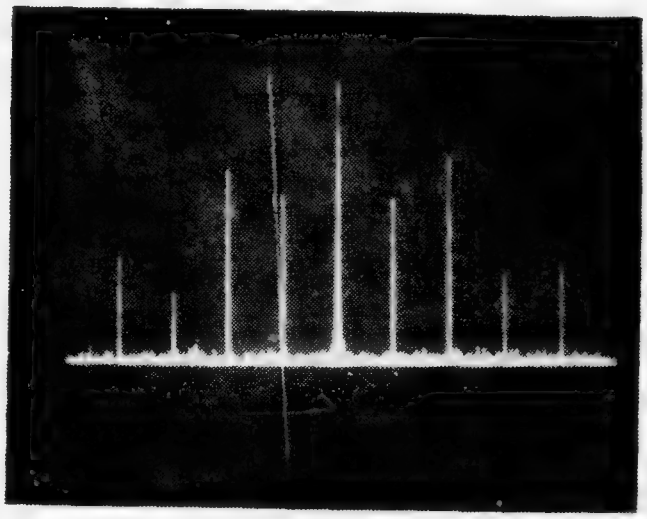

Spectrum Analyzer

f_0 = 445 MHZ
20 MHZ/DIV
10 KHZ BW
2 SEC/DIV
Attenuation = 20 dB
Log. reference = -20 dBm
Video Filter = 10 kHz
10 dB/DIV

Figure 31: Spectrum of intermodulation products generated by a HF CW signal @ 20 MHZ (E7) and an UHF/RADAR at 445 MHZ, PRF = 1 kHZ, PW = 100 μsec (E5). (The settings of the attenuators in NONLINEARITY #1 were: E7 = 7 dB, E5 = 10 dB, N1 = 0 dB. Measured at "TEST OUT" in C1.)

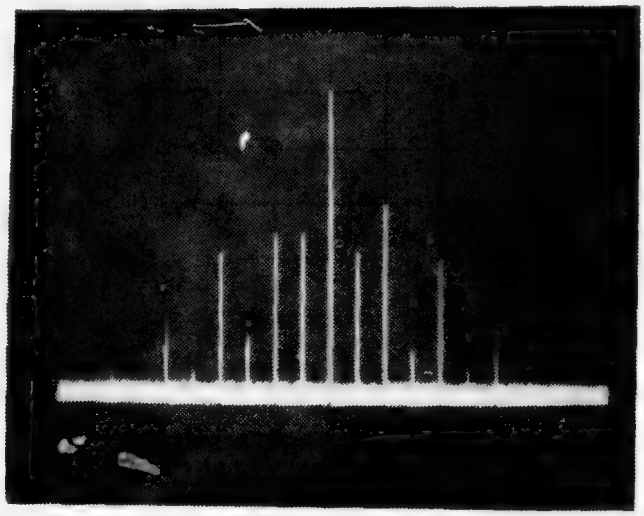

Spectrum Analyzer

f_0 = 300 MHZ
10 MHZ/DIV
100 KHZ BW
.5 SEC/DIV
Attenuation = 10 dB
Log reference = -20 dBm
Video Filter = 10 KHZ
10 dB/DIV

Figure 32: Spectrum of intermodulation products generated by a HF CW signal at 5 MHZ (E8) and an UHF/PSK @ 300 MHZ, 4.8 kHz data rate (E2). (The settings of the attenuators in NONLINEAPITY #1 were: E2 = 5 dB, E8 = 10 dB, N1 = 0 dB. Measured at "TEST OUT" in C1.)

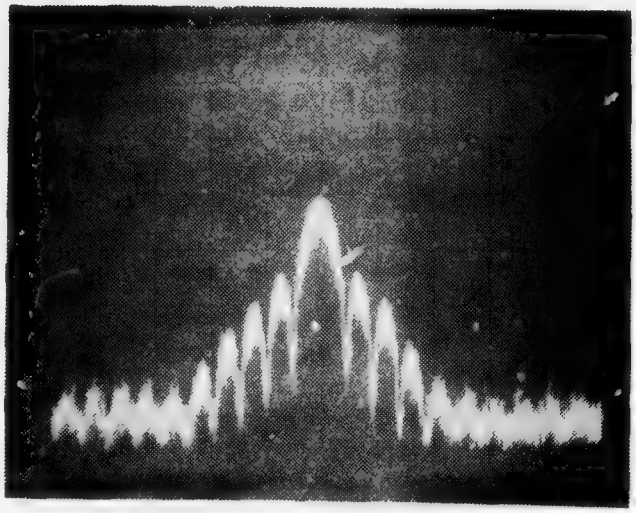

Spectrum Analyzer

f_0 = 290 MHZ
10 kHZ/DIV
.3 kHZ BW
1 SEC/DIV
Attenuation = 10 dB
Log. reference = -40 dBm
Video Filter = 100 HZ
10 dB/DIV

Figure 33: Expanded view of a 3rd order intermodulation product ($f_2 - 2f_8$) .

(Same conditions as in Figure 32.)

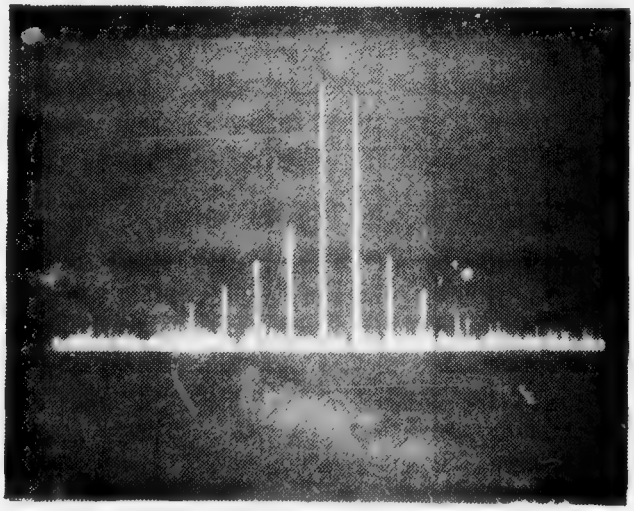

Spectrum Analyzer

f_0 = 305.8 MHZ
1 MHZ/DIV
3 kHZ BW
.5 SEC/DIV
Attenuation = 30 dB
Log. reference = -20 dBm
Video Filter = 10 KHZ
10 dB/DIV

Figure 34: Spectrum of intermodulation products generated by an UHF/LOS signal @ 305.8 MHZ (E3) and an UHF/PSK signal @ 306.4 MHZ & 4.8 KHZ data rate (E2). (The settings of the attenuators in NONLINEARITY #1 were: E2 = 5 dB, E3 = 10 dB, N1 = 0 dB. Measured at "TEST OUT" in C1.)

Table 7

Attenuation from Input Ports to Input of Amplifiers in Nonlinearities N1 and N2

FREQUENCY (MHz)	5		10		20		60		150	
UNIT	N1	N2	N1	N2	N1	N2	N1	N2	N1	N2
E6	-	-	-	-	-	-	32.0	31.8	33.0	32.8
E7	-	-	31.9	31.9	31.7	31.6	-	-	-	-
E8	28.7	28.7	28.6	28.6	-	-	-	-	-	-

C. EMITTER E1

The measurement set up for the determination of the linear operation of Emitter 1 (units E1A, E1B and E1C connected) as a function of the 30 MHz reference input and the resulting data, is shown in Figure 35. The operating point, as determined by careful analysis of distortions on the spectrum of E1, is indicated in the figure. Time and frequency domain signatures of the signal are shown in Figures 36 and 37. The photos are from samples of the signal at the "OUTPUT" port of C1 combining unit.

The total power available at the "OUT" port with the signal as defined in Figures 36 and 37 was 2.5 dBm.

D. EMITTER E2

As for the case of Emitter 1, the overall characterization of the linear operation of Emitter 2 was made and an operating point, obeying the same criteria used for Emitter 1, was chosen as indicated in Figure 38.

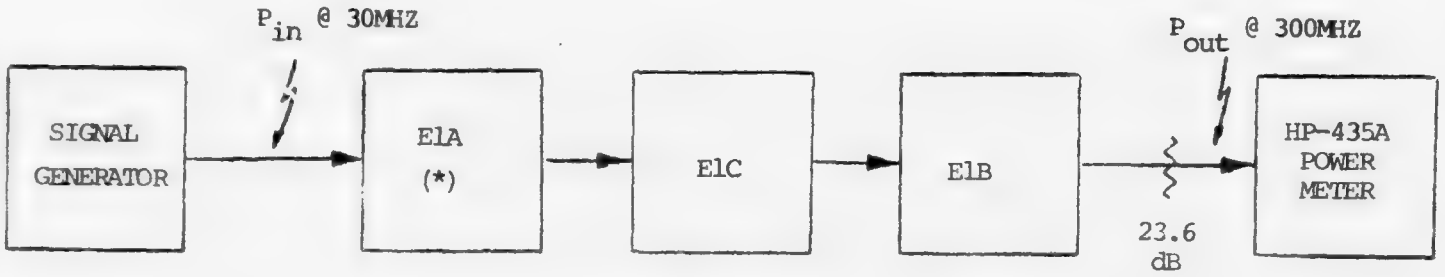

(*) encoding="PSW", rate "19.2 KHZ", register length = "5".

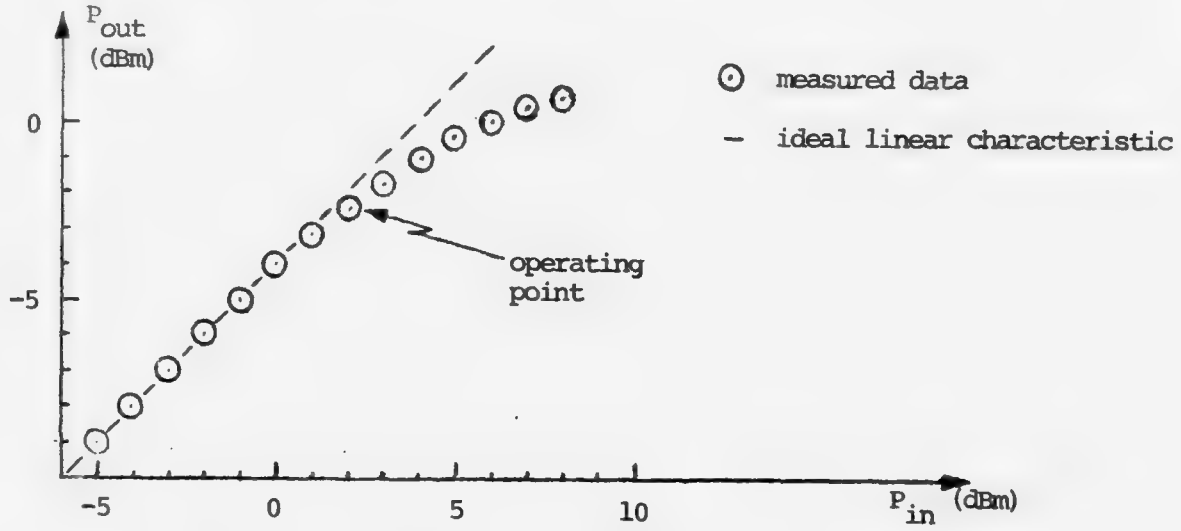

Figure 35: Measured input-output characteristic of E1

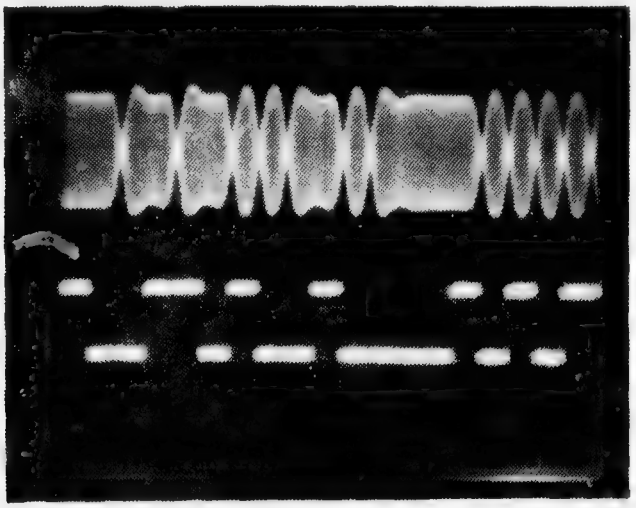

Oscilloscope

50 μs/DIV

CH1 = .2 V/DIV

CH2 = 2V/DIV

Figure 36: Time-domain view of E1. (Signal parameters are: f_0 = 240 MHZ, DATA RATE = 19.2 kHZ, REG. LENGTH = 5, ENCODING = PSK, LO = 7 dBm @ 270 MHZ. Upper trace (CH1) is the signal. Lower trace (CH2) is measured at "OUTPUT" in C1.)

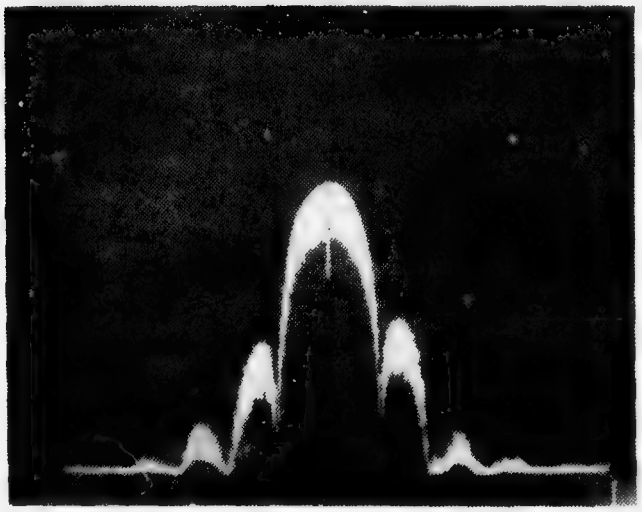

Spectrum Analyzer

f_0 = 240 MHZ

20 kHZ/DIV

.3 kHZ BW

2 SEC/DIV

Attenuation = 20 dB

Log. reference = -10 dBm

Video Filter = 100 HZ

10 dB/DIV

Figure 37: Frequency-domain view of E1. (Signal parameters same as in Figure 36. Measured at "TEST OUT" in C1.)

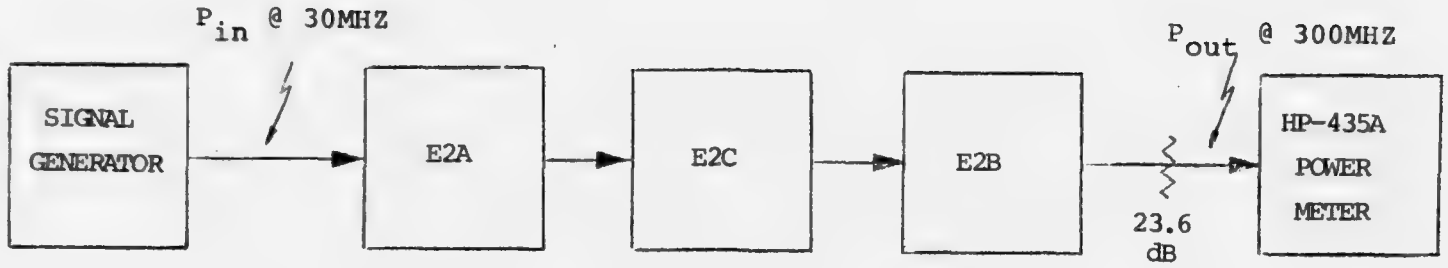

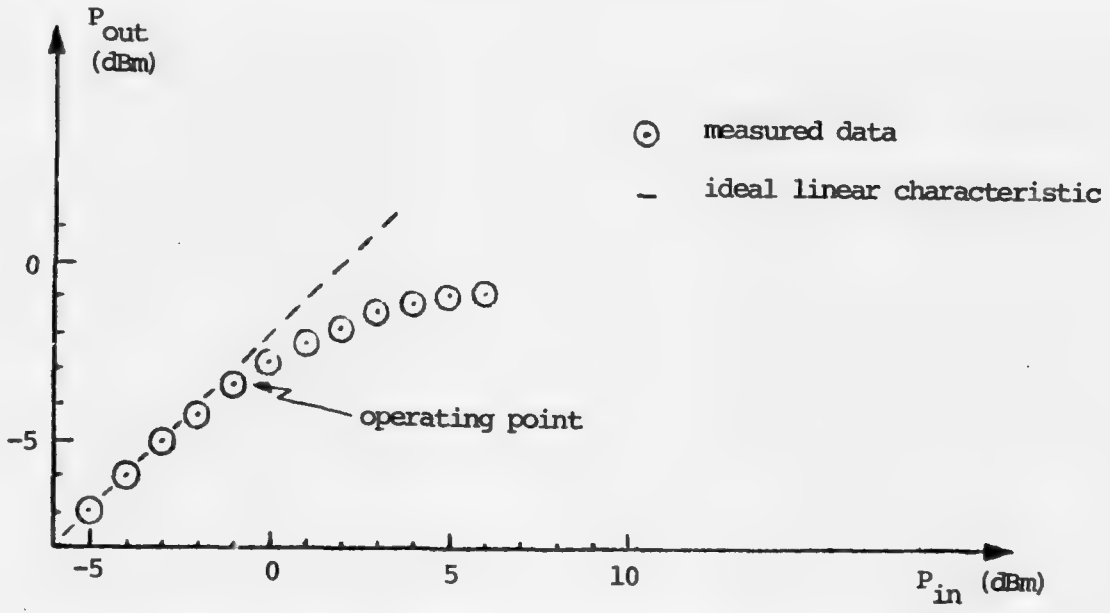

Figure 38: Measured Input-Output Characteristic of E2

The time and frequency domain signatures of a 240 MHz, PSK modulated at 9.6 KHz data rate, signal is shown in Figures 39 and 40. The signal was measured at the "OUT" port of C1 and had a power level of .5 dBm.

E. EMITTER 3

The two most relevant factors to consider in the performance evaluation of Emitters 3 and 4 are the physical characteristics of the signal itself (frequency, modulation, level, etc.) and the duty cycle (Push-to-Talk) statistics. As we have described in Chapter IV the PTT statistics were generated by using two independent pseudo-Poisson processes to turn the AN/SRC-21 transmitter on and off. A sample of the resultant control signal is shown in Figure 41. An important comment about the use of the controls in this unit is that the "PTT RATE" and the "PTT AVG ON TIME" controls are calibrated in terms of the start and stop pseudo-Poisson process rates. The actual PTT rate and average on time will depend on the combination of the two controls used. For example, if we set the "PTT RATE" to 4 per minute, the actual number of times that the control will be on will depend on the average on time selected. The bigger the "on time" selected the bigger the decrease on the actuall PTT rate from the selected value. That happens because, by construction, the start pulses are blocked when the PTT is in ON and the bigger the "On time" the more start pulses we lose. A similar phenomenon occurs when we fix the "PTT AVG ON

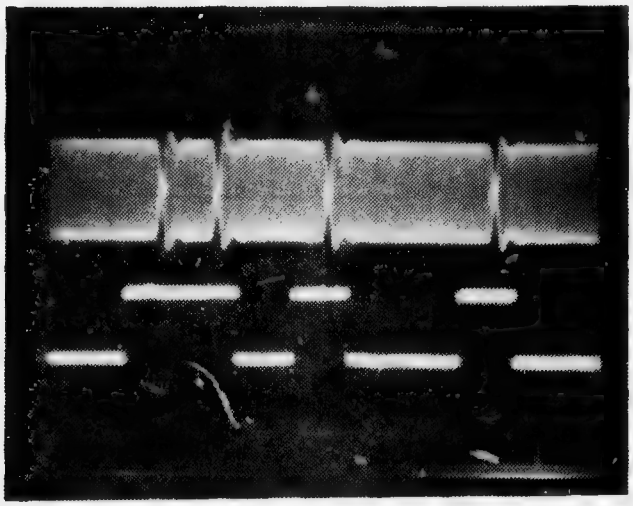

Oscillscope

.2 ms/DIV

CH1 = .2 V/DIV

CH2 = 2 V/DIV

Figure 39: Time-domain view of E2. (Signal parameters: f_0 = 240 MHZ, DATA RATE = 4.8 KHZ, REG. LENGTH = 5, ENCODING = DPSK, LO = 7 dBm @ 270 MHZ. Upper trace (CH1) is the signal. Lower trace (CH2) is the data stream. Measured at "OUTPUT" in C1.)

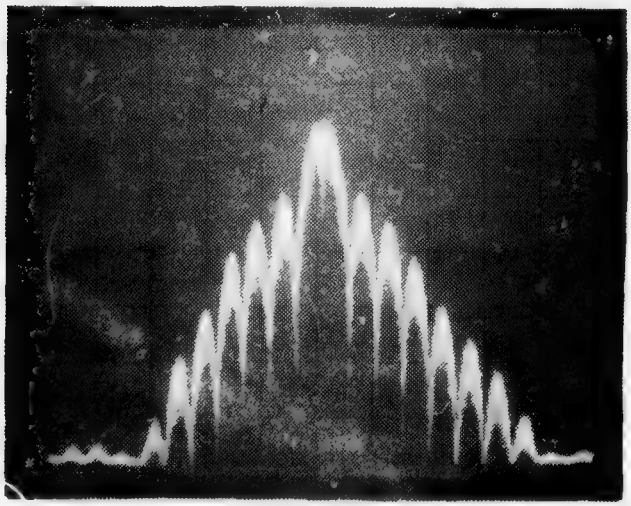

Spectrum Analyzer

f_0 = 240 MHZ

10 KHZ/DIV

.3 KHZ BW

1 SEC/DIV

Attenuation = 20 dB

Log. reference = -20 dBm

Video Filter = 100 HZ

10 dB/DIV

Figure 40: Frequency-domain view of E2. (Signal parameters same as in Figure 39. Measured at "TEST OUT" in C1.)

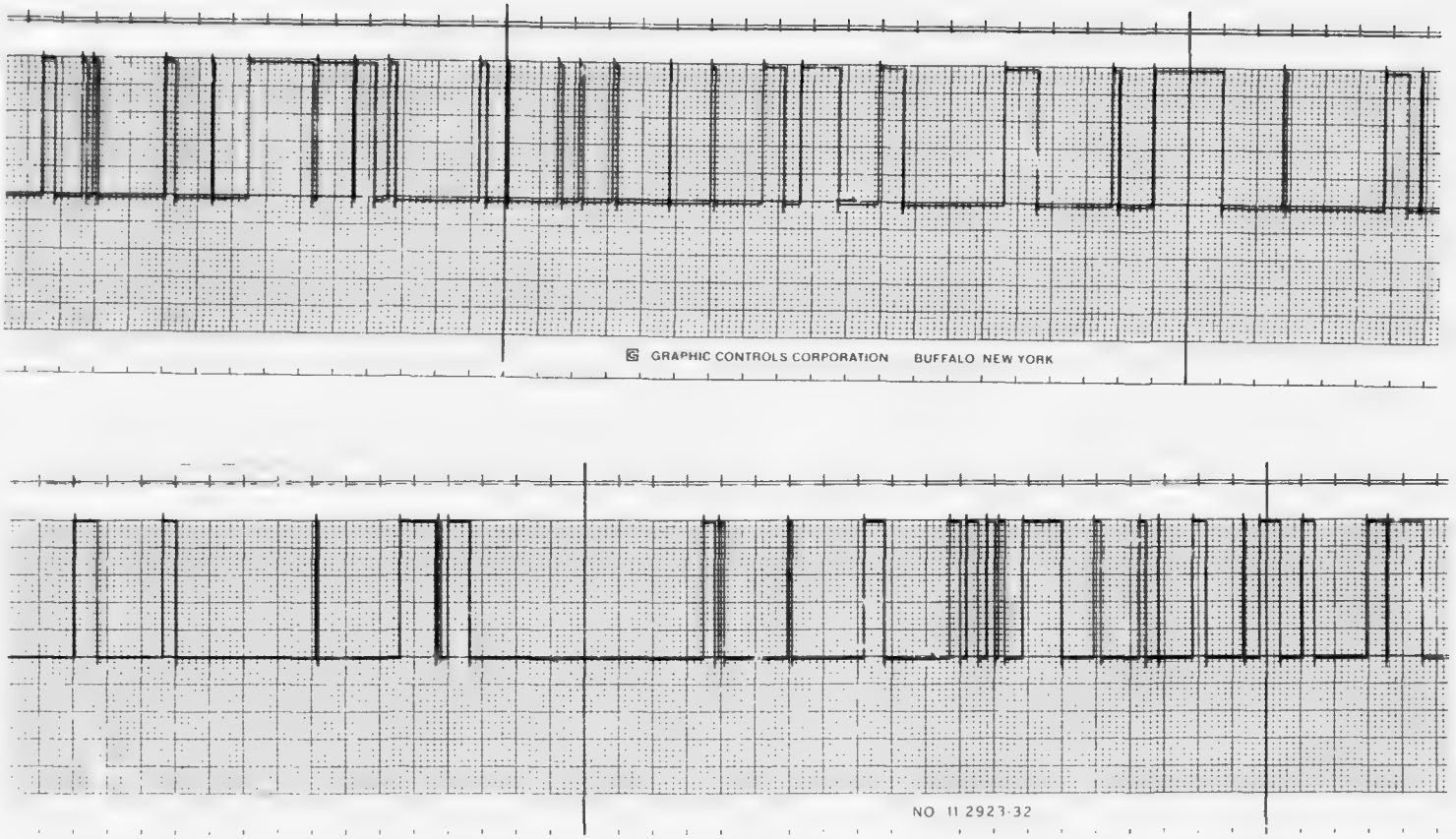

Figure 41: Emitter 3 PTT Control Signal. (Chart scale 1 mm/sec. controls set ot RATE = 8/min; AVG ON TIME = 2 sec)

TIME" control and vary the setting in "PTT RATE." The physical characteristics of E3 are best described by its spectrum signature. Since we are using the same sources of signal used aboard ships and since the complex modulation is of the same nature (a "voice process") we see that the physical characteristics of Emitter 3 will be identical to the LOS emitters aboard ships. In Figures 42 and 43 we give the spectrum characteristics of typical unmodulated and modulated Emitter 3 signals.

The total power available at "OUT port of C1 is 7 dBm under the conditions: Frequency 308.5 MHz (CH 8), MODULATION - OFF.

F. EMITTER 4

The same comments made for Emitter 3 apply for Emitter 4. A sample of the PTT control signal is given in Figure 44 for a different set of controls selection. Spectrum signatures of the unmodulated and voice modulated carrier are given in Figures 45 and 46.

The total power available at "OUT" terminals in C1 is 7 dBm when Emitter 4 is at 308.5 MHz and MODULATION is "OFF".

G. EMITTER 5

The UHF/RADAR interferer, as described previously, has two components: A pulsed RF and a pulsed noise. For the pulsed RF, the best way to characterize it is by its spectrum signature. A pulsed modulated RF with PRF - 1 KHz and

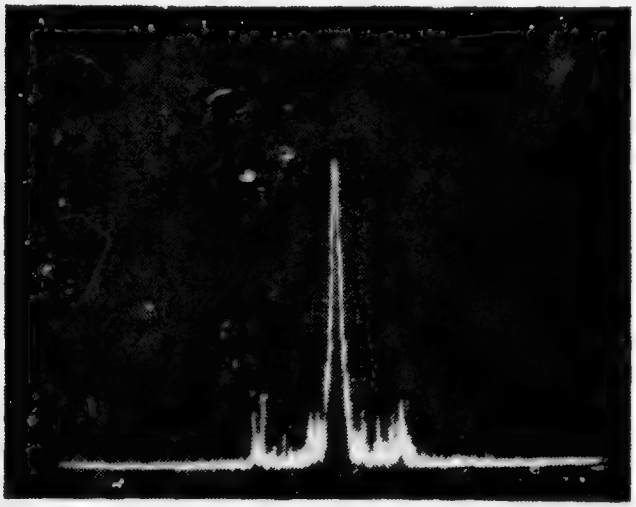

Spectrum Analyzer

f_0 = 305.8 MHZ
2 KHZ/DIV
.1 KHZ BW
1 SEC/DIV
Attenuation = 30 dB
Log. reference = 10 dBm
Video Filter = 100 HZ
10 dB/DIV

Figure 42: Frequency-domain view of E3 with modulation OFF (Measured at "TEST OUT" in C1.)

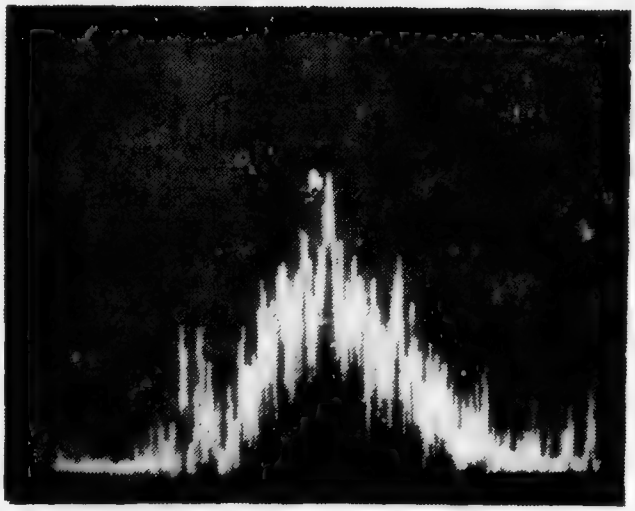

Spectrum Analyzer

Same as Figure 42.

Figure 43: Frequency-domain view of E3 with modulated ON. (Measured at "TEST OUT" in C1.)

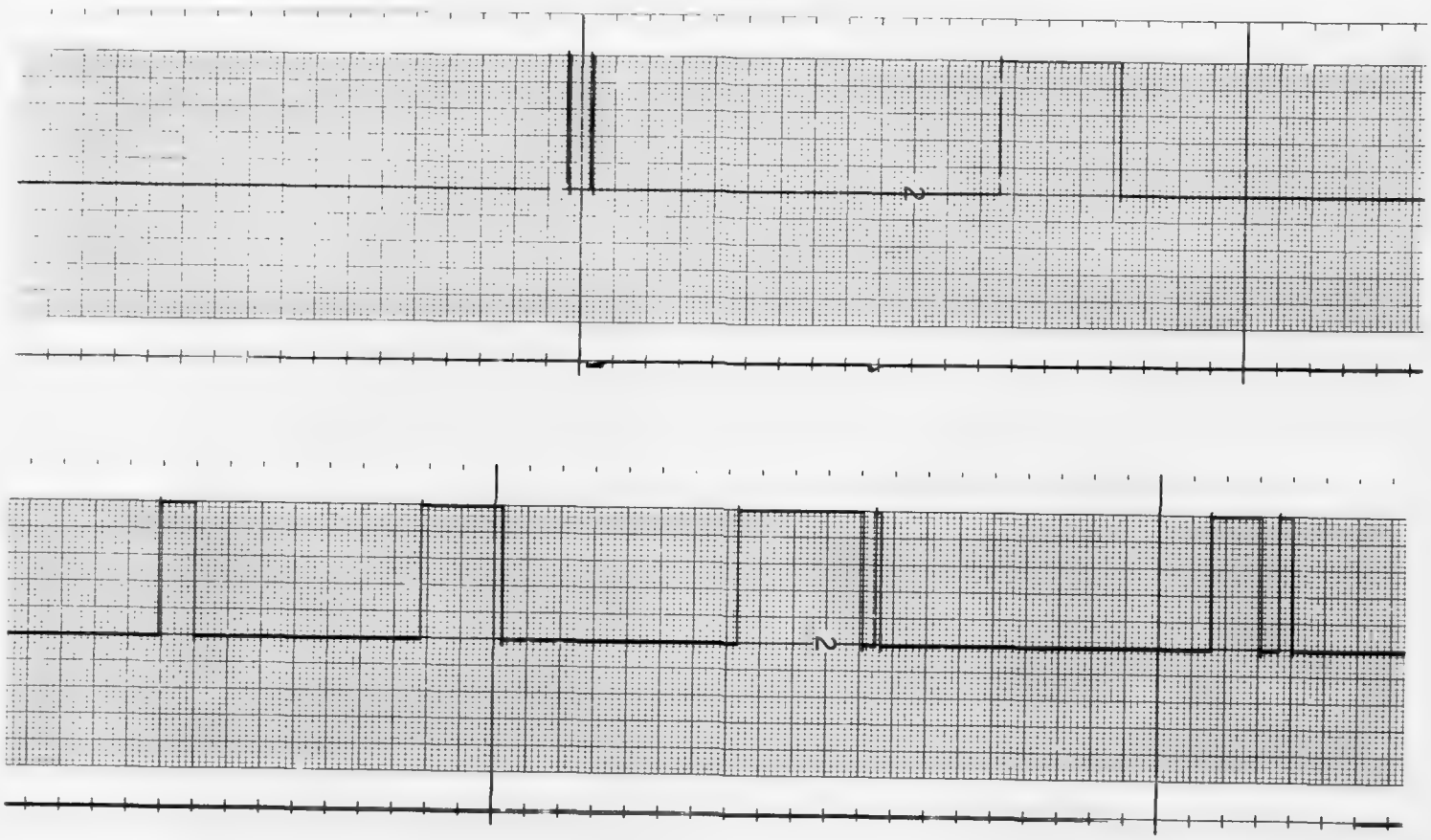

Figure 44: Emitter 4 PTT Control Signal. (Chart scale 1 mm/sec. Controls set to: RATE = 2/min, PTT AVG. ON TIME = 8 sec.)

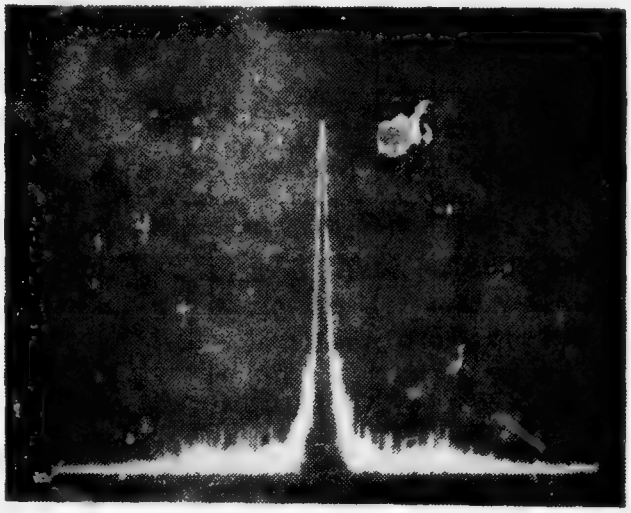

Spectrum Analyzer

f_0 = 319.1 MHZ
2 KHZ/DIV
.1 MHZ BW
1 SEC/DIV
Attenuation = 30 dB
Log. reference = 0 dBm
Video filter = 100 HZ
10 dB/DIV

Figure 45: Frequency-domain view of E4 with modulation OFF. (Measured at "TEST OUT" in C1.)

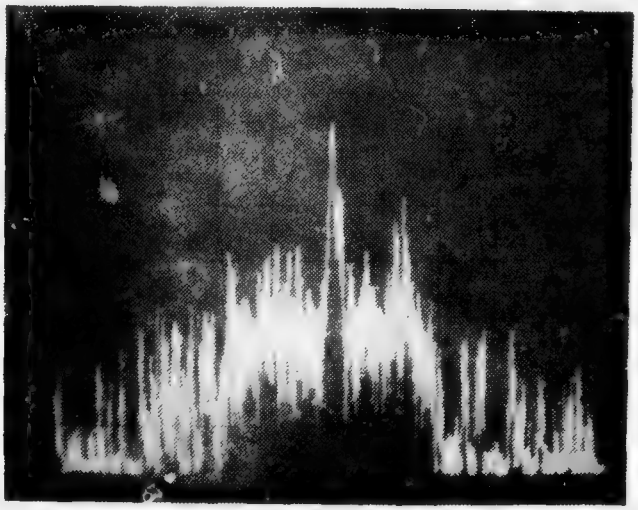

Spectrum Analyzer

Same as Figure 45.

Figure 46: Frequency-domain view of E4 with modulation ON. (Measured at "TEST OUT" in C1.)

PW = 100 μsec (10 dB duty cycle) is shown in Figure 47. In Figure 48 a wider bandwidth view of the same signal shows the effect of filtering on the same signal.

Since the pulsed-noise component of the RADAR emitter has a uniform power spectrum density, no useful information can be derived from its spectrum signature. A more important characteristic is its time domain behavior. In order to give a more real idea of the effects of the various components of the radar interferer on a receiver, a detected sample of each one is in Figures 49 to 51. The photos used were taken from a spectrum analyzer operating in the video mode and show the results of detection of the three possible combinations of the component signals: pulsed RF, pulsed noise and the sum of the two signals. Figure 52 shows the original modulating signal.

Unfortunately one main parameter of the UHF/RADAR could not be evaluated at the time of this writing because the INTERDATA 7/32 computer used to generate the scan pattern is still not operative due to delays in delivery. Until the computer is ready, the pin-diode attenuators in E5C-RADAR SCAN MODULATOR unit are hardwired to 0 dB attenuation by grounding pins A through H on connector P11. Manual control of attenuation for testing purposes can be obtained from a control box that can be attached to P11.

The average power available at the "OUT" terminal in unit C1, when a 210 MHz, pulsed signal at 1 kHz PRF and 100 μsec PW is produced is 18.3 dBm (28.3 dBm peak).

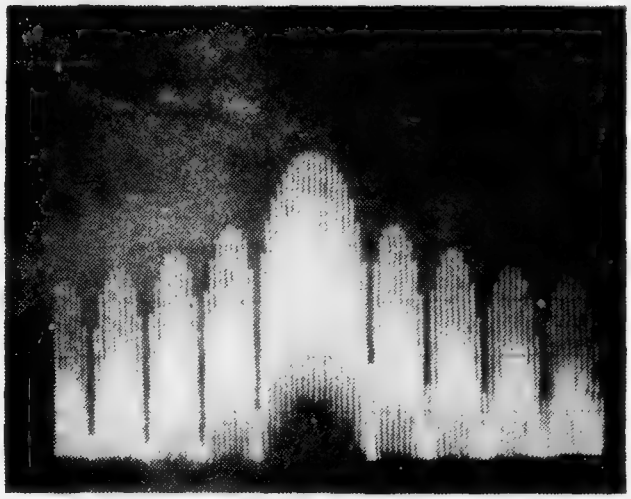

Spectrum Analyzer

f_0 = 210 MHZ
10 KHZ/DIV
.1 KHZ BW
5 SEC/DIV
Attenuation = 30 dB
Log. reference = -10 dBm
Video Filter = 100 HZ
10 dB/DIV

Figure 47: Frequency-domain view of E5. (Signal parameters: for 210 MHZ, PRF = 1 KHZ, PW = 100μsec. Measured at "TEST OUT" in C1 with E5 attenuator at 20 dB.)

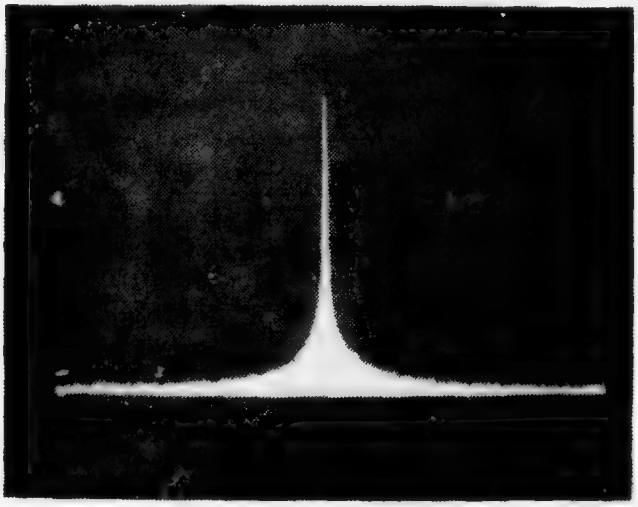

Spectrum Analyzer

f_0 = 210 MHZ
10 MHZ/DIV
30 KHZ BW
1 SEC/DIV
Attenuation = 30 dB
Log. reference = 0 dBm
Video Filter = 10 KHZ
10 dB/DIV

Figure 48: Frequency-domain view of E5. (Signal and measurement conditions same as in Figure 47.)

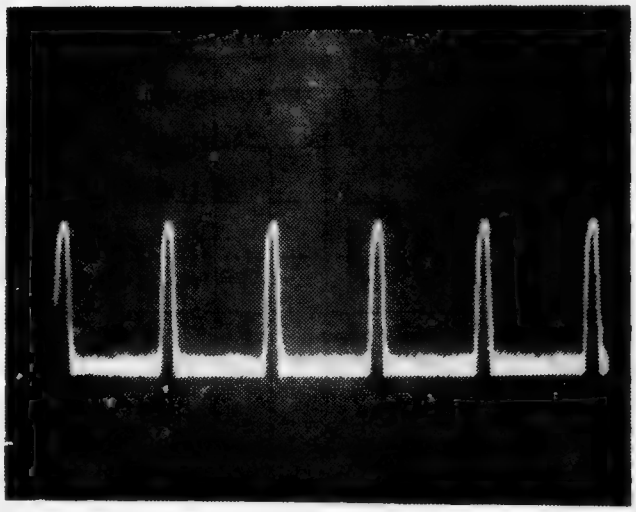

Spectrum Analyzer

f_0 = 210 MHZ
Scan width = zero
30 KHZ BW
.5 msec/DIV
Attenuation = 30 dB
Log. reference = -10 dBm
Video Filter = 10 KHZ
Scan trigger = VIDEO

Figure 49: Detected radar signal. Pulsed RF only. (Signal parameters: f_0 = 210 MHZ, PRF = 1 KHZ, PW = 100 μs, NOISE OFF. Measured at "TEST OUT" in C1. E5 attenuator at 50 dB.)

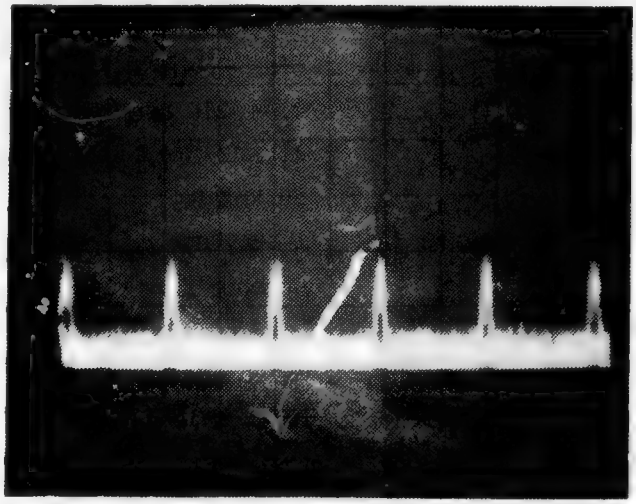

Spectrum Analyzer

f_0 = 210 MHZ
Scan width = zero
30 KHZ BW
.5 msec/DIV
Attenuation = 0 dB
Log. reference = -40 dBm
Video Filter = 100 KHZ
Scan trigger = VIDEO

Figure 50: Detected radar signal. Pulsed NOISE only. (Signal parameters: PRF = 1 KHZ, PW = 100 μsec, NOISE attenuator = 0 dB. Measured at "TEST OUT" in C1. E5 attenuator at 0 dB.)

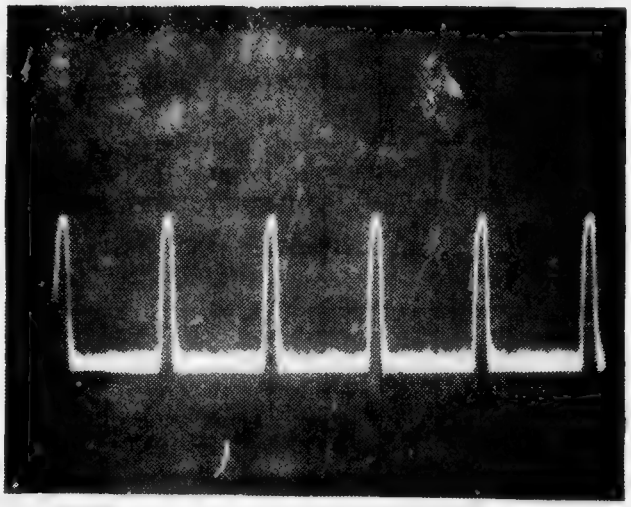

Spectrum Analyzer

f_0 = 210 MHZ
Scan width = zero
30 KHZ BW
.5 msec/DIV
Attenuation = 30 dB
Log. reference = -10 dBm
Video Filter = 10 kHZ
Scan trigger = VIDEO

Figure 51: Detected radar signal. Pulsed RF+NOISE. (Signal parameters: f_0 = 210 MHZ, PRF = 1 KHZ, PW = 100 μsec, NOISE attenuator = 0 dB. Measured at "TEST OUT" in C1. E5 attenuator 50 dB.)

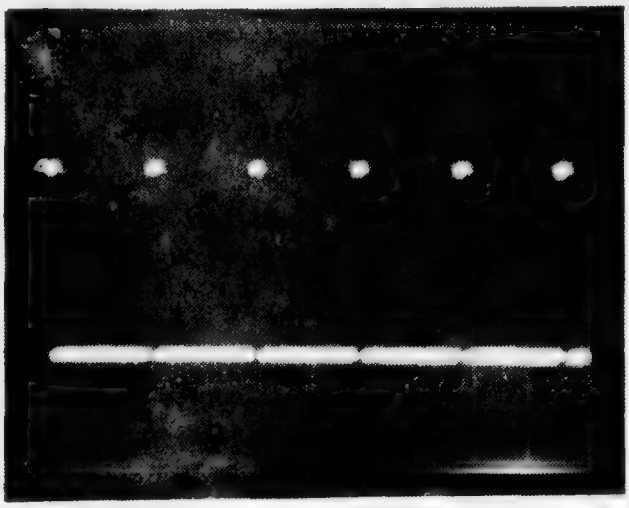

Oscilloscope

.5 msec/DIV
1 V/DIV

Figure 52: Radar modulating signal. (PRF = 1 KHZ, PW = 100 μsec.)

H. EMITTERS 6 AND 7

Since these are CW signals, the only parameter of importance is the available power at the "TEST OUT" port on each of the emitters and the input-output characteristics since this gives an idea of the necessary driving power from the signal generators. The input-output characteristics for Emitters 6 and 7 are given in Figures 53 and 54 respectively. As can be seen from each figure the available power from each emitter is about 28 dBm.

I. EMITTER 8

Since we do not have any control over the power level of the transmitter T-827B/URT the only data of interest is the total available power at the "TEST OUT" terminal which is about 25 dBm.

J. EMITTER 9

The two most important characteristics of the impulsive noise as modeled in Chapter II were the randomness of its occurrence in time and its ability to cause interference to the SATCOM receiver through the whole band of operation (240 to 400 MHz). The randomness of the impulses can be determined by matching the distribution of the number of impulses occurring in a given time slot against a theoretical Poisson distribution. This measurement was made and the data obtained is plotted in Figure 55. We can see that the impulses occur very closely to a Poisson process. The broadband nature of Emitter 9 was established by using a

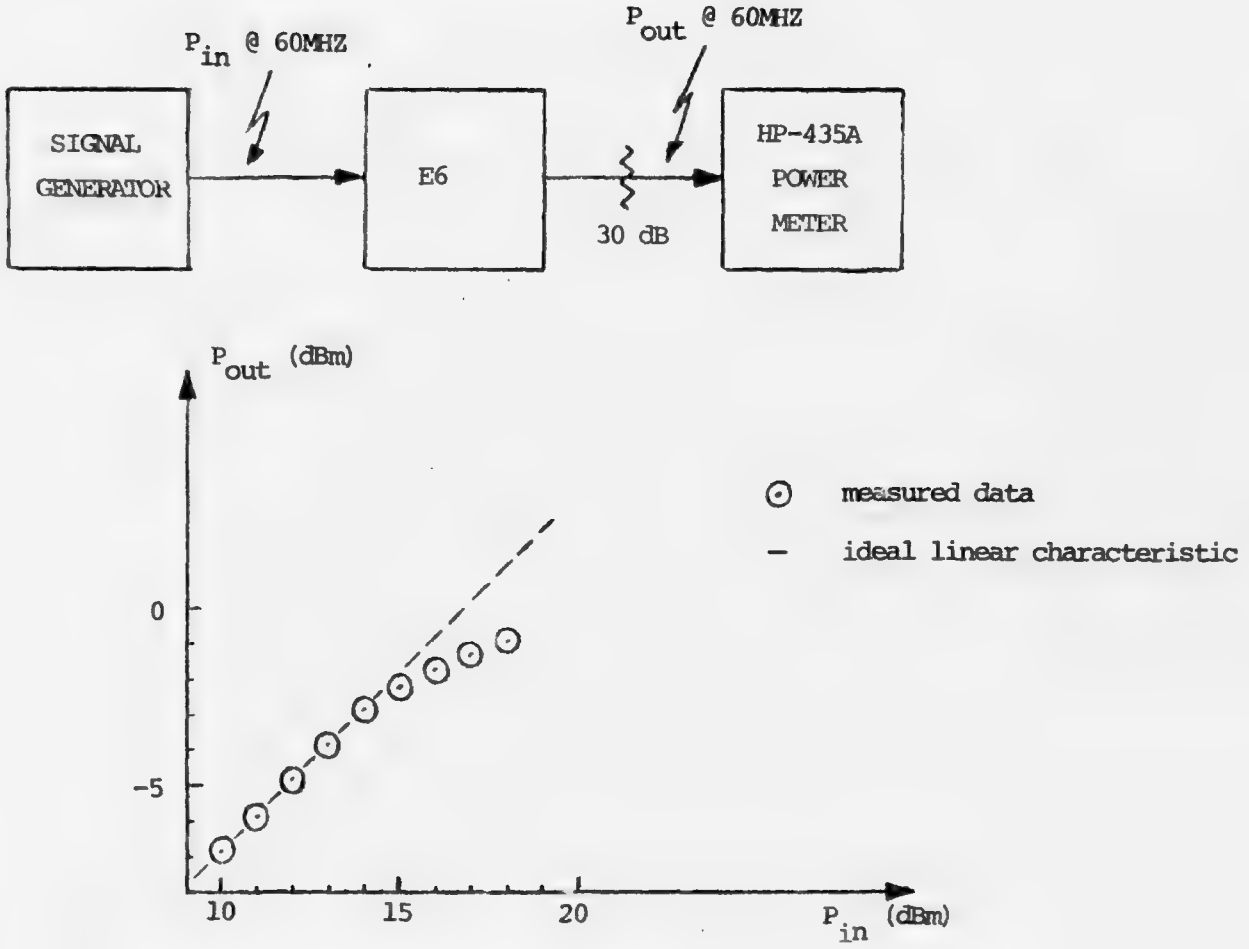

Figure 53: Measured Input-output Characteristic for E6.

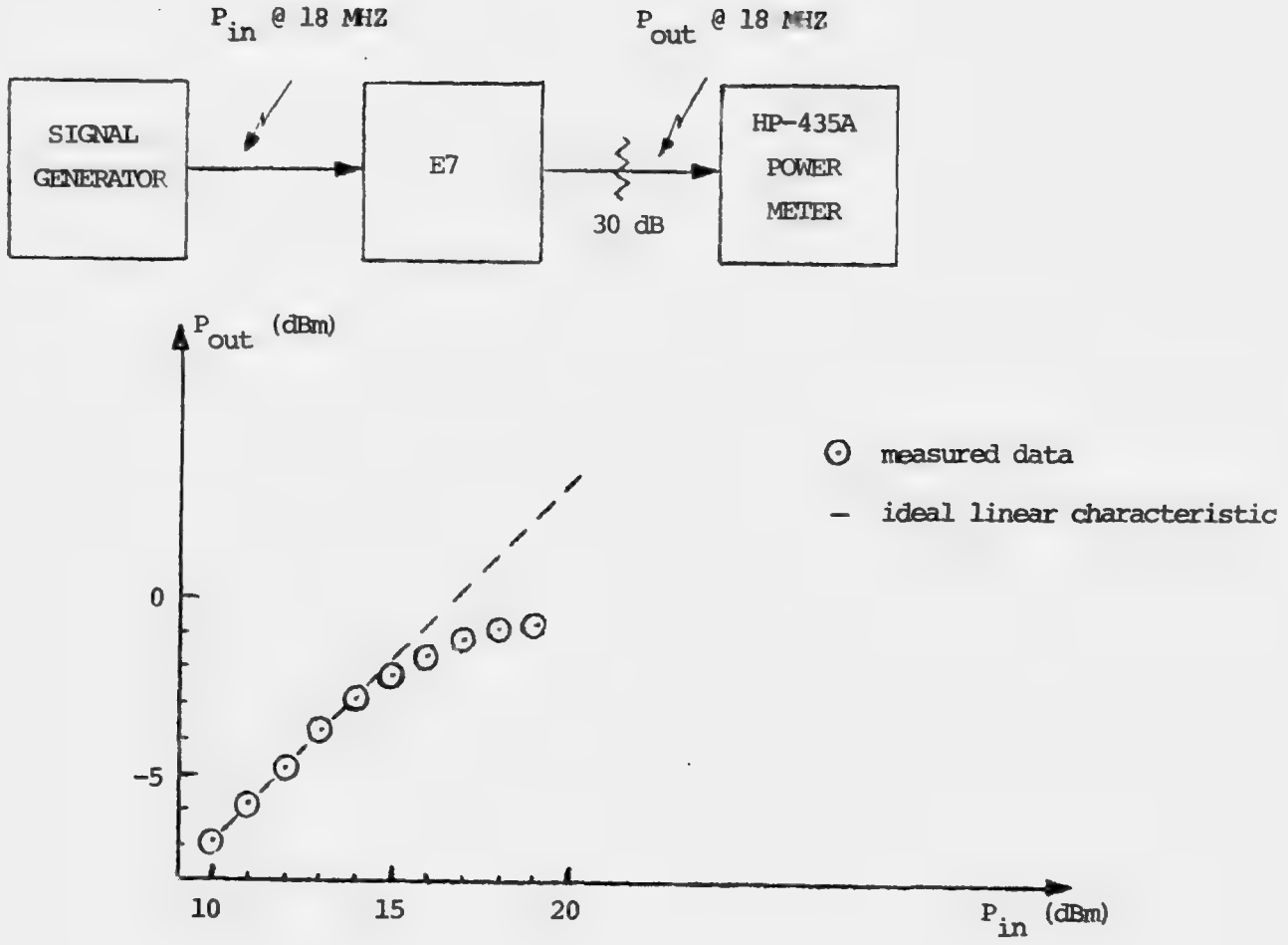

Figure 54: Measured Input-output Characteristic of E7.

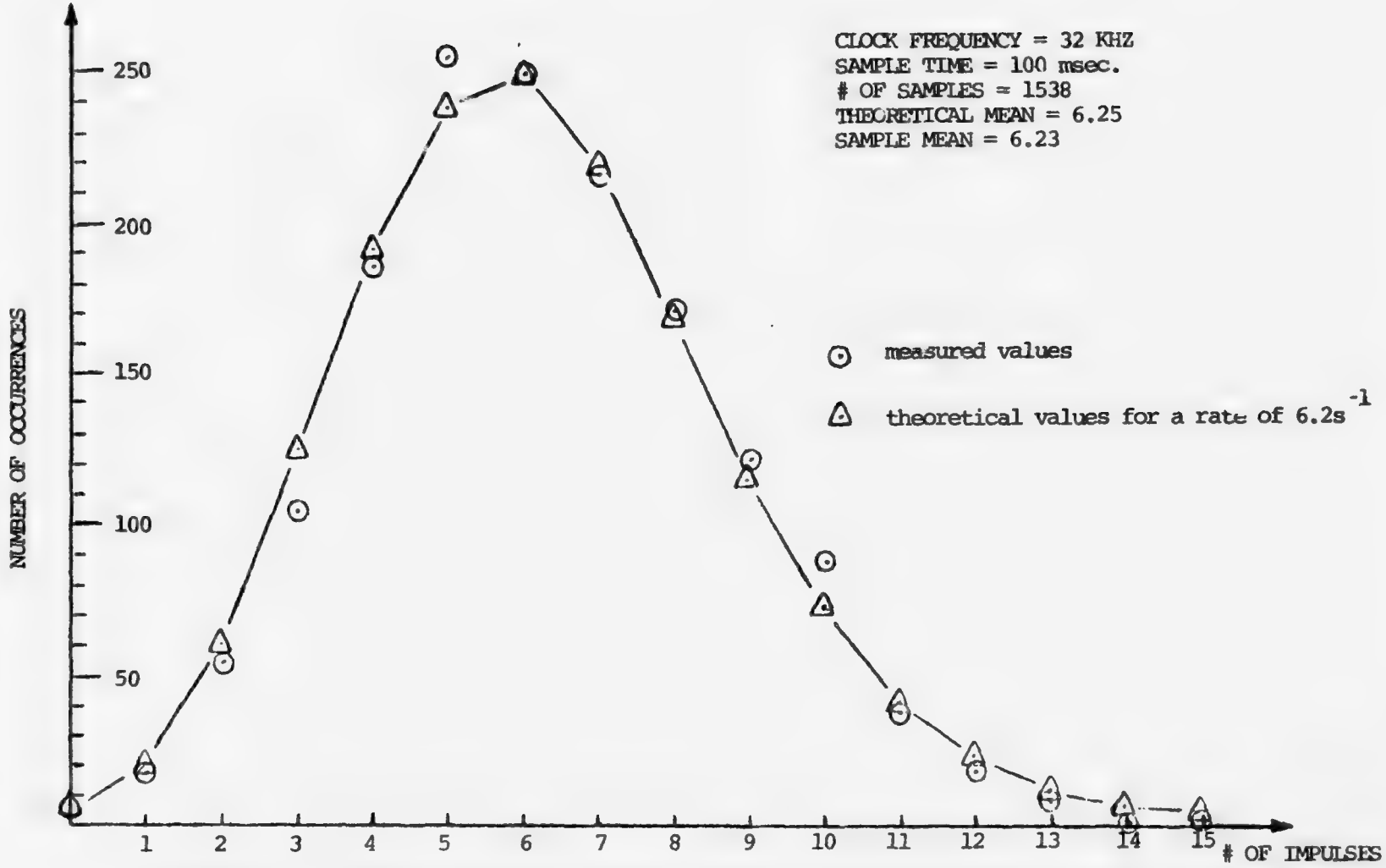

Figure 55: Theoretical and Measured Distribution of Timing Pulses for E9.

spectrum analyzer to detect the signal at three different frequencies (240, 300 and 400 MHz). Single sweep measurements of the detected signals are shown in Figures 56 through 58. Since on these photos the horizontal axis is the time axis, the randomness of the impulses can be observed.

K. EMITTER 10

Emitter 10 is a source of broadband Gaussian noise. As such it is totally characterized by its power spectrum density at the "OUT" terminal in C1 as shown in Figure 59.

L. SIGNAL

The signal unit (S1) was tested by comparing results of bit error measurements using an AN/WSC-3 SATCOM RECEIVER at different data rates and signal levels, against results of measurements using different setups.[30] The data from these measurements is given in Figures 60 and 61. Also important for the overallperformance of S1 is its amplitude stability. Since this is given, in great extent, by the ability of the 30 MHz reference signal circuit to absorb level variations on the 5 MHz frequency standard, an overall input-output characteristic was drawn in Figure 62. The chosen operating point is also shown in the figure.

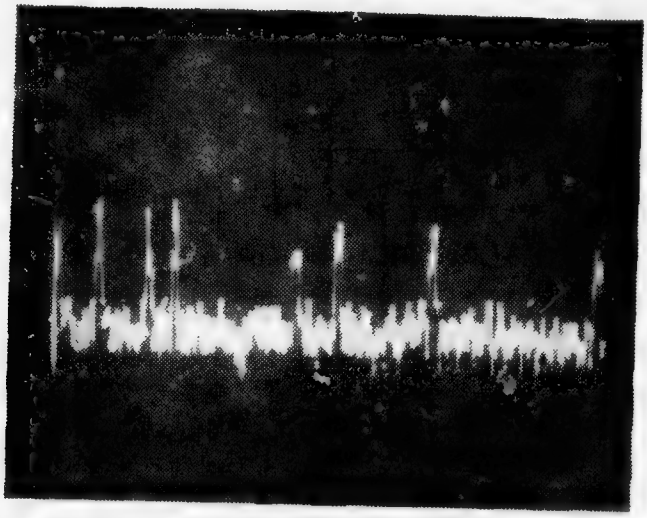

Spectrum Analyzer

f_0 = 240 MHZ
Scan width = zero
30 KHZ BW
1 msec/DIV
Attenuation = 0 dB
Log. reference = -50 dBm
Scan trigger = VIDEO
Single scan

Figure 56: Detected impulsive-noise. (Noise parameters: RATE = $1000s^{-1}$, PW = 100 μsec, Attenuation = 0 dB. Measured at "OUT" in C1.)

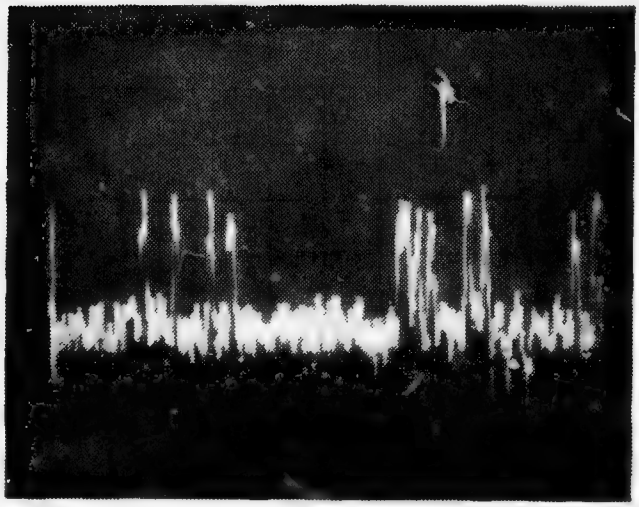

Spectrum Analyzer

f_0 = 320 MHZ

Figure 57: Detected impulsive-noise. (Same conditions as Figure 56.)

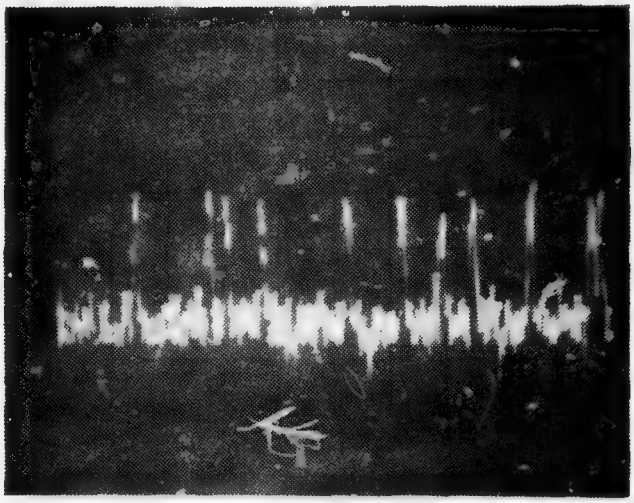

Spectrum Analyzer

f_0 = 400 MHZ

Figure 58: Detected impulsive-noise. (Same conditions as Figure 56.)

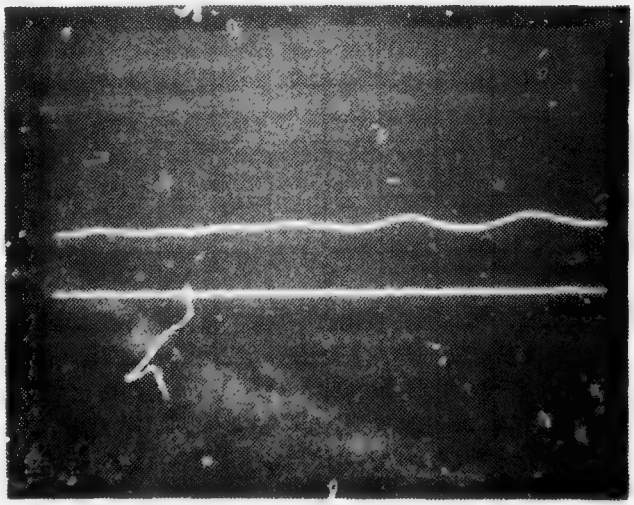

Spectrum Analyzer

f_0 = 300 MHZ
20 MHZ/DIV
300 KHZ BW
10 SEC/DIV
Attenuation = 0 dB
Log. reference = -50 dBm
Video Filter = 10 HZ
10 dB/DIV

Figure 59: Power spectrum density of E10-GAUSSIAN NOISE. (Noise attenuator at 0 dB. Measured at "OUTPUT" in C1. Lower trace = spectrum analyzer noise level. Upper trace = E10 power spectrum density.)

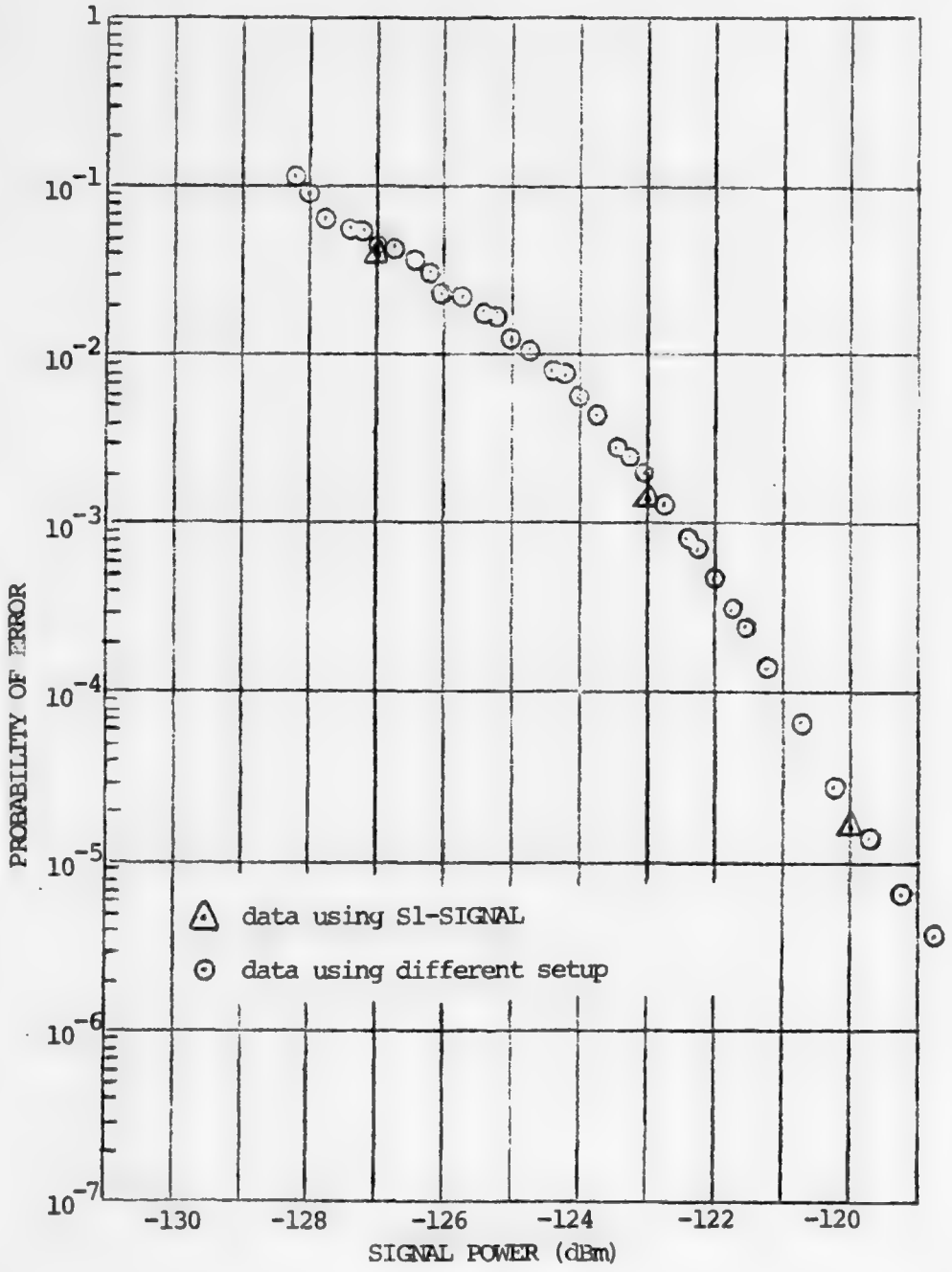

Figure 60: AN/WSC-3 Bit Error Rate at 9600 b/s, Sequence n=20

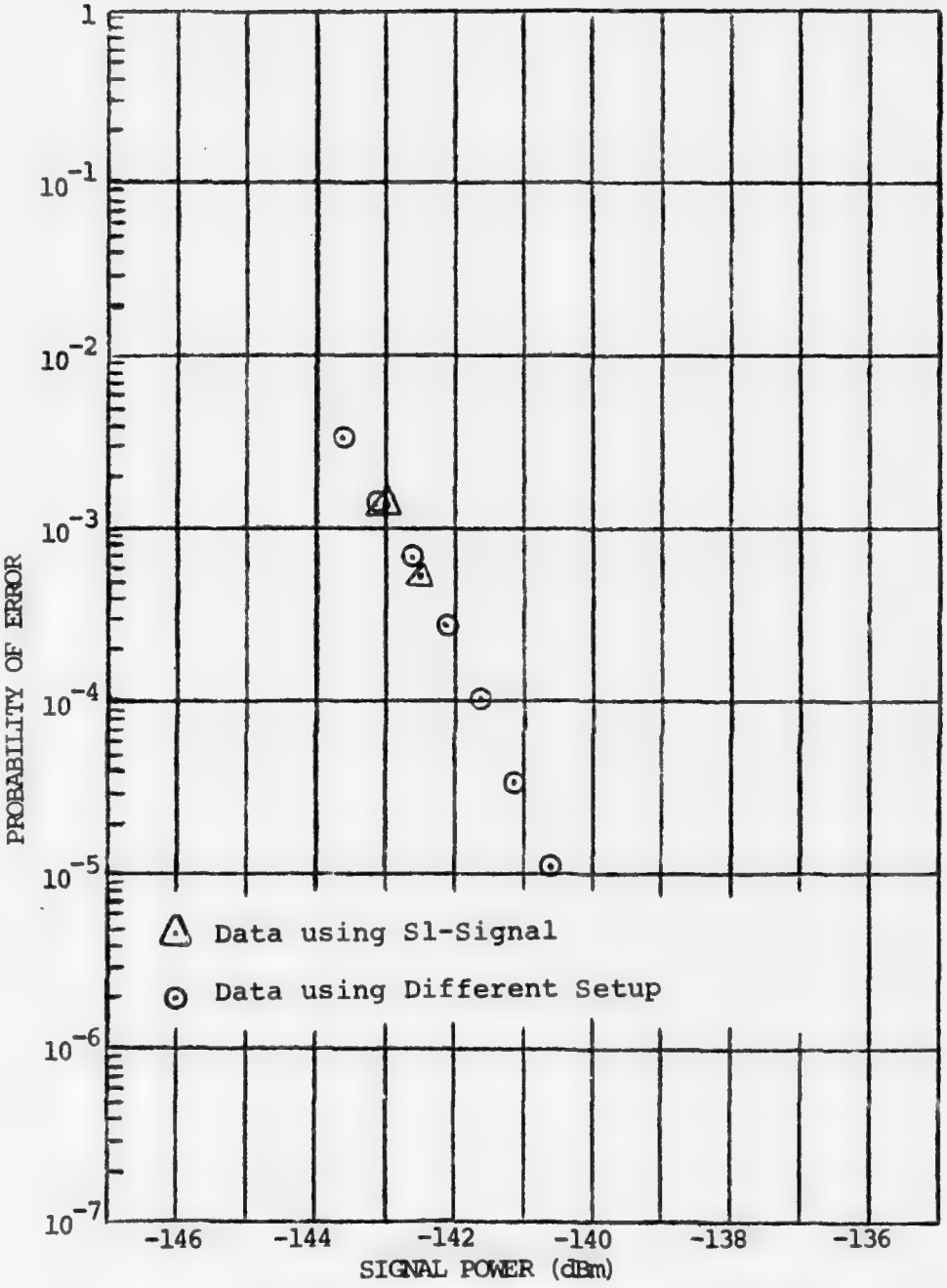

Figure 61: AN/WSC-3 Bit Error Rate at 75 b/s, Sequence n=6

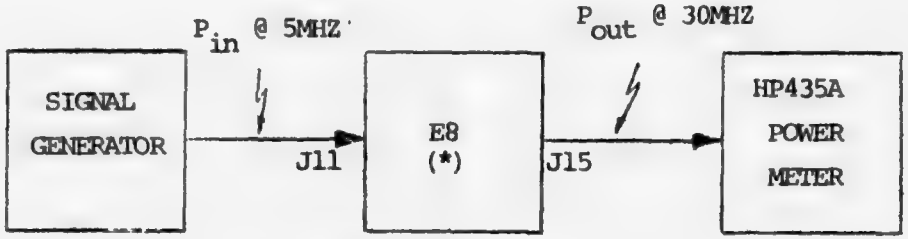

(*) J12-14 terminated in 50Ω

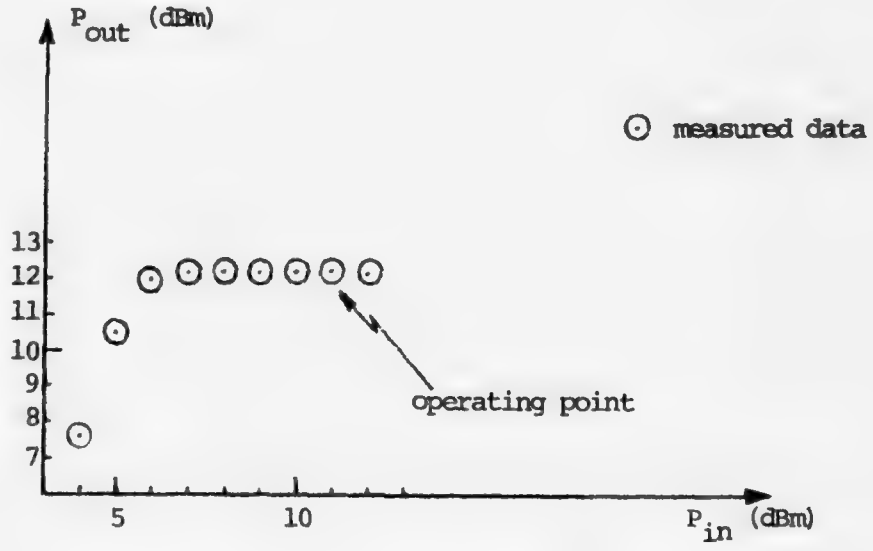

Figure 62: Measured Input-output Characteristics for 30 MHz Reference Signal.

VI. CONCLUSIONS

White Gaussian noise is seldom the only source of interference affecting shipboard communications systems. The presence of a variety of other systems, operating in the same environment, with high power levels and sharing the same frequency bands, causes additional degradation to those systems. This is particularly true for the new tactical UHF satellite communications system being introduced in the U.S. Navy fleet, due to the higher sensitivity of this system.

In order to be able to characterize the performance of this system in the shipboard electromagnetic environment, a simulator based on a model established in Chapter III was designed and built. The interference model used is a Physical-statistical model similar to one developed by Middleton. This model of the interference process describes the sources of interference (emitters) by considering all the important physical characteristics of these sources and inserting them in a statistical framework to account for the randomness of some parameters. The simulator is capable of generating ten complex emitters which incorporate all the main physical and statistical characteristics of the ones found on a ship plateofrm.

A description of the implemented system, at the block diagram level, is shown in Chapter IV, which also describes

the controls and ports available on the front panels of the various units.

Performance of the simulator is shown in Chapter V. In this chapter, basically two types of information is presented. Spectrum and time domain signatures of the various emitters, as well as intermodulation generation capability were shown with the purpose of validating the simulator performance against measured data. Results of measurements on the overall transfer characteristics of the various units and available power levels at various points in the circuit were also shown with the double purpose of providing data for checking the operation of the simulator and as a help for troubleshooting. Detailed description of various units is given in the appendices.

Problems deserving further attention and that were not treated in this research are the following: the need for better understanding of the characteristics of topside nonlinearities and further development of an analytical model for shipboard RFI with application to the problem of optimal estimation and detection in this environment.

APPENDIX 1

DETAILED DESCRIPTION OF UNITS C1, N1 AND N2

A. C1 - COMBINING UNIT

The schematic diagram for C1 COMBINING UNIT is shown in Figure 63. The signal (S1), Emitter 10 and Emitter 9 are fed through connectors J11, J12, J13 on the back of the unit. Emitters 1 through 5 and the signals from nonlinear processing in NONLINEARITIES 1 and 2 are brought by semi-rigid coaxial cables running internally from Units N1 and N2. Emitters 1 to 4 are then attenuated by attenuators R1 to R4 (which are 0-60 dB, 10 dB steps, rotary attenuators) and directed by switches S1 to S4 (SPDT RF switches) either to connectors on the front panel of the unit ("OFF" position) or to the inputs of two-way power dividers PD1 and PD2, used as summers. The output signals of PD1 and PD2 are then combined again on power divider PD3. The results of nonlinear processing on Emitters 1 to 8 in NONLINEARITIES N1 and N2 are combined in Power Divider PD5. Emitter 9, which is available from Connector J13 on the back of the unit, is directed by a SPDT RF switch either to a connector on the front panel ("OFF" position of the switch) or to one input of power divider PD6. The other input of PD6 is derived from the output of PD5. PD6 thus provides an output which contains the results of nonlinear processing in Emitters 1 to 8 and Emitter 9. Thus signal and the sum of Emitters

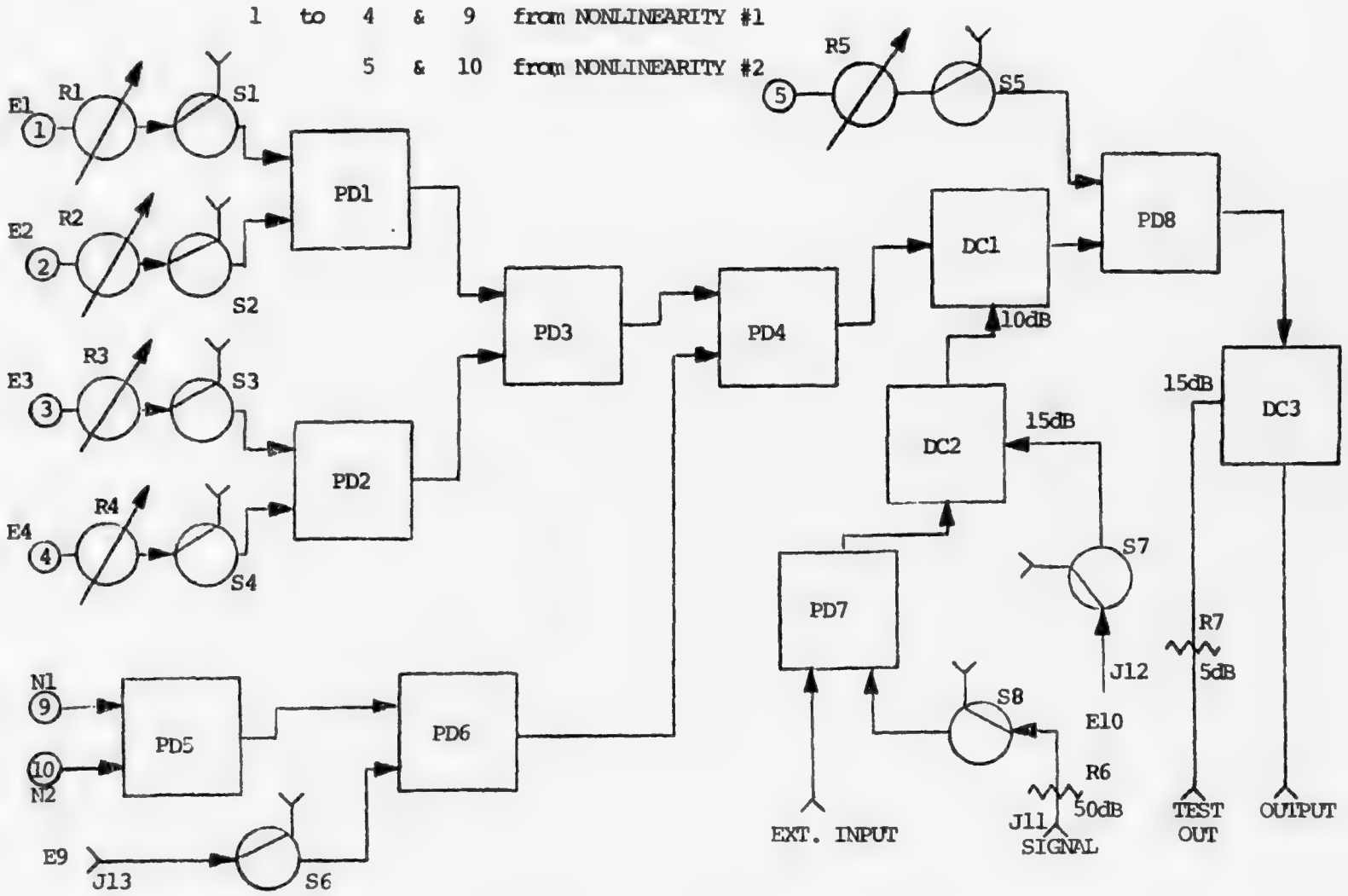

Figure 63: C1 - Combining Unit Schematic Diagram.

1 to 4 (output of PD3) are then added by power divider PD4.

The SIGNAL (S1) is fed to the COMBINING UNIT by means of a connector (J11) on the back. A 50 dB attenuator pad is used to decrease the signal level which can also be switched on and off by Switch S8 (SPDT RF switch) on the front panel. On the "OFF" position, a replica of the signal, 103 dB below the level obtained at the "TEST OUTPUT" jack on Unit S1, is available at a connector on the front panel of C1. In the "ON" position the signal is fed to one of the input ports of Power Divider PD7. The other port is fed by any external signal connected to the "EXT. INPUT" jack on the front panel. Emitter 10 is brought to the COMBINING UNIT through Connector J12 on the back. E10 is then directed by Switch S7 (SPDT RF switch) either to a connector on the front panel ("OFF" position) or to the coupled port of a 15 dB directional coupler DC2 which is used to combine E10 with the signal and the external input, fed to the output port of DC2. The input of DC2 is then connected to the coupled output of DC1 (10 dB directional coupler) which is also used as a combiner having as the other input the output of PD4. At the input port of DC1 we thus have the combination of EMITTERS 1 to 4, 9 and 10, the signal and the external input. The radar emitter (E5), obtained from a connector in Unit N2, is brought to attenuator R5 in C1 by internal connections. E5, after being attenuated by R5 can be switched on and off by S5. In the

"OFF" position, E5 is available at a connector on the front panel of C1. In the ON position, E5 is combined with all the other signals (available at the input port in DC1) in power divider PD8. The output of PD8 is then fed to the input port of a 15 dB directional coupler (DC3). The direct output of DC3 is connected to the "OUTPUT" port of C1. The coupled port of DC3 after being attenuated by a 5 dB pad (20 dB total attenuation) is connected to the "TEST OUT" port of C1. A table containing the attenuation of the various signals in Unit C1, from the input connectors to the "OUTPUT port, is given in Table 3, Chapter V.

B. N1 - NONLINEARITY #1

The schematic diagram for Unit N1 is shown in Figures 64, 66 and 68. Emitters 1 to 4 are fed to the unit through connectors J14, J13, J12 and J11 on the back. Each of these emitters is then split in three by two power dividers as shown in Figure 64. The outputs taken from the first power divider go to Attenuators R1 to R4 in C1-COMBINING UNIT (Figure 63). The two other outputs of each emitter go to Attenuators R1 to R4 in Units N1 (Figure 64) and N2 (Figure 65). The power dividers used to split Emitters 1 to 4 are PD1 to PD8 as shown in Figure 64. Emitters 5 to 8 are connected to ports on the back of N2. After a similar power splitting in N2, a sample of each of them is brought by internal connectors to attenuators R1 to R4 in Units N1 (Figure 64) and N2 (Figure 65). The power dividers used

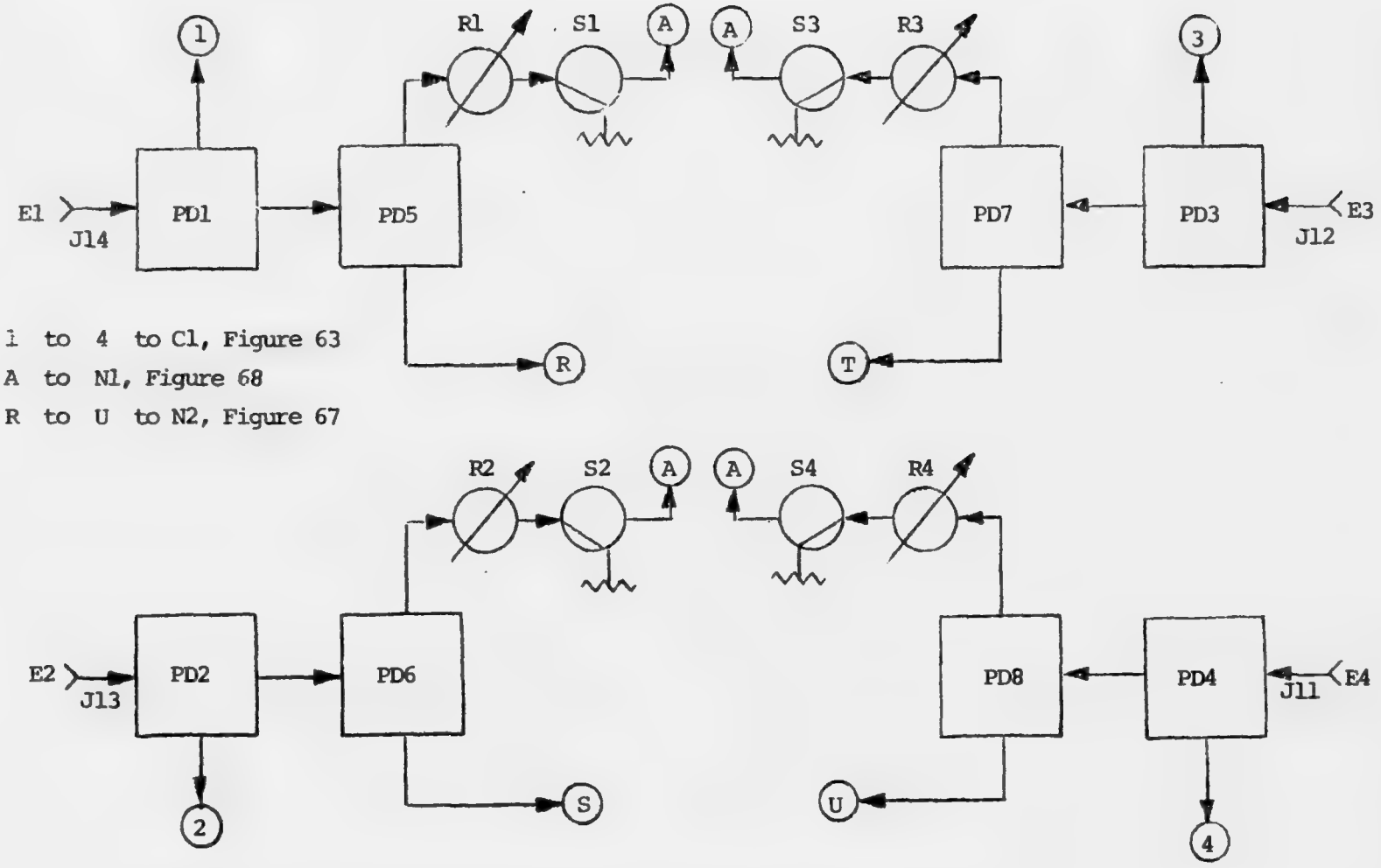

Figure 64: N1-Nonlinearity #1 Schematic Diagram (1 of 3).

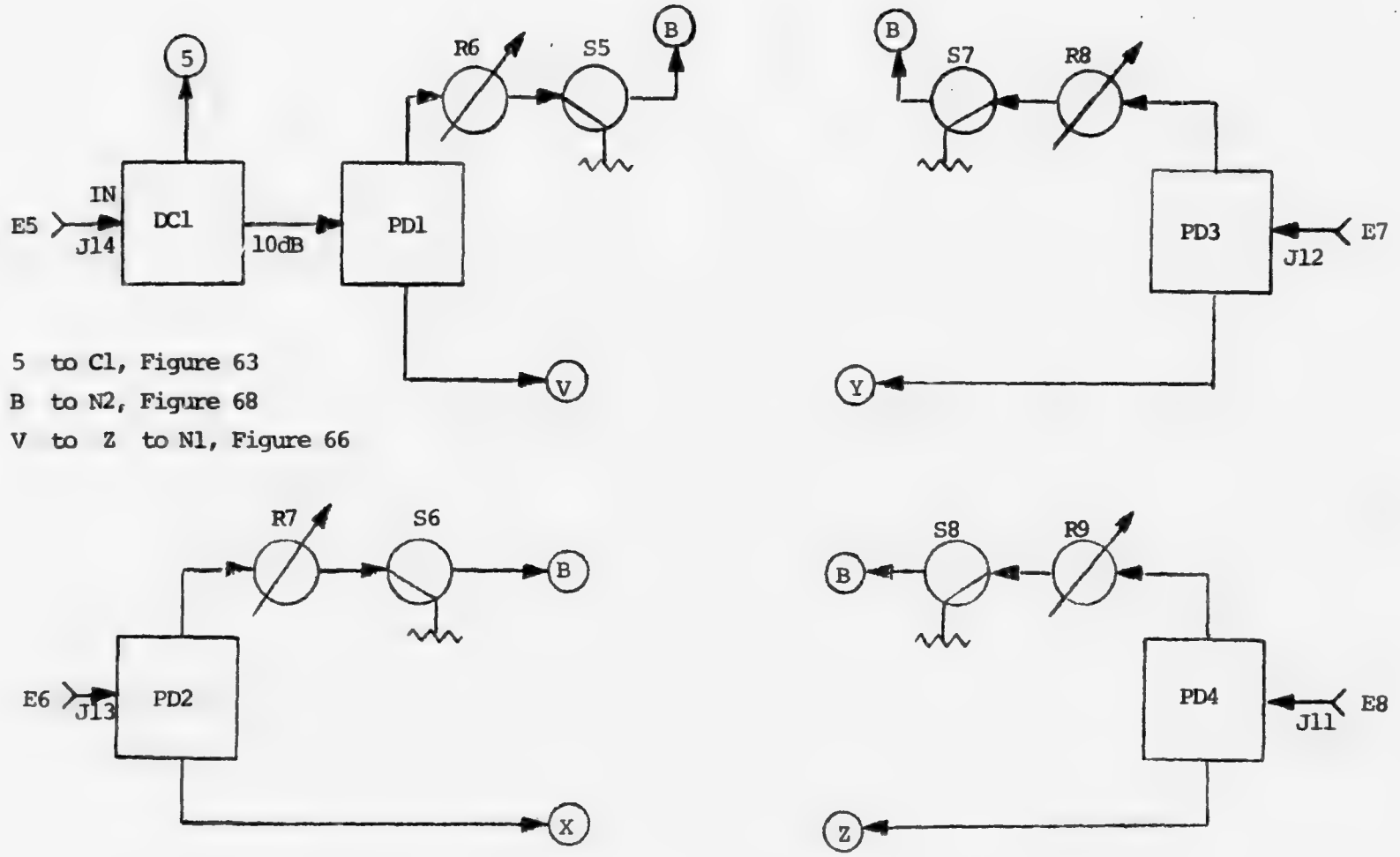

Figure 65: N2-Nonlinearity #2 Schematic Diagram (1 of 3).

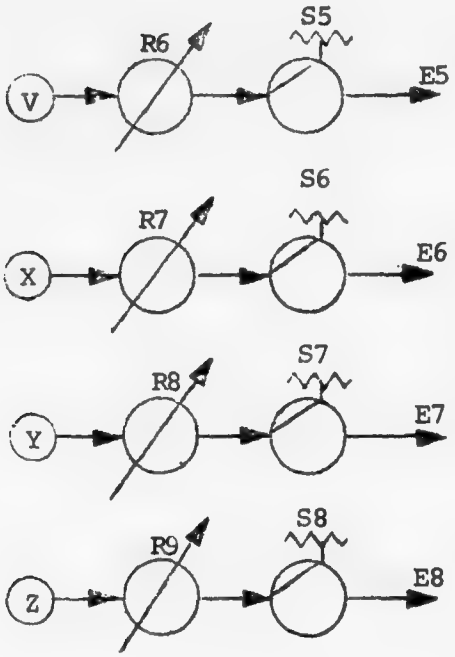

Figure 66: N1-Nonlinearity #1 Schematic Diagram (2 of 3).

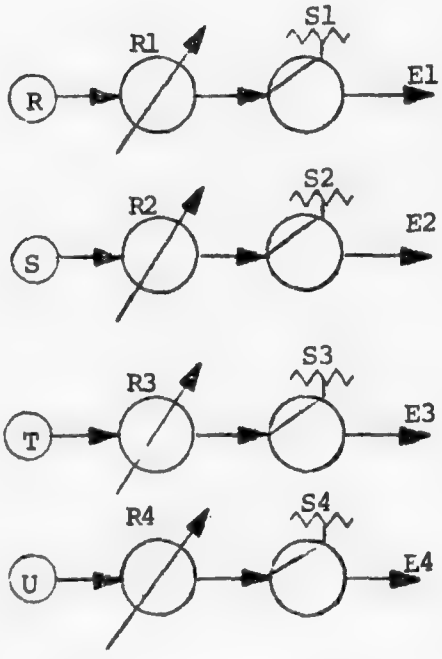

Figure 67: N2-Nonlinearity #2 Schematic Diagram (2 of 3).

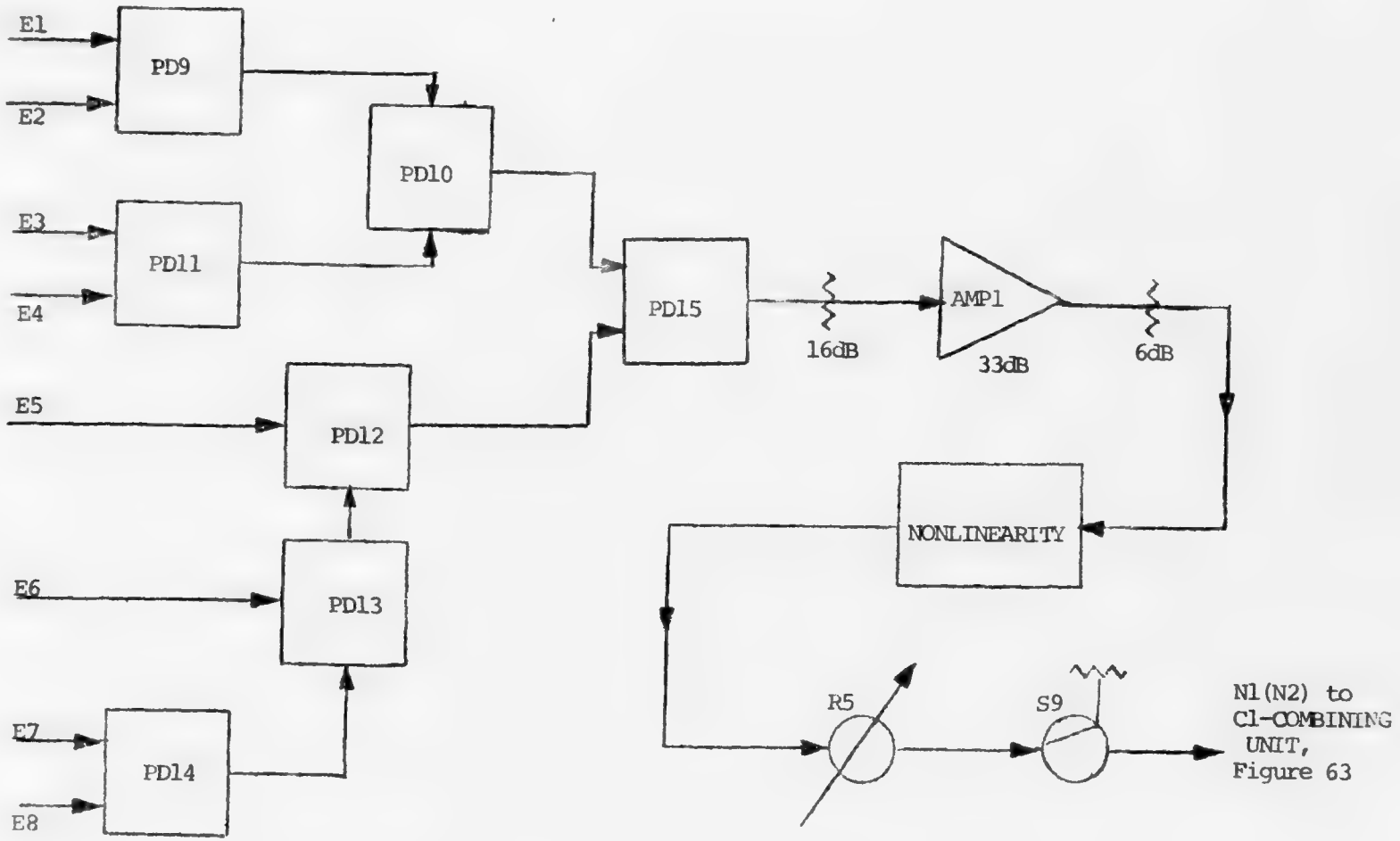

Figure 68: N1(N2) - Nonlinearity #1 (#2) Schematic Diagram (3 of 3).

to split Emitters 1 to 4 are PD1 to PD8 as shown in Figure 64. Emitters 5 to 8 are connected to ports on the back of N2. After a similar power splitting in N2, a sample of each of them is brought by internal connections to Attenuators R6 to R9 in N1 as shown in Figure 66. In cascade with Attenuators R1 to R4 and R6 to R9 we have Switches S1 to S4 and S5 to S8 which are SPDT RF switches used to turn Emitters 1 to 8 on or off. In the OFF position each emitter is dissipated in internal loads connected to one of the switch's ports. The attenuators above mentioned are 1 dB steps, 0-60 dB total attenuation components and allow for precise control of emitter levels to the nonlinearities.

After being attenuated, Emitters 1 to 8 are combined by power dividers PD9 to PD15 as shown in Figure 68. A 33 dB gain, 22 dBm 1 dB compression point amplifier (AMP1) is then used with the double purpose of guaranteeing that the weakest emitter will have a level well above the nonlinearity threshold and that enough reverse isolation is provided between the nonlinearity and the main signal lines as explained in Chapter V. A 16 dB pad at the input of AMP1 and a 6 dB pad at the output, guarantee that the weakest signal will have more than 10 dBm of pwer to the nonlinearity.

The nonlinearity was built by loading a 50Ω micro-strip transmission line with two back-to-back Schottky diodes. The transmission was built using inexpensive double sided printed circuit boards with a relative dielectric constant

(ε_r) of approximately 2.5. Measurements of the nonlinearity threshold were made as explained in Chapter V, which also contains results of the performance measurements on N1.

The results of nonlinear processing on Emitters 1 to 8 can then be attenuated by a 0-60 dB, 10 dB step attenuator (R5) and switched on and off by Switch S9. In the OFF position of S9 the signal is dissipated in an internal load. A word of caution should be made for the operation of the unit. Since AMP1 puts a noise level of 30 dB above thermal at the input of R5 and the total attenuation from the output of R5 to the "OUTPUT" port in C1 is only 16 dB, we see that in order to eliminate the contribution of this broadband noise to the interference appearing at the receiver front end, we must use R5 with a minimum of 20 dB of attenuation. While setting the levels of the intermodulation products, before running a test, R5 can be set at 0 dB to facilitate observation of the signals in a spectrum analyzer.

C. N2 - NONLINEARITY #2

The schematic diagram for Unit N2 is shown in Figures 65, 67 and 68. N2 is conceptually and physically identical to N2. The construction differences between them are due to the fact that parts of the circuit that is common to C1, N1 and N2 are located in N1 or N2. Emitters 5 to 8 are fed to the unit through connectors J14, J13, J12 and J11 on the back. Emitter 5 is split in three parts by a 10 dB directional coupler (DC1) and a power divider (PD1) as shown in

Figure 65. The direct output of the coupler provides the E5 signal to C1-COMBINING UNIT. The two outputs of PD1 provide the E5 signal to attenuator R6 in N1 and N2 as shown in Figures 65 and 66. Emitters 6 to 7 are split in two by power dividers PD2 to PD4. The outputs of these power dividers provide the E6, E7, and E8 signals to attenuators R7, R8 and R9 in units N1 and N2 as shown in Figures 65 and 66. As in N1, signals E1 to E8 can be individually switched on and off by SPDT RF Switches (S1 to S8). The combining and nonlinear processing of Emitters 1 to 8 in NONLINEARITY #2 is exactly the same as in N1. Thus, the same description and Figure 68 apply.

Parts lists for C1, N1 and N2 is given in Appendix 12.

Interconnection tables for Units C1, N1 and N2 are given below.

Table 8

Connection Information for C1

Connector	Function	Connected to
C1 - J11	Signal (S1) input	S1 - J11
C1 - J12	Emitter 10 (E10) input	E10 - J12
C1 - J13	Emitter 9 (E9) input	E9 - J12

Table 9

Connection Information for N1

Connector	Function	Connected to
N1 - J11	Emitter 4 (E4) input	SRC/21 OUT (COM. LAB)
N1 - J12	Emitter 3 (E3) input	SRC/21 OUT (RADAR LAB)
N1 - J13	Emitter 2 (E2) input	E2A - J15
N1 - J14	Emitter 1 (E1) input	E1A - J15

Table 10

Connection Information for N2

Connector	Function	Connected to
N2 - J11	Emitter 8 (E8) input	E8 - J18
N2 - J12	Emitter 7 (E7) input	E6/E7 - J12
N2 - J13	Emitter 6 (E6) input	E6/E7 - J13
N2 - J14	Emitter 5 (E5) input	E5C - J14
N2 - P11	+24V DC power	PS1 - J11

APPENDIX 2

DETAILED DESCRIPTION OF EMITTERS 1 AND 2 (E1,E2)

Emitters 1 and 2, having been built in the same way, will necessitate only one description. A schematic diagram for Unit E1A (E2A) is given in Figure 69 and for Units E1B (E2B) and E1C/E2C in Figure 70. Unit E1A (E2A) performs the following functions:

a) Generates a pseudo-random data stream to modulate a carrier,

b) Performs PSK modulation of a 30 MHz carrier,

c) Filters the modulated carrier with a 30 KHz bandwith XTAL filter,

d) Up-converts the signal to the UHF band,

e) Selects the modulated or unmodulated signal either to a counter or to processing by units C1, N1 and N2.

Functions a) to e) above are executed by A2, DBM2, FL1, DBM1 and S2, respectively as shown in Figure 69. The 30 MHz carrier is obtained from Unit E8 and is fed to connector J13 with a level of 2 dBm for E1 and -1 dBm for E2. These levels were determined by looking to the spectrum of the signal at the J15 port and observing the distortion caused by nonlinear effects of amplification by E1C/E2C on the two side-bands of the signal that exist as a result of the up-conversion in DBM1. These operating points are at the beginning of the nonlinear region of E1C/E2 as shown

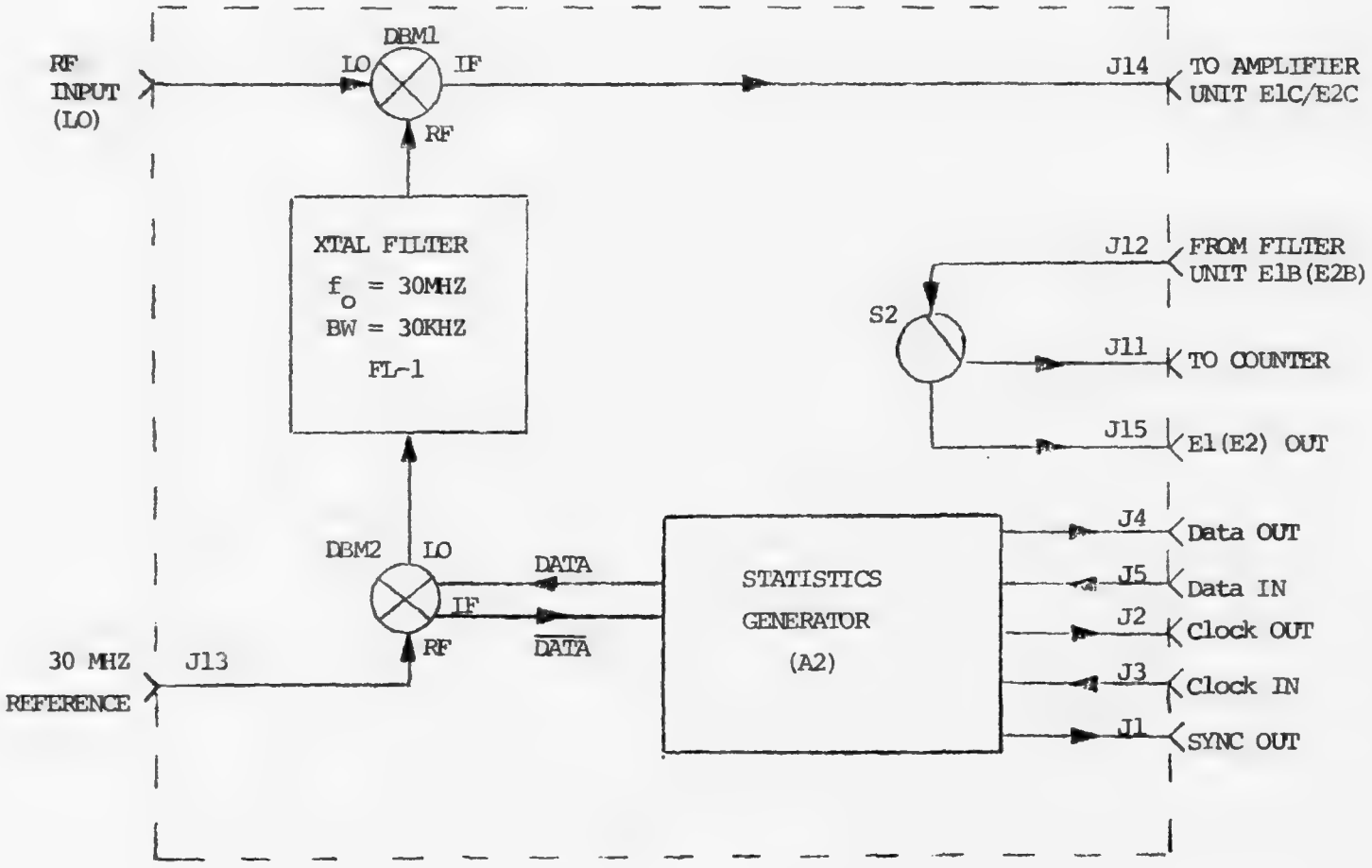

Figure 69: E1A(E2A) UHF/PSK Modulator Schematic Diagram.

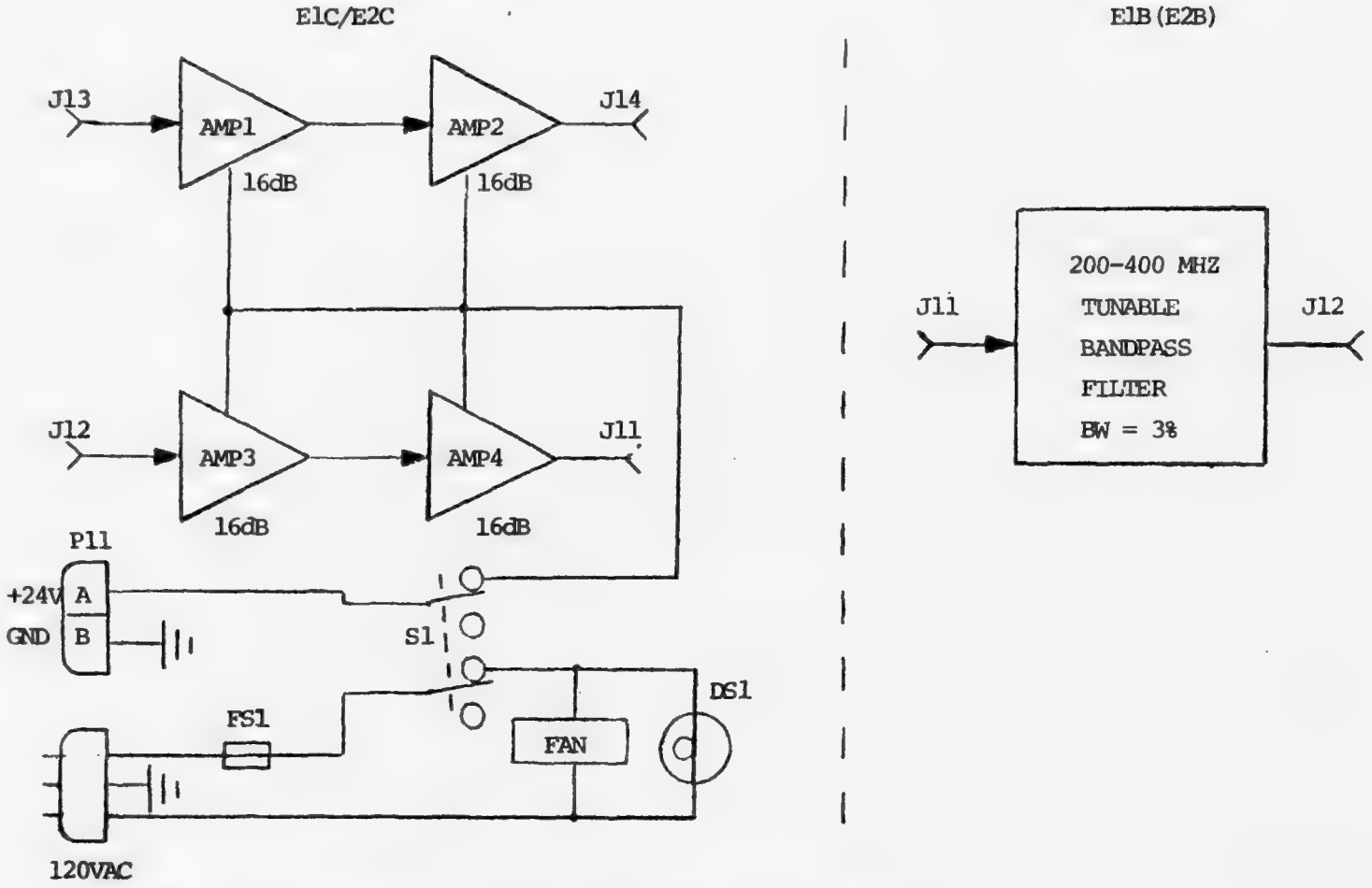

Figure 70: E1B(E2B) & E1C/E2C Schematic Diagrams.

by Figures 35 and 38 in Chapter V and the difference in levels is due to different overall transfer characteristics for E1 and E2 including amplification and filtering.

DBM2 is a very high level (+23 dBm LO) double-balanced mixer used to PSK modulate the 30 MHz carrier. After modulation the signal is then filtered by FL-1 a 30 KHz bandwidth, 30 MHz XTAL filter. DBM1 performs then an up-conversion of this signal. DBM1 is a high-level (+17 dBm LO) mixer and requires a L.O. power of at least 7 dBm at the "RF INPUT" port (J6) on the front panel of E1A (E2A). The loss in DBM1 will vary from -7.5 dB to -6.3 dB depending on LO level. At J14, the two sidebands which resulted from the up-conversion of the signal, are available for amplification in Unit E1C/E2C.

Switch S2 is a RF SPDT switch used to control the flow of the signal as explained before. Detailed description of A2-STATISTICS GENERATOR used as a source of pseudo-random data is reserved for Appendix 9 since A2 is used to generate statistics for various units.

The up-converted signal is amplified by a two amplifier chain in E1C/E2C. Each amplifier has a nominal 16 dB gain and 28 dBm compression point. DC power for the amplifiers can be switched on and off by Toggle Switch S1, at the same time that AC power is switched on and off for a cooling fan d for a neon lamp DS1 on the front panel. The amplified signal is E1C/E2C is filtered by Unit E1B/E2B and brought

back to E1A (E2A) where RF Switch S2 controls it as explained before.

Results of performance measurements in Units E1 and E2 are given in Chapter V. Parts list for E1 and E2 are given in Appendix 12. Interconnection information for E1 and E2 is given in Tables 11 and 12.

Table 11

Interconnection Information for E1

Connector	Function	Connected to
E1A - J11	Output to counter	HP 5383A - J15
E1A - J12	Input from filter unit E1B	E1B - J12
E1A - J13	30 MHz reference input	E8 - J12
E1A - J14	Output to amplifier	E1C/E2C - J13
E1A - J15	E1 output for processing	N1 - J14
E1B - J11	Filter input	E1C/E2C - J14
E1B - J12	Filter output	E1A - J11
E1C/E2C - J13	Amplifier input	E1A - J14
E1C/E2C - J14	Amplifier output	E1B - J11
E1C/E2C - P11	+24 VDC input	PS1 - J17

Table 12

Interconnection Information for E2

Connector	Function	Connected to
E2A - J11	Output to counter	HP5383A - J11
E2A - J12	Input from filter	E2B - J12
E2A - J13	30 MHz reference input	E8 - J13
E2A - J14	Output to amplifier	E1C/E2C - J12
E2A - J15	E2 output	N1 - J13
E2B - J11	Filter input	E1C/E2C - J11
E2B - J12	Filter output	E2A - J12
E1C/E2C - J11	Amplifier output	E2B - J11
E1C/D2C - J12	Amplifier input	E2A - J14

APPENDIX 3

DETAILED DESCRIPTION OF EMITTERS 3 AND 4 (E3,E4)

A block diagram of Emitter 3(4) is given in Chapter V. In this appendix a schematic diagram of E3A(E4A) is presented in Figure 71. Two STATISTICS GENERATOR (A2) boards are used to generate two pseudo-Poisson processes as explained in Appendix 9. One will be a start signal and the other a stop signal that will control the PTT output of E3A(E4A). The PTT signal is used to switch a reed-relay (K1) that controls a SRC/21 transmitter. A front panel OUTPUT (J1) of the PTT signal is available at the "PTT OUT" port of E3A(E4A). A LED (DS1) in parallel with this output furnishes visual indication of PTT operation. Switch S11 in the back of the unit, selects the signal that will control the transmitter. Internal (I) or external (E) control can be chosen. In the external position a TTL compatible signal at J11 will be necessary.

Audio output from the R-390A receiver is fed to P11 and "MODULATION" switch directs this signal either to the AN/SRC-21 audio input or to a 620Ω internal load. CLOCK #1 and CLOCK #2 output connectors (J12 and J14) provide an output of the clocks of the two pseudo-random impulse generators in E3A(E4A). These outputs are derived from TTL line drivers and thus will accept a 50Ω load. CLOCK #1 and CLOCK #2 input connectors (J13 and J15) can be fed with

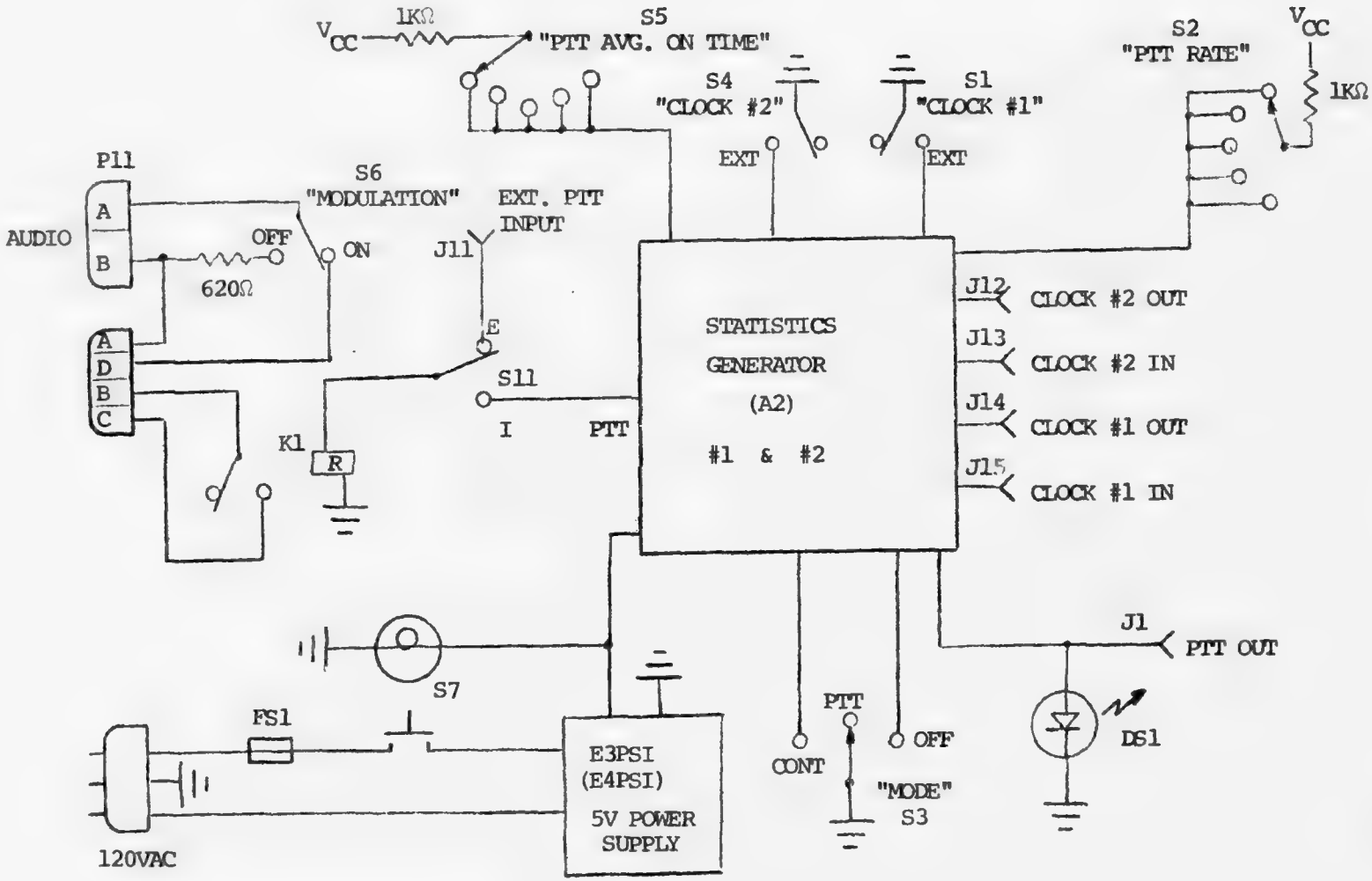

Figure 71: E3A(E4A) Schematic Diagram.

a TTL compatible clock source when "CLOCK #1" and (or) "CLOCK #2) switches are in "EXT".

Interconnection information for E3A (E4A) is given in Tables 13 and 14.

Performance results for E3(E4) are given in Chapter V, and parts list in Appendix 12.

Table 13

Interconnection Information for E3

Connector	Function	Connected to
E3A - P11	Audio input	R 390A - J11
E3A - P12	Remote control	SRC/21 - J104 (Radar Lab)
E3A - J11	External PTT input	TTL compatible source
E3A - J12	Clock #2 output	Any 50Ω load
E3A - J13	Clock #2 input	TTL compatible source
E3A - J14	Clock #1 output	Any 50Ω load
E3A - J15	Clock #1 input	TTL compatible source

Table 14

Interconnection Information for E4

Connector	Function	Connected to
E4A - P11	Audio input	R390A - J12
E4A - P12	Remote control	SRC/21 - J104 (Com Lab)
E4A - J11	External PTT input	TTL compatible source
E4A - J12	Clock #2 output	Any 50Ω load
E4A - J13	Clock #2 input	TTL compatible source
E4A - J14	Clock #1 output	Any 50Ω load
E4A - J15	Clock #1 input	TTL compatible source

APPENDIX 4

DETAILED DESCRIPTION OF E5

The UHF/RADAR interferer, being the most important of all sources of interference, was implemented with great care. In order to account for all relevant characteristics of the emitter, its implementation required the use of six units as described below:

E5A	RADAR pulse modulator
E5B	RADAR AMPLIFIER (HUGHES 1416 H AMPLIFIER)
E5C	RADAR SCAN MODULATOR
HP3200B	SIGNAL GENERATOR
HP8011A	PULSE GENERATOR
INTERDATA 7/32	MINICOMPUTER

Detailed description and operating instructions for Units E5B, HP3200B, HP8011A and INTERDATA 7/32 can be found in technical and operating manuals for these equipments. Detailed description with the presentation of schematic diagrams for Units E5A and E5C will be given in this appendix.

Performance results for E5 are given in Chapter V.

Parts list for E5 are given in Appendix 12. Interconnection information for the units of E5 is given in Table 15.

Table 15

Interconnection Information for E5

Connector	Function	Connected to
E5A - J11	Scan modulated noise input	E5C - J11
E5A - J12	Scan & pulse modulated noise input	E5C - J12
E5A - J13	Scan modulated RF input	E5C - J15
E5A - J14	Pulse output to counter	HP5383A - J12
E5A - P11	+5 VDC power	PS1 - J14
E5C - J11	Scan modulated noise output	E5A - J11
E5C - J12	Scan & pulse modulated noise input	E5A - J12
E5C - J13	Noise output to E9	E9 - J11
E5C - J14	E5 output	N2 - J14
E5C - J15	Scan modulated RF output	E5A - J13
E5C - J16	RF input	HP-3200B - OUT
E5C - J17	RF output to counter	HP-5383A - J16
E5C - P11	Computer input and output	INTERDATA 32
E5C - P11	+24 VDC, ±15 VDC, +5 VDC power	PS1 - J13

A. E5A - RADAR PULSE MODULATOR

In order to obtain a pulsed RF signal a double balanced mixer (DBM) was used as the modulating device. Since a real life DBM is capable only of a finite amount of attenuation,

expressed as an ON/OFF RATIO (relation between maximum and minimum output signal taken from LO port when IF current is being used to control the attenuation) it can be seen that there will always exist a residual carrier in addition to the pulsed RF signal at the mixer output. In order to obtain a signal with a spectrum resembling that of a true pulsed RF signal a more careful analysis had to be made.

When we are using a DBM as pulse modulator, the output signal Fourier transform will have the following expression:

$$O(f) = F(f) + \frac{C}{2}\delta(f - f_0) + \frac{C}{2}\delta(f + f_0) \qquad \text{(A4-1)}$$

where F(f) is the Fourier transform of a true pulsed RF signal as given by (3.11) and C is the amplitude of the residual carrier. In formula (3.11), B is the amplitude of the input unmodulated RF carrier and A represents the minimum attenuation (insertion loss) of the DBM (usually given as 20 log A in the specification sheets). Recalling again from expression (3.11) that the carrier amplitude after modulation is $\frac{ABT_p}{2T}$, the total carrier amplitude after modulation in a DBM will be

$$\text{Carrier} = \frac{ABT_p}{2T} + \frac{C}{2} \qquad \text{(A4-2)}$$

where the first term corresponds to a true pulsed signal and the second represents the effect of the residual carrier. As before, T_p is the modulating pulse width and T is the

pulse repetition period. In order to obtain a faithful representation of the true pulsed signal we want the first term in (A4-2) to be much greater than the second one. Thus we have as a desirable condition:

$$AB \frac{T_p}{T} >> C \qquad \text{(A4-3)}$$

or

$$\frac{T}{T_p} << \frac{AB}{C} \qquad \text{(A4-4)}$$

Taking 20 log( ) of both sides of (A3.4) we get

$$2 \times (10 \log \frac{T}{T_p}) << 20 \log \log \frac{AB}{C} \qquad \text{(A4-5)}$$

since $10 \log \frac{T}{T_p}$ is the radar "DUTY CYCLE" in dB and $20 \log \frac{AB}{C}$ is the expression for the DBM ON/OFF RATIO we obtain:

$$\text{DUTY CYCLE} << \frac{\text{ON/OFF RATIO}}{2} \qquad \text{(A4-6)}$$

Since DUTY CYCLES of 30 dB or more can be expected and ON/OFF RATIOS for DBM's are less than 50 dB it was found that we needed to use two DBM's in series to provide the necessary attenuation.

For the pulsed noise modulation a similar problem was confronted. The model for the impulsive noise being:

$$n(t) = a(t)n_c(t) \qquad (3.14)$$

where $n_c(t)$ is a broadband Gaussian process and $a(t)$ the modulating signal. Again, since a DBM was used to implement the model, we could represent the signal after modulation as

$$n(t) = Aa(t)n_c(t) + n_R(t)$$

where $n_R(t)$ is a residual (non-impulsive) Gaussian process. Since we want to avoid any uncontrollable contribution of Gaussian noise to the simulator output, we must provide that this residual Gaussian process will be below thermal noise. For this reason, 2 DBM's in series were also used as modulators.

The actual implementation of E5A RADAR PULSE MODULATOR is shown in Figure 72. The RF carrier after being modulated in E5C-RADAR SCAN MODULATOR is fed to the "R" port of DBM1 from J13. Signal level at this point is 14 dBm. After being modulated by DBM1 and DBM2 the pulsed RF signal will be fed to E5B RADAR AMPLIFIER from "PULSED RF" connector (J1) in the front panel. The signal level at J1 is 6 dBm peak since the two DBM's in cascade have a measured insertion loss of 8 dB. Similarly, the signal path for the noise is described in the following manner. At J11 a scan modulated Gaussian noise signal with a power spectrum density of approximately 88 dB above KT is presented. This signal is modulated in

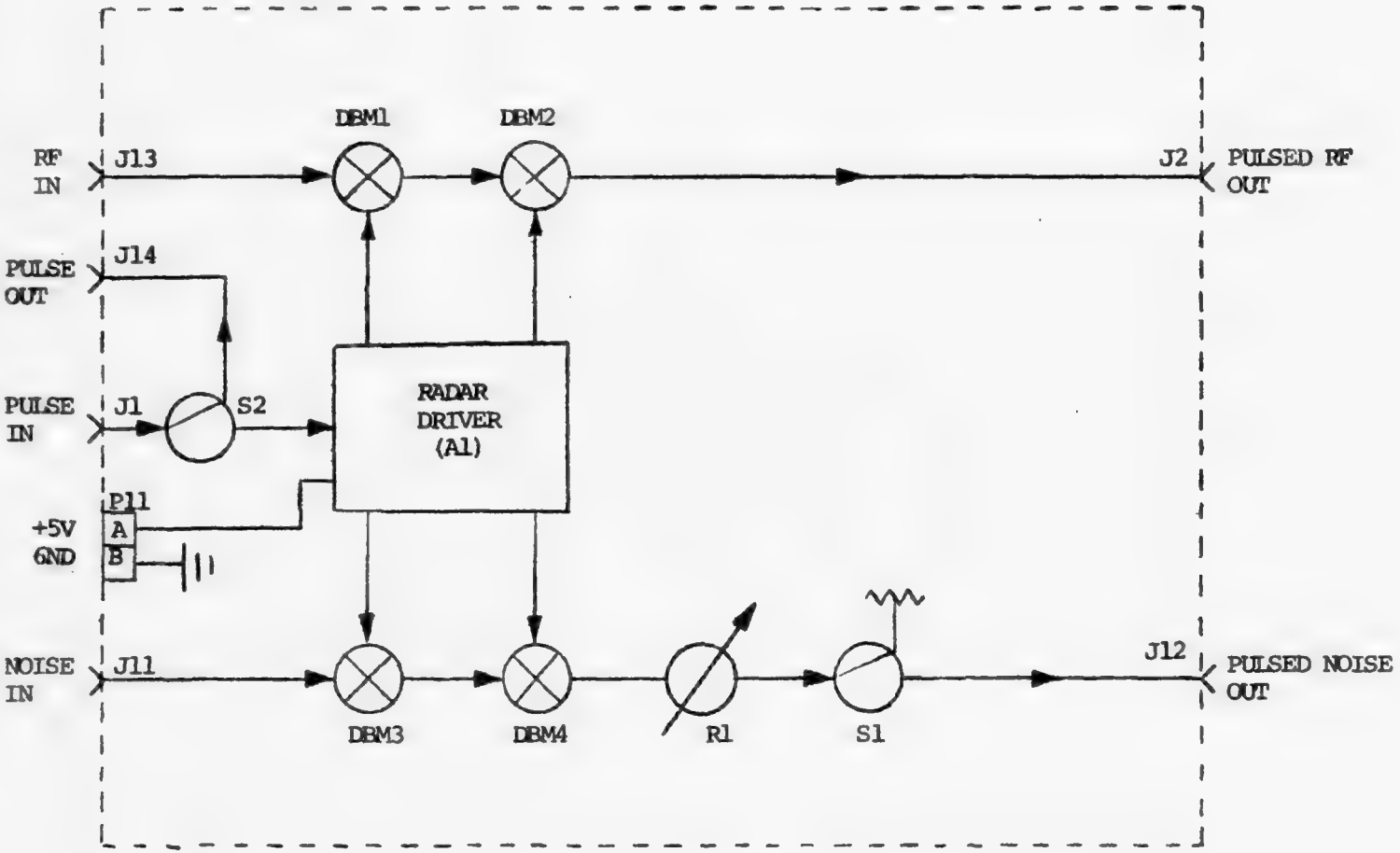

Figure 72: E5A - Radar Pulse Modulator Schematic Diagram.

DBM's 3 and 4 and can be attenuated from 0 to 60 dB in 10 dB steps by rotary attenuator R1. Switch S2 on the signal line can be used to turn off this signal. All four DBM's are driven in parallel from the same modulating signal s(t). Figure 73 shows the DRIVER schematic diagram. In that figure IC1 is a simple inverter and IC's 2 and 3 are line drivers. Resistor R1 is used to present a 50 Ohm load at the input J1 and Resistors R2 to R13 have the double purpose of controlling the currents to the DBM's IF ports and presenting a 50 Ohm load to these ports simultaneously.

The modulating signal s(t) is derived from an HP8011A PULSE GENERATOR which provides pulse width control from 25 nsec. to .1 sec and pulse repetition periods from 50 nsec to 10 sec. Switch S1 provides the means of switching s(t) to the DRIVER or to connector J14 which is connected to the frequency counter that permits quick measurement of PRF. To obtain an accurate measurement of pulse width, on the other hand, the PULSE GENERATOR must be previously calibrated with the help of an oscilloscope.

B. E5C - RADAR SCAN MODULATOR

The RADAR SCAN MODULATOR UNIT performs various functions on the implementation of Emitter 5. It contains a source of broadband Gaussian noise used in E5 and also in E9. It generates a clock at 360 times the scan rate selected by the "SCAN RATE" switch on the front panel of the unit, which is used as an interrupt for the computer on the creation of the antenna pattern scan. Unit E5C also performs scan

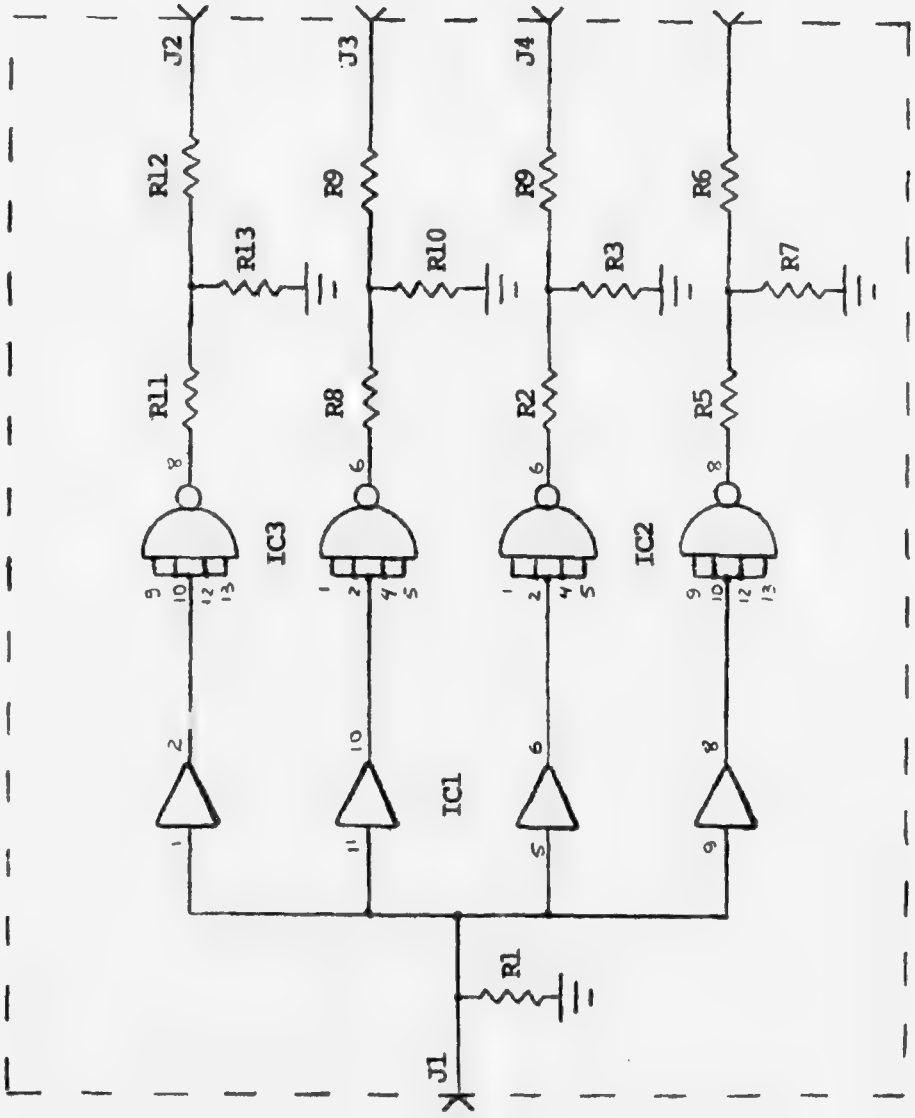

Figure 73: Radar Driver (A1) Schematic Diagram.

modulation on both the RF and noise component of E5 and has the filters for the pulsed RF component of E5. In addition to that the pulsed RF and noise components of E5 are added in E5C. Finally, Unit E5C provides the switch that allows one to turn the RF source "ON" or to the counter for frequency measurements. Schematic diagrams for E5C are given in Figures 74 and 75.

The Gaussian noise source was small with three amplifiers with 33 dB of gain and noise figure of 3 dB. A high pass-filter (FL3) was used to eliminate low frequency oscillations in this high-gain, wideband amplifier chian. The 10 dB pad (R4) was used to limit the noise power to the pulse modulator. Power divider PD1 splits the noise in two parts. One, after further amplification by AMP3 will constitute the pulsed noise component of E5. The other will be used as the Gaussian noise source in E9 - IMPULSIVE NOISE. The RF and the noise are modulated with the antenna pattern, at the scan rate, by two digitally controllable pin-diode modulators. The antenna pattern is stored in the computer memory and released at 360 times the scan rate by interrupts created by the scan rate selection circuit. Switch S2 is a SPDT RF switch on the RF line, used to switch the RF source to the counter for frequency measurements. Bandpass filters FL-1 and FL-2 in Figure 75, cover the bands from 200-224 MHz and 420-470 MHz respectively and are used to filter the RF component of E5. Coupler DC1 is used as a combining unit to add the pulsed RF with the pulsed noise signal.

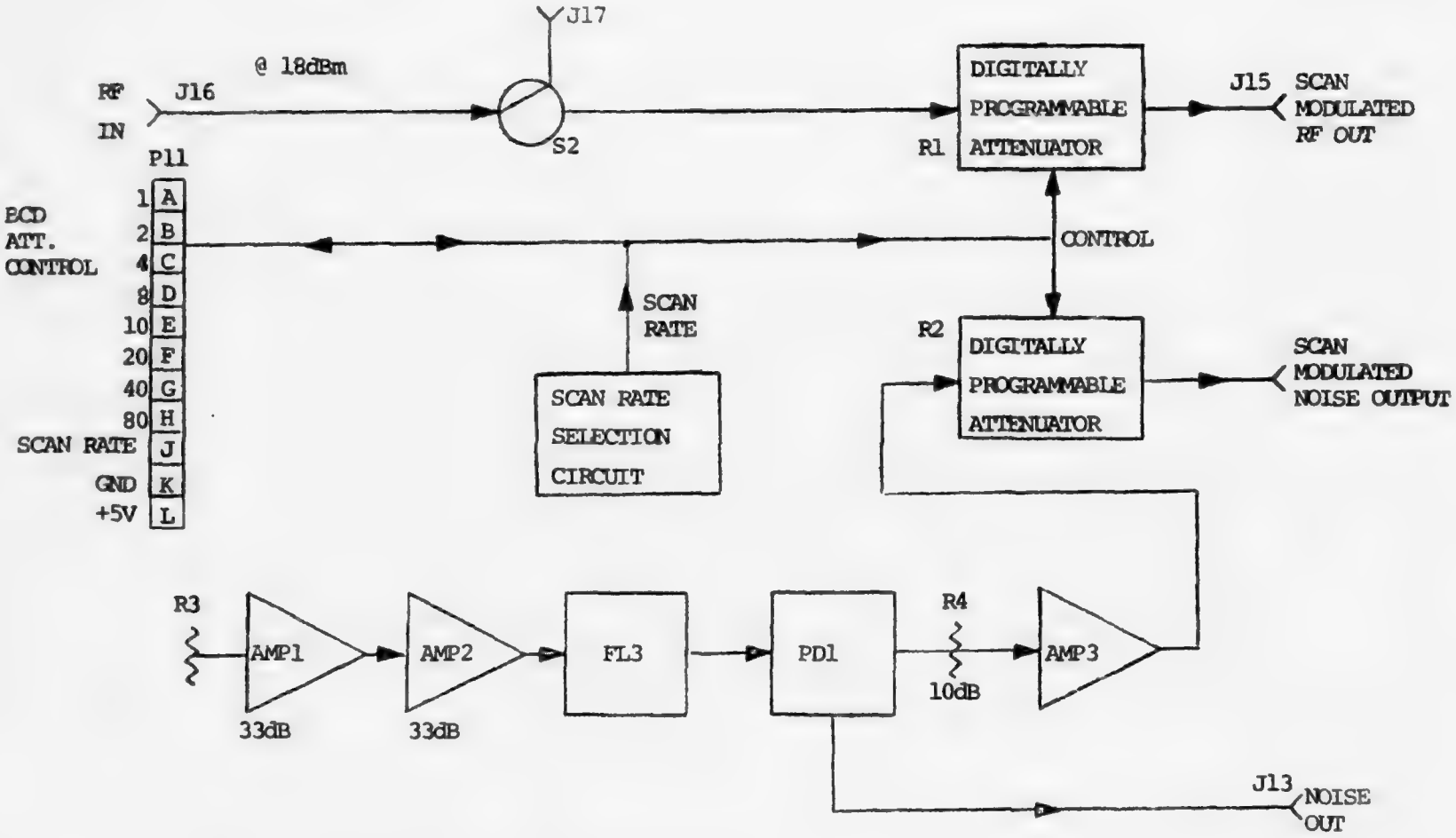

Figure 74: E5C-RADAR SCAN MODULATOR Schematic Diagram (1 of 2).

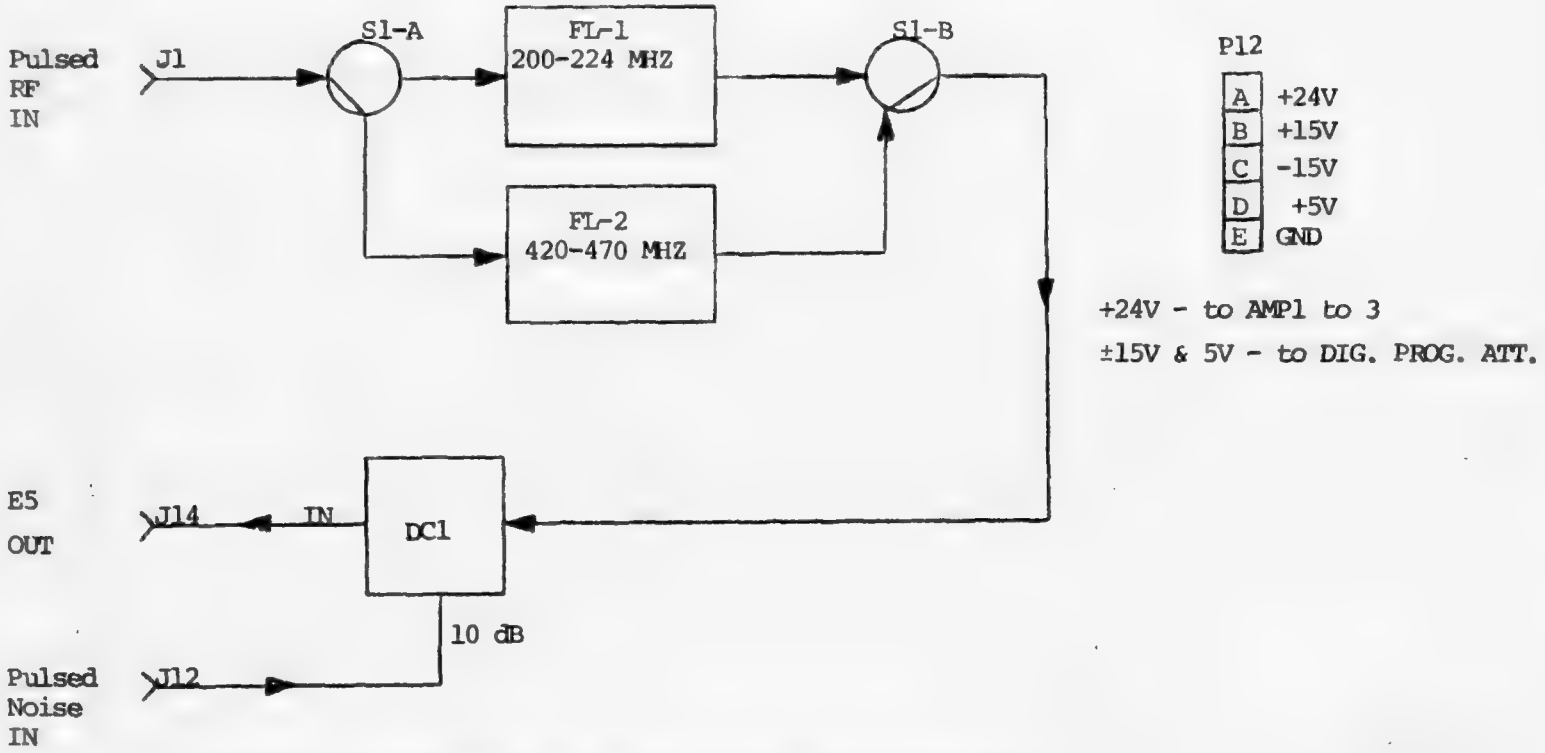

Figure 75: E5C Radar Scan Modulator Schematic Diagram (2 of 2)

The scan rate selection circuit was implemented as shown in Figure 76. A 1.024 MHz XTAL oscillator is divided by 700 by a dividing chain of 3 fixed counters (IC1 to IC3). Two additional counters (IC4 and IC6) can be programmed by the "SCAN RATE" switch on the front panel to give the total divide ratio for the dividing chain as shown in Table 16. In this fashion, by varying the divide ratio we can obtain the nominal scan rates with an accuracy better than 1.6%.

Table 16

Scan Rate Programming

NOMINAL SCAN RATE (RPM)	DIVIDE RATIO	ACTUAL SCAN RATE (RPM)	PROGRAMMING INPUTS (*)							
			1	2	4	8	10	20	40	80
5	2.016×10^5	5.079	0	0	1	0	0	1	0	0
6	1.68×10^5	6.095	0	0	0	0	0	1	1	0
7	1.47×10^5	6.966	1	1	0	0	1	0	1	0
12	8.4×10^4	12.190	0	0	0	0	0	0	0	1
15	6.7×10^4	15.238	0	1	0	0	0	0	0	1

(*) 0 = GND

1 = OPEN

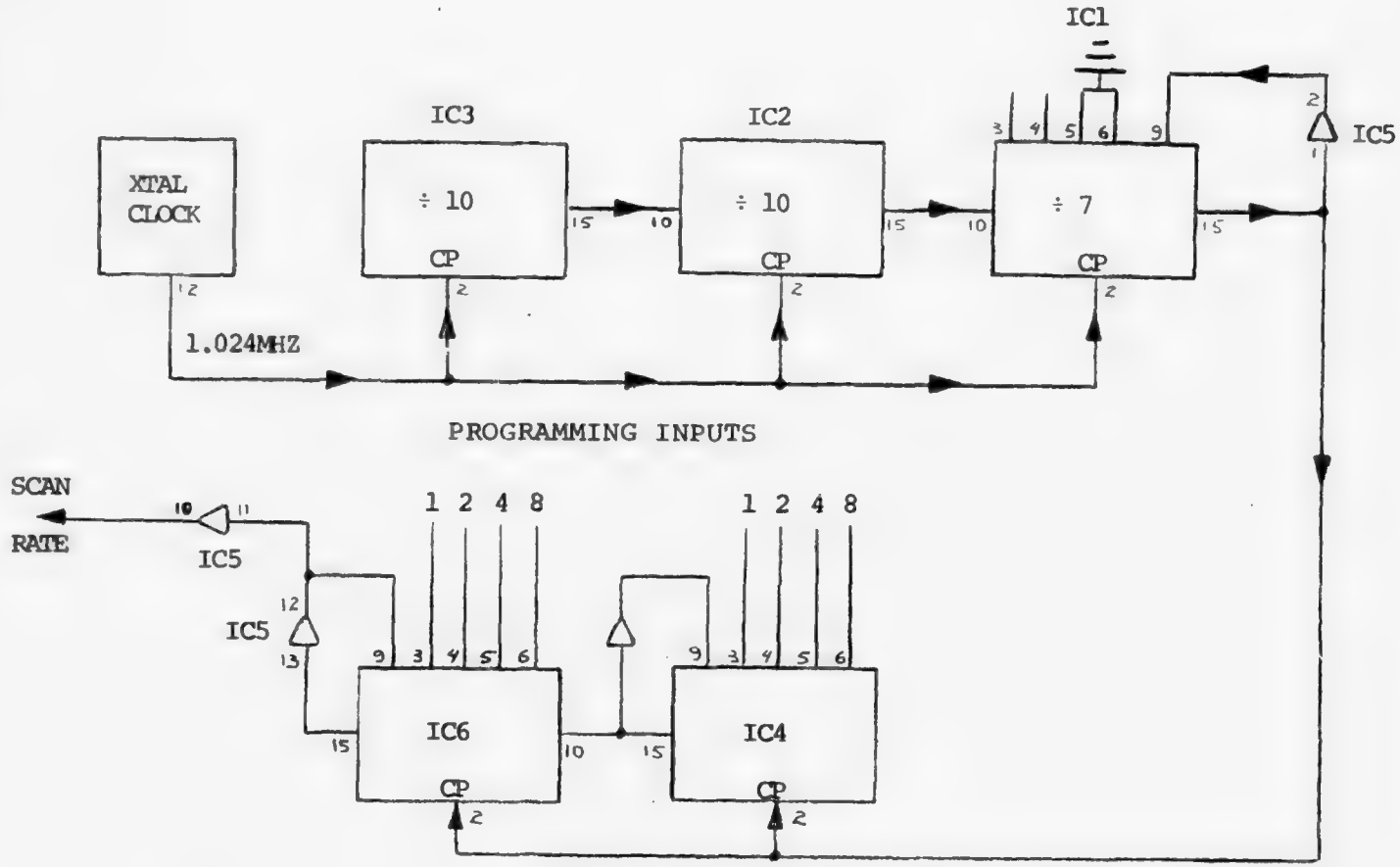

Figure 76: Scan Rate Selection Circuit Schematic Diagram.

APPENDIX 5

DETAILED DESCRIPTION OF EMITTERS 6,7,8 AND 30 MHz REFERENCE

A. EMITTERS 6 AND 7

Emitters 6 and 7 are located in the same unit E6/E7 - VHF/HF INTERFERERS. Both emitters have identical construction except for the band of operation. Schematic diagram for E6 is given in Figure 77 and for E7 in Figure 78.

A HP-3200B signal generator is the source of RF signal. This signal is amplified by a 16 dB gain amplifier with a 1 dB compression point bigger than 28 dBm. The amplified signal can be switched "ON" or to the "COUNTER" for frequency measurements purposes by a SPDT RF switch. Another switch, this time a DPDT RF switch, can select one of two bandpass filters according to the desired band of operation. For E6 the options are 40-75 MHz and 108-200 MHz. For E7 the options are 10-16 MHz and 16-26 MHz. These filters are used to reduce the harmonic contents of the signals to comply with military specifications and also to present "clean" signals to the processing part of the simulator in order to guarantee that the effects being created are due to the processing and not to the signal itself. After filtering the signal is split in two by a power divider. One of the outputs is the interferer and the other is available at the "TEST OUTPUT" of the unit for monitoring or any other purpose.

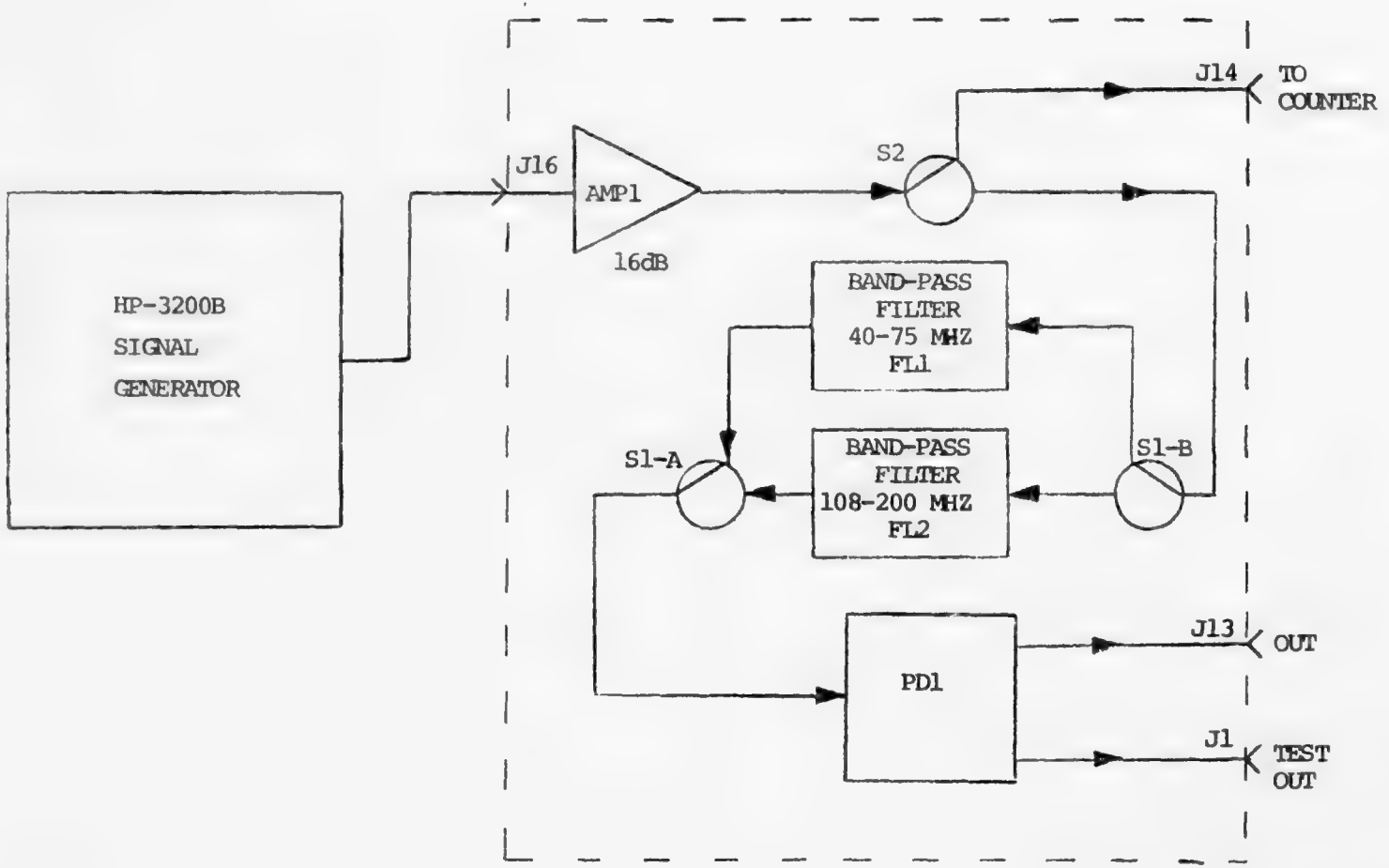

Figure 77: E6 Schematic Diagram.

AD-A035 743 NAVAL POSTGRADUATE SCHOOL MONTEREY CALIF F/G 17/2.1
A SIMULATOR FOR SHIPBOARD RADIO FREQUENCY INTERFERENCE IN SATEL--ETC(U)
OCT 76 E S BRICK, J E OHLSON
UNCLASSIFIED NPS-620L76109 NL

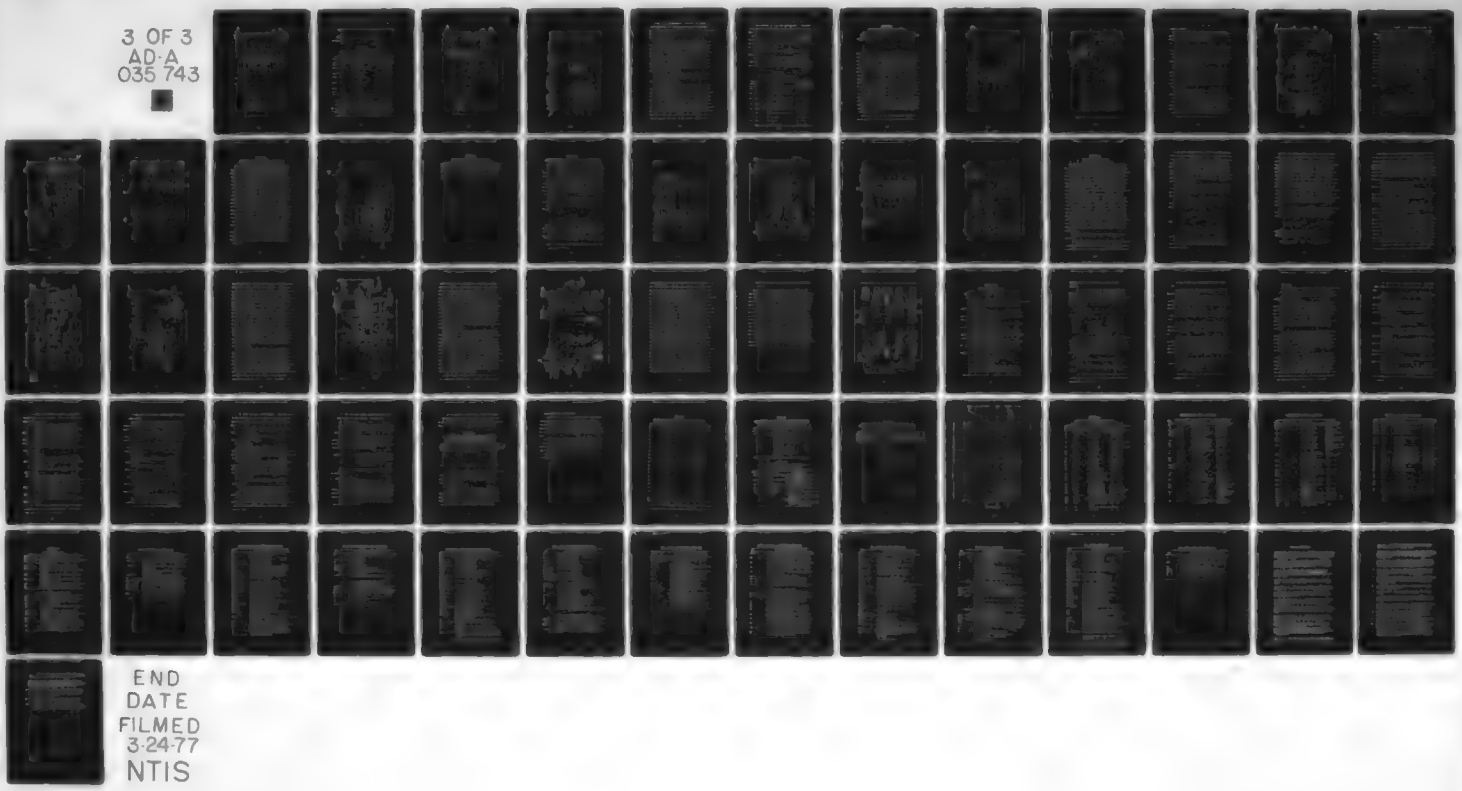

3 OF 3
AD-A
035 743

END
DATE
FILMED
3-24-77
NTIS

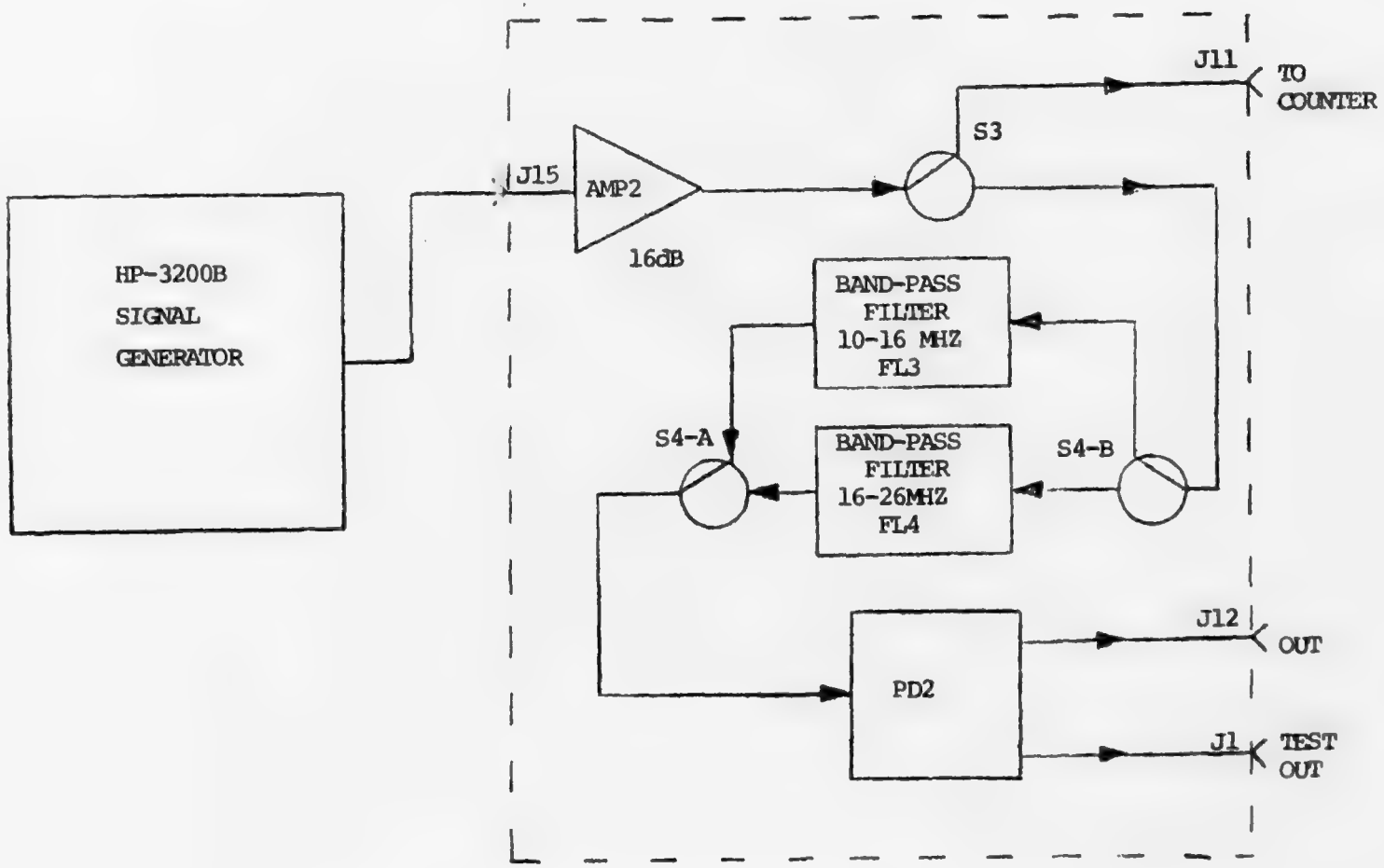

Figure 78: E7 Schematic Diagram.

Parts list for emitters 6 and 7 is given in Appendix 12.

Performance measurements for E6/E7 is given in Chapter V.

Interconnection information for Emitters 6 and 7 is given in Table 17.

Table 17

Interconnection Information for E6 and E7

Connector	Function	Connected to
E6/E7 - J13	E6 Output	N2 - J13
E6/E7 - J14	E6 RF output to counter	HP 5383A - J13
E6/E7 - J16	E6 RF input	HP 3200B - OUT
E6/E7 - P11	+24 VDC power	PS1 - J12
E6/E7 - J11	E7 RF output to counter	HP 5383A - J17
E6/E7 - J12	E7 output	N2 - J12
E6/E7 - J15	E7 RF input	HP 3200 B - OUT

B. EMITTER 8 AND 30 MHZ REFERENCE

As we mentioned in Chapter IV, Emitter 8 and the 30 MHz reference circuit are located in the same unit (E8 - HF INTERFERER). A schematic diagram for Emitter 8 is given in Figure 79 and one for the 30 MHz reference in Figure 80.

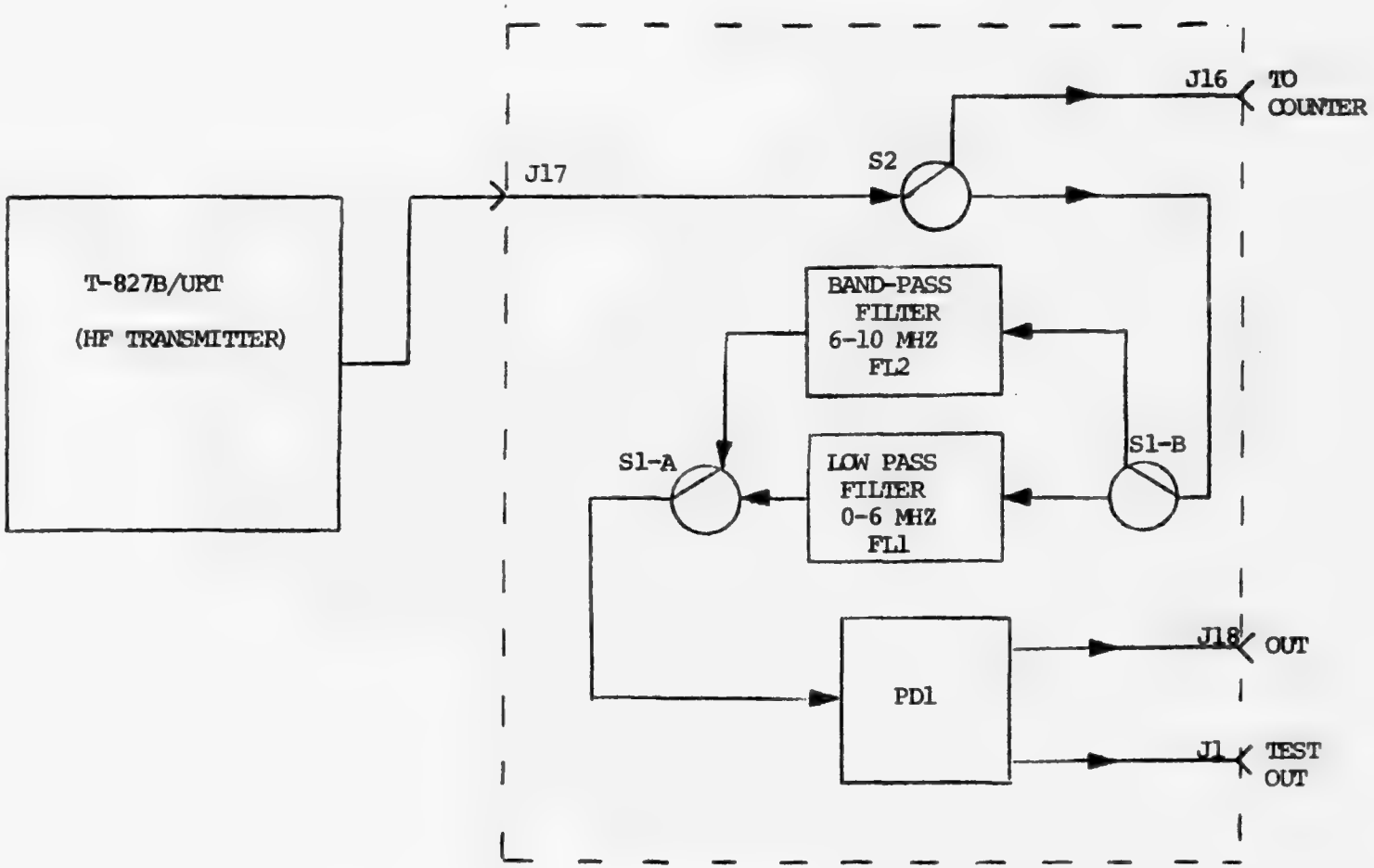

Figure 79: E8 Schematic Diagram.

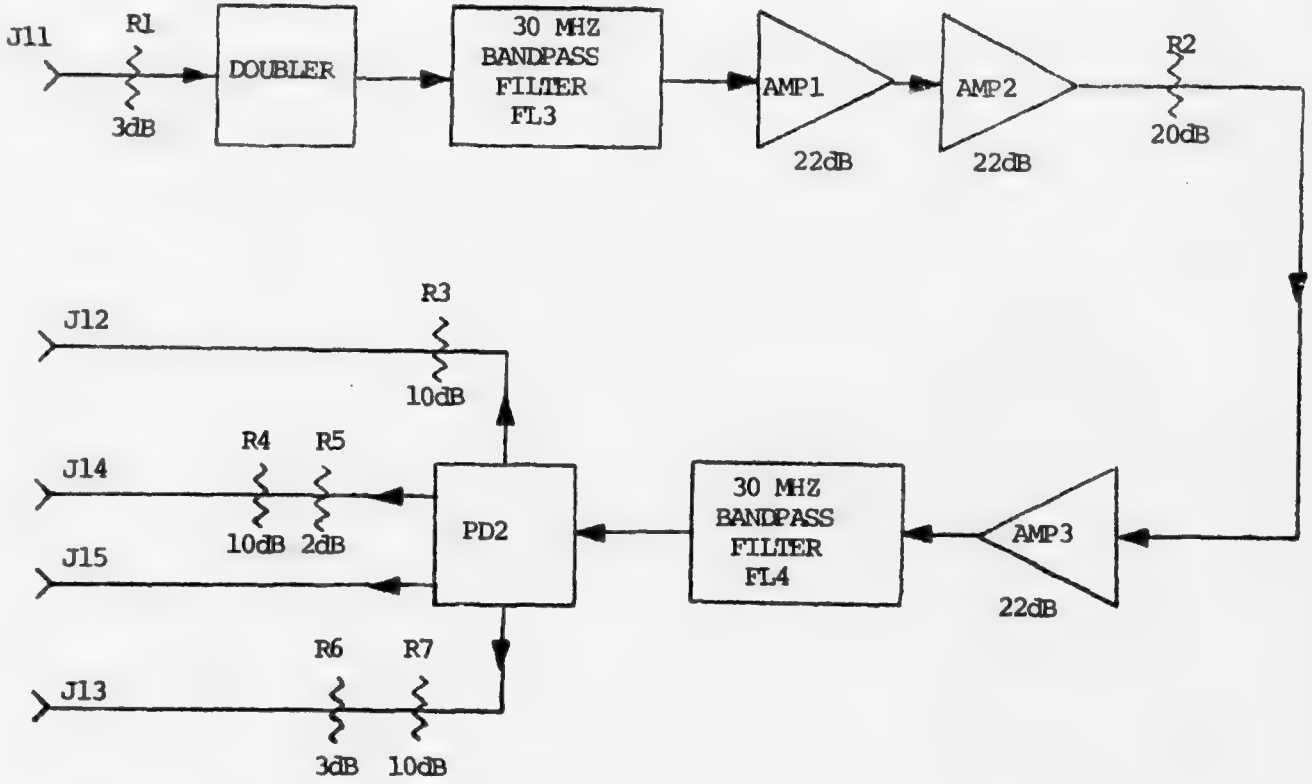

Figure 80: 30 MHz Reference Schematic Diagram.

Emitter 8 is implemented by filtering the output of T-827B/URT which is a synthesizer capable of delivering up to 28 dBm of power at the HF band. Before being filtered this signal can be switched "ON" or to a "COUNTER" for frequency measurements.

The filters are used with the same purpose as the ones for E6 and E7 (to provide a "clean" signal for processing by C1, N1 and N2) and the bands of operation are 0-6 MHz and 6-10 MHz. After filtering, a power divider splits the signal in two. One component is Emitter 8 and the other is available at the "TEST OUTPUT" port for monitoring or other purposes. The 30 MHz reference circuit, which was located in the same unit as E8 due to space availability, performs two basic functions.

a) Generates a 30 MHz signal from a 5 MHz standard.

b) Provides a certain degree of level control on the 30 MHz reference signal.

The operation of this circuit is as follows. A 5 MHz frequency standard existing in the Communications Laboratory is buffered by the AM-2123A(V)U-DISTRIBUTION AMPLIFIER which provides 4 paralleled outputs of the 5 MHz standard. One of these outputs is used to drive a frequency doubler in the 30 MHz reference circuitry. The sixth harmonic of the standard is selected by a 30 MHz, 1 MHz bandwidth filter and amplified by amplifiers AMP1, AMP2 and AMP3. The third amplifier in the chain is driven into saturation and that is used to control the level of the signal. Another 30 MHz,

1 MHz bandwidth filter is used to clean the signal of the harmonics generated by the leveling amplifier. The output of this filter is then split in four equal signals with a level of 12 dBm at 30 MHz. Attenuator pads are then used to adjust the level of the signals to the levels required by units E1, E2 and S1. A spare 30 MHz, 12 dBm output is available at port J15 on the back of E8 (when used, it should be loaded with a 50Ω load).

Parts list for Unit E8 - HF INTERFERER is given in Appendix 12.

Performance measurements for Emitter 8 and 30 MHz reference circuit are presented in Chapter 5. Interconnection information for Unit E8 is presented in Table 18 below.

Table 18

Interconnection Information for E8

Connector	Function	Connected to
E8 - J11	5 MHz standard input	AM-2123A(V)U - J4
E8 - J12	30 MHz output to E1 (2 dBm)	E1A - J13
E8 - J13	30 MHz output to E2 (-1 dBm)	E2A - J13
E8 - J14	30 MHz output to S1 (0 dBm)	S1 - J12
E8 - J15	30 MHz spare output (12 dBm)	Any 50Ω load
E8 - J16	E8 RF output to counter	HP 5383A - J18
E8 - J17	E8 RF input	T-827B/URT - J23
E8 - J18	E8 output	N2 - J11
E8 - P11	+15 VDC power	E10 - J11

APPENDIX 6

DETAILED DESCRIPTION OF EMITTER 9

As mentioned in Chapter III, the impulsive noise interference was modeled as:

$$n(t) = a(t)\ n_c(t)$$

where a(t) is a randomly occurring sequence of rectangular pulses with pulse width and pulse rate as the two variable parameters, and $n_c(t)$ is a broadband Gaussian noise process. Since DBM's were used in the physical implementation of the model, the same considerations made for the pulse noise modulator in the radar emitter apply here. Thus, it was necessary to use two DBM's in series to obtain the pulsed noise. Figure 81 shows the schematic diagram for this unit. Broadband Gaussian noise with power spectrum density approximately 65 dB above thermal is fed to the "R" port of DBM 1 via J11. After modulation, attenuator R1 provides means of inserting attenuation from 0 to 60 dB in 10 dB steps. The impulsive noise is available at J12. Driver (A5) is just a resistive network as shown in Figure 82 and has the double function of controlling the current available at the DBM's IF ports and of presenting a 50 Ohm load to these IF ports to maintain a match.

The signal input to this driver must be a positive pulse sequence with peak amplitude strictly between 1 and

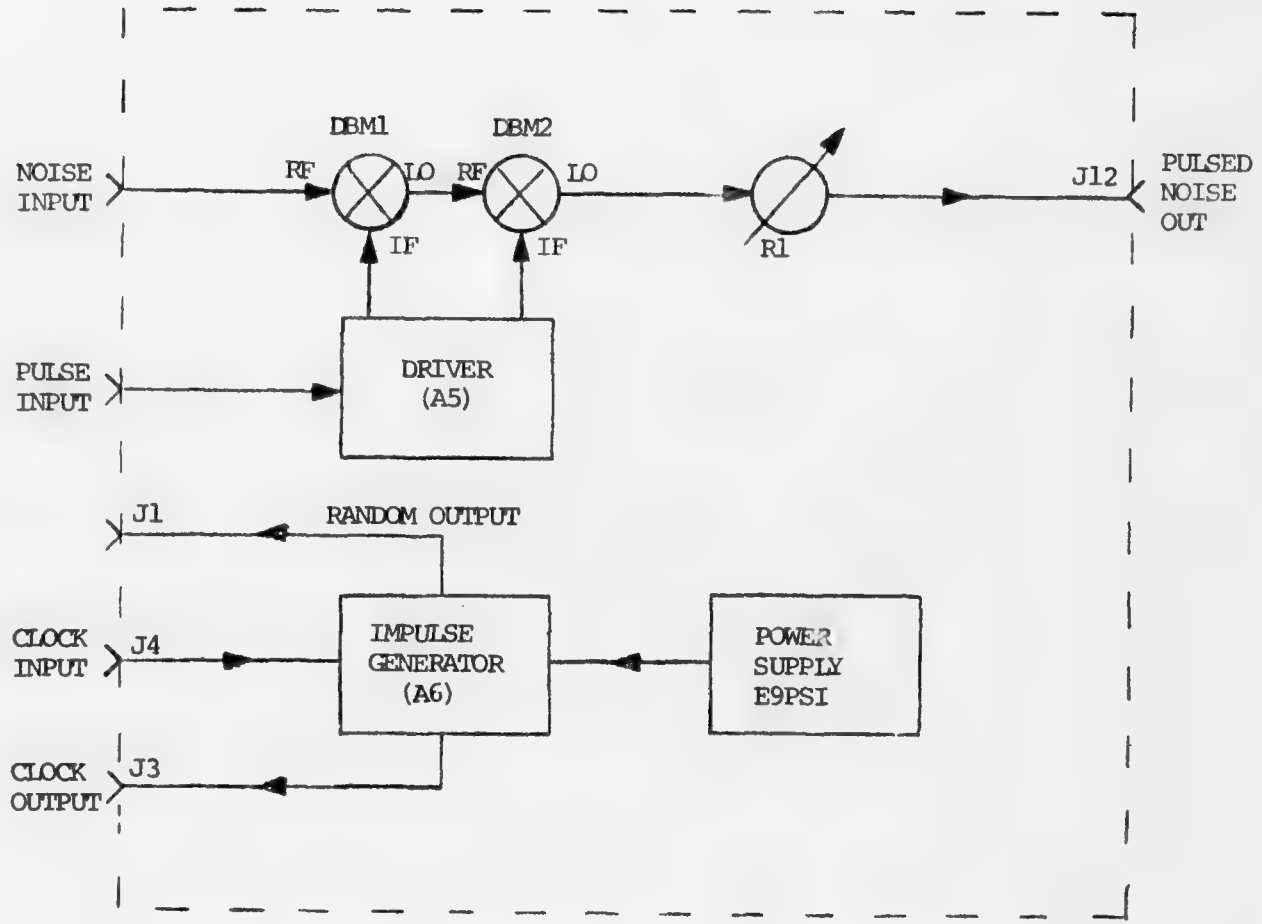

Figure 81: E9 - Impulsive Noise Schematic Diagram.

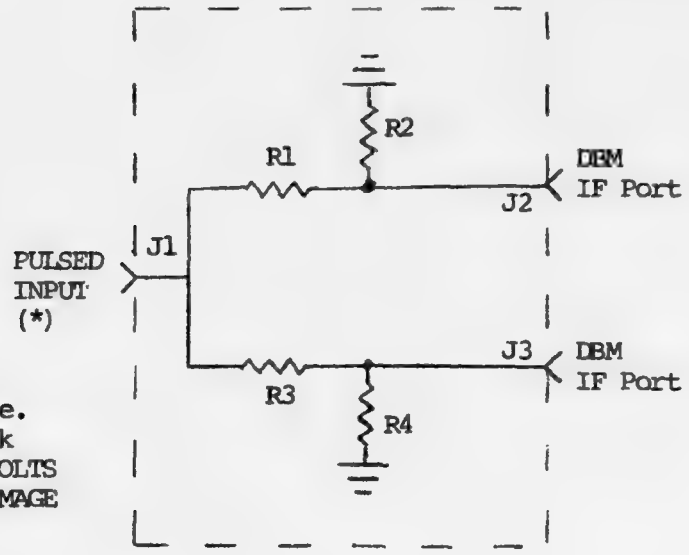

(*) Positive pulse.
2.5 Volts peak
MORE THAN 3 VOLTS
AT J1 WILL DAMAGE
MIXERS.

Figure 82: Driver (A5)

CONTROL L LINE	CLOCK RATE (KHz)	IMPULSE RATE (S^{-1})
2000	1024	2000
1000	512	1000
500	256	500
250	128	250
125	64	125
60	32	62.5
30	16	31.25
15	8	15.0625

Table 19: E9 - Rate Control Lines Description

3 volts (ideally 2.5 Volts). More than 3 volts will damage the DBM's.

IMPULSE GENERATOR (A6) uses the same process used in the STATISTICS GENERATOR (A2) of Emitters 3 and 4 to generate a pseudo-Poisson process. The only basic differences are:

i) Since higher pulse rates are needed, a longer PRBS (register length 28) is used in order to keep the period of the sequence long enough (more than 4 minutes was achieved.

ii) More possibilities of fixed rate selection (8) were made available to span the expected range of pulse rates of known impulsive interference.

IMPULSE GENERATOR (A6) is functionally divided in two sections: a clock section, depicted in Figure 83, which consists of a clock, a frequency divider (IC's 1 and 6), a frequency selection scheme (IC's 2, 3, 4 and 5), a clock selection scheme (IC's 3 and 9) and a clock output buffer (IC's 11 and 13).

The control lines for frequency selection and the corresponding clock and impulse rates are shown in Table 19. All the control lines are connected to the "RATE" switch on the front panel, which at the same time provides a "1" logic state to the selected line, provides a "0" logic state to all other lines. In this fashion only one of the frequencies derived from the clock by the binary dividers IC 6 and IC1, can be selected at a given time. If an impulse

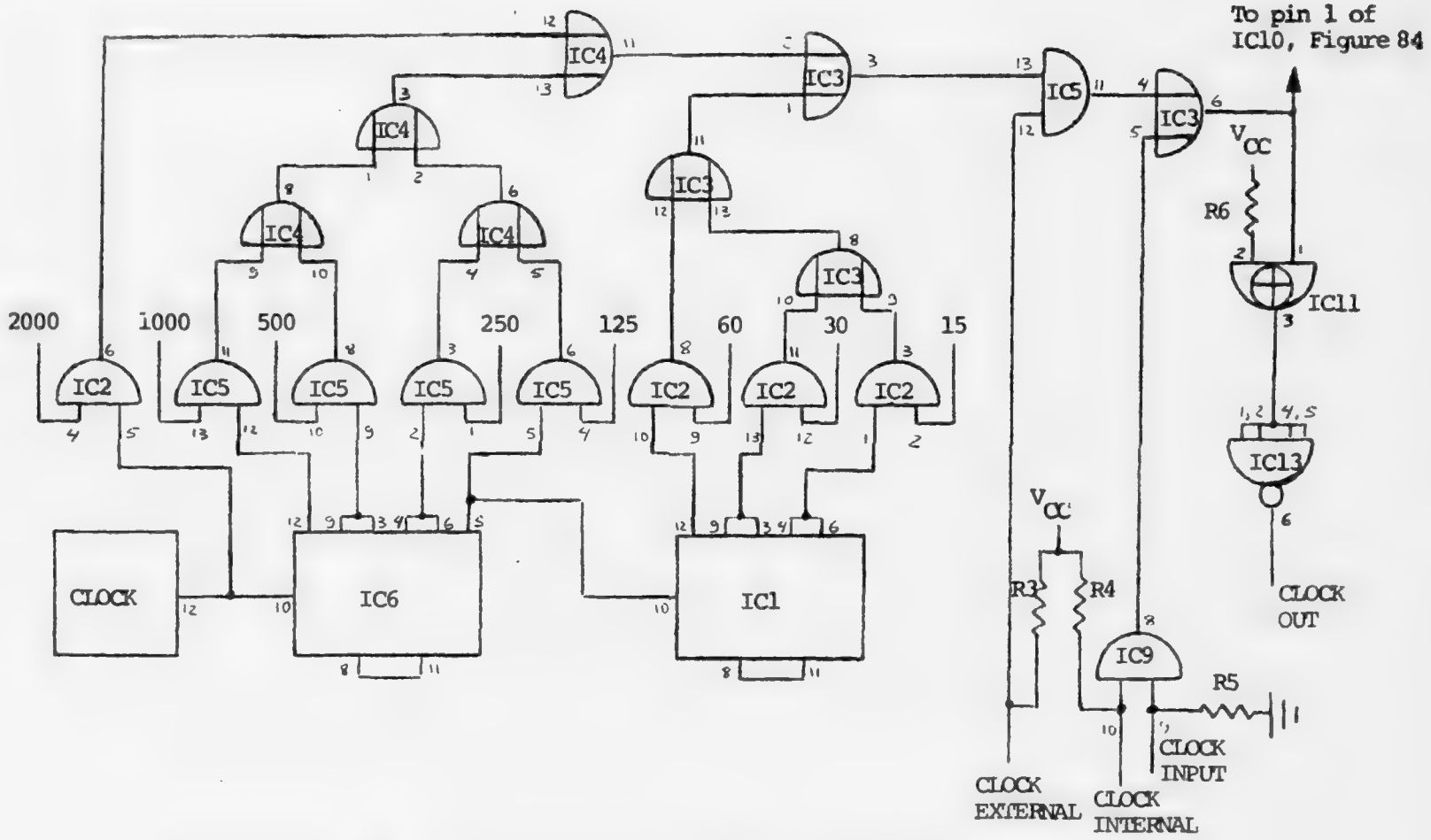

Figure 83: A6 - Clock Section Schematic Diagram.

rate different from the fixed ones available is needed, an external clock with frequency 512 times the desired rate (in S^{-1}) can be used and the selection is also made from a front panel "CLOCK SELECTION" switch.

The other section in A6 is the IMPULSE GENERATOR SECTION which is constituted by a PRBS generator of register length 28 (IC's 10, 11, 12, 14, 15, 16), an automatic restart feature (IC8) to avoid the possibility of the sequence being trapped in the all zero's state, a subsequence selector (C7) which is responsible for deriving the Poisson sequence from the PRBS as explained before, and finally a line driver (IC13) which acts as a buffer. Since the operation of this circuit is the same as the one in (A2) - STATISTIC GENERATOR, no further explanation will be made here.

Parts list for Emitter 9 is given in Appendix 12 and performance measurements results in Chapter V.

Interconnection information for Emitter 9 is given in Table 20 below.

Table 20

Interconnection Information for Emitter 9

Connector	Function	Connected to
E9 - J11	Noise input	E5C - J13
E9 - J12	E9 output	C1 - J13

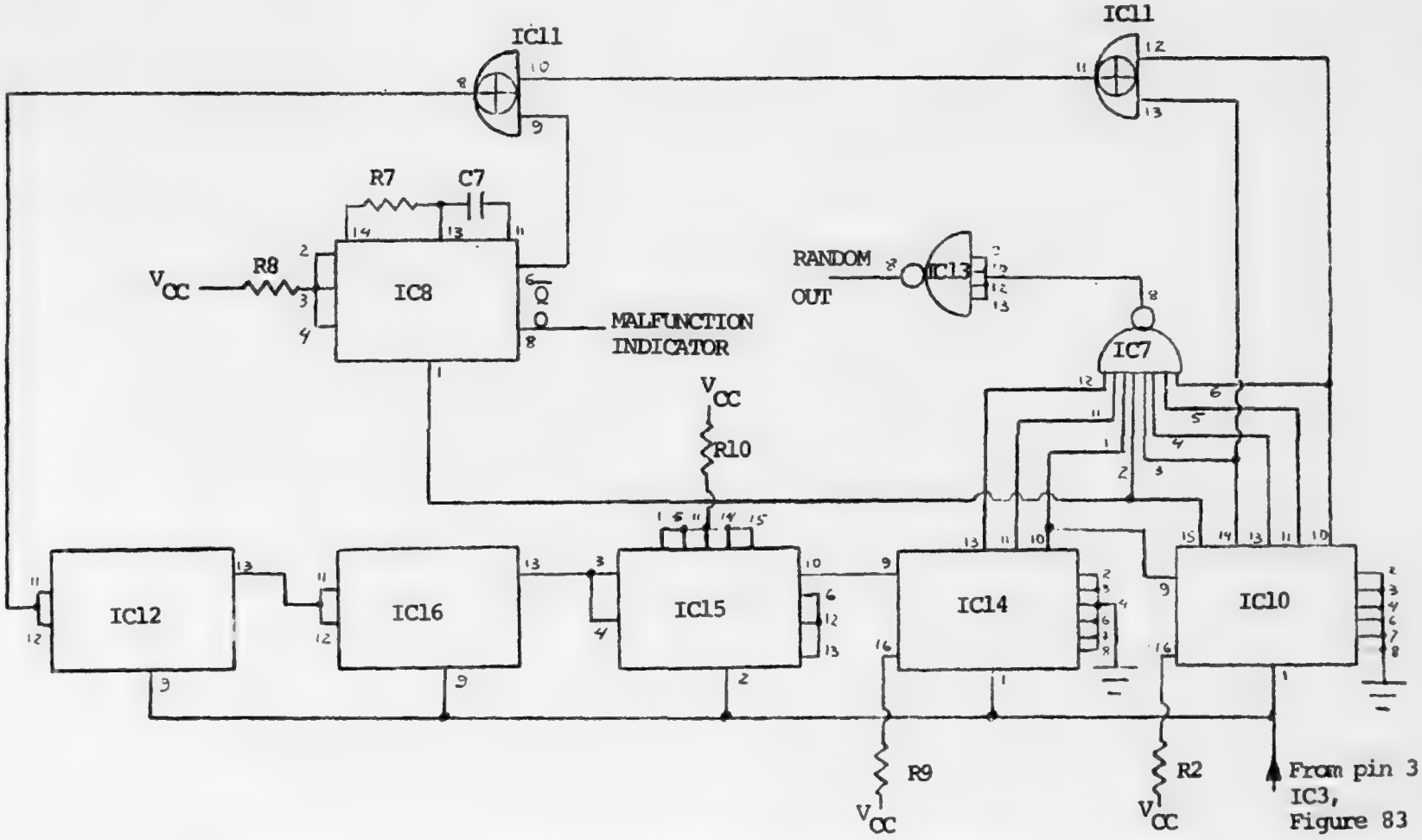

Figure 84: A6 - Impulsive Generator Section Schematic Diagram.

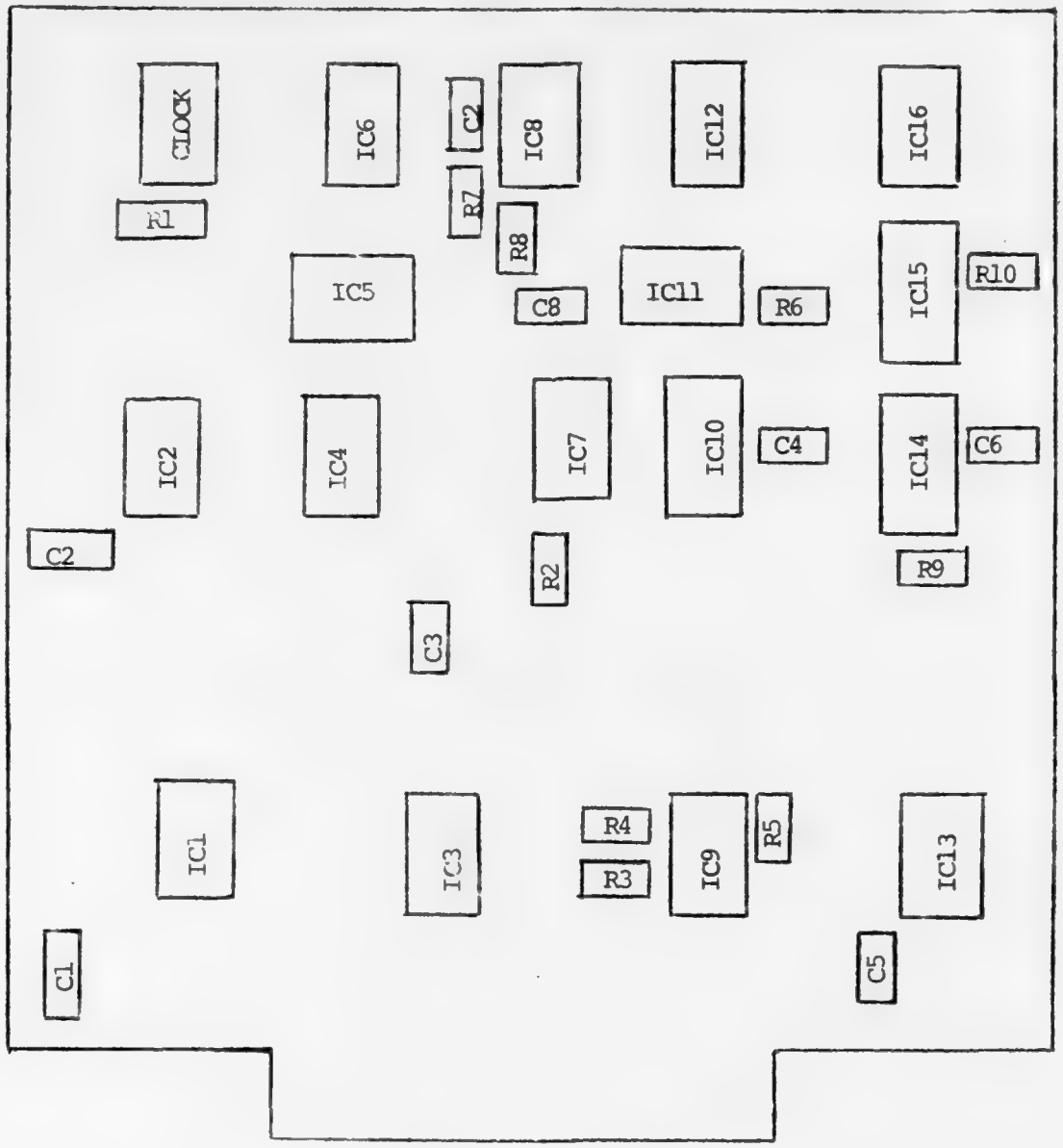

Figure 85: A6 Board Layout.

APPENDIX 7

DETAILED DESCRIPTION OF THE SIGNAL UNIT

The schematic diagram for S1 is given in Figure 86. Pseudo-random data is generated by an A2 - STATISTICS GENERATOR circuit board, PSK modulates a 0 dBm, 30 MHz carrier. This modulated signal can be filtered or not by a 30 KHz bandwidth depending on the position of a transfer switch S1, electrically commanded by a toggle switch on the front panel. The signal is then attenuated by a 0-60 dB, 1 dB step attenuator (R1) and up-converted in mixer DBM2. A tunable bandpass filter with 3% bandwidth selects one of the sidebands due to the up-conversion and AMP1, a 22 dB gain amplifier increases the level of the signal to 21 dBm. A power divider (PD1) splits the signal in two equal parts. One is made available at the "TEST OUTPUT" port on the front of the unit. The other, after being attenuated by 50 dB is available at the J11 output port. An extra 3 dB pad is connected externally to this port to allow for easy variation in the dynamical range of signal level.

Complete parts list for S1 is given in Appendix 12 and performance measurements results in Chapter V. Detailed description of A2-STATISTICS GENERATOR can be found in Appendix 9. Interconnection information for S1 is given in Table 21.

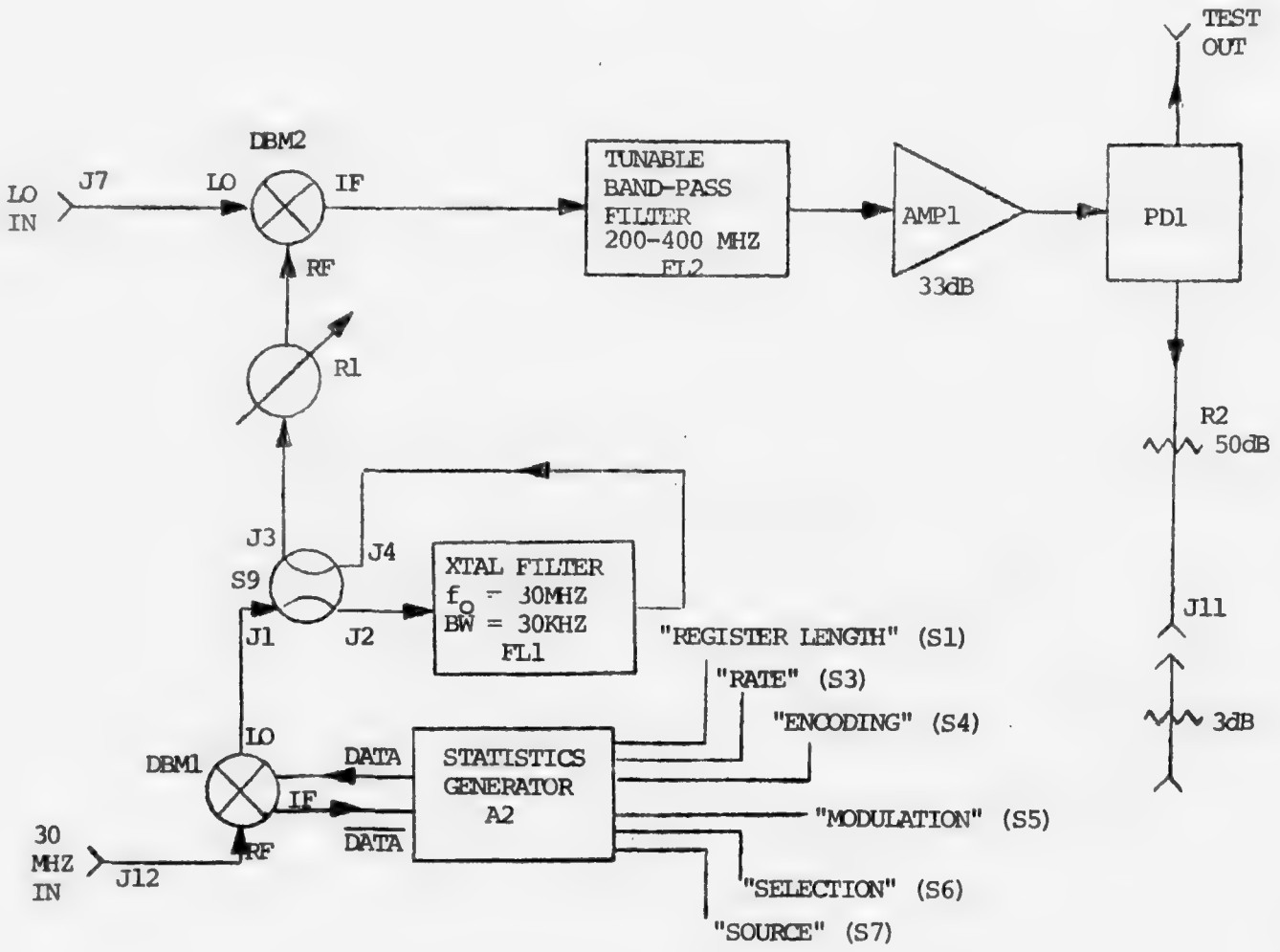

Figure 86: S1 - Signal Schematic Diagram.

Table 21

Interconnection Information for S1

Connector	Function	Connected to
S1 - J11	Signal output	C1 - J11
S1 - J12	30 MHz reference input	E8 - J14

APPENDIX 8

Schematics Diagrams for Units E10, PS1 and Counter

A schematic diagram of Emitter 10 is given in Figure 87. The Gaussian noise source was implemented using two 33 dB gain, 3 dB noise figure amplifiers, that gives a noise power spectrum density approximately 70 dB above thermal.

A 0-60 dB, 1 dB step attenuator (R1) is then used to control the level of this noise source. The 15 VDC power supply located in this unit is also used as the source of power for unit E10. This voltage is available at connector J11 on the back of E10.

A complete parts list for E10 is given in Appendix 12 and performance measurements are presented in Chapter V.

Interconnection information for E10 is presented in Table 22 below.

Table 22

Interconnection Information for E10

Connector	Function	Connected to
E10 - J11	+15 V DC power to E8	E8 - P11
E10 - J12	E10 - output	C1 - J12

Schematics for PS1 and COUNTER selection circuit are given in Figures 88 to 90.

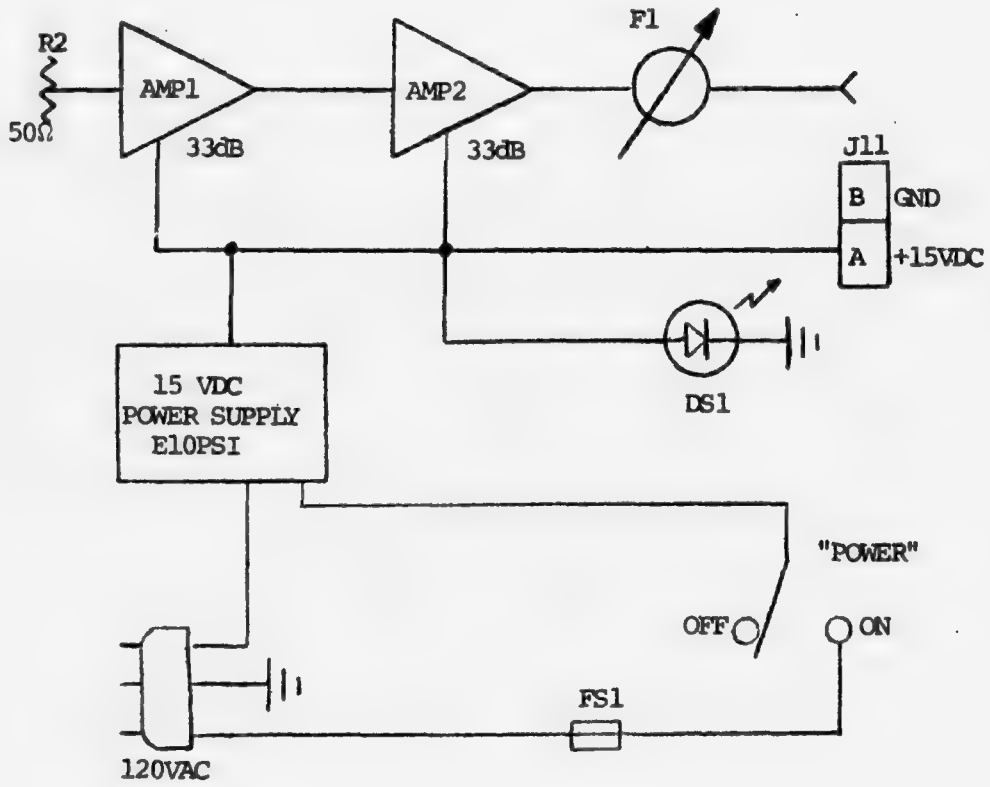

Figure 87: E10 - Gaussian Noise Schematic Diagram.

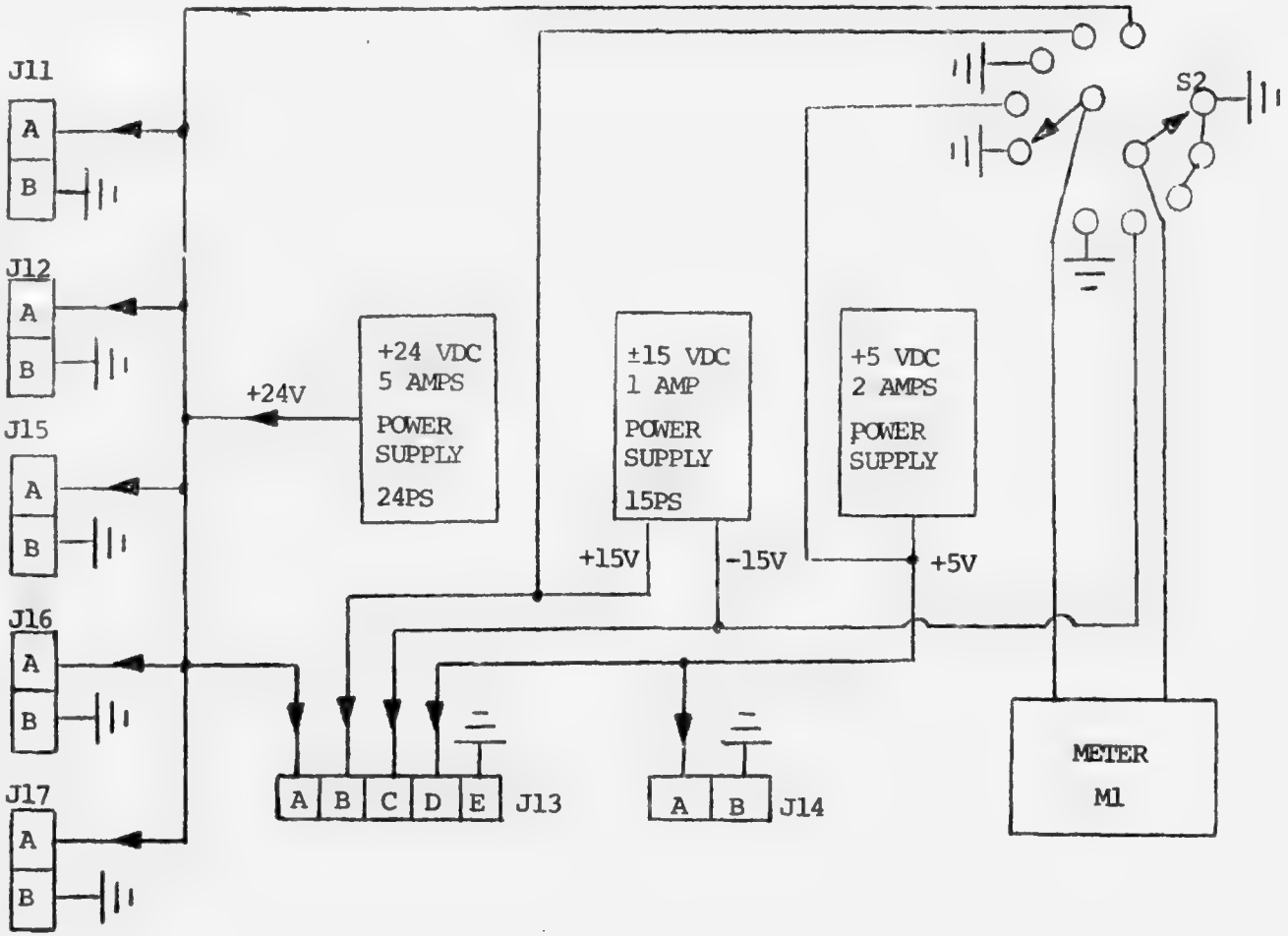

Figure 88: PS1 - Power Supply DC Wiring Diagram.

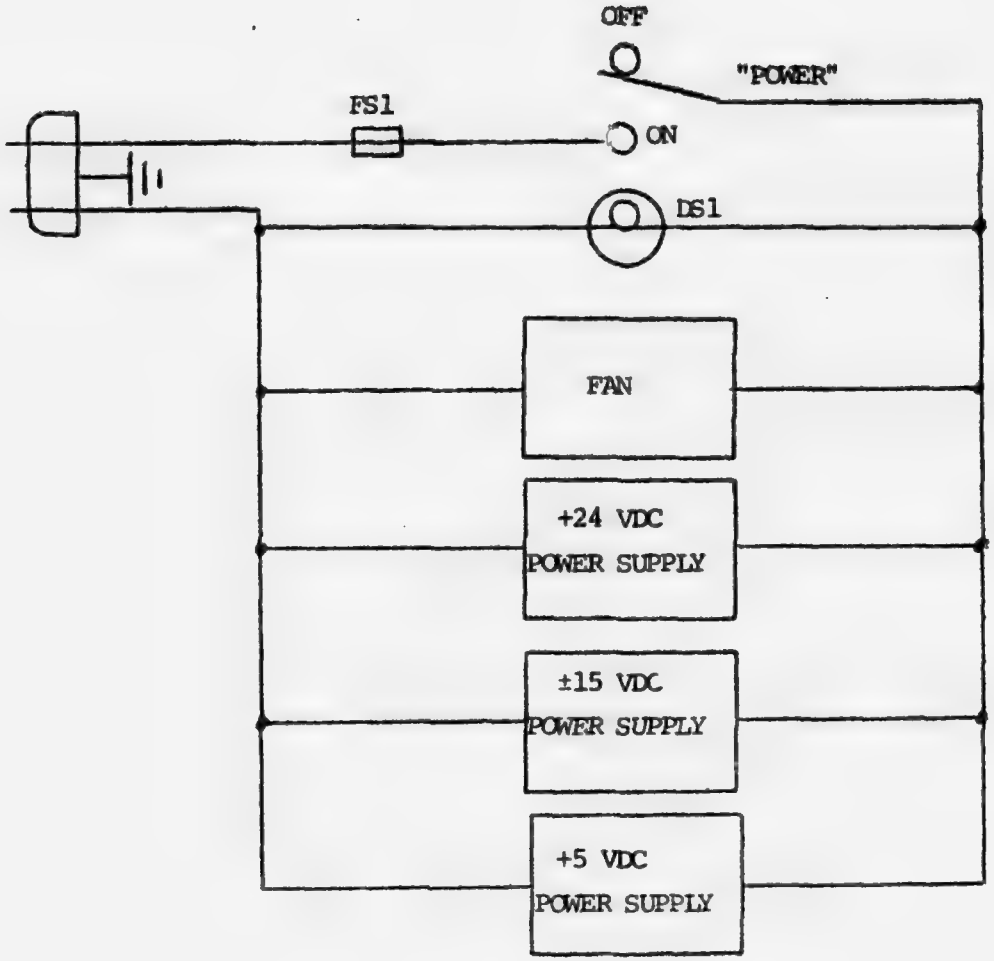

Figure 89: PS1 - Power Supply AC Wiring Diagram.

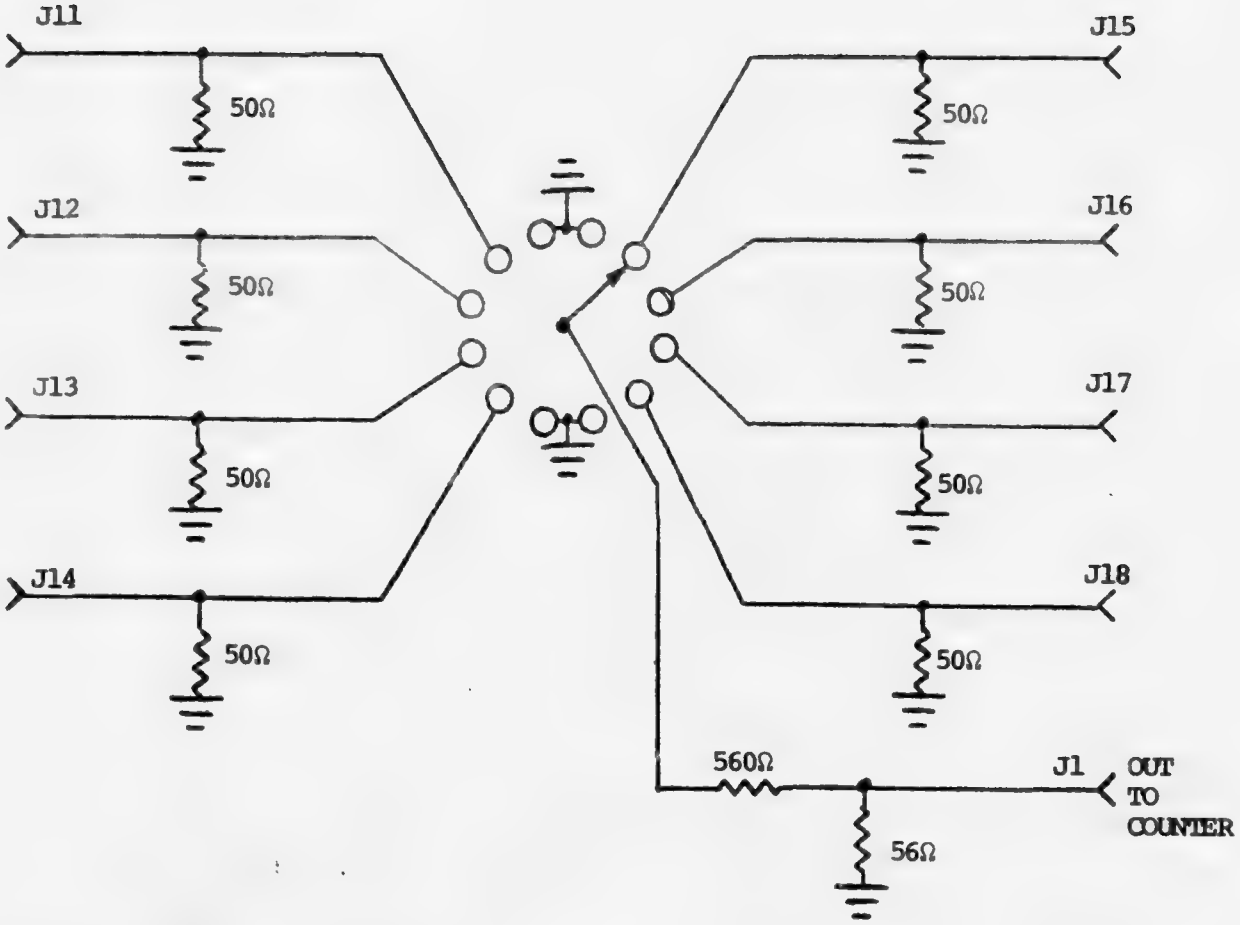

Figure 90: Counter Schematic Diagram.

APPENDIX 9

Statistics Generator (A2)

One of the most important characteristics of the model for UHF shipboard interference, as developed in this work, is given by the statistical assumptions made for the various emitters. Since the objective was to be able to simulate the interference process, it is obvious that this could not have been done unless a method of generating the necessary statistics had been devised. As we have seen in the discussions of Emitters 3, 4 and 10, two types of random process used to generate statistics for our model were easily obtained from available sources. In the case of Emitters 3 and 4 a "voice process" necessary to provide a modulating signal for the emitter was obtained by sampling the signal from a broadcast station. In the case of Emitter 10 (and also Emitters 5 and 9) a Gaussian noise source was implemented by using the noise generated by a high-gain chain of broadband amplifiers which is known to be of Gaussian nature. This leaves two other stochastic processes whose implementation was necessary for the generation of all necessary statistics:

- a random stream of data used to modulate the PSK emitters,

- a randomly occurring sequence of impulses with Poisson counting properties necessary to implement the PTT statistics of Emitters 3 and 4 and also to generate the impulsive noise.

It has been known for quite a while that pseudo random binary sequences generated by providing feedback from some of the stages of a shift-register chain, possess properties similar to a random sequence of ones and zeros (see for example References 19 and 20). This means that the ones and zeros occur approximately according to a binomial distribution. That is, if U(k) is the maximum length sequence generated by a digital binary shift register, it possesses the following properties:

a) The sequence is periodic with period $T = N\delta$ where N is the sequence length and δ is the period of the clock driving the shift register. Also, $N = 2^n - 1$ where n is the register length.

b) The amplitude probability density function for the sequence consists of two impulses of almost equal amplitude centered at 1 and 0. That is,

$$P(U(k) = 1) = 2^{n-1}/(2^n - 1)$$

and

$$P(U(k) = 0) = (2^{n-1} - 1)/(2^n - 1)$$

for all k = 1, N.

Because of these properties PRBS are very suitable for generating pseudo-random data and this was the approach taken in this work.

Another less known property of PRBS is its usefulness in generating pseudo-random signals with different statistics. This is illustrated by References 21 to 26 where generation of pseudo-noise signals with arbitrary amplitude distribution properties is discussed. Fortunately PRBS have also been used to generate pseudo-random Poisson processes as explained in References 27 and 28. Since the individual samples of a PRBS occurs according to a binomial distribution it is well known (see Papoulis, Ref. 29) that the probability of obtaining a fixed sequence of 1's and 0's in a certain time slot will approach a Poisson distribution if this sequence is long enough. Thus, by detecting a given subsequence of length L < n we can obtain an approximation of a Poisson process as explained in References 27 and 28.

In our implementation a subsequence of all 1's was used with the result that the rate γ of the resulting Poisson process can be calculated by the formula below.

$$\gamma = \frac{1}{2^{(L+1)} \times T} \text{ sec}^{-1} \qquad \text{(A9-1)}$$

where T is the clock period in seconds and L is the subsequence length. For L = 8 (our case),

$$\gamma = \frac{1}{512 \times T} \text{ sec}^{-1} \quad \text{or} \quad \gamma = \frac{60}{512 \times T} \text{ min}^{-1}$$

Since PRBS's are used for both the generation of random data and of the Poisson process it was convenient to build a circuit that would be able to perform both functions with little modification. This was accomplished with the A2 - STATISTIC GENERATOR board of which a functional block diagram is given in Figure 91. From that figure we can see that the STATISTICS GENERATOR is functionally divided in the following sections:

a) A CLOCK SECTION that includes a clock, a binary divider and a clock selection circuitry,

b) A STATISTICS GENERATION SECTION including a PRBS generator, an automatic restart circuitry, a register length selection circuitry and a subsequence selector to obtain the random impulses from the PRBS,

c) A PTT and ENCODING SECTION which generates a PTT signal from two random sequences of impulses and provides the means to differentially encode the data.

In the CLOCK SECTION, shown in Figure 92, a TTL compatible, DIP type of RC or XTAL oscillator generates a clock frequency according to the particular use being considered. A binary divider (IC6) provides four other outputs containing the clock frequency divided by 2, 4, 8 and 16, respectively. A selection circuitry (IC's 3, 4, 5) is then used to select one of the five available frequencies by putting a "1" on one of the control lines (named 19.2, 9.6, 4.8, 2.4, 1.2) and "0" on the others. This is accomplished by connecting all lines to a special type of switch that at

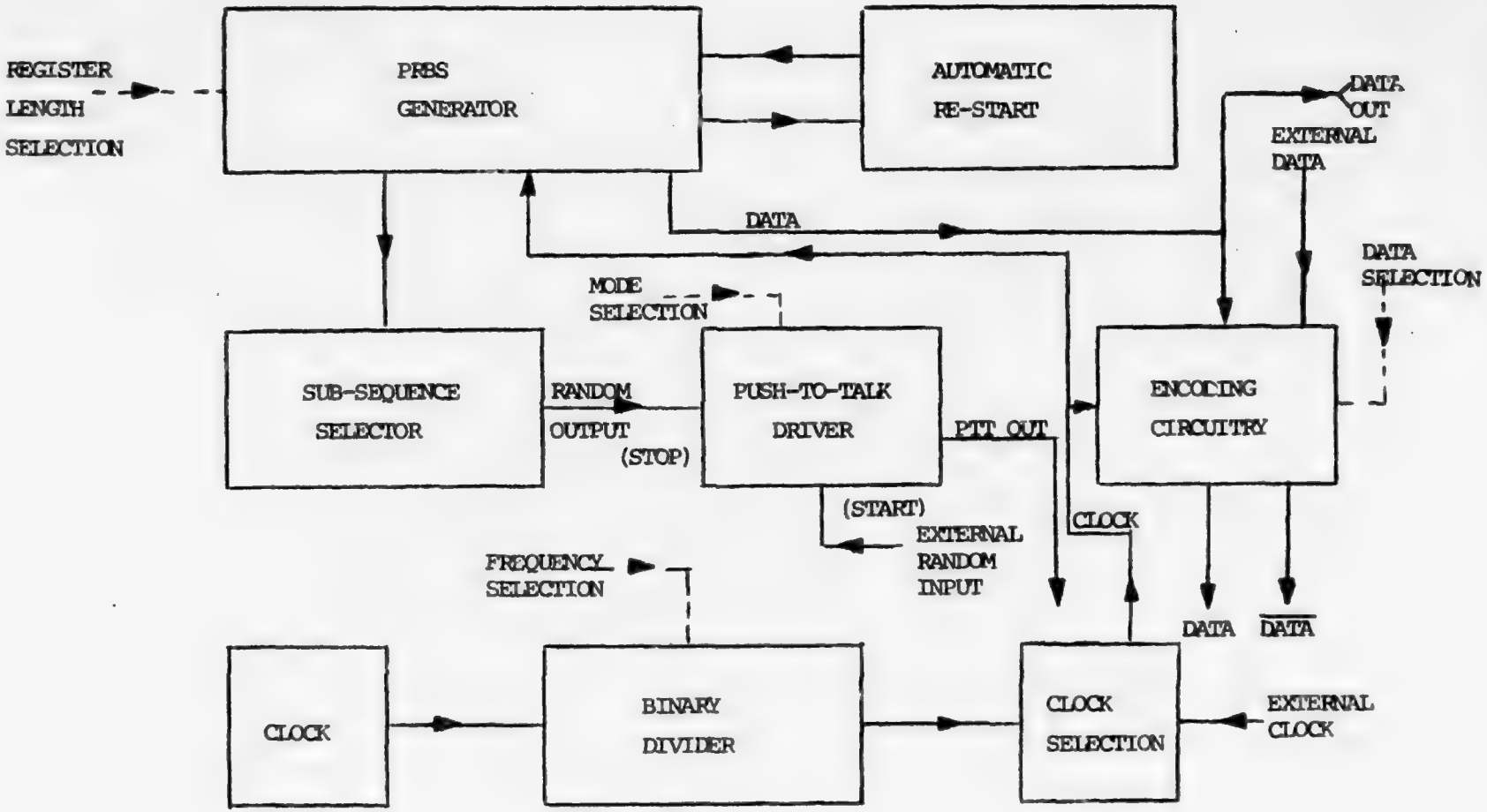

Figure 91: A2 - Statistics Generator Block Diagram.

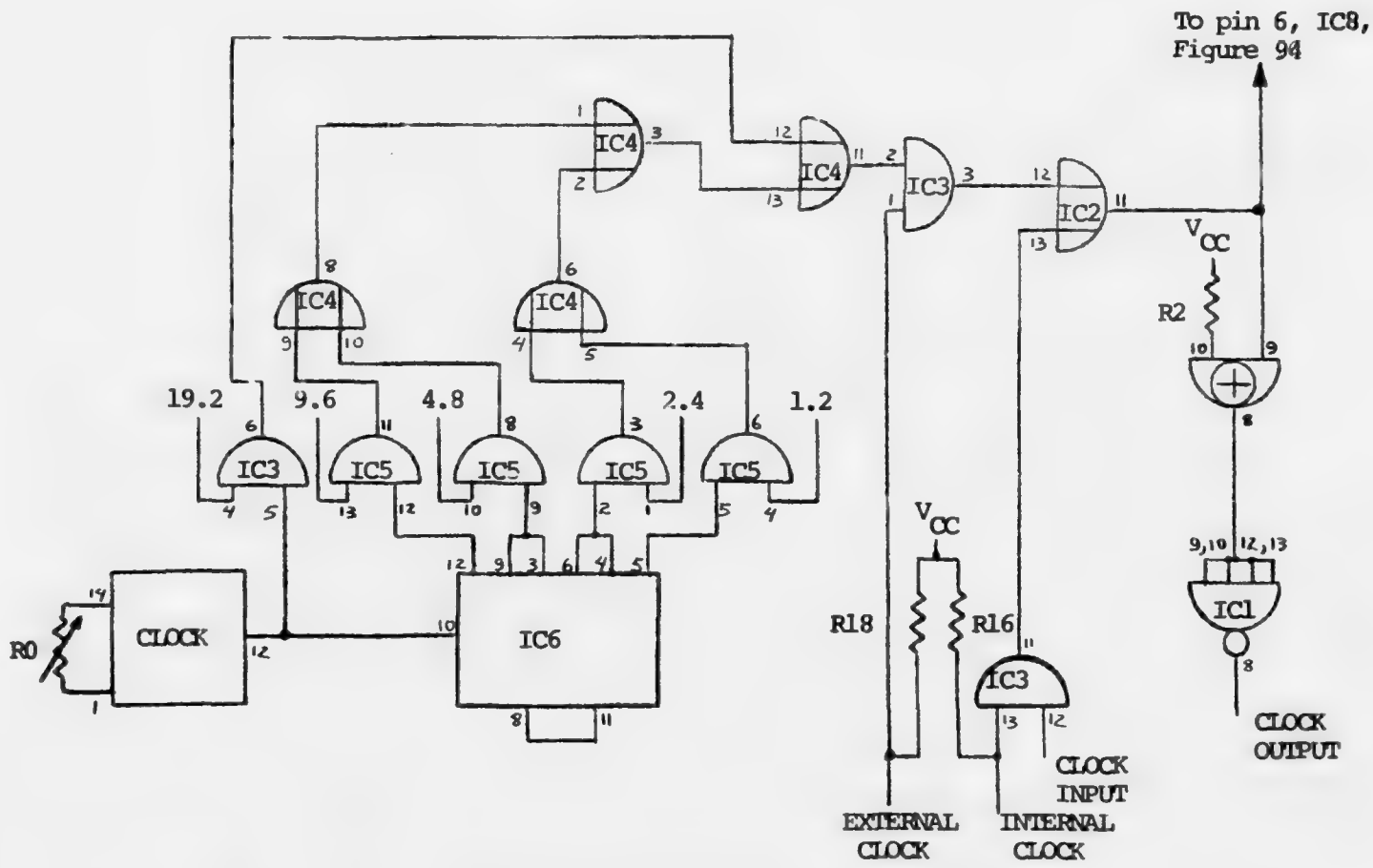

Figure 92: A2 - Clock Selection Schematic Diagram.

the same time that connects the pole to a selected position, grounds all other positions not selected. Thus only one of the control lines can be at state "1", the others necessarily being at "0". As can easily be seen in Figure 93, this will select one of the frequencies only. The selection switch can be graduated for CLOCK RATE, PTT RATE or PTT AVG. ON TIME depending on the use of the A2 board. The selected internal clock is then available at Pin 11 of IC4 but another selection can be made as to what clock source we want to use. IC's 2 and 3 and a "CLOCK SELECTION" switch can be used to select an external or the internal clock source. This is done by putting a ground at Pin 1 of IC3 or Pin 13 of IC 13 respectively as shown. Finally, the selected clock (internal or external) is available at Pin 11 of IC2 from where it goes to clock inputs of the shift-registers on the PRBS generator and is also used to drive a TTL line driver (IC1) the output of which is available for external uses.

In the STATISTICS GENERATION SECTION, IC's 13, 18, 19 and 20 makes a shift register of length 20 which can be reduced, operationally speaking, to lengths 10 and 5 by the control lines L10 and L5. This is done by directing the feedback from Flip-flops 1 and 4 in the chain to the input of Flip-flops 10 or 5 (according to the selection made) and at the same time disabling the input from the Flip-flops of number greater than the register length selected. This selection is done by IC's 14, 15 and 17 as shown. Control

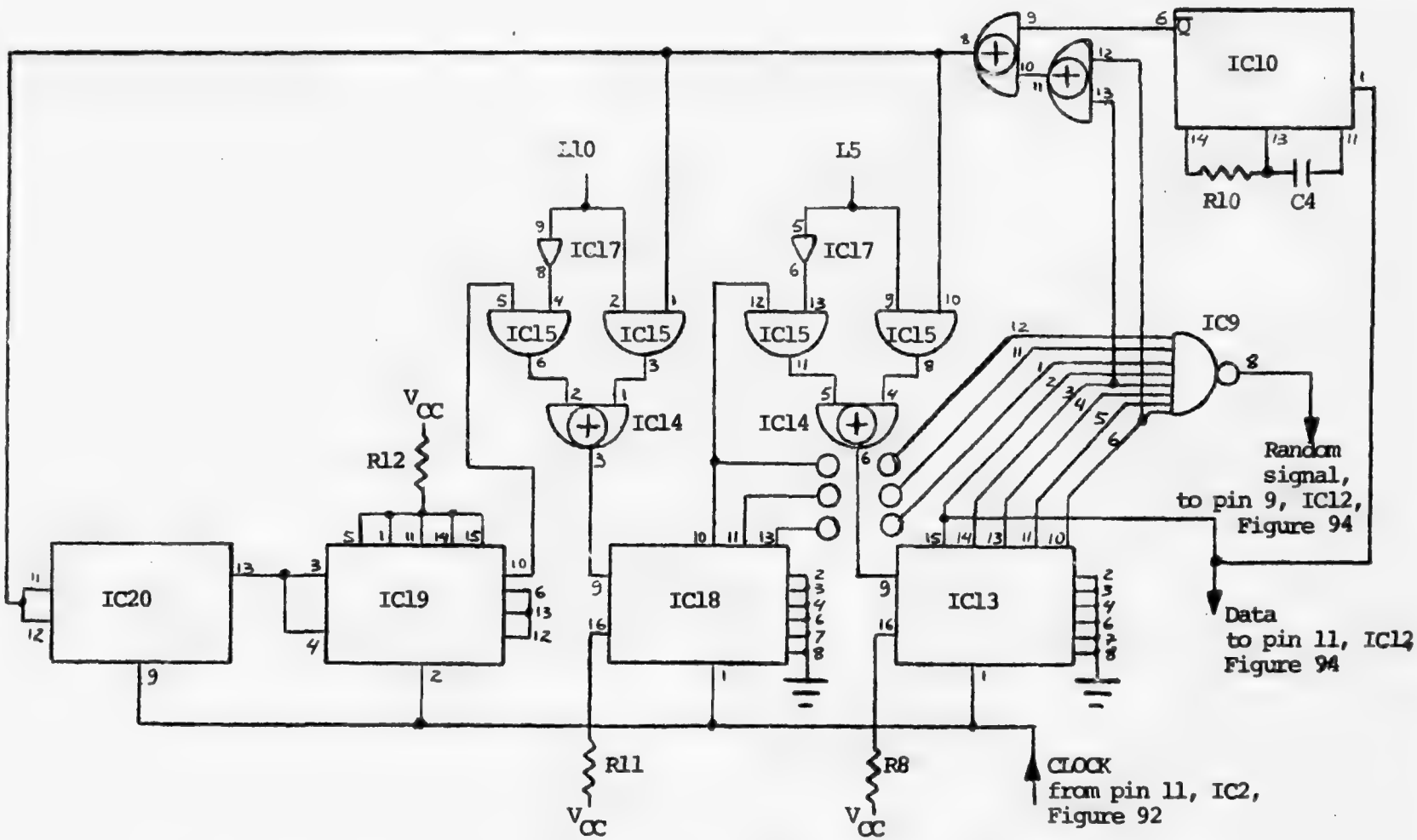

Figure 93: A2 - Statistics Generation Section Schematic Diagram.

lines L5 and L10 are connected to a 3-position switch of the same type used for clock rate selection. The selected position of the switch will be at state "1" while all others at "0". The automatic restart was implemented by triggering a retriggerable monostable (1C10) with the PRBS. The monostable is set to a time bigger than the maximum possible time between two 1's on the sequence. Thus, the monostable will never go off on a normal operation and $\overline{Q}$ will be "0". When the shift register gets trapped in the all zeros state, the mono will not be triggered and will go off. $\overline{Q}$ will then go high and since this output is on the feedback path of the shift-register it will cause the sequence to start again.

IC9, an 8-input NAND gate, performs the subsequence selection function. Its inputs are connected to the eight first flip-flops on the chain so each time we have a sequence of eight or more 1's, the output of IC9 goes down and this occurs in a random fashion with a Poisson distribution. When used to generate this pseudo-Poisson process, the board is hardwired for a register of length 20 operation (L5 and L10 are grounded). When used to generate random data IC9 is reconfigured to generate a synchronism pulse each time the sequence of length 31 (register length 5) is repeated. This is done by connecting Pins 1, 11 and 12 of IC9 to V_{CC} through a 1 kΩ resistor.

In the PTT and ENCODING SECTION (Figure 94) IC's 2, 3 and 12 are used together with a "SOURCE" switch to select

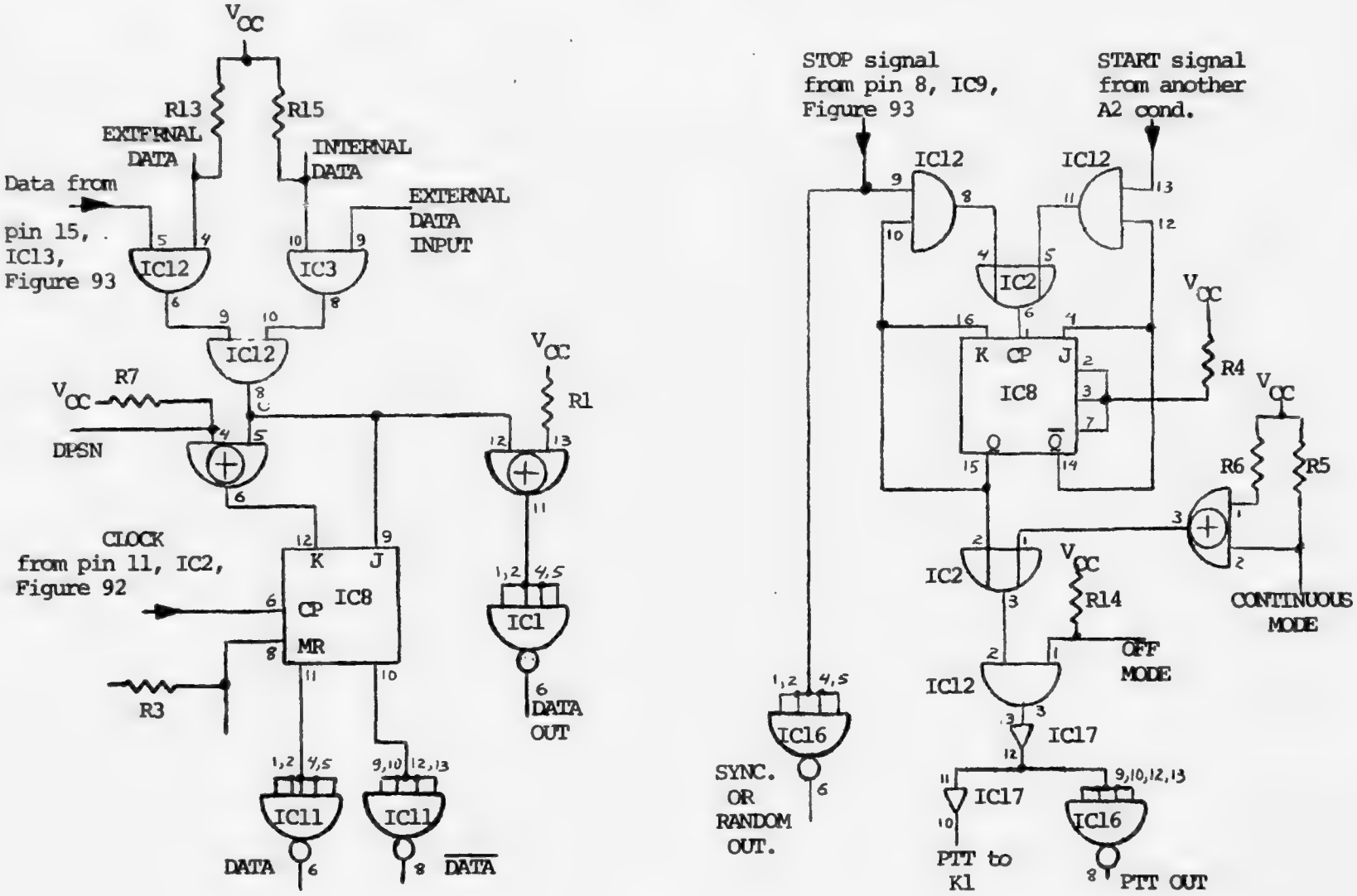

Figure 94: A2 - PTT and Encoding Sections Schematic Diagrams.

the source of data being available to the encoding circuitry. The "SOURCE" switch selects the internal or external data by putting a ground at Pin 10 of IC3 or Pin 4 of IC12 respectively. The encoding circuitry was built with IC's 7 and 8. IC8 is a J-K edge triggered flip-flop. When the "ENCODING" switch is in the DPSK position a ground is put at Pin 4 of IC7. Thus, the data will be presented at both the J and K inputs of the flip-flop. This flip-flop is triggered on the trailing edge of the clock while the data is changed on the leading edge of the clock. Thus the leading edge of the clock will change the data and during the trailing edge, if the data is in the "1" state, the flip-flop will flip. If the data is "0", the flip-flop will remain at the same state. Thus, while the data remains in "1" the output of the flip-flop will continue to change state. With the "ENCODING" switch and the PSK position, IC7 will function as an inverter and the flip-flop will follow exactly the input data. It is important to observe that since there must be a perfect synchronism between the data and the clock, when using external data, the clock used to generate that data should also be used. It is also important to notice that the only external data sources compatible with this unit are the ones in which the data transitions occur on the leading edge of the clock. Another thing to observe is that the data available at Pin 6 of IC1 (a line driver)

will be half-clock period in advance of the encoded data (Pin 6 of IC11).

The circuit generating the PTT signal works in the following fashion. A J-K edge-triggered flip-flop is turned "on" and "off" by the occurrence of pulses on a start and a stop signal respectively. When the flip-flop is in the "On" state, the start pulses are blocked by sensing the output $\overline{Q}$. When in the "off" state the stop pulses are similarly disabled. The flip-flop is wired to work as a binary divider and its clock input is the "start" or the "stop" as explained above. A "MODE" switch can be used to select the above generated signal ("PTT" position) or to make the "PTT OUT" terminal (IC 16 Pin 8) and IC17 Pin 10 remain continuously "on" (CONT" position) or "off" (OFF" position). The selection is made by IC's 2, 7, 12 as shown in Figure 95. Performance measurements of this circuit were done by testing the units in which this circuit was used as explained in Chapter V.

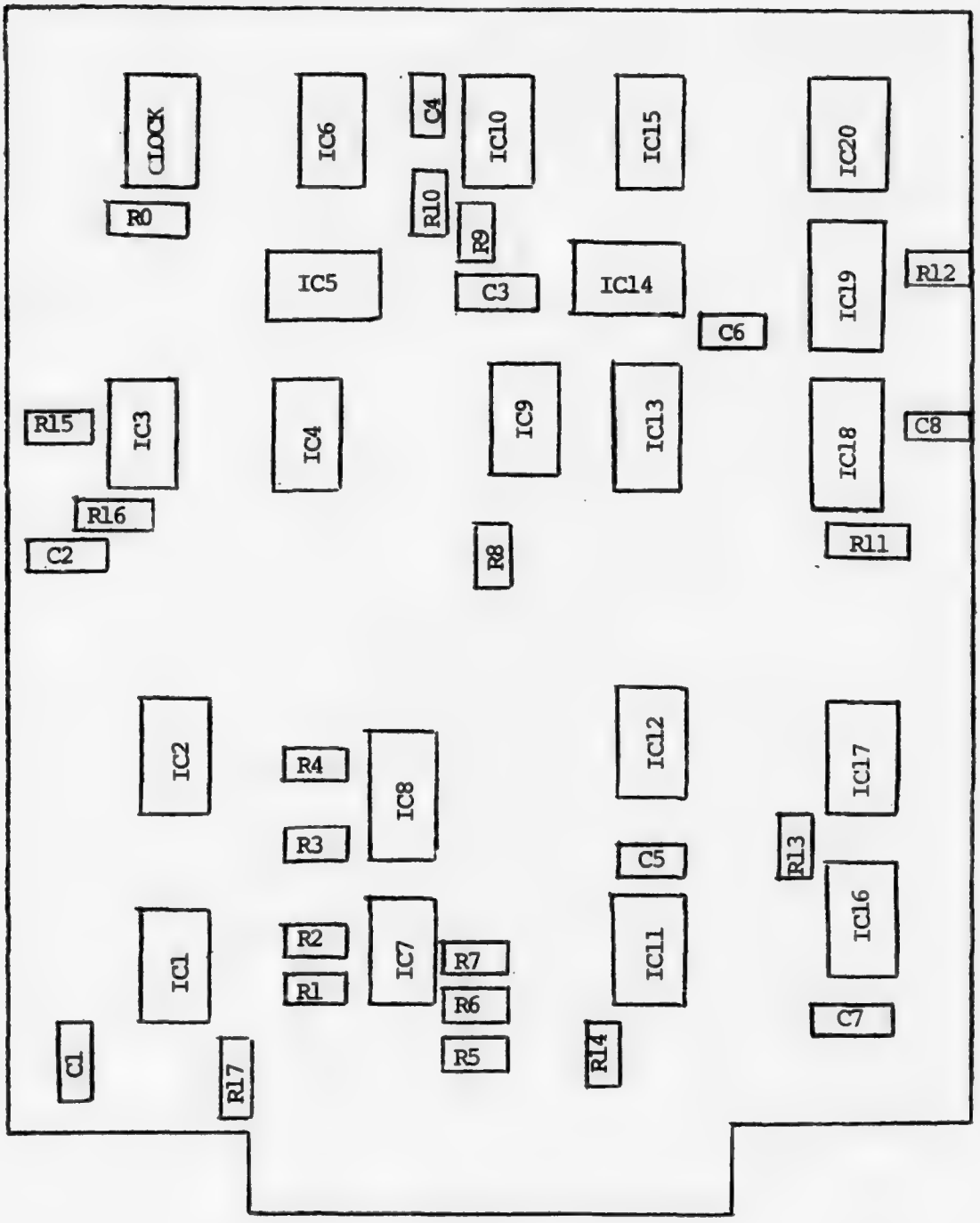

Figure 95: A2 Board Layout.

APPENDIX 10

Operating Instructions

A. SETTING UP THE EMITTERS

1. Emitter 1

To put Emitter 1 in operation follow these instructions:

a) Verify if AC plugs in E1A and E1C/E2C are connected to an outlet.

b) Verify if the connectors on the back of Units E1A, E1B and E1C/E2C are connected according to the interconnection table given in Appendix 11.

c) Connect the HP-608C signal generator output to the "RF IN" port on the front panel of E1A.

d) Select the frequency of the HP-608C signal generator to be 30 MHz above or below the desired frequency of operation and set the level to 7 dBm.

e) Since E1A receives a 30 MHz carrier from Unit E8, check the operation of that unit and turn it "on".

f) Turn Unit PS1 - POWER SUPPLY "On". This will supply +24 VDC for E1C/E2C - UHF/PSK AMPLIFIERS.

g) Turn E1B knob to the desired frequency.

h) Turn "On" Unit E1C/E2C.

i) Turn "On" Unit E1A.

j) Turn "MODULATION" switch in E1A to "OFF".

k) Turn "RF" switch to counter and the counter "SELECTION" switch to the "1" position. Read the emitter

frequency adjusting HP-608C to get the desired frequency.

1) Turn "RF" switch to "ON" and readjust E1E setting to get maximum power at the "OUTPUT" port of C1 - COMBINING UNIT. The power meter should read approximately 2.5 dBm when the E1 attenuator in C1 is set to 0 dB.

2. Emitter 2

Instructions a) to k) apply if the following substitutions are made:

E1A → E2A

E1B → E2B

HP 608C → WAVETEK 3000

In addition to the substitutions above the instructions differ on the available power at the "OUTPUT" port of C1. For Emitter 2, the available power is only about .5 dBm. Also "SELECTION" switch on the counter should be put in "2" when measuring Emitter 2 frequency.

3. Emitter 3

To put Emitter 3 in operation, follow these instructions.

a) Verify if AC plug in E3A is connected to an outlet.

b) Verify if the connectors on the back of Unit E3A and E3B are connected according to the interconnection table given in Appendix 11.

c) Turn "MODE" and "MODULATION" switch in E3A to "OFF".

d) Turn "On" transmitter AN/SRC-21 in RADAR LAB and set it for remote control.

e) Dial the desired frequency of operation in E3B. For Channels 1 to 9 dial directly the desired number. For Channels 10 to 19 dial A plus the last digit of the desired channel. Ex.: Channel 13, dial A3.

f) Turn mode switch to "CONT". The available power at "OUTPUT" terminal in C1 - COMBINING UNIT should be about 7 dBm.

g) To operate in the "PTT" mode turn "CLOCK #1" and CLOCK #2" switches in E3A to "INT", put S11 switch in the back of E3A to "I" (internal) and the "MODE" switch to PTT.

h) If external control of PTT is desired, connect an external, TTL compatible, PTT source to connector J11 on the back of E3A and put S11 to "E" (external). In this mode of operation all controls on the front panel, with the exception of the "MODULATION" switch, will be inoperative.

4. Emitter 4

Instructions for the operation of E4 are the same as a) to h) above with the following exceptions:

- Substitute: E3A → E4A

E3B → E4B

- The SRC/21 transmitter used for E4 is located in the Communications Lab.

5. Emitter 5

To put Emitter 5 in operation follow these instructions.

OPERATION WITHOUT ANTENNA PATTERN SCAN MODULATION.

a) Verify if AC plug in Unit E5B - RADAR AMPLIFIER is connected to an outlet.

b) Verify if the connectors on the back of Units E5A and E5C are connected according to the interconnection table given in Appendix 11. The only exception is Connector E5C - P11 which should be terminated with a mating socket that grounds Pins A to H of P11. This will provide a hardwire programming of the pin-diode modulators inside E5C to 0 dB of attenuation, disabling the scan modulation function.

c) Choose the frequency of operation of the radar, and tune the HP 3200B signal generator to that frequency. Adjust the OUTPUT level of HP-3200B to 18 dBm. Switch "RF" on Unit E5C on. The "COUNTER" position can then be used to direct this signal for direct frequency measurement on the counter ("SELECTION" switch in 3).

d) Connect an oscilloscope to the output of the HP 8011A pulse generator. Turn the pulse generator on and adjust PRF and PW to the desired values. The pulse output should be 0 to 4V peak (TTL compatible signal) on a 50Ω load. After adjusting the desired parameters reconnect the output of HP 8011A to the "PULSE IN" port in E5A. The PRF can be measured in Position 4 of the counter "SELECTION" switch when the switch in E5A is set in "COUNTER".

e) Turn unit PS1 - POWER SUPPLY "on". This will supply +24, ±15 and +5 VDC to Unit E5C and +5 VDC to Unit E5A.

f) Turn "BAND" switch in E5C to the selected band and "RF" switch to "ON".

g) Turn PULSE switch in E5A "ON". Adjust the "ATTENUATION" control for the noise component of the radar to a desired value. Turn noise component "ON" or "OFF" according to necessity.

h) Turn "ON" unit E5B - RADAR AMPLIFIER

i) The signal level of "OUTPUT" port in Unit C1 - COMBINING UNIT will be about 30 dBm peak.

OPERATION WITH ANTENNA PATTERN SCAN MODULATION

Repeat a) to i) above with the following additions and modifications.

a) Connect P11 on E5C to the designated connector on the INTERFACE of the INTERDATA 7/32 computer.

b) Follow the instructions of operation of the INTERDATA 7/32 Computer and leave the program for antenna pattern scan control running.

c) Select the desired scan rate by means of "SCAN RATE" switch on the front panel of E5C.

6. Emitter 6

To put Emitter 6 in operation, follow these instructions.

a) Verify if connectors in the back of Unit E6/E7 are connected according to the interconnection table given in Appendix 11.

b) Choose the desired frequency of operation and tune HP-3200B to this frequency. Adjust the output level of HP-3200B to 14 dBm.

c) Turn "BAND" switch to the desired band.

d) Turn "On" Unit PS1 - POWER SUPPLY. This will provide the +24 VDC for the amplifiers in E6/E7.

e) By turning the "RF" switch in E6 to "COUNTER" and "SELECTION" switch to Position "5", the frequency of E6 can be accurately measured by the counter.

f) The power available at "TEST OUT" in E6 should be about 27 dBm.

7. Emitter 7

To put Emitter 7 in operation follow the same instructions given above with the following modifications:

- Substitute E6 → E7.

- "SELECTION" switch on the counter will select E7 at Position 6.

8. Emitter 8 (Includes 30 MHz Reference Signal)

To put Emitter 8 in operation, follow these instructions:

a) Verify if connectors on the back of E8 are connected according to interconnection table in Appendix 11.

b) Select the frequency of operation and turn "BAND" switch to cover the desired band.

c) Turn "ON" transmitter T-827B/URT and select the desired frequency.

d) "RF" switch can be used to direct the signal to the counter where by selecting position 7 of "SELECTION" switch, its frequency can be measured.

e) The power available at "TEST OUTPUT" of Emitter 8 is about 25 dBm.

To make operative the 30 MHz signal generation located in this unit, follow the additional instructions below:

f) Verify if AM-2123A(V)U - DISTRIBUTION AMPLIFIER is properly connected to the 5 MHz STANDARD and both are turned "ON".

g) Turn "On" "Power switch in Unit E10. This will provide +15 VDC to the amplifiers in the 30 MHz reference circuitry.

9. Emitter 9

To put Emitter 9 in operation, follow these instructions.

a) Verify if AC plug on E9 is connected to an outlet.

b) Verify if all connectors are connected according to Interconnection Table in Appendix 11.

c) Connect an oscilloscope to the output of HP 8011A and make the following adjustments.

- Level 0 to 2.5V on a 50Ω load (3V or more will damage the mixers in E9).

- Pulse width adjusted to the desired value.

d) Connect "RANDOM OUT" in E9 to "TRIGGER IN" in HP 8011A and "PULSE IN" in E9 to "OUT" in HP 8011A.

e) Select "PULSE PERIOD" in HP 8011A to "EXT".

f) Turn "On" PS1 - POWER SUPPLY. This will provide +24 VDC to the noise source located in Unit E5C which provides the necessary Gaussian noise for the operation of E9.

g) Turn E9 "On", "CLOCK SELECTION" to "INT" and "RATE" to desired value.

h) Adjust the level of E9 to the desired value by using "ATTENUATION" control.

10. Emitter 10

To put Emitter 10 in operation just turn "ON" "POWER" switch on the front panel after having verified that all connectors and AC cord on the back are properly connected as explained in Appendix 11.

Since this is not a calibrated source of Gaussian noise, the actual power at the "OUTPUT" port of C1 - COMBINING UNIT has to be measured. "ATTENUATION" control in 1 dB steps are available at the front panel of E10.

11. S1 - Signal

To put the signal in operation, follow these instructions.

a) Verify if AC plug is connected to an outlet.

b) Verify if connectors on the back are connected according to interconnection diagram in Appendix 11.

c) Connect the output of HP to "LO IN" on the front panel of S1. Select its frequency to be 30 MHz below or above the desired frequency of operation. Adjust its level to 7 dBm.

d) Turn "On" the 30 MHz signal by following the instructions given to put Emitter 8 in operation.

e) Turn "On" S1.

f) Connect a power meter to the "TEST OUT" in S1.

g) Adjust the filter tuning in S1 to obtain a peak in the power at "TEST OUT".

h) Adjust the level of the signal to the desired value by using the "ATTENUATION" control. The level of the signal at the "OUTPUT" port in C1 - COMBINING UNIT can be calculated with the following formula

SIGNAL LEVEL (dBm) = POWER LEVEL MEASURED AT "TEST OUT" (dBm)- 102.9dB - ATTENUATION VALUE GIVEN BY FIGURE 28 in dB.

Figure 28 is repeated at the end of this appendix for convenience.

B. USING THE SIMULATOR

1. N1 and N2 Nonlinearities #'s 1 and 2

After setting up the various emitters as explained before, the operator can generate intermodulation products caused by the various combinations of them by varying the controls on the front panel of the units.

The operator has available ON/OFF and attenuation control for Emitters 1 to 8.

It is important to note that in order to prevent the amplifier preceding the nonlinearity from being saturated by any individual emitter, the minimum amount of attenuation from each emitter must be as given in Table 23 below.

Table 23

Minimum Attenuation from Each Emitter to Prevent Saturation of Amplifiers in N1 and N2.

EMITTER	MINIMUM ATTENUATION	EMITTER	MINIMUM ATTENUATION
1	0 dB	5	10 dB
2	0 dB	6	8 dB
3	7 dB	7	7 dB
4	8 dB	8	7 dB

In addition, in order to maintain the noise generated by the amplifier at a level below thermal noise, the attenuator at the output of the nonlinearity should be set at least to 20 dB.

2. C1 - Combining Unit

After having set up all emitters as desired and also the INTERMODS to match a known interference scenario, the operator has ON/OFF control of signals E1 to E5, E9, E10 and the SIGNAL. In addition, Emitters E1 to E5 have attenuation control from 0 to 60 dB in 10 dB steps.

C. OTHER OPERATIONAL INFORMATION

In order to facilitate the operator task in using this simulator additional tables are given below. Table 24 provides a list of all power supplies used for each unit and gives its location. Table 25 describes which signals are connected to the counter in each position of "SELECTION" switch.

Table 26 gives the noise power density level available at the "OUTPUT" port in C1 from each of the emitters. It also gives information about the filters that control the noise and spurious level of each emitter.

Table 27 gives attenuation of "TEST OUT" in relation to "OUTPUT" port in C1.

Table 24

Relation of Power Supplies and Their Locations

UNIT	POWER SUPPLY	LOCATION
E1	+5 VDC	E1A
E1	+24 VDC	PS1
E1	+15 VDC	E10
E2	+5 VDC	E2A
E2	+24 VDC	PS1
E2	+15 VDC	E10
E3	+5 VDC	E3A
E4	+5 VDC	E4A
E5	+5 VDC, ±15 VDC, +24 VDC	PS1
E6	+24 VDC	PS1
E7	+24 VDC	PS1
E8	+15 VDC	E10
E9	+5 VDC	E9
E9	+24 VDC	PS1
E10	+15 VDC	E10
S1	+5 VDC, +24 VDC	S1
S1	+15 VDC	E10
N1	+24 VDC	PS1
N2	+24 VDC	PS1

Obs: In order that the units listed in the "UNIT" column can operate, units listed in column "LOCATION" must be "ON".

Table 25

List of Frequency Measurements That Can be Made at Each Position of Counter "SELECTION" switch

Position	Measurement
1	Emitter 1 center frequency
2	Emitter 2 center frequency
3	Radar center frequency
4	Radar PRF
5	Emitter 6 frequency
6	Emitter 7 frequency
7	Emitter 8 frequency
8	Not used

Table 26

Information for Noise Level Computation At "OUTPUT" Port in C1

EMITTER	NOISE LEVEL (dB above kT)	FILTER INFORMATION
1	22	BW = 3%; $\frac{30\text{ dB BW}}{3\text{ dB BW}} = 2.1$
2	22	BW = 3%; $\frac{30\text{ dB BW}}{3\text{ dB BW}} = 2.1$
3	Not known	Not known
4	Not known	Not known
5	35 dB	200 MHz Band: 3 dB points = 200 & 224 MHz 35 dB points = 180 & 240 MHz 400 [redacted] Band: 3 dB points = 418 & 471 MHz 35 dB points = 385 & 495 MHz

Table 27

Attenuation of "TEST OUT" in relation to "OUTPUT" Port in C1

FREQUENCY	200	220	240	260	280	300	320	340	360	380	400
ATTENUATION	20.2	20.2	20.15	20.15	20.2	20.2	20.15	20.15	20.15	20.15	20.15

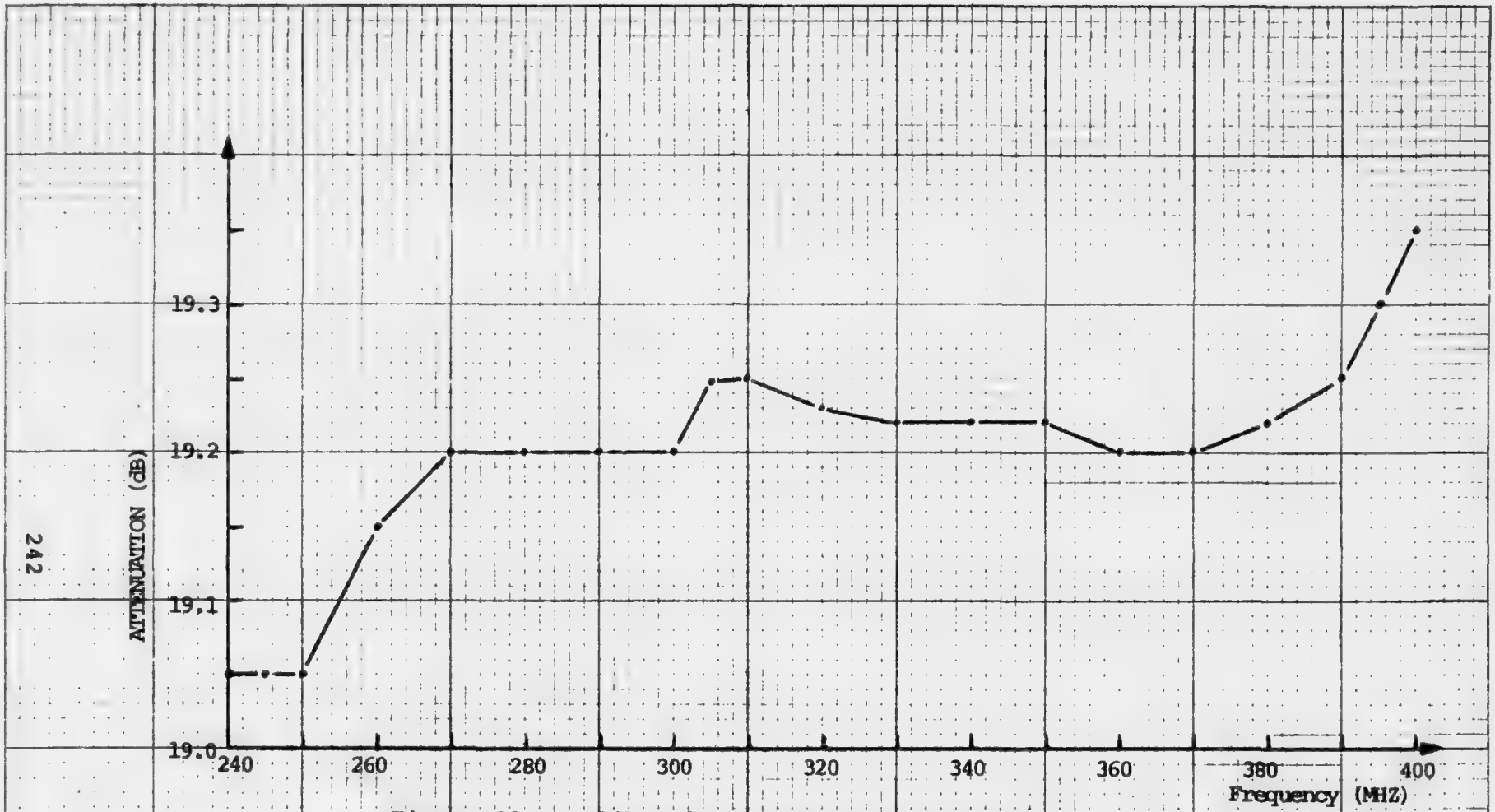

Figure 28: Calibration Curve for the Signal.

APPENDIX 11

INTERCONNECTION TABLE FOR ALL UNITS

UNIT	CONNECTOR	FUNCTION	CONNECTED TO
C1	J11	SIGNAL IN	S1 - J11
C1	J12	E10 INPUT	E10 - J12
C1	J13	E9 INPUT	E9 - J12
N1	J11	E4 INPUT	SRC/21 - OUT (COM LAB)
N1	J12	E3 INPUT	SRC/21 - OUT (RADAR LAB)
N1	J13	E2 INPUT	E2A - J15
N1	J14	E1 INPUT	E1A - J15
N2	J11	E8 INPUT	E8 - J18
N2	J12	E7 INPUT	E6/E7 - J12
N2	J13	E6 INPUT	E6/E7 - J13
N2	J14	E5 INPUT	E5C - J14
N2	P11	+24V DC POWER	PS1 - J11
PS1	J11	+24V DC OUTPUT	N2 - P11
PS1	J12	+24V DC OUTPUT	E6/E7 - P11
PS1	J13	±15V, +5, +24V DC OUTPUT	E5C - P12
PS1	J14	+5V DC OUTPUT	E5A - P11
PS1	J15	+24V DC OUTPUT	400 mA TOTAL
PS1	J16	+24V DC OUTPUT	CURRENT AVAILABLE
PS1	J17	+24V DC OUTPUT	E1C/E2C - P11
E1A	J11	OUTPUT TO COUNTER	HP 5383A - J15
E1A	J12	INPUT FROM FILTER	E1B - J12
E1A	J13	30 MHz REFERENCE INPUT	E8 - J12
E1A	J14	OUTPUT TO AMPLIFIER	E1C/E2C - J13
E1A	J15	E1 OUTPUT	N1 - J14

INTERCONNECTION TABLE (Continued)

UNIT	CONNECTOR	FUNCTION	CONNECTED TO
E1B	J11	FILTER INPUT	E1C/E2C - J14
E1B	J12	FILTER OUTPUT	E1A - J11
E1C/E2C	J13	AMPLIFIER INPUT	E1A - J14
E1C/E2C	J14	AMPLIFIER OUTPUT	E1B - J11
E1C/E2C	P11	24V INPUT	PS1 - J17
E2A	J11	OUTPUT TO COUNTER	HP 5383A - J11
E2A	J12	INPUT FROM FILTER	E2B - J12
E2A	J13	30 MHz REFERENCE INPUT	E8 - J13
E2A	J14	OUTPUT TO AMPLIFIER	E1C/E2C - J12
E2A	J15	E2 OUTPUT	N1 - J13
E2B	J11	FILTER INPUT	E1C/E2C - J11
E2B	J12	FILTER OUTPUT	E2A - J12
E1C/E2C	J11	AMPLIFIER OUTPUT	E2B - J11
E1C/E2C	J12	AMPLIFIER INPUT	E2A - J14
E3A	P11	AUDIO INPUT	R390A - J11
E3A	P12	REMOTE CONTROL	SRC/21 - J104 (RADAR LAB)
E3A	J11	EXTERNAL PTT INPUT	TTL COMPATIBLE SOURCE
E3A	J12	CLOCK #2 OUTPUT	ANY 50 OHMS LOAD
E3A	J13	CLOCK #2 INPUT	TTL COMPATIBLE SOURCE
E3A	J14	CLOCK #1 OUTPUT	ANY 50 OHMS LOAD
E3A	J15	CLOCK #1 INPUT	TTL COMPATIBLE SOURCE
E3B		FREQUENCY SELECTION CONTROL LINES	SRC/21 - J103 (RADAR LAB)

INTERCONNECTION TABLE (Continued)

UNIT	CONNECTOR	FUNCTION	CONNECTED TO
E4A	P11	AUDIO/INPUT	R390A - J12
E4A	P12	REMOTE CONTROL	SRC/21 - J104 (COM. LAB)
E4A	J11	EXT PTT INPUT	TTL COMPATIBLE SOURCE
E4A	J12	CLOCK #2 OUTPUT	ANY 50 OHMS LOAD
E4A	J13	CLOCK #2 INPUT	TTL COMPATIBLE SOURCE
E4A	J14	CLOCK #1 OUTPUT	ANY 50 OHMS LOAD
	J15	CLOCK #1 INPUT	TTL COMPATIBLE SOURCE
E4B		FREQUENCY SELECTION CONTROL LINES	SRC/21 - J103 (COM. LAB)
E5A	J11	SCAN MODULATED NOISE IN	E5C - J11
E5A	J12	SCAN & PULSE MODUL. NOISE OUT	E5C - J12
E5A	J13	SCAN MODULATED RF IN	E5C - J15
E5A	J14	PULSE OUT TO COUNTER	HP 5383A - J12
E5A	P11	+5V DC POWER	PS1 - J14
E5C	J11	SCAN MODULATED NOISE OUT	E5A - J11
E5C	J12	SCAN & PULSE MODUL. NOISE IN	E5A - J12
E5C	J13	NOISE OUTPUT	E9 - J11
E5C	J14	E5 OUTPUT	N2 - J14
E5C	J15	SCAN MODULATED RF OUT	E5A - J13
E5C	J16	RF INPUT	HP 3200B - OUT
E5C	J17	RF OUTPUT TO COUNTER	HP 5383A - J16
E5C	P11	COMPUTER INPUT/OUTPUT	
E5C	P12	DC POWER INPUT	PS1 - J13

INTERCONNECTION TABLE (Continued)

UNIT	CONNECTOR	FUNCTION	CONNECTED TO
E6/E7	J13	E6 OUTPUT	N2 - J13
E6/E7	J14	RF OUTPUT TO COUNTER	HP 5383A - J13
E6/E7	J16	RF INPUT	HP 3200B - OUT
E6/E7	P11	+24V DC POWER	PS1 - J12
E6/E7	J11	RF OUTPUT TO COUNTER	HP 5383A - J17
E6/E7	J12	E7 OUTPUT	N2 - J12
E6/E7	J15	RF INPUT	HP 3200B - OUT
E8	J11	5 MHz REFERENCE INPUT	AM-2123A(V)U-J4
E8	J12	20 MHz OUTPUT @ 2 DBm	E1A - J13
E8	J13	30 MHz OUTPUT @ 1 DGm	E2A - J13
E8	J14	30 MHz OUTPUT @ 0 DBm	S1 - J12
E8	J15	30 MHz OUTPUT @ 12 DBm	ANY 50 OHMS LOAD
E8	J16	RF OUTPUT TO COUNTER	HP 5383A - J18
E8	J17	RF INPUT	T-827B/URT - J23
E8	J18	E8 OUTPUT	N2 - J11
E8	P11	+15 V DC POWER IN	E10 - J11
E9	J11	NOISE INPUT	E5C - J13
E9	J12	E9 OUTPUT	C1 - J13
E10	J11	+15V DC POWER OUT	E8 - P11
E10	J12	GAUSSIAN NOISE OUT	C1 - J12
S1	J11	SIGNAL OUTPUT	C1 - J11
S1	J12	30 MHz REF. INPUT	E8 - J14

APPENDIX 12

COMBINER C1 PARTS LIST

ITEM	DESCRIPTION AND MANUFACTURER
R1 to R5	TELONIC, 8121-S; 0-60 dB, 10 dB steps, rotary attenuator
S1 to S8	TEXSCAN SW-10/TNC; SPDT RF switch
PD1 to PD8	MERRIMAC PDM-20-500; 5-1000 MHz two way power divider with 1 watt internal loads
DC1	MERRIMAC CRM-10-500; 50-500 MHz, 10 dB directional coupler
DC2, DC3	MERRIMAC CRM-15-500; 10-500 MHz, 15 dB directional coupler
R6	WEINSCHEL MODEL 50-50; 50 dB fixed attenuator
R7	ELCOM AT-50; 5 dB fixed attenuator

N1 - NONLINEARITY #1 PARTS LIST

ITEM	DESCRIPTION AND MANUFACTURER
R1 to R4	TEXSCAN LA 54; 0-60 dB, 1 dB steps
R6 to R9	rotary attenuator
R5	TELONIC 8121-S; 0-60 dB, 10 dB steps, rotary attenuator
S1 to S9	TEXSCAN SW-10/TNC; SPDT RF switch
PD1 to PD11	TECHNICAL RESEARCH AND MANUFACTURING DL206; two-way power divider, 5-500 MHz
PD13, PD14	ANZAC THV-50; two-way power divider
PD12, PD15	MERRIMAC PDM-20-500; 5-1000 MHz two-way power divider with 1 watt internal loads
AMP1	Q-BIT CORP; QB-538; 2-500 MHz, 33 dB gain 22 dBm linear amplifier

N2 - NONLINEARITY #2 PARTS LIST

ITEM	DESCRIPTION AND MANUFACTURER
R1 to R4	TEXSCAN LA54; 0-60 dB, 1 dB steps rotary attenuator
R6 to R9	TEXSCAN LA54; 0-60 dB, 1 dB steps rotary attenuator
R5	TELONIC 8121-S; 0-60 dB, 10 dB steps rotary attenuator
S1 to S9	TEXSCAN SW-10/TNC; SPDT RF switches
DC1	ANZAC DCG-10-4; 10 dB directional coupler
PD1 and PD9 to PD11	TECHNICAL RESEARCH AND MANUFACTURING DL 206; 5-500 MHz two-way power divider
PD2 to PD4, PD13, PD14	ANZAC THV-50; 2-200 MHz two-way power divider
PD12, PD15	MERRIMAC PDM-20-500; 5-1000 MHz two-way power divider with 1 watt internal load
AMP1	Q-BIT; QB-538; 2-500 MHz, 33 dB gain, 22 dBm linear amplifier

E1A OR E2A UHF/PSK MODULATORS PARTS LIST

ITEM	DESCRIPTION AND MANUFACTURER
A2	Statistics generator
A2RO	10 KΩ potentiometer
A2R10	33 KΩ 1/4W resistor
A2R1 to A2R9 A2R11 to A2R17	1 KΩ, 1/8W resistor
A2C1	47 µF, 35V DC electrolitic capacitor
A2C4	47 µF, 35V DC electrolitic capacitor
A2C2, C3	.02 µF, 50V DC ceramic capacitor
A2C5 to C7	.02 µF, 50V DC ceramic capacitor
A2IC1, IC11, IC16	74S140 line drivers
A2IC2, IC4	7432 QUAD, 2 INPUT OR gate
A2IC3, IC5	7408 QUAD, 2 INPUT AND gate
IC12, IC15	7408 QUAD, 2 INPUT AND gate
A2IC7, IC14	7480 QUAD, 2 INPUT EXCLUSIVE OR gate
A2IC8	74H106 DUAL JK flip-flop
A2IC6	9305 variable modulo counter
A2IC9	7430 8 INPUT NAND gate
A2IC1	9601 retriggerable monostable multivibrator
A2IC13, IC18	9396 5-bit shift register
A2IC19	9022 DUAL JK M-S flip-flop
A2IC20	9391 8-bit shift register
A2 CLOCK	CONNOR-WINFIELD L13R - RC oscillator (19.2 KHz)
DBM 1	MINICIRCUITS LABORATORY ZAD-1HB or ZLW-1HWB mixers (1) (2)
DBM2	MINICIRCUITS LABORATORY RAY-1 mixer
FL1	PIEZO TECHNOLOGY INC. - 5152 XTAL filter
S2	TEXSCAN CORP. SW-10 SPDT RF switch
S1	CENTRALAB 1P3T SWITCH (PA-300 + PA-18)
S3	CENTRALAB 1P5T SWITCH (PA-300 + PA-18)
S4, S5, S6, S7	ALCOSWITCH 105D SPDT

E1B OR E2B UHF/PSK PARTS LIST (Continued)

ITEM	DESCRIPTION AND MANUFACTURER
S6	MICROSWITCH 3G34A SPDT switch and indicator light
J1 to J5	BNC/F connector
J6	N/F connector
J11 to J15	TNC/F connector
PSE3, E4	ACOPIAN 5E100 power supply
E1B (E2B)	K & L MICROWAVE 5BT 200/400-3-0 tunable band-pass filter

ELC/E2C UHF/PSK AMPLIFIER PARTS LIST

ITEM	DESCRIPTION AND MANUFACTURER
AMP 1 to AMP 4	MINICIRCUITS LABORATORY ZHL-1, 2-500 MHz, 16 dB gain amplifier
FAN	PAMOTOR 8500 P
S1	DPDT toggle switch
DS1	120V neon lamp

E3A OR E4A - UHF/LOS MODULATOR PARTS LIST

ITEM	DESCRIPTION AND MANUFACTURER
A2	STATISTICS GENERATOR (2 each)
A2RO	10 KΩ potentiometer
A2R1 - R9	1 KΩ 1/8W resistor
A2R11 - R17	1 KΩ 1/8W resistor
A2R10	47 KΩ 1/4W resistor
A2C1	47 µF, 35V DC elect. capacity
A2C4	47 µF or 330 µF electrol. capacity
A2C2, C3, C5 to C8	.02 µF ceramic capacitor
A2IC1, IC11, IC16	74S 140 line driver
A2IC2, IC4	7432 QUAD-2 INPUT OR gate
A2IC3, 5, 12, 15	7408 QUAD-2 INPUT AND gate
A2IC7, 14	7486 QUAD-2 INPUT EXC. OR gate
A2IC8	74H106 DUAL JK flip-flop
A2IC6	9305 variable modulo counter
A2IC9	7430 8 INPUT NAND gate
A2IC10	9601 retriggerable monostable
A2IC13, IC18	9396 5-bit shift register
A2IC19	9022 DUAL JK flip-flop
A2IC20	9391 8-bit shift register
A2 CLOCK	CONNOR-WINFIELD L13R - RC oscillators (512 and 70 Hz)
K1	MAGNECRAFT DIP-107 reed relay
S1, S4, S6, S11	ALCOSWITCH 105D, SPDT toggle switch
S2, S5	SWITCHCRAFT SP5T, rotary switch
S3	SPDT toggle switch, with "stop" position
E3PS1 (E4PS1)	ACOPIAN 5E150, 5V DC, 1.5 AMP, power supply
S7	MICROSWITCH 3G34A SPDT switch with indicator light
DS1	DIALCO 507-4756-3731-500 3.6V LED indicator

E5A - RADAR PULSE MODULATOR PARTS LIST

ITEM	DESCRIPTION AND MANUFACTURER
A1	RADAR DRIVER
A1IC1	7404 HEX-INVERTER
A1IC2	74S104 line driver
A1IC3	74S104 line driver
A1R1	56 ohms 1/2W resistor
A1R2, R4, R5, R6	18 ohms 1/2W resistor
A1R3, R7	56 ohms 1/2W resistor
A1R8 to A1R13	30 ohms 1/2W resistor
A1J1 to A1J5	SMA/female connectors (modpack)
DBM1, 2	MINICIRCUITS LABORATORY ZAY-1B mixer
DBM 3, 4	MINICIRCUITS LABORATORY ZAD-1B mixer
J1	BNC/female connector
J2	N/female connector
J11 to J14	TNC/female connector
P11	AMPHENOL 3002A 12S-3-P connector
R1	TELONIC 8120S rotary attenuator
R2	ELCOM CT-52/TNC 50 ohms termin.
S1, S2	TEXSCAN SW-10-TNC switch

E5B - RADAR AMPLIFIER PARTS LIST

ITEM	DESCRIPTION AND MANUFACTURER
E5B	HUGHES 1416H, 50-500 MHz, 30 dB gain, 4 Watts linear amplifier

E5C - RADAR SCAN MODULATOR PARTS LIST

ITEM	DESCRIPTION AND MANUFACTURER
IC1 to IC4 and IC6	9310 programmable decade counter
IC5	7404 HEX INVERTER
clock	L13C - CONNOR-WINFIELD 1.024 MHz XTAL oscillator
DC1	DCG-4-ANZAC 10 dB directional coupler
FL1	5B114-212/24-0/0-K & L MICROWAVE, bandpass tubular filter
FL2	5B114-445/50-0/0-K & L MICROWAVE bandpass tubular filter
FL3	30 MHz RC, high pass filter
PD1	T-1000-ANZAC power divider
AMP1 → AMP3	Q-BIT - QB-538, 2-500 MHz, linear amplifier
R1, R2	325-80-1 - GENERAL MICROWAVE, 0-80 dB programmable attenuator
R3	CT-50 - ELCOM 50 ohms termination
R4	AT-50 ELCOM 10 dB attenuator
S1	SW-20/TNC - TEXSCAN DPDT, RF switch
S2	SW-10/TNC - TEXSCAN SPDT RF switch

E6/E7 - VHF/UHF - INTERFERERS PARTS LIST

ITEM	DESCRIPTION AND MANUFACTURER
AMP1, 2	ZHL-1 2-500 MHz, 16 dB gain, 1 Watt linear amplifier, MINICIRCUITS LABORATORY
FL1	8B50-57 5/35-0/0; 40 to 75 MHz bandpass filter, K & L MICROWAVE
FL2	8B50-154/92 - 0/0; 108 to 200 MHz bandpass filter, K & L MICROWAVE
FL3	7B50 - 13/6.5 - 0/0; 10-16 MHz bandpass filter, K & L MICROWAVE
FL4	7B50-21/11-0/0; 16-26 MHz bandpass filter, K & L MICROWAVE
PD1, 2	THV-50 power divider, ANZAC
S2, S3	SW-10-TNC; SPST RF switch, TEXSCAN
S1, S4	SW-20-TNC, DPDT RF switch, TEXSCAN

E8 - HF INTERFERER PARTS LIST

ITEM	DESCRIPTION AND MANUFACTURER
S1	SW-20-TNC, DPDT RF switch, TEXSCAN
S2	SW-10-TNC, SPST RF switch, TEXSCAN
PD1	THV-50 power divider, ANZAC
PD2	DS-312 four-way power divider, ANZAC
FL1	10L50-6.5 - 0/0; 0 to 6.5 MHz lowpass filter, K & L MICROWAVE
FL2	8B50-8/4.25 - 0/0; 6 to 10 MHz bandpass filter, K & L MICROWAVE
FL3	5B114-30/1 - 0/0; 29.5 to 30.5 MHz tubular bandpass filter, K & L MICROWAVE
FL4	5C20-30/1-0.0, 30 MHz, 1 MHz BW bandpass filter, K & L MICROWAVE
AMP1, 2, 3	QB-300 - 1 to 300 MHz amplifier, Q-BIT CORP.
DBL	GK-3B doubler, MINICIRCUITS LABORATORY
R1, R7	AT-50; attenuators, ELCOM

E9 - IMPULSIVE NOISE PARTS LIST

ITEM	DESCRIPTION AND MANUFACTURER
A5	DRIVER
A5R1, R3	100Ω 1/2 watt resistor
A5R2, R4	67Ω 1/2 watt resistor
A5J1 to J3	SMA/female connectors (MODPACK)
A6	IMPULSE GENERATOR
A6IC1, IC6	9305 variable modulo counter
A6IC2, IC5	7408 QUAD-2 INPUT NAND gate
IC9	
A6IC3, IC4	7432 QUAD-2 INPUT OR gate
A6IC7	7430 8 INPUT NAND gate
A6IC8	9601 retriggerable monostable multivibrator
A6IC10, IC14	9396/7496 5 bit shift register
A6IC11	7486 QUAD-2 INPUT EXCLUSVIE OR gate
A6IC12, IC16	9391/7491 8 bit shift register
A6IC15	9022 DUAL JK master-slave flip-flop
A6IC13	945140 line driver
A6C1	15 µF/35V DC electrolitic capacitor
A6C2 to C6 and A6C8	.02 µF/50 DC ceramic capacitor
A6C7	.47 µF/12V DC ceramic capacitor
A6R1	not used
A6R2, R3, R4, R6, R8, R9, R10	1 KΩ/1/8@ resistor
A6R5	56Ω/1/2W resistor
A6R7	47 KΩ/1/4W resistor
A6 clock	CONNOR-WINFIELD CORP. L13C-XTAL oscillator (1.024 MHz)
DS1	DIALCO 249-7867-3731-504 LET indicator
DBM1, DBM2	MINICIRCUITS LABORATORY ZAD-1B mixer
F1	CORCOM 3EF1 EM1 filter
FS1	AMP fuse
J1 to J4	BNC/female connector

E9 PARTS LIST (Continued)

ITEM	DESCRIPTION AND MANUFACTURER
PS1E9	power supply; ACOPINA 5E100
R1	TELONIC INDUSTRIES INC. - 8121-S 0-60 dB (10 dB steps) rotary attenuator
R2	1KΩ/1/8W resistor
R3	56Ω/1/2W resistor
S1	ALCOSWITCH 105D SPDT switch
S2	CENTRALAB 1P8T switch (PA-300 30° index + PA-18 ceramic section)
S3	SWITCHCRAFT SPDT momentary switch
S4	MICROSWITCH 3G34A SPDT switch with indicator light

E10 - GAUSSIAN NOISE PARTS LIST

ITEM	DESCRIPTION AND MANUFACTURER
E10/PS1	ACOPIAN B15 GT100V, 15 VOLTS, 1 AMP power supply
AMP1, AMP2	Q-BIT: QB-538, 2-500 MHz, 33 dB gain linear amplifier
R1	TEXSCAN LA-54, 0-60 dB, 1 dB step rotary attenuator
DS1	DIALCO 249-7871-3731-504, 14V DC LED indicator
S1	ALCOSWITCH 105D, SPDT toggle switch

PS1 - POWER SUPPLY PARTS LIST

ITEM	DESCRIPTION AND MANUFACTURER
24PS	ACOPIAN B24GT500V, +24V DC, 5 AMP power supply
15 PS	ACOPIAN TD15-100V, ±15V DC, 1 AMP power supply
5 PS	ACOPIAN B5GT210V, +5VOC, 2 AMP power supply
FAN	INC BS2107F-0-1
M1	SYMPSON 1227, 0-30V DC meter
S1	ALCOSWITCH 105D, SPDT toggle switch
S2	SWITCHCRAFT DP5T rotary switch
DS1	115 VAC neon lamp

S1 - SIGNAL PARTS LIST

ITEM	DESCRIPTION AND MANUFACTURER
A2	STATISTICS GENERATOR
A2R1-R9	1KΩ, 1/8W resistor
A2R11-R17	1KΩ, 1/8W resistor
A2R10	33KΩ 1/4W resistor
A2C1	47 µF, 35V DC elect. capacitor
A2C4	47 µF, 35V DC elect. capacitor
A2C2, C3, C5-C8	.02 µF, 50V DC ceramic capacitor
A2IC1, 11, 16	74S140 line driver
A2IC2, 4	7432 QUAD-2 INPUT OR gate
A2IC3, 5, 12, 15	7408 QUAD-2 INPUT AND gate
A2IC7, 14	7486 QUAD-2 INPUT EXCL. OR gate
A2IC8	74H106 DUAL JK flip-flop
A2IC6	9305 variable module counter
A2IC9	7430 8 INPUT NAND gate
A2IC10	9601 retriggerable monostable
A2IC13, 18	9396 5 bit shift register
A2IC19	9022 DUAL JK flip-flop
A2IC20	9391 8 bit shift register
A2 clock	CONNOR-WINFIELD L13C XTAL oscillator (19.2 KHz)
FL1	PIEZO TECHNOLOGY 5152 XTAL filter
FL2	K & L MICROWAVE 5 BT 200/400-3-0 tunable bandpass filter
DBM1	MINICIRCUITS LABORATORY SRA-6 mixer
DBM2	MINICIRCUITS LABORATORY ZAD-1B mixer
R1	TEXSCAN LA-54, 0-60 dB, 1 dB step attenuator
R2	WEINSCHEL MODEL 50-50, 50 dB pad
S1	SWITCHCRAFT, SP3T rotary switch
S2, 4, 5, 6, 7	ALCOSWITCH 105D, SPDT toggle switch
S3	SWITCHCRAFT SP5T rotary switch
S8	MICROSWITCH 3G34A SPDT switch w/ indicator light
S9	TELEDYNE CS-37S1C coaxial transfer switch with indicator

S1 - SIGNAL PARTS LIST (Continued)

ITEM	DESCRIPTION AND MANUFACTURER
S9	TELEDYNE CS-37S1C coaxial transfer switch with indicator
AMP1	Q-BIT; QB-538, 2-500 MHz, 33 dB gain linear amplifier
PD1	ANZAC, T-1000 power divider
S1/PS1	ACOPIAN 5E100, 5V, 1 AMP power supply
S1/PS2	ACOPIAN 24E60, 24V, .6 AMP power supply
DS1, 2	DIALCO 249-7871-3731-504 14V DC LED indicator

LIST OF REFERENCES

1. Ohlson, J.E. and Landry, T.C., Shipboard Radio Frequency Interference in UHF Satellite Communications, Technical Report, Naval Postgraduate School, Monterey, California, in preparation, 1976.

2. Middleton, D., "Statistical Physical Models of Urban Radio-Noise Environments - Part I: Foundations," IEEE Trans. on Electromagnetic Compatibility, VOL. EMC14, No. 2, May 1972.

3. Hall, H. M., A New Model for Impulsive Phenomena: Application to Atmospheric-Noise Communications Channels, Stanford Electronics Laboratories SEL-66-052, August 1966.

4. Ibukun, O., "Structural Aspects of Atmospheric Radio Noise," Proceedings of the IEEE, Vol. 54, No. 3, March 1966.

5. Giordano, A. A., "Modeling of Atmospheric Noise," Radio Science, Vol. 7, No. 11, pp. 1011-1023, November 1972.

6. Spaulding, A. D., Optimum Reception in an Impulsive Interference Environment, Ph.D. Thesis, University of Denver, May 1975.

7. Furutsu, K. and Ishida, T., "On the Theory of Amplitude Distribution of Impulsive Random Noise," Journal of Applied Physics, Vol. 32, No. 2, July 1961.

8. Ishida, T., "Statistical Characteristics of Atmospheric Noise, 1966-1969," Report of the Radio Research Laboratory, Ministry of Posts and Telecommunications, Tokyo, Japan, 1969.

9. Nakai, T. and Nagatani, M., "Synchronous Analysis of Statistical Parameters of the Atmospheric Noise," Proc. Inst. Atmos. (Japan), Vol. 17, pp. 29-41, 1970.

10. Electromagnetic Impact on Ship Design, IIT Research Institute Report IITRI-6904-F.

11. Chase, W. M., A Dialogue on Conducting Shipboard RFI Surveys and Locating Interference Sources, Report of the U.S. Naval Electronics Laboratory Center TD338, 7 October 1974.

12. Chase, W. M., Ship RFI Survey Procedure for HF Frequencies, Report of the U.S. Nav. Elec. Lab. Ctr. TD 336, 21 June 1974.

13. Horn, J. M., HF Shipboard Antenna System Design and Utilization Criteria, Report of the U.S. Nav. Elec. Lab. Ctr. TR1808, 12 January 1971.

14. Salisbury, G. C., Analysis of Very High Order Frequency Components of the Intermodulation Interference Spectrum, Report of the U.S. Nav. Elec. Lab. Ctr. TR1852, 27 December 1972.

15. Salisbury, G. C., Topside Intermodulation Aboard USS MOUNT WHITNEY (LCC20), USS BLUE RIDGE (LCC99) and USS IWOJIMA (LPH2), Report of the U.S. Naval Electronics Laboratory Center TD206, 27 December 1972.

16. Higa, W. H., "Spurious Signals Generated by Electron Tunneling on Large Reflector Antennas," Proceedings of the IEEE, Vol. 63, No. 2, February 1975.

17. Carlson, R. F., and Ohlson, J. E., Receiver Desensitization of the AN/WSC-3 Satellite Communications Set, Technical Report NPS 620L 76072, Naval Postgraduate School, July 1976.

18. Interference Notebook, Rome Air Development Center RADC-TR-66-1, June 1966.

19. Peterson, W. W., Error Correcting Codes, MIT Press, 1961.

20. Advisory Group for Aerospace Research and Development, Spread Spectrum Communications, Lecture Series No. 58, 1973.

21. Roberts, P. D. and Davis, R. H., "Statistical Properties of Smoothed Maximal-Length Linear Binary Sequences," Proceedings of IEEE, Vol. 113, No. 1, January 1966.

22. Anderson, G. C., Finnie, B. W. and Roberts, G. T., "Pseudo-Random and Random Test Signals," Hewlett-Packard Journal, pp. 1-17, September 1967.

23. Davies, A. C., "Digital Filtering of Binary Sequences," Electronics Letters, Vol. 3, No. 7, July 1967.

24. Rowe, I. H. and Kerr, I. M., "A Broad-Spectrum Pseudo-Random Gaussian Noise Generator," IEEE Trans. on Automatic Control, Vol. AC15, No. 5, October 1970.

25. Sobolewski, J. J. and Payne, W. H., "Pseudonoise with Arbitrary Amplitude Distribution – Part I: Theory," IEEE Trans. on Computers, Vol. C-21, No. 4, April 1972.

26. "Pseudonoise with Arbitrary Amplitude Distribution – Part II: Hardware Implementation," IEEE Trans. on Computers, Vol. C-21, No. 4, April 1972.

27. Ku, W. H., et al., Analysis and Digital Hardware Realization of Non-Gaussian Impulsive Noise in Wideband Communications Systems, Technical Report AD-774 443, Cornell University, October 1973.

28. Y. Neuvo and Ku, W. H., "Analysis and Digital Realization of a Pseudorandom Gaussian and Impulsive Noise Source," IEEE Trans. on Com., Vol. COM-23, No. 9, p. 849-858, September 1975.

29. Papoulis, A., Probability, Random Variables and Stochastic Processes, McGraw-Hill, 1965.

30. R. F. Carlson and J. E. Ohlson, "Bit-Error Rate Measurements on the AN/WSC-3 and AN/SSR-1 Satellite Communications Sets," Technical Report NPS-62OL76102, Naval Postgraduate School, October 1976.